Universiteit Leiden
The Netherlands

Development of the sinus venosus myocardium from the posterior second heart field : implications for sinoatrial and atrioventricular mode development

Vicente Steijn, R.

Citation
Vicente Steijn, R. (2011, June 16). *Development of the sinus venosus myocardium from the posterior second heart field : implications for sinoatrial and atrioventricular mode development*. Retrieved from https://hdl.handle.net/1887/17712

Version:	Corrected Publisher's Version
License:	Licence agreement concerning inclusion of doctoral thesis in the Institutional Repository of the University of Leiden
Downloaded from:	https://hdl.handle.net/1887/17712

Note: To cite this publication please use the final published version (if applicable).

Development of the sinus venosus myocardium from the posterior second heart field

Implications for sinoatrial and atrioventricular node development

Rebecca Vicente Steijn

© Rebecca Vicente Steijn, Den Haag
All rights reserved. No part of this book may be reproduced or transmitted, in any form or by any means, without written permission of the author.

ISBN nr: 978-94-6108-162-9
Cover: Barcelona design by Monste Breda Biada
Layout: Tiny Wouters
Printed by Gildeprint Drukkerijen- www.gildeprint.nl

The work presented in this thesis was carried out at the Department of Anatomy and Embryology of the Leiden University Medical Center.

Development of the sinus venosus myocardium from the posterior second heart field

Implications for sinoatrial and atrioventricular node development

Proefschrift

ter verkrijging van
de graad van Doctor aan de Universiteit van Leiden,
op gezag van de Rector Maginificus prof.mr. P.F.van der Heijden,
volgens het besluit van het College voor Promoties
te verdedigen op donderdag 16 juni 2011
klokke 11.15 uur

door

Rebecca Vicente Steijn

geboren te Barcelona, Spanje
in 1983

Promotiecommissie

Promotores: Prof. dr. A.C. Gittenberger-de Groot
Prof. dr. R.E. Poelmann

Co-promotor: Dr. M.R.M. Jongbloed

Overige leden: Prof. dr. A van der Laarse
Prof. dr. N.A. Blom
Prof. dr. R.N.W. Hauer (Universitair Medisch Centrum Utrecht)

Financial support of the Netherlands Heart Foundation for the publication of this thesis is gratefully acknowledged.
The realization of this thesis was also financially supported by Boston Scientific B.V, Sorin Group Nederland N.V. and Toshiba Medical Systems Nederland.

Contents

1	General introduction	6
2	*Podoplanin* deficient mice show a RhoA related hypoplasia of the sinus venosus myocardium including the sinoatrial node *Developmental Dynamics 2009;238:183–193*	26
3	Electrical activation of sinus venosus myocardium and expression patterns of RhoA and Isl-1 in the chick embryo *J Cardiovasc Electrophysiol 2010;21:1284-1292*	48
4	Platelet-derived growth factor is involved in the differentiation of second heart field-derived cardiac structures in chicken embryos *Developmental Dynamics 2009;238:2658-2669*	68
5	Expression of Id2 in the second heart field and cardiac defects in *Id2* knockout mice *Submitted for publication*	92
6	The funny current channel HCN4 delineates the developing cardiac conduction system in the chicken heart *Heart Rhythm 2011 in press*	118
7	Development of the sinoatrial and atrioventricular node in the avian embryo: morphological and electrophysiological changes during maturation *Submitted for publication*	138
8	General discussion	166
	Summary	186
	Samenvatting	192
	List of publications	198
	Curriculum Vitae	202
	Dankwoord	206

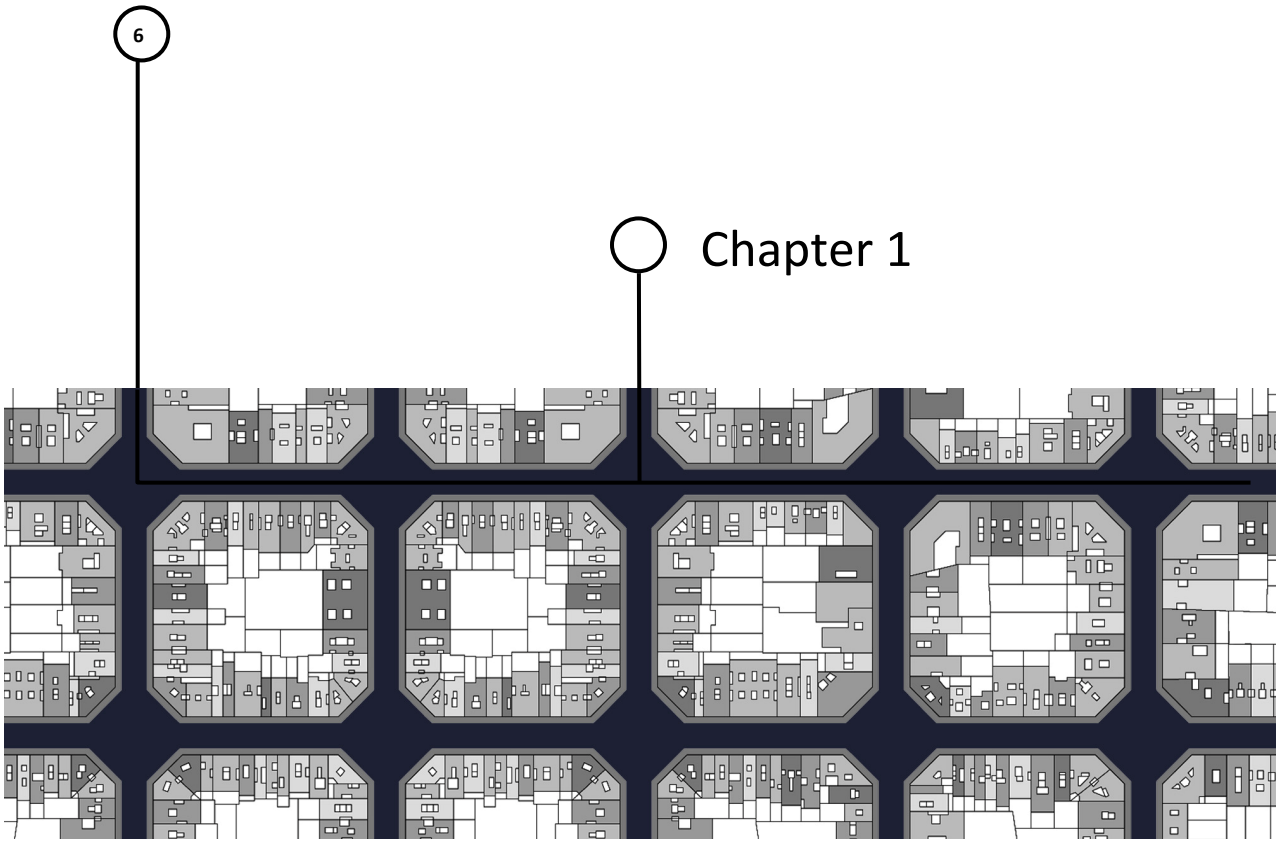
6
Chapter 1

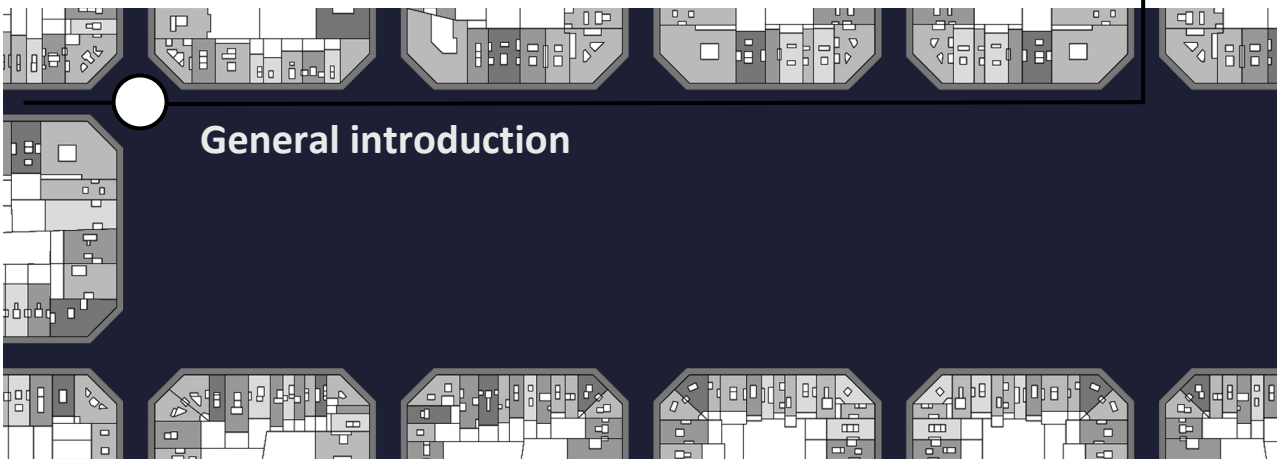
General introduction

Background

While the embryonic heart is developing and maturing towards its four-chambered form, the cardiac conduction system (CCS) of the heart is developing as well. The CCS will provide the heart with the required wiring system to ensure the proper contraction of the myocardial chambers. Both in the young and adult population rhythm disturbances or cardiac arrhythmias can occur. Electrophysiological studies have shown that these events do not occur randomly in the heart but rather at anatomical predilection sites. Specifically, ectopic foci have been reported in sinus venosus-related structures at the venous pole of the heart like the crista terminalis,[1] the ostia of the caval veins,[2] the coronary sinus[3] and the pulmonary veins.[4] Interestingly, during embryonic development, the area covered by the developing CCS includes structures that will not contribute to the mature CCS,[5,6] like for example the left cardinal vein, which during development goes in regression to become the ligament of Marshall, a known arrhythmogenic substrate. Therefore, we hypothesize that by studying the development of the CCS we may better understand the etiology of known arrhythmogenic events. This is the reason why we have focused on embryonic development of the CCS in relation to arrhythmias.

Early embryonic development: mesoderm formation

During embryonic development prior to gastrulation, the bilaminar embryonic disc is almost flat and consists of two layers, the epiblast and the hypoblast. The epiblast will give rise to the embryo and some of the extraembryonic structures, while the hypoblast will contribute entirely to the extraembryonic membranes. During gastrulation, cells from the epiblast undergo epithelial-to-mesenchymal transformation (EMT) and delaminate in the primitive streak to form the mesodermal as well as the endodermal layer. Thus, the bilaminar embryonic disc transforms into a trilaminar embryonic disc consisting of the three germ layers (ectoderm, mesoderm and endoderm). During formation of the primitive streak, the antero-posterior axis of the embryo is established. The ectoderm will contribute to the epidermis and the nervous system, the endoderm will contribute to the epithelium of the respiratory system and the intestinal tract, and the mesoderm will contribute to the cardiovascular system, the skeleton and striated muscles as well as the reproductive and excretory organs.[7] The mesoderm will initially divide into four compartments: the axial, the paraxial, the intermediate and the lateral plate mesoderm. The lateral mesodermal layer will split into two layers, the somatic (outer) and the splanchnic (inner) mesoderm layer. The space between the two layers will give rise to the coelomic cavity at Hamburger & Hamilton (HH) stage 7 in chick and at embryonic day (E) 7.5 in mice, just before the first somite is formed.[8-10] The somatic mesoderm will

contribute to the formation of the body wall and the extremities while the splanchnic mesoderm will contribute to the formation of the viscera, including the heart.

Cardiogenesis: heart forming fields and additional cellular contributions

The myocardial progenitors can be identified in the chick at HH5-6[11] and at E7.5 in the mice[12] organized in bilateral structures of the anterior splanchnic mesoderm or cardiac mesoderm, which has the potential to form myocardial cells. These cardiogenic plates will eventually fuse at the midline of the embryo to form the cardiac crescent (Figure 1.1a) in the antero-lateral mesoderm which already expresses specific cardiac transcription factors like Nkx2.5, Tbx5 and GATA4.[10,13,14] The myocardial potential of this population is also highly influenced by signals emitted by the underlying endoderm.[14] Additionally we now know that specific regions of the cardiac crescent will give rise to specific cardiac segments. Supporting evidence shows regional gene expression patterns in the cardiac crescent, like for example in the mouse fibroblast growth factor 8 (*Fgf8*) and 10 (*Fgf10*) which are important for outflow tract formation[13] or *Tbx18* which is involved in sinus venosus formation.[15] Eventually the cardiac crescent will remodel and give rise to the primary heart tube that rapidly starts to pump blood.[10] This heart tube is formed by a myocardial layer on the outside, an endocardial layer covering the inside and cardiac jelly in between (Figure 1.1b). In the chicken, the heart tube is formed as a linear structure at HH10, and then it starts to loop from HH11 onwards,[16] first transforming into a C-shaped and then into a S-shaped structure. In the mouse the linear heart tube starts looping immediately (5-7 somite stage) and becomes a looped heart by E8.5 (9 somite stage).[8] The embryonic heart is formed by two different myocardial progenitor populations that will contribute to specific segments of the heart.[17] Initially, this primary heart tube will consist mainly of a left ventricle, an atrioventricular canal and a part of the atria. The myocardial progenitor population that will contribute to this primary heart has been named the first heart field. Additionally, cells from a second progenitor pool of myocardial precursors are necessary for the proper development of the heart tube into a matured four-chambered heart. This pool of cells is located in the splanchnic mesoderm dorsal to the primary heart tube and has been named the second heart field (SHF) (Figure 1.1b). Both heart field populations can already be distinguished in the early stages of the cardiac crescent (first heart field), the SHF lying medial to the first heart field (Figure 1.1a).[10,14,17] The myocardial cells from the SHF will be added at the arterial and venous poles of the heart. Several molecular markers are expressed throughout the second heart field and have an important role in the development of both the arterial and venous pole, like for example the LIM homeodomain transcription factor *Islet-1* (*Isl-1*). Mice lacking this transcription factor do not develop an outflow tract, right ventricle and part of the atria, showing the role of this gene in

the SHF.[17] Like *Isl-1*, other genes expressed in the second heart field are also required for proper development of the heart, like the inhibitor of differentiation *Id2*[18,19] or the platelet-derived growth factor receptor α (*Pdgfr-α*).[20] In this thesis we have investigated the expression patterns of members of the PDGF family as well as PDGFR-α in relation to second heart field development in the chicken **(Chapter 4)** as well as the role of Id2 during mouse heart development **(Chapter 5)**.

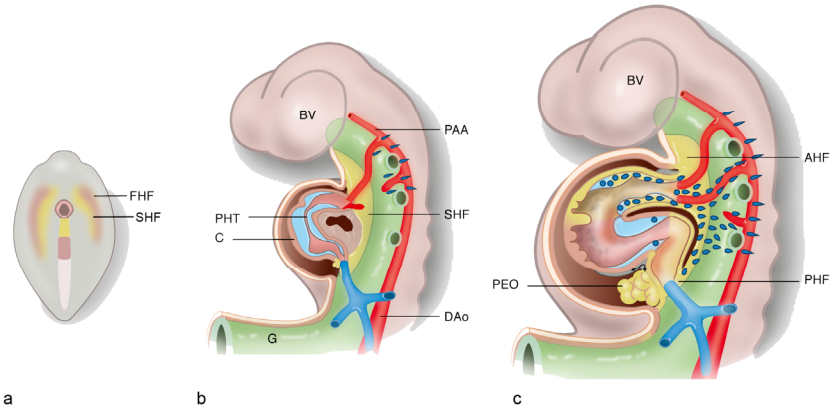

Figure 1.1 **Development of the heart from the first (FHF) and second (SHF) heart fields.**
a. Initially, early in development, the bilateral fields of cardiac mesoderm are present in the primitive plate. Cells depicted in yellow will contribute to the SHF-derived parts of the heart, whereas cells depicted in brown depict the FHF that will contribute the primary myocardial heart tube (PHT). **b**. Schematic representation of the PHT (brown) after fusion of the bilateral plates of mesoderm. The tube is lined on the inside by cardiac jelly (blue). The mesoderm of the SHF is depicted by the yellow area behind the PHT. This region will contribute myocardium to both the arterial and venous poles of the heart (depicted by the yellow myocardium in c) during development. **c**. As time progresses, segments of the heart will develop by contribution of myocardium from the FHF and SHF (brown or yellow respectively). The SHF can be divided into the anterior heart field (AHF) and posterior heart field (PHF). The yellow lobulated structure that protrudes into the pericardial cavity at the venous pole of the heart is the proepicardial organ (PEO). Cardiac neural crest cells (depicted by blue dots) migrate from the neural crest along the arterial and venous pole into the heart. BV: brain ventricles, C: coelomic cavity, DAo: dorsal aorta, G: gut, PAA: pharyngeal arch arteries. Modified after Gittenberger-de Groot et al.[96]

Anterior second heart field and arterial pole development

The cellular addition at the arterial pole will contribute to the formation of the outflow tract (i.e. where the pulmonary trunk and the aorta will develop)[21-23] and the right ventricle.[24] This progenitor population was called the anterior or secondary heart field (AHF) (Figure 1.1c) and this mesoderm already expresses the myocardial transcription factors *Nkx2.5*, *Gata4* and *Mef2c.*[23] The term secondary heart field was

attributed by Waldo and colleagues to the cellular population that would contribute to the distal part of the outflow tract which is impaired in the absence of cardiac neural crest cells that normally colonize this region.[23] Additionally they proposed that a balance between fibroblast growth factor (FGF) signals, driving cell proliferation, and bone morphogenetic protein (BMP) signals, promoting cell differentiation, was required to regulate the growth of the arterial pole. The AHF contributes to the myocardium of the proximal outflow tract and requires *Fgf10* expression.[21,22] Both populations can be integrated into one considering two phases of addition of cells to the arterial pole: an initial contribution which gives rise to the right ventricle and the proximal outflow tract myocardium before the neural crest population is involved, and a second neural crest-dependent contribution which gives rise to the myocardium of the distal outflow tract.[21] Understanding the development of the arterial pole within heart development has led to a better comprehension of specific congenital heart defects like those found in cases of DiGeorge syndrome. Genes like *Tbx1*[25], *Fgf8* and *Fgf10*[21] have been associated with outflow tract abnormalities, that include lack of outflow tract septation and abnormal alignment with the ventricles and can result in a double outlet right ventricle (DORV).[26] In this thesis we will show that mice lacking *Id2* show outflow tract malformations **(Chapter 5)**.

Posterior second heart field and venous pole development

Complementary to the arterial contribution, the venous pole progenitor population has been referred to by our lab as the posterior heart field (PHF) (Figure 1.1c).[27] The PHF can be subdivided into a mesenchymal component that will contribute to the development of the dorsal mesenchymal protrusion (DMP) important for atrial septation and to the proepicardial organ (PEO) with its derivatives, the epicardium and epicardium-derived cells (EPDCs). The other component of the PHF is myocardial and will contribute to the development of the sinus venosus myocardium, which comprises the myocardium that surrounds the cardinal (embryonic) or caval (adult) veins where the sinoatrial node (SAN) will develop and the pulmonary veins. Until recently, the PEO and its derivatives were described as an extracardiac contribution. However, based on recent studies by our own group and others, it is becoming clear that this population is in close relation to the developing heart and should not be seen separately.[28-31]

Just like its counterpart the AHF, a subset of genes and transcription factors have been found to be necessary for proper PHF-derived cardiac development. Some of these genes include the transcription factors *Tbx18,*[32] the transmembrane glycoprotein podoplanin[27] and one of its downstream effectors the small GTPase RhoA. The absence of either *Tbx18* or *podoplanin* during cardiac development results in abnormalities in both mesenchymal and myocardial components of the PHF[30,32] **(Chapter 2)**.

Dorsal mesenchymal protrusion

The dorsal mesenchymal protrusion (DMP) rises from the dorsal mesocardium of the heart. In the past, this mesenchyme has been described as the spina vestibuli or vestibular spine[33] and is continuous with the mesenchymal cap on the primary atrial septum. The mesenchymal cap initially forms as a small cushion-like tissue in the Anlage of the primary atrial septum. During normal atrioventricular (AV) septation the DMP and the mesenchymal cap fuse with the superior and inferior AV cushions forming the AV mesenchymal complex closing the primary atrial foramen. The DMP has been described as a mesenchymal second heart field derivative as it expresses *Isl-1*. Eventually it undergoes mesenchymal to myocardial differentiation to form the myocardial base of the primary atrial septum. Disruption of the development of the DMP can result in atrioventricular septal defects (AVSD).[33-36]

Proepicardial organ and derivatives

The proepicardial organ (PEO) is an accumulation of villous protrusions of the pericardial mesothelium that forms in close proximity to the liver and the sinus venosus myocardium at the venous pole of the heart.[29,37-39] In both the mammalian and avian systems the PEO starts off as bilateral structures. In chicken, the left PEO Anlage does not persist while the right PEO Anlage will develop into a cauliflower-like structure.[40] During cardiac looping, cells from the PEO cross the coelomic cavity floating freely in cell aggregates (mammals and fish)[37,41] or using tissue bridges of extracellular matrix (avian)[38] and attach to the naked heart tube at the AV sulcus. From there they spread over the heart to cover it with an epicardial layer.[39] The derivatives of the epicardium, the EPDCs, are a subset of cells that detach from the epicardium, undergo EMT and colonize the subepicardium, the subendocardial space in an early stage, the myocardium and the AV endocardial cushions.[42] After EMT, EPDCs will contribute to the interstitial fibroblast population of the heart and to the smooth cell and fibroblast population of the coronary vasculature. Additionally, EPDCs have a regulatory role in AV valve differentiation and appear to be important for the formation of compact myocardium.[42-44] Cardiac looping and development of the Purkinje fiber system are also EPDC-dependent,[45] stating the importance of EPDCs during cardiogenesis. Multiple signaling cascades are involved in epicardial-myocardial signaling for proper migration of the EPDCs and normal inductive function. One of these signaling cascades involves the PDGF family and its receptors. Previous results in our lab have demonstrated a role for PDGF-signaling in relation to coronary vasculature development.[46,47] In this thesis we have investigated the role of PDGF signaling in epicardial-myocardial interaction in stages previous to coronary vasculature development **(Chapter 4)**.

Sinus venosus myocardium and CCS

The sinus venosus myocardium of the heart comprises the myocardium that surrounds the cardinal veins including the SAN and the pulmonary veins. Recently, we described in the mouse the expression of podoplanin, a 43kDa mucin-type transmembrane glycoprotein, in the active epithelium lining the coelomic cavity, in second heart field-derived structures at the venous pole of the heart and in the CCS (Figure 1.2).[27] Based on the expression pattern observed we propose that cells from the PHF are being incorporated via a process of EMT from the coelomic epithelium.[27] Interestingly, podoplanin expression is found initially at the left side of the embryo, followed by expression in a U-shaped myocardial population surrounding the sinus venosus including the left and right cardinal veins and the SAN. The sinus venosus myocardium is further characterized by expression of the cation channel protein HCN4,[48,49] Shox2[50] and lack of expression of Nkx2.5,[27,32] partially overlapping with expression of the transcription factors *Tbx18*[32] and *Tbx3*.[6] The sinus venosus myocardium has also been described to form a left-sided nodule of cells, referred to as a 'transient left' sinoatrial nodal area (transient left SAN),[27] that is continuous with the myocardial sleeve developing around the pulmonary veins. Interestingly, podoplanin expression was also found in other components of the CCS in addition to the SAN, providing a possible link between PHF-derived myocardium and other parts of the CCS. In this thesis we have investigated the role of *podoplanin* in PHF-derived CCS development by studying *podoplanin* knockout mice and a proposed downstream effector, the small GTPase RhoA **(Chapter 2)**. RhoA is a member of a family of small GTPases which act as molecular switches in a variety of processes such as cell migration, cytoskeletal reorganization, myogenic differentiation[51] and podoplanin-mediated EMT.[52] Adult mice with an over- or underexpression of RhoA present phenotypes with atrial fibrillation and AV-block, indicating a possible role for RhoA in the function of specific ion channels in the CCS.[53,54]

The avian embryonic system is a frequently used model and easy to manipulate. However, studies of the development of the sinus venosus myocardium in the chicken are not available. Given the broad sinus venosus-wide expression patterns in the sinus venosus myocardium including the SAN, we were interested in the functional implications the expression of CCS-related markers could have. Thus, in this thesis we have studied the expression patterns of known markers in the sinus venosus myocardium in the chicken as well as the sequences of atrial activation patterns during development **(Chapter 3)**.

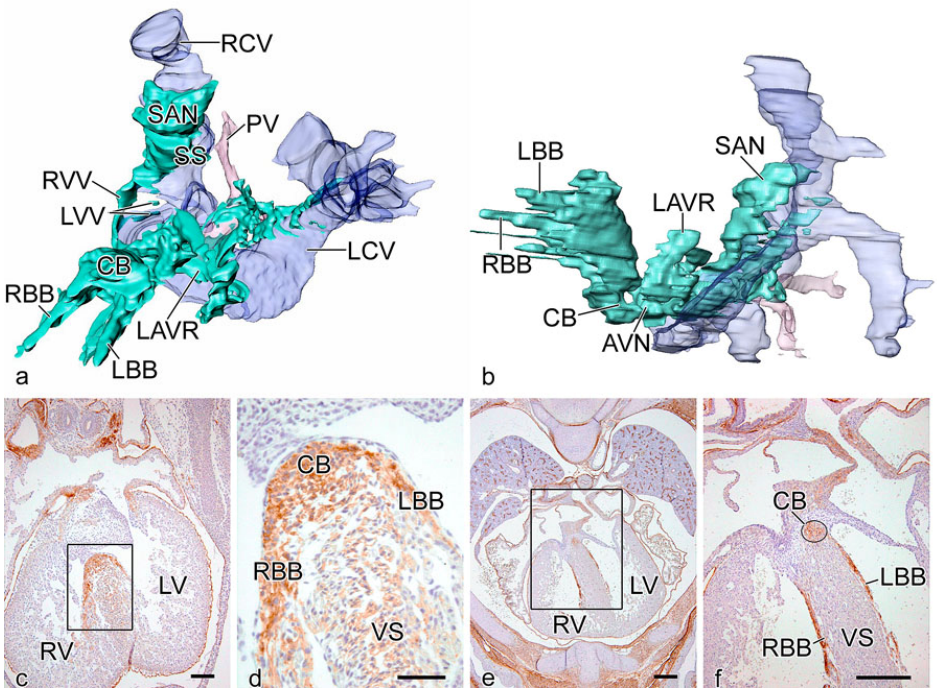

Figure 1.2 **Expression of podoplanin in the embryonic cardiac conduction system.**
a. Left frontal view of a 3D reconstruction of podoplanin expression (turquoise) in relation to the lumen of the cardinal veins (right (RCV) and left (LCV)) and the lumen of the pulmonary vein (PV) of a E13.5 embryo. This view shows expression in the sinoatrial node (SAN) next to the RCV and the right (RVV) and left (LVV) venous valves eventually merging in the region of the atrioventricular node (AVN). **b**. Left lateral view of the same reconstruction as a. The expression is also found in the left atrioventricular ring (LAVR), the common bundle (CB) and the right (RBB) and left (LBB) bundle branches. **c-f**: Sections of the thorax and heart of wildtype mouse embryos of E13.5 (c with magnified box in d) and E15.5 (e with magnified box in f) stained for podoplanin which is visible in the CB, RBB and LBB on top of the ventricular septum (VS). LV: left ventricle; RV: right ventricle, SS: septum spurium. Scale bars for c-f: 100µm. Modified after Gittenberger-de Groot et al.[27]

Extracardiac contribution: Cardiac neural crest cells

The cardiac specific population of neural crest cells that migrates from the rhombencephalon is the so-called cardiac neural crest cell (CNC) population[55,56] and can be regarded as a true extracardiac population. CNCs contribute to the development of the embryonic heart through the arterial and venous pole (blue dots in Figure 1.1c).[57] The role of CNCs at the arterial pole has been studied extensively. CNCs in this region play a role in remodeling of the pharyngeal arch arteries,[58] contribute to the arterial smooth muscle population,[59] the neurons and ganglia of

cardiac innervation,[60] and are involved in septation and myocardialisation of the outflow tract.[61,62] At the venous pole, the CNCs play an inductive role as the great majority undergo apoptosis within the heart.[56,57,63] These CNCs have been located in close proximity to distal components of the CCS and neural crest ablation in the chick has resulted in impaired progress towards a mature apex-to-base activation pattern and a lack of proper electrical isolation of the common bundle.[64]

CCS development: origin, formation and maturation

In the adult heart, the CCS is responsible for initiating and propagating the cardiac electrical impulse. This impulse originates in the SAN, located at the entrance of the right caval vein into the right atrium. It is then conducted via Bachmann's bundle to the left atrium and through the atrial muscle to the atrioventricular node (AVN) located at the right side of the base of the atrial septum in the triangle of Koch,[65] where it is delayed. The impulse is then propagated through the common bundle, situated on the top of the ventricular septum, and the left and right bundle branches located at each side of the ventricular septum, to the Purkinje fiber network. The electrical impulse will then be conducted rapidly to the working ventricular myocardium allowing the ventricles to contract in an apex to base manner (Figure 1.3).

Origin of the CCS cells

The origin of the CCS has been a matter of debate for many years. The question was prompted because both muscle and neuron-specific genes were co-expressed in cells of the CCS, like α and β Myosin Heavy Chain isoforms[66] or the neural crest-associated markers HNK-1[67] and EAP-300.[68] Initially, given the specific function of this tissue within the heart and the similarities in function and morphology with neuronal tissue, a neurogenic origin was suggested. However, an elegant series of retroviral lineage tracing studies have shown that both central and peripheral CCS cells originate from a myocardial progenitor pool present in the looped heart.[69,70]

Models of CCS development

Molecular genetic studies in the mouse have demonstrated that a complex network of transcription factors is required for the formation of the CCS.[71]
Specific transitional zones can be identified after looping of the heart has started, which are interposed between the developing cardiac chambers that consist of working myocardium (Figure 1.4a-c). These zones have a different expression profile compared to the working myocardium and have been identified based on the patterns of several immunohistochemical and molecular markers, e.g. the transcriptional

repressor *Tbx3,*[6] HNK-1,[72] MinK,[73] engrailed-2-LacZ/CCS-LacZ,[5] and podoplanin.[27] The transitional zones include the sinus venosus myocardium (i.e. the myocardium developing at the inflow portion of the heart covering the cardinal veins) where the SAN will develop. Also the atrioventricular canal where the AVN will form, the primary fold, which is the myocardium between the primitive right ventricle and left ventricle where the common bundle and the bundle branches will develop, and finally regions of the outflow tract.[5,6] These zones are of particular relevance in some of the models explaining CCS development. However, the molecular pathways guiding the cells towards either a working or pacemaking myocardium still remain unclear.[70,74]

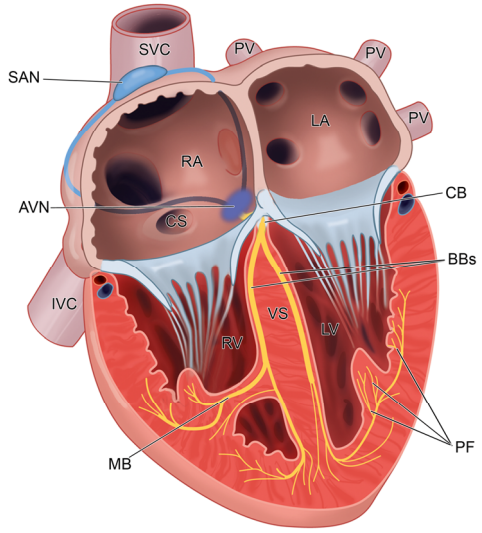

Figure 1.3 **Components of the mature cardiac conduction system.**
Schematic respresentation of the components of the adult cardiac conductions system. The electrical impulse is generated in the sinoatrial node (SAN) which is located at the entrance of the superior caval vein (SCV) into the right atrium (RA). The impulse is then conducted through the atrial muscle to the atrioventricular node (AVN) located at the right side of the base of the atrial septum in the triangle of Koch, where it is delayed. Controversy exists on whether preferential conduction tracts known as internodal tracts are present between the SAN and the AVN. These tracts have been identified in the embryo and run in the RA between the SAN and the AVN. Specifically they run along the terminal crest, which is formed by the remnant of the right venous valve in the posterior atrial wall and the interatrial septum (blue lines between SAN and AVN). After reaching the AVN, the impulse is then propagated through the common bundle (CB), situated on the top of the ventricular septum, and the left and right bundle branches (BBs) located at each side of the ventricular septum, to the Purkinje fiber network (PF) resulting in the contraction of the ventricular myocardium. CS: coronary sinus, IVC: inferior vena cava, LV: left ventricle, MB: moderator band, PV: pulmonary vein, RV: right ventricle.

The first model to be postulated was the so-called ring theory. This theory stated that cells from the CCS are derived from specialized tissue distributed in 4 rings that can be

distinguished from the working myocardium.[75] These rings overlap with the previously described transitional zones, and should be regarded as such (Figure 1.4c). Only small remnants of the embryonic transitional zones will be found in the mature components of the adult CCS (Figure 1.4d-e). The second model to be postulated was the recruitment model. Here, the CCS is formed on the one hand by an initial or primary framework of conduction cells present in the tubular heart. Secondarily, inductive recruitment of multipotent cardiogenic precursor cells occurs for further development of the CCS.[69,70] The third model proposed was the specification model which states that the precursors of the CCS are specified early in development, proliferate slowly, and develop further into the components of the CCS.[74] The cells expressing markers of the CCS early in development can either continue in this path of differentiation or loose their CCS markers and differentiate further into working myocardium. However, according to this model, examples of working myocardial cells differentiating into a CCS cell are rare to none.[76] In this thesis we have studied the development of the CCS in the chicken embryo on a electrophysiological as well as a morphological level based on the developmental expression pattern of some of the mentioned CCS markers like the cation channel HCN4 **(Chapters 2, 6 and 7)**. Our results provide additional information on the development of the CCS.

Development of the Pacemaker of the heart (SAN)

The first morphological signs of the SAN are present at Carnegie stage 15 in the human embryo, ~HH18 in chicken and ~E11.5 in mouse[77] in the anteromedial wall of the right common cardinal vein, which will ultimately give rise to the superior caval vein. Recent studies have shown that this primordium is recognizable even earlier in development and will continue to grow by proliferation and differentiation of its mesodermal progenitors.[27,78] This developing area of the sinus venosus myocardium includes the primordium of the SAN at the right side and a cluster of cells at the left side ('transient left SAN') where the left cardinal vein will enter the atrium.[27] This entire area shares the expression pattern of multiple genes and transcription factors specifically involved in pacemaking, like *Shox2,*[50] *Tbx3,*[6] *Tbx5*[79] and *Hcn4.*[80] Functionally, in the early avian embryo (HH10) the first spontaneous action potentials are generated at the left posterior inflow-site of the heart (putative sinus venosus region).[81] In the adult, the dominant pacemaker activity is located in the SAN at the entrance of the right caval vein in the right atrium. Initially, the primary heart tube presents a nodal-like functional phenotype in that it shows automaticity, slow conduction of the electrical signal and a peristaltic-like contraction pattern.[74,82] In the adult, the cells of the SAN will show the most rapid intrinsic rate of excitation and therefore determine the activation rate of the heart. In this thesis we have looked at the development of the sinus venosus myocardium including the SAN **(Chapters 2, 3, 5-7)** as well as the pacemaker potential of this myocardium **(Chapters 3 and 7)**.

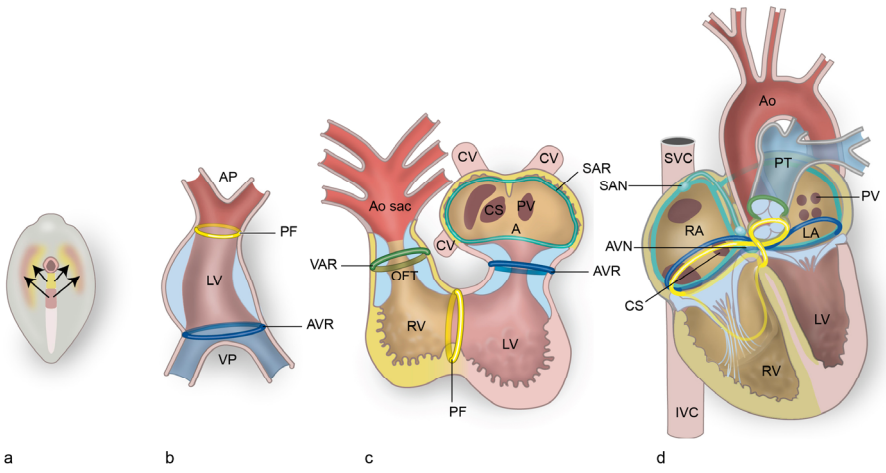

Figure 1.4 **Transitional zones and development of the cardiac conductions system.**
a. In the primitive plate, bilateral fields of cardiac mesoderm are present. Progenitor cells migrate from the primitive streak to the bilateral mesoderm (arrows). Cells depicted in yellow will contribute to the second heart field-derived parts of the heart, whereas cells depicted in brown depict the first heart field that will contribute the primary myocardial heart tube. **b**. Schematic representation of the primary heart tube, consisting of endocardium and myocardium, with myocardial jelly interposed between the two layers (light blue). Initially the primitive heart tube consists mainly of the atrioventricular (AV) canal and the left ventricle (LV). **c**. After looping, several transitional zones can be distinguished in the tube, being the sinoatrial transition (turquoise, SAR) in between the sinus venosus and common atrium, the AV transition (dark blue, AVR) in between the common atrium and common ventricle, the primary fold (yellow, PF) in between the primitive right ventricle (RV) and LV, and a ventriculo-arterial transition (green, VAR) at the outflow tract (OFT) of the heart. Second heart field-derived parts of the heart are depicted in yellow. **d**. Part of the transitional zones will contribute to definitive elements of the cardiac conduction system. A: common atrium, AP: arterial pole, Ao: aorta, Ao sac: aortic sac, AVN: atrioventricular node, CV: cardinal vein, CS: coronary sinus, ICV: inferior caval vein, LA: left atrium, LBB: left bundle branch, PT: pulmonary trunk, PV: pulmonary vein, RA: right atrium, SCV: superior caval vein, VP: venous pole.

Development of the AVN

The developing AVN becomes gradually identifiable from Carnegie stage 16/17 in the human embryo,[83] ~HH29[84] in the chick and ~E13.5 in the mouse[85] which is considerably later than the SAN. Interestingly, an AV-delay is already detected much earlier in development and has been initially attributed to the myocardium of the atrioventricular canal, a myocardial band between the developing atria and ventricles with a slow conducting phenotype.[82,84,86-90] Later in development the AVN, consisting of a compact node bordered by transitional cells, will develop and become responsible for the AV-delay.[84,89] Whether the avian system has an AVN is still a

matter of debate. Some studies have stated that the atrioventricular ring (AVR) myocardium functions as the AVN in the chicken, at least until late stages of development.[86] Several theories have been postulated on the origin of the AVN from the AVR myocardium,[75,91] the lower and dorsal part of the interatrial segment,[84] the dorsal atrial wall[92] or as a counterpart of the left sinus horn.[93,94] The hypothesis of multiple cellular contributions to the AVN is also based on electrophysiological data.[95] The morphological and electrophysiological development of the AVN in the avian system has been extensively studied in **Chapter 7** of this thesis. Additional lineage tracing experiments were also carried out to elucidate a possible cellular contribution from the PHF to the AVN.

Aim and Chapter Outline of the Thesis

In this thesis we have studied the cellular contribution of SHF-derived cells to the developing heart, focusing on the morphological and functional development of the sinus venosus myocardium and components of the central CCS, specifically the SAN and the AVN. We have studied the incorporation of cells from the PHF to the venous pole of the heart in mouse, chicken and quail using several immunohistochemical and molecular markers like *podoplanin*, *RhoA*, *PDGF*-family, *Id2* and *Hcn4*. We have also studied the changes in the embryonic electrogram in relation to potential arrhythmogenic substrates that could be explained by events during development.

In **Chapter 2** we show the role of *podoplanin* in mouse PHF development, specifically focusing on the myocardial population. We provide evidence that cells of the coelomic epithelium contribute to the PHF through a process of EMT.

In **Chapter 3** we describe RhoA and Isl-1 expression during chick embryonic heart development in relation to the sinus venosus myocardium. We also provide an overview of the possible atrial activation patterns present during development.

Chapter 4 provides an overview of PDGF-A, -C and their receptor PDGFR-α during embryonic chicken heart development in relation to SHF-derived structures.

Chapter 5 describes the expression of *Id2* during mouse embryonic heart development and studies the effects of *Id2* mutation on SHF-derived structures, focusing on the venous pole.

In **Chapter 6** we describe for the first time in chicken the expression of the cation channel *Hcn4* in relation to the developing CCS. We also provide the full-length sequence of *Hcn4*.

Chapter 7 provides an overview of morphological and electrophysiological development of the SAN and AVN in the avian system, as well as a possible sinoatrial cellular contribution to the AVN as shown by lineage tracing experiments.

Finally, **Chapter 8** provides a general discussion on the role of PHF in heart development in relation to the formation of the sinus venosus myocardium, the SAN and the AVN. The data obtained from this thesis is related to arrhythmogenesis and is thoroughly discussed and placed in perspective with the most recent findings in the field.

References

1. Kalman JM, Olgin JE, Karch MR, Hamdan M, Lee RJ, Lesh MD. "Cristal tachycardias": origin of right atrial tachycardias from the crista terminalis identified by intracardiac echocardiography. *J Am Coll Cardiol*. 1998;31:451-459.
2. Tsai CF, Tai CT, Hsieh MH, Lin WS, Yu WC, Ueng KC, Ding YA, Chang MS, Chen SA. Initiation of atrial fibrillation by ectopic beats originating from the superior vena cava: electrophysiological characteristics and results of radiofrequency ablation. *Circulation*. 2000;102:67-74.
3. Katritsis D, Ioannidis JP, Giazitzoglou E, Korovesis S, Anagnostopoulos CE, Camm AJ. Conduction delay within the coronary sinus in humans: implications for atrial arrhythmias. *J Cardiovasc Electrophysiol*. 2002;13:859-862.
4. Haissaguerre M, Jais P, Shah DC, Takahashi A, Hocini M, Quiniou G, Garrigue S, Le MA, Le MP, Clementy J. Spontaneous initiation of atrial fibrillation by ectopic beats originating in the pulmonary veins. *N Engl J Med*. 1998;339:659-666.
5. Jongbloed MRM, Schalij MJ, Poelmann RE, Blom NA, Fekkes ML, Wang Z, Fishman GI, Gittenberger-de Groot AC. Embryonic conduction tissue: a spatial correlation with adult arrhythmogenic areas? Transgenic CCS/lacZ expression in the cardiac conduction system of murine embryos. *J Cardiovasc Electrophysiol*. 2004;15:349-355.
6. Hoogaars WM, Tessari A, Moorman AF, de Boer PA, Hagoort J, Soufan AT, Campione M, Christoffels VM. The transcriptional repressor Tbx3 delineates the developing central conduction system of the heart. *Cardiovasc Res*. 2004;62:489-499.
7. William J.Larsen. Human Embryology. 3 ed. Churchill Livingstone, 2001.
8. DeRuiter MC, Poelmann RE, VanderPlas-de Vries I, Mentink MMT, Gittenberger-de Groot AC. The development of the myocardium and endocardium in mouse embryos. Fusion of two heart tubes? *Anat Embryol*. 1992;185:461-473.
9. Moreno-Rodriguez RA, Krug EL, Reyes L, Villavicencio L, Mjaatvedt CH, Markwald RR. Bidirectional fusion of the heart-forming fields in the developing chick embryo. *Dev Dyn*. 2006;235:191-202.
10. Abu-Issa R, Kirby ML. Heart field: from mesoderm to heart tube. *Annu Rev Cell Dev Biol*. 2007;23: 45-68.
11. Yang X, Dormann D, Munsterberg AE, Weijer CJ. Cell movement patterns during gastrulation in the chick are controlled by positive and negative chemotaxis mediated by FGF4 and FGF8. *Dev Cell*. 2002;3:425-437.
12. Tam PP, Parameswaran M, Kinder SJ, Weinberger RP. The allocation of epiblast cells to the embryonic heart and other mesodermal lineages: the role of ingression and tissue movement during gastrulation. *Development*. 1997;124:1631-1642.
13. Harvey RP. Patterning the vertebrate heart. *Nat Rev Genet*. 2002;3:544-556.
14. Buckingham M, Meilhac S, Zaffran S. Building the mammalian heart from two sources of myocardial cells. *Nat Rev Genet*. 2005;6:826-835.
15. Mommersteeg MT, Dominguez JN, Wiese C, Norden J, de Gier-de Vries C, Burch JB, Kispert A, Brown NA, Moorman AF, Christoffels VM. The sinus venosus progenitors separate and diversify from the first and second heart fields early in development. *Cardiovasc Res*. 2010;87:92-101.
16. Stalsberg H, DeHaan RL. The precardiac areas and formation of the tubular heart in the chick embryo. *Dev Biol*. 1969;19:128-159.
17. Cai CL, Liang X, Shi Y, Chu PH, Pfaff SL, Chen J, Evans S. Isl1 identifies a cardiac progenitor population that proliferates prior to differentiation and contributes a majority of cells to the heart. *Dev Cell*. 2003; 5:877-889.
18. Martinsen BJ, Frasier AJ, Baker CV, Lohr JL. Cardiac neural crest ablation alters Id2 gene expression in the developing heart. *Dev Biol*. 2004;272:176-190.
19. Moskowitz IP, Kim JB, Moore ML, Wolf CM, Peterson MA, Shendure J, Nobrega MA, Yokota Y, Berul C, Izumo S, Seidman JG, Seidman CE. A molecular pathway including Id2, Tbx5, and Nkx2-5 required for cardiac conduction system development. *Cell*. 2007;129:1365-1376.

20. Prall OW, Menon MK, Solloway MJ, Watanabe Y, Zaffran S, Bajolle F, Biben C, McBride JJ, Robertson BR, Chaulet H, Stennard FA, Wise N, Schaft D, Wolstein O, Furtado MB, Shiratori H, Chien KR, Hamada H, Black BL, Saga Y, Robertson EJ, Buckingham ME, Harvey RP. An Nkx2-5/Bmp2/Smad1 negative feedback loop controls heart progenitor specification and proliferation. *Cell*. 2007;128:947-959.
21. Kelly RG, Brown NA, Buckingham ME. The arterial pole of the mouse heart forms from Fgf10-expressing cells in pharyngeal mesoderm. *Dev Cell*. 2001;1:435-440.
22. Mjaatvedt CH, Nakaoka T, Moreno-Rodriguez R, Norris RA, Kern MJ, Eisenberg CA, Turner D, Markwald RR. The outflow tract of the heart is recruited from a novel heart-forming field. *Dev Biol*. 2001;238: 97-109.
23. Waldo K, Kumiski DH, Wallis KT, Stadt HA, Hutson MR, Platt DH, Kirby ML. Conotruncal myocardium arises from a secondary heart field. *Development*. 2001;128:3179-3188.
24. Zaffran S, Kelly RG, Meilhac SM, Buckingham ME, Brown NA. Right ventricular myocardium derives from the anterior heart field. *Circ Res*. 2004;95:261-268.
25. Xu H, Morishima M, Wylie JN, Schwartz RJ, Bruneau BG, Lindsay EA, Baldini A. Tbx1 has a dual role in the morphogenesis of the cardiac outflow tract. *Development*. 2004;131:3217-3227.
26. Lindsay EA, Vitelli F, Su H, Morishima M, Huynh T, Pramparo T, Jurecic V, Ogunrinu G, Sutherland HF, Scambler PJ, Bradley A, Baldini A. Tbx1 haploinsufficieny in the DiGeorge syndrome region causes aortic arch defects in mice. *Nature*. 2001;410:97-101.
27. Gittenberger-de Groot AC, Mahtab EAF, Hahurij ND, Wisse LJ, DeRuiter MC, Wijffels MCEF, Poelmann RE. Nkx2.5 negative myocardium of the posterior heart field and its correlation with podoplanin expression in cells from the developing cardiac pacemaking and conduction system. *Anat Rec*. 2007; 290:115-122.
28. Kruithof BP, van Wijk B, Somi S, Kruithof-de Julio M, Perez Pomares JM, Weesie F, Wessels A, Moorman AF, van den Hoff MJ. BMP and FGF regulate the differentiation of multipotential pericardial mesoderm into the myocardial or epicardial lineage. *Dev Biol*. 2006;295:507-522.
29. Lie-Venema H, van den Akker NMS, Bax NAM, Winter EM, Maas S, Kekarainen T, Hoeben RC, DeRuiter MC, Poelmann RE, Gittenberger-de Groot AC. Origin, fate, and function of epicardium-derived cells (EPCDs) in normal and abnormal cardiac development. *ScientificWorldJournal*. 2007;7:1777-1798.
30. Mahtab EAF, Wijffels MCEF, van den Akker NMS, Hahurij ND, Lie-Venema H, Wisse LJ, DeRuiter MC, Uhrin P, Zaujec J, Binder BR, Schalij MJ, Poelmann RE, Gittenberger-de Groot AC. Cardiac malformations and myocardial abnormalities in podoplanin knockout mouse embryos: correlation with abnormal epicardial development. *Dev Dyn*. 2008;237:847-857.
31. van Wijk B, van den Hoff M. Epicardium and myocardium originate from a common cardiogenic precursor pool. *Trends Cardiovasc Med*. 2010;20:1-7.
32. Christoffels VM, Mommersteeg MT, Trowe MO, Prall OW, Gier-de Vries C, Soufan AT, Bussen M, Schuster-Gossler K, Harvey RP, Moorman AF, Kispert A. Formation of the venous pole of the heart from an Nkx2-5-negative precursor population requires Tbx18. *Circ Res*. 2006;98:1555-1563.
33. Blom NA, Ottenkamp J, Wenink AG, Gittenberger-de Groot AC. Deficiency of the vestibular spine in atrioventricular septal defects in human fetuses with down syndrome. *Am J Cardiol*. 2003;91:180-184.
34. Snarr BS, O'Neal JL, Chintalapudi MR, Wirrig EE, Phelps AL, Kubalak SW, Wessels A. Isl1 expression at the venous pole identifies a novel role for the second heart field in cardiac development. *Circ Res*. 2007;101:971-974.
35. Snarr BS, Wirrig EE, Phelps AL, Trusk TC, Wessels A. A spatiotemporal evaluation of the contribution of the dorsal mesenchymal protrusion to cardiac development. *Dev Dyn*. 2007;236:1287-1294.
36. Snarr BS, Kern CB, Wessels A. Origin and fate of cardiac mesenchyme. *Dev Dyn*. 2008;237:2804-2819.
37. Viragh S, Challice CE. The origin of the epicardium and the embryonic myocardial circulation in the mouse. *Anat Rec*. 1981;201:157-168.
38. Manner J. The development of pericardial villi in the chick embryo. *Anat Embryol (Berl)*. 1992;186: 379-385.
39. Vrancken Peeters M-PFM, Mentink MMT, Poelmann RE, Gittenberger-de Groot AC. Cytokeratins as a marker for epicardial formation in the quail embryo. *Anat Embryol*. 1995;191:503-508.
40. Schulte I, Schlueter J, Bu-Issa R, Brand T, Männer J. Morphological and molecular left-right asymmetries in the development of the proepicardium: a comparative analysis on mouse and chick embryos. *Dev Dyn*. 2007;236:684-695.

41. Munoz-Chapuli R, Macias D, Ramos C, Fernandez B, Sans-Coma V. Development of the epicardium in the dogfish *(Scyliorhinus canicula)*. *Acta Zool*. 1997;78:39-46.
42. Gittenberger-de Groot AC, Vrancken Peeters M-PFM, Mentink MMT, Gourdie RG, Poelmann RE. Epicardium-derived cells contribute a novel population to the myocardial wall and the atrioventricular cushions. *Circ Res*. 1998;82:1043-1052.
43. Gittenberger-de Groot AC, Vrancken Peeters MP, Bergwerff M, Mentink MM, Poelmann RE. Epicardial outgrowth inhibition leads to compensatory mesothelial outflow tract collar and abnormal cardiac septation and coronary formation. *Circ Res*. 2000;87:969-971.
44. Lie-Venema H, Gittenberger-de Groot AC, van Empel LJP, Boot MJ, Kerkdijk H, de Kant E, DeRuiter MC. Ets-1 and Ets-2 transcription factors are essential for normal coronary and myocardial development in chicken embryos. *Circ Res*. 2003;92:749-756.
45. Eralp I, Lie-Venema H, Bax NAM, Wijffels MC, Van der Laarse A, DeRuiter MC, Bogers AJ, van den Akker NM, Gourdie RG, Schalij MJ, Poelmann RE, Gittenberger-de Groot AC. Epicardium-derived cells are important for correct development of the Purkinje fibers in the avian heart. *Anat Rec*. 2006; 288A:1272-1280.
46. van den Akker NMS, Lie-Venema H, Maas S, Eralp I, DeRuiter MC, Poelmann RE, Groot ACG. Platelet-derived growth factors in the developing avian heart and maturating coronary vasculature. *Developmental Dynamics*. 2005;233:1579-1588.
47. van den Akker NMS, Caolo V, Wisse LJ, Peters PPWM, Poelmann RE, Carmeliet P, Molin DGM, Gittenberger-de Groot AC. Developmental coronary maturation is disturbed by aberrant cardiac VEGF-expression and Notch-signaling. *Cardiovasc Res*. 2008; 78:366-375.
48. Garcia-Frigola C, Shi Y, Evans SM. Expression of the hyperpolarization-activated cyclic nucleotide-gated cation channel HCN4 during mouse heart development. *Gene Expr Patterns*. 2003;3:777-783.
49. Mahtab EA, Vicente-Steijn R, Hahurij ND, Jongbloed MR, Wisse LJ, DeRuiter MC, Uhrin P, Zaujec J, Binder BR, Schalij MJ, Poelmann RE, Gittenberger-de Groot AC. Podoplanin deficient mice show a Rhoa-related hypoplasia of the sinus venosus myocardium including the sinoatrial node. *Dev Dyn*. 2009;238:183-193.
50. Blaschke RJ, Hahurij ND, Kuijper S, Just S, Wisse LJ, Deissler K, Maxelon T, Anastassiadis K, Spitzer J, Hardt SE, Schöler H, Feitsma H, Rottbauer W, Blum M, Meijlink F, Rappold GA, Gittenberger-de Groot AC. Targeted mutation reveals essential functions of the homeodomain transcription factor Shox2 in sinoatrial and pacemaking development. *Circulation*. 2007;115:1830-1838.
51. Wei L, Roberts W, Wang L, Yamada M, Zhang S, Zhao Z, Rivkees SA, Schwartz RJ, Imanaka-Yoshida K. Rho kinases play an obligatory role in vertebrate embryonic organogenesis. *Development*. 2001; 128:2953-2962.
52. Martin-Villar E, Megias D, Castel S, Yurrita MM, Vilaro S, Quintanilla M. Podoplanin binds ERM proteins to activate RhoA and promote epithelial-mesenchymal transition. *J Cell Sci*. 2006;119:4541-4553.
53. Sah VP, Minamisawa S, Tam SP, Wu TH, Dorn GW, Ross J, Jr., Chien KR, Brown JH. Cardiac-specific overexpression of RhoA results in sinus and atrioventricular nodal dysfunction and contractile failure. *J Clin Invest*. 1999;103:1627-1634.
54. Wei L, Taffet GE, Khoury DS, Bo J, Li Y, Yatani A, Delaughter MC, Klevitsky R, Hewett TE, Robbins J, Michael LH, Schneider MD, Entman ML, Schwartz RJ. Disruption of Rho signaling results in progressive atrioventricular conduction defects while ventricular function remains preserved. *FASEB J*. 2004; 18:857-859.
55. Kirby ML, Waldo KL. Role of neural crest in congenital heart disease. *Circulation*. 1990;82:332-340.
56. Boot MJ, Gittenberger-de Groot AC, van Iperen L, Poelmann RE. The myth of ventrally emigrating neural tube (VENT) cells and their contribution to the developing cardiovascular system. *Anat Embryol*. 2003;206:327-333.
57. Poelmann RE, Gittenberger-de Groot AC. A subpopulation of apoptosis-prone cardiac neural crest cells targets to the venous pole: multiple functions in heart development? *Dev Biol*. 1999;207:271-286.
58. Kirby ML, Turnage KL, Hays BM. Characterization of conotruncal malformations following ablation of "cardiac" neural crest. *Anat Rec*. 1985;213:87-93.

59. Bergwerff M, Verberne ME, DeRuiter MC, Poelmann RE, Gittenberger-de Groot AC. Neural crest cell contribution to the developing circulatory system. Implications for vascular morphology? *Circ Res*. 1998;82:221-231.
60. Verberne ME, Gittenberger-de Groot AC, Poelmann RE. Lineage and development of the parasympathetic nervous system of the embryonic chicken heart. *Anat Embryol*. 1998;198:171-184.
61. Waldo K, Miyagawa-Tomita S, Kumiski D, Kirby ML. Cardiac neural crest cells provide new insight into septation of the cardiac outflow tract: Aortic sac to ventricular septal closure. *Dev Biol*. 1998;196: 129-144.
62. Poelmann RE, Mikawa T, Gittenberger-de Groot AC. Neural crest cells in outflow tract septation of the embryonic chicken heart: differentiation and apoptosis. *Dev Dyn*. 1998;212:373-384.
63. Poelmann RE, Molin DGM, Wisse LJ, Gittenberger-de Groot AC. Apoptosis in cardiac development. *Cell Tissue Res*. 2000;301:43-52.
64. Gurjarpadhye A, Hewett KW, Justus C, Wen X, Stadt H, Kirby ML, Sedmera D, Gourdie RG. Cardiac neural crest ablation inhibits compaction and electrical function of conduction system bundles. *Am J Physiol Heart Circ Physiol*. 2007;292:H1291-H1300.
65. Koch W. Ueber die Blutversorgung der Sinusknotens und etwaige Beziehungen des Letzteren zum Atrioventrikularknoten. *Munch Med Wochenschr*. 1909;56:2362-2364.
66. de Jong F, Geerts WJC, Lamers WH, Los JA, Moorman AFM. Isomyosin expression pattern during formation of the tubular chicken heart: a three-dimensional immunohistochemical analysis. *Anat Rec*. 1990;226:213-227.
67. Chuck ET, Watanabe M. Differential expression of PSA-NCAM and HNK-1 epitopes in the developing cardiac conduction system of the chick. *Dev Dyn*. 1997;209:182-195.
68. McCabe CF, Gourdie RG, Thompson RP, Cole GJ. Developmentally regulated neural protein EAP-300 is expressed by myocardium and cardiac neural crest during chick embryogenesis. *Dev Dyn*. 1995;203: 51-60.
69. Gourdie RG, Mima T, Thompson RP, Mikawa T. Terminal diversification of the myocyte lineage generates purkinje fibers of the cardiac conduction system. *Development*. 1995;121:1423-1431.
70. Cheng G, Litchenberg WH, Cole GJ, Mikawa T, Thompson RP, Gourdie RG. Development of the cardiac conduction system involves recruitment within a multipotent cardiomyogenic lineage. *Development*. 1999;126:5041-5049.
71. Srivastava D, Olson EN. A genetic blueprint for cardiac development. *Nature*. 2000;407:221-226.
72. Blom NA, Gittenberger-de Groot AC, DeRuiter MC, Poelmann RE, Mentink MM, Ottenkamp J. Development of the cardiac conduction tissue in human embryos using HNK-1 antigen expression: possible relevance for understanding of abnormal atrial automaticity. *Circulation*. 1999;99:800-806.
73. Kondo RP, Anderson RH, Kupershmidt S, Roden DM, Evans SM. Development of the cardiac conduction system as delineated by minK-lacZ. *J Cardiovasc Electrophysiol*. 2003;14:383-391.
74. Moorman AFM, Christoffels VM. Cardiac chamber formation: Development, genes and evolution. *Physiol Rev*. 2003;83:1223-1267.
75. Wenink ACG. Development of the human cardiac conducting system. *J Anat*. 1976;121/3:617-631.
76. Christoffels VM, Moorman AF. Development of the cardiac conduction system: why are some regions of the heart more arrhythmogenic than others? *Circ Arrhythm Electrophysiol*. 2009;2:195-207.
77. Moorman AF, de Jong F, Denyn MM, Lamers WH. Development of the cardiac conduction system. *Circ Res*. 1998;82:629-644.
78. Mommersteeg MT, Hoogaars WM, Prall OW, Gier-de Vries C, Wiese C, Clout DE, Papaioannou VE, Brown NA, Harvey RP, Moorman AF, Christoffels VM. Molecular pathway for the localized formation of the sinoatrial node. *Circ Res*. 2007;100:354-362.
79. Puskaric S, Schmitteckert S, Mori AD, Glaser A, Schneider KU, Bruneau BG, Blaschke RJ, Steinbeisser H, Rappold G. Shox2 mediates Tbx5 activity by regulating Bmp4 in the pacemaker region of the developing heart. *Hum Mol Genet*. 2010;19:4625-4633.
80. Stieber J, Herrmann S, Feil S, Loster J, Feil R, Biel M, Hofmann F, Ludwig A. The hyperpolarization-activated channel HCN4 is required for the generation of pacemaker action potentials in the embryonic heart. *Proc Natl Acad Sci U S A*. 2003;100:15235-15240.
81. Kamino K, Hirota A, Fujii S. Localization of pacemaking activity in early embryonic heart monitored using voltage-sensitive dye. *Nature*. 1981;290:595-597.

82. de Jong F, Opthof T, Wilde AA, Janse MJ, Charles R, Lamers WH, Moorman AF. Persisting zones of slow impulse conduction in developing chicken hearts. *Circ Res*. 1992;71:240-250.
83. De Haan RL. Differentiation of the atrioventricular conducting system of the heart. *Circulation*. 1961; 24:458-470.
84. Arguello C, Alanis J, Valenzuela B. The early development of the atrioventricular node and bundle of His in the embryonic chick heart. An electrophysiological and morphological study. *Development*. 1988;102:623-637.
85. Viragh S, Challice CE. The development of the conduction system in the mouse embryo heart. *Dev Biol*. 1980;80:28-45.
86. Lieberman M, Paes de CA. The Electrophysiological Organization of the Embryonic Chick Heart. *J Gen Physiol*. 1965;49:351-363.
87. Lieberman M, Paes de CA. The Spread of Excitation in the Embryonic Chick Heart. *J Gen Physiol*. 1965; 49:365-379.
88. Paff GH, Boucek RJ, Harrell TC. Observations on the development of the electrocardiogram. *Anat Rec*. 1968;160:575-582.
89. Arguello C, Alanis J, Pantoja O, Valenzuela B. Electrophysiological and ultrastructural study of the atrioventricular canal during the development of the chick embryo. *J Mol Cell Cardiol*. 1986;18: 499-510.
90. Chuck ET, Meyers K, France D, Creazzo TL, Morley GE. Transitions in ventricular activation revealed by two-dimensional optical mapping. *Anat Rec A Discov Mol Cell Evol Biol*. 2004;280:990-1000.
91. Benninghoff A. Uber die Beziehungen des Reizleitungssystems und der Papillarmuskeln zu den Konturfasern des Herzschlandes. *Anat Anz*. 1923;57:186-208.
92. Marino TA, Truex RC, Marino DR. The development of the atrioventricular node and bundle in the ferret heart. *Am J Anat*. 1979;154:135-150.
93. Patten BM. The development of the sinoventricular conduction system. 1956;22:1-21.
94. James TN. Structure and function of the sinus node, AV node and His bundle of the human heart: part I - structure. *Progress in Cardiovascular Diseases*. 2002;45:235-267.
95. Scheinman MM, Yang Y. The history of AV nodal reentry. *Pacing Clin Electrophysiol*. 2005;28: 1232-1237.
96. Gittenberger-de Groot AC, Jongbloed MRM, Poelmann RE. Normal and abnormal cardiac development. In: Moller JH, Hoffmann JIE, eds. *Pediatric Cardiovascular Medicine*. 2011; *in press.*

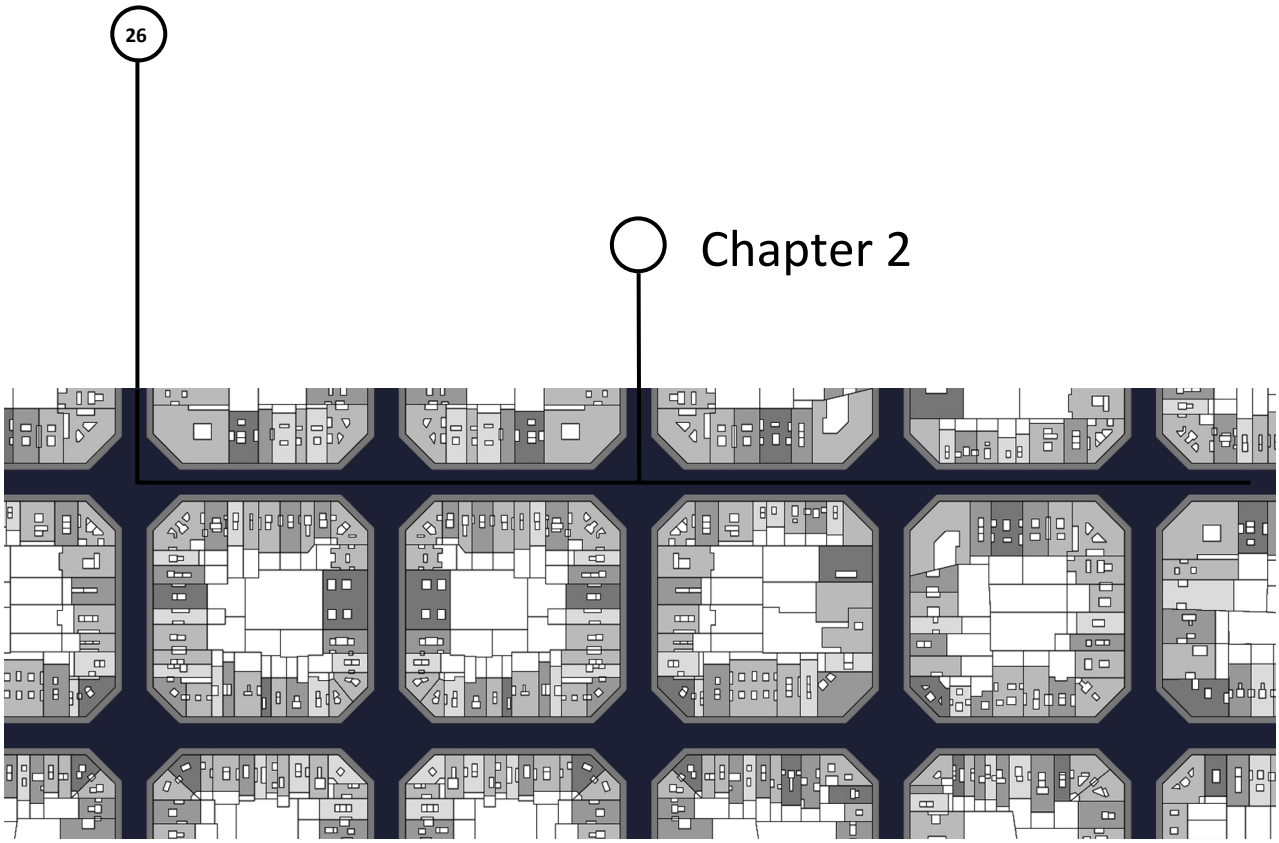
26
Chapter 2

Podoplanin deficient mice show a RhoA related hypoplasia of the sinus venosus myocardium including the sinoatrial node

Edris AF Mahtab, Rebecca Vicente-Steijn, Nathan D Hahurij, Monique RM Jongbloed, Lambertus J Wisse, Marco C DeRuiter, Pavel Uhrin, Jan Zaujec, Bernd R Binder, Martin J Schalij, Robert E Poelmann, Adriana C Gittenberger-de Groot

Modified after Developmental Dynamics 2009;238:183-193

Abstract

We investigated the role of *podoplanin* in development of the sinus venosus myocardium comprising the sinoatrial node, the dorsal atrial wall and the primary atrial septum as well as the myocardium of the cardinal and pulmonary veins. We analyzed *podoplanin* wildtype and knockout mouse embryos between embryonic day (E) 9.5-15.5 using immunohistochemical marker podoplanin, sinoatrial node marker HCN4, myocardial markers MLC-2a, Nkx2.5 as well as Cx43, coelomic marker WT-1 and epithelial-to-mesenchymal transformation markers E-cadherin and RhoA. 3D-reconstructions were made and myocardial morphometry was performed. *Podoplanin* mutants showed hypoplasia of the sinoatrial node, the primary atrial septum and dorsal atrial wall. Myocardium lining the wall of the cardinal and pulmonary veins was thin and perforated. Impaired myocardial formation is correlated with abnormal epithelial-to-mesenchymal transformation of the coelomic epithelium due to upregulated E-cadherin and downregulated RhoA, which are controlled by *podoplanin*. Our results demonstrate an important role for *podoplanin* in the development of sinus venosus myocardium.

Introduction

During early embryogenesis the lateral plate mesoderm splits into two layers: the somatic and the splanchnic mesoderm forming the outer and the inner layer of the coelomic cavity.[1,2] The somatic mesoderm is involved in the development of the body wall and extremities while myocardial precursors are restricted to the splanchnic mesoderm.[3,4] Subsequently, the left and right primary heart fields (cardiogenic plates) fuse at the ventral midline resulting in the primary linear heart tube which starts looping at E8.5.[1,2,5]

Previous studies of heart development[5-7] have shown that further development of the heart tube is related to the addition of cells at both the arterial and venous pole of the heart, forming the outflow and the inflow tract myocardium, respectively. These observations on the addition of the secondary myocardium have been supported by several studies describing the addition of myocardium at the arterial pole, by the secondary[8] or anterior heart field.[9-12] The posterior heart field (PHF) was described at the venous pole[12-15] of the developing heart. The complete length of the splanchnic mesoderm contributing to the addition of myocardium at both poles of the heart was called second heart field[14] or second lineage.[10,12,14]

A number of genes and proteins, considered as early markers of the second heart field at the outflow and inflow tract have been reported, such as *MesP1,*[16] *Fibroblast growth factor* (*Fgf*) *8* and *10,*[9] *Bmp-2* and Nkx2.5,[8,13,15] *Isl-1*,[14] inhibitor of differentiation *Id2*,[17] GATA factors targeting *Mef2c*,[18,19] *Tbx1*, *Tbx3* and *Tbx18*[15,20] and *Shox2.*[21] Recently we have added *podoplanin* to this list as a novel gene in cardiac development.

As a coelomic and myocardial marker, podoplanin is specifically expressed in the mesenchyme and in the myocardium at the venous pole.[13,22,23] Studying the mesenchymal population, podoplanin expression was observed in the proepicardial organ and epicardium.[13,22,24] In the cardiomyocyte population podoplanin staining was seen in major parts of the developing atrioventricular cardiac conduction system, in sinus venosus myocardium including the sinoatrial node, the venous valves, the dorsal mesocardium, the dorsal atrial wall and the primary atrial septum. Also the myocardium surrounding the cardinal veins and the common pulmonary vein belongs to this population.[13,22,23] In earlier publications, podoplanin, a 43-kd mucin type transmembrane glycoprotein, first named E11 antigen as a new marker for an osteoblastic cell line,[25] was also reported in the nervous system, the epithelia of lung, eye, oesophagus and intestine,[26] the mesothelium of the visceral peritoneum,[25] the coelomic wall (pericardium) lining the pericardial cavity,[13] the epicardium,[22] the podocytes of the kidney[27] and the lymphatic endothelium.[28]

To elucidate a possible functional role of *podoplanin* in cardiac development and more specifically in the development of the sinus venosus myocardium, we studied *podoplanin* knockout mouse embryos and used several immunohistochemical markers. To investigate the sinus venosus myocardium including the sinoatrial node

we have used hyperpolarization-activated, cyclic nucleotide-gated cation 4 (HCN4).[29-31] In addition, atrial myosin light chain 2 (MLC-2a), NK2 transcription factor related locus 5 (Nkx2.5) and connexin 43 (Cx43) were used. Furthermore, we studied E-cadherin, a cell to cell adhesion protein, and RhoA important for epithelial-to-mesenchymal transformation (EMT) of the coelomic epithelium, a process that allows epithelial cells to become mobile mesenchymal cells.[32] To visualize the epithelium and mesothelium of the coelomic cavity, the epicardium and sites of active EMT we have used Wilm's tumor suppressor protein (WT-1).[33-35] It has been described that the PHF and resulting myocardium are derived from the epithelial lining of the coelomic cavity (splanchnic mesothelium) by EMT.[13] During normal development, loss of E-cadherin is needed for proper EMT resulting in loss of epithelial features[36] and consecutive development into migratory mesenchymal cells. During abnormal development, an upregulated state of E-cadherin, by e.g. lack of *podoplanin*, presents an altered EMT.[37] Podoplanin can, therefore, be considered as an inhibitor of E-cadherin stimulating EMT. In addition, RhoA activation by podoplanin and ezrin interaction have been described to lead to podoplanin-induced EMT.[38] Similar to E-cadherin, lack of *podoplanin* might lead to downregulated RhoA and altered EMT.
In the current paper we studied the role of *podoplanin* in the development of the sinus venosus myocardium derived from the PHF. We demonstrate that knocking out the *podoplanin* gene leads to myocardial abnormalities in sinus venosus myocardium at the venous pole of the developing mouse heart.

Materials and Methods

Generation of *podoplanin*$^{-/-}$ mice and harvesting of embryos

The *podoplanin* wild type as well as knockout mouse embryos were kindly provided by Prof. dr. B.R. Binder. The knockout mice were generated by homologous recombination in embryonic stem cells from the 129S/v mouse line by inserting a neomycin phosphotransferase cassette in a 7.7kb genomic fragment encompassing exons II to V. The complete description of this model was reported previously.[22] Briefly, the heterozygous ES cell clones were test-bred for germline transmission with Swiss mice to generate *podoplanin*$^{+/-}$ offspring (50% 129S/v: 50% Swiss genetic background) using standard procedures. These mice were crossed to obtain *podoplanin*$^{-/-}$ embryos and *podoplanin*$^{+/+}$ (wildtype) littermates. The morning of the vaginal plug was stated embryonic day (E) 0.5. Pregnant females were sacrificed and embryos were harvested.

General description

We investigated the lining of the coelomic cavity and the morphology of the sinus venosus myocardium of the heart in 27 wildtype mouse embryos of E9.5 (n=4), E10.5

(n=4), E11.5 (n=3), E12.5 (n=4), E13.5 (n=5), E14.5 (n=4) and E15.5 (n=3) and compared these with 37 *podoplanin* knockout mouse embryos of E9.5 (n=4), E10.5 (n=4), E11.5 (n=6), E12.5 (n=8), E13.5 (n=6), E14.5 (n=5) and E15.5 (n=4). All embryos were fixed in 4% paraformaldehyde (PFA) and routinely processed for paraffin immunohistochemical investigation.

Immunohistochemistry

Immunohistochemistry was performed with antibodies against MLC-2a (1/6000, kindly provided by S.W. Kubalak, Charleston, SC, USA), Nkx2.5 (1/4000, Santa Cruz Biotechnology, Inc., CA, USA, SC-8697), podoplanin (clone 8.1.1., 1/500, Hybridomabank, Iowa, USA), WT-1 (1/1000, Santa Cruz Biotechnology, Inc., CA, USA, sc-192), E-cadherin (1/150, Santa Cruz Biotechnology, Inc., CA, USA, SC-7870), HCN4 (1/1000, Alomone labs, The Netherlands, APC-052), RhoA (1/2000, Santa Cruz Biotechnology, Inc., CA, USA, SC-418) and Cx43 (1/200, Sigma-Aldrich Chemie, USA, C6219). The primary antibodies were dissolved in phosphate buffered saline (PBS)-Tween-20 with 1% Bovine Serum Albumin (BSA, Sigma Aldrich, USA). Between subsequent incubation steps all slides were rinsed in PBS (2x) and PBS-Tween-20 (1x). The slides were incubated with the secondary antibody for 45 min: for MLC-2a, WT-1, E-cadherin, HCN4 and Cx43 with 1/200 goat-anti-rabbit-biotin (Vector Laboratories**,** USA, BA-1000) and 1/66 goat serum (Vector Laboratories, USA, S1000) in PBS-Tween-20; for Nkx2.5 with 1/200 horse-anti-goat-biotin (Vector Laboratories, USA, BA-9500) and 1/66 horse serum (Brunschwig Chemie, Switserland, S-2000) in PBS-Tween-20; for podoplanin with 1/200 goat-anti-Syrian hamster-biotin (Jackson Imunno research, USA, 107-065-142) and 1/66 goat serum in PBS-Tween-20 and for RhoA with 1/200 horse-anti-mouse-biotin (Santa Cruz Biotechnology, Inc., CA, USA, SC-9996-FITC) and 1/66 horse serum in PBS-Tween-20. The slides were incubated with ABC-reagent (Vector Laboratories,USA**,** PK 6100) for 45 min. For visualization the slides were incubated with 400 µg/ml 3-3'di-aminobenzidin tetrahydrochloride (DAB, Sigma-Aldrich Chemie, USA, D5637) dissolved in Tris-maleate buffer pH 7.6 to which 20 µl H_2O_2 was added: MLC-2a, and E-cadherin 5 min; Nkx2.5, HCN4, Cx43, WT-1 and podoplanin 10 min. Counterstaining was performed with 0.1% haematoxylin (Merck, Darmstadt, Germany) for 5 sec, followed by rinsing with tap water for 10 min. All slides were dehydrated and mounted with Entellan (Merck, Darmstadt, Germany).

3-D reconstruction

We made 3-D reconstructions of the sinus venousus myocardium based on MLC-2a, Nkx2.5 and HCN4 stained sections of wildtype as well as podoplanin knockout embryos of E12.5 in which the morphological differences were shown. The reconstructions were made as previously described[39] using the AMIRA software package (Template Graphics Software, San Diego, USA).

Morphometry of the myocardium

Based on HCN4, MLC-2a and Nkx2.5 stained sections, sinus venosus and separately sinoatrial node myocardial volume estimation was performed in 12 wildtype mouse hearts of E11.5 (n=3), E12.5 (n=3), E13.5 (n=3) E14.5 (n=3) and 12 *podoplanin* knockout mouse hearts of E11.5 (n=3), E12.5 (n=3), E13.5 (n=3) E14.5 (n=3) based on Cavalieri's principle as described previously.[40] Statistical analysis was performed with an independent sample-*t*-test ($P<0.05$) using the SPSS 11.0 software program (SPSS Inc, Chicago, III). In summary, regularly spaced points (100 mm^2 grid for sinus venosus myocardium and 49 mm^2 grid for sinoatrial node myocardium) were randomly positioned on the HCN4 stained myocardium. The distance between the subsequent sections of the slides was 0.075 mm for sinus venosus myocardium and 0.025 mm for sinoatrial node. The volume measurement was done using the HB2 Olympus microscope with a 100x 'final magnification' objective for sinus venosus myocardium and 200x 'final magnification' for sinoatrial node.

Results

General description

We studied the embryonic phenotype of the *podoplanin* knockout mice, which show an increased embryonic death of approximately 40% of the homozygote embryos between E10-E16. Additionally, 50% of the neonatal homozygote knockout mice die within the first weeks of life, while heterozygous mutants reach sexual maturity. The cause of embryonic death has been correlated to the cardiac defects[22] while the cause of neonatal death is still unknown.

Several marked morphological cardiac abnormalities were observed in the knockout mouse embryos. In the younger stages a hypoplastic proepicardial organ (E10.5) as well as ventricular myocardium were observed with discontinuous epicardium, a thin layer of subepicardial mesenchyme and a diminished amount of epicardium-derived cells (EPDCs).[22] These hearts also presented outflow tract abnormalities such as severe dextroposition of the aorta, coronary artery abnormalities, spongious myocardium of the developing interventricular septum and impaired formation and fusion of the atrioventricular cushions. At the sinus venosus region, which is the area of our focus, myocardial hypoplasia and morphological abnormalities were observed.

Below, morphology and immunohistochemical expression patterns of the sinus venosus myocardium will be described in the knockout embryos and compared to wildtype embryos in subsequent stages of heart development.

Podoplanin expression in the heart

In wildtype mice the first expression of podoplanin can be recognized as early as E9.5 in the coelomic mesothelium and in the proepicardial organ.[13,22] Moreover, podoplanin was observed in the myocardium of the medial wall of the left cardinal vein shortly before entering the sinus venosus. At E10.5 podoplanin staining in this region was more extensive and extended into the dorsal mesocardium. At the right side the staining was evaluated for the first time at the level of the future sinoatrial node, in the medial wall of the right cardinal vein. The venous valves showed also podoplanin positivity. At E12.5 podoplanin was clearly observed in the pericardium, epicardium, sinoatrial node, venous valves, dorsal mesocardium, myocardium of the pulmonary vein, atrial septum and ventricular conduction system. Remarkably, podoplanin staining was also observed at the left side bordering the medial contour of the left cardinal vein. The pattern and intensity of this region was similar to the sinoatrial node region at the right side, although the left-sided region was smaller at this stage.[13]

Sites of epithelial-to-mesenchymal transformation

To demarcate the coelomic mesothelium and sites of active EMT, we used WT-1, E-cadherin and RhoA staining. WT-1 was observed in both the coelomic mesothelium and proepicardial organ at E9.5 in the wildtype. In the mutants, compared to the wildtype embryos, these regions were smaller and E-cadherin was upregulated. At E10.5 in wildtype embryos WT-1 positivity was found in the single layer of mesothelium of the coelomic cavity and epicardium (Figure 2.1a and 2.1b). Marked staining was seen at the corners of the coelomic cavity at both sides adjacent to the cardinal veins, where the expression of WT-1 was more extensive and the cells of the coelomic mesothelium appeared to be cuboidal and well organized (Figure 2.1b). In *podoplanin* knockout embryos WT-1 was also present in these regions (Figure 2.1e and 2.1f), however, the coelomic mesothelium was disorganized, the cells were irregular in shape and size and seemed to have maintained their epithelial confinement (Figure 2.1, compare a and b with e and f). The defective spreading of the epicardium at several locations was shown after WT-1 staining that followed this pattern and did not normally cover the myocardium in the knockout mouse embryos (Figure 2.1a and 2.1e). Increased E-cadherin staining has been observed clearly in both the epicardium and mesothelium lining the coelomic wall in the *podoplanin* knockout embryos (Figure 2.1g) compared to the wildtype mouse embryos (Figure 2.1c). Remarkably, in the mutants E-cadherin staining was not only upregulated in the epithelium of the coelomic cavity but also in the underlying mesenchymal cells (Figure 2.1c and 2.1g), supporting the observation of disturbed EMT. At E10.5 in wildtype embryos major RhoA expression was seen in the mesenchyme and epithelium of the coelomic cavity and epicardium (Figure 2.1d). In the mutants overall expression of RhoA was downregulated (Figure 2.1h).

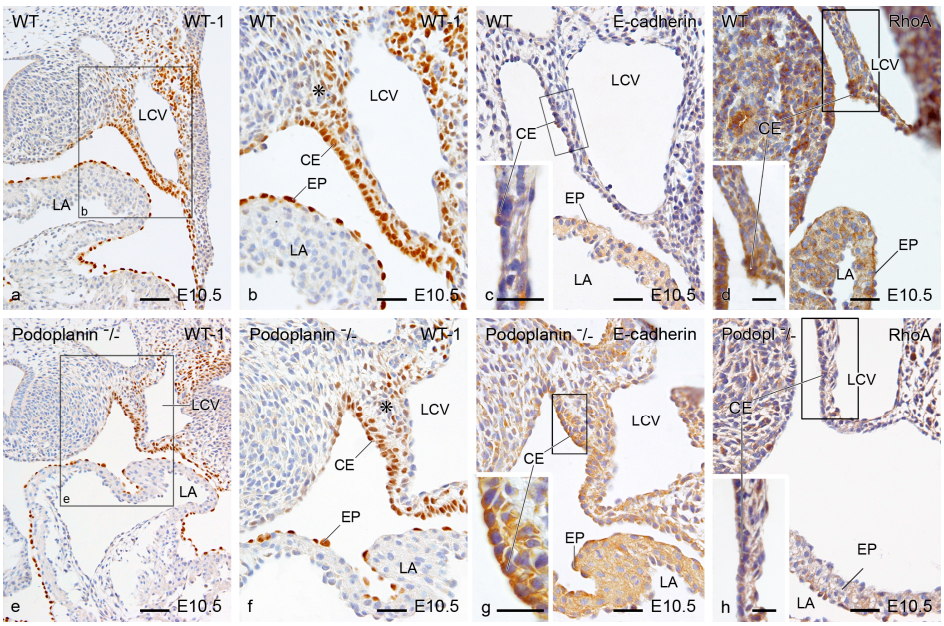

Figure 2.1 **Transverse sections showing epithelial-to-mesenchymal transformation (EMT) sites of the coelomic cavity epithelium in the epithelium in E10.5 hearts of wildtype (WT) and *podoplanin* knockout (*podoplanin*$^{-/-}$) mouse embryos**. To demarcate the coelomic mesothelium and sites of active EMT, we studied WT-1 staining (**a,b,e** and **f**) and E-cadherin staining (**c** and **g**). WT-1 positivity was found in the mesothelium (asterisk in **b** and **f**), in the epithelium (CE) of the coelomic cavity and in the epicardium (EP) of the WT embryos (**a** and **b**). WT-1 staining was more extensive at the corners of the coelomic cavity (asterisk) below the left cardinal vein (LCV), where the CE appeared to be cuboidal and well organized (**b**). In *podoplanin*$^{-/-}$ embryos WT-1 was also present in these regions (**e** and **f**), however, the CE was disorganized and the cells were irregular in shape and size (compare **a** and **b** with **e** and **f**). E-cadherin staining appeared stronger in both the EP and CE of the *podoplanin*$^{-/-}$ embryos (**g**) when compared to the WT mouse embryos (**c**). Remarkably, in the *podoplanin*$^{-/-}$ E-cadherin staining was not only upregulated in the CE but also in the underlying mesothelial cells (**c** and **g**). In WT embryos RhoA expression was seen in the coelomic mesenchyme, CE and epicardium (**d**). In the mutants overall expression of RhoA was downregulated (**h**). LA: left atrium. Scale bars: a,e = 60µm; b,c,d,f,g,h = 30µm; magnification box in c,d,g and h = 20µm.

The sinus venosus myocardium

The HCN4 positive region of the sinus venosus area (Figure 2.2i, 2.2k and Figure 2.3d, 2.3f, 2.3m, 2.3o) overlaps the Nkx2.5 negative (Figure 2.2g, 2.2j and Figure 2.3h-k) and MLC-2a positive sinus venosus region (Figure 2.2c-f and Figure 2.3c, 2.3e, 2.3l, 2.3n). Podoplanin is also expressed in these regions of the sinus venosus myocardium, almost completely overlapping with the Nkx2.5 negative and HCN4 positive regions.

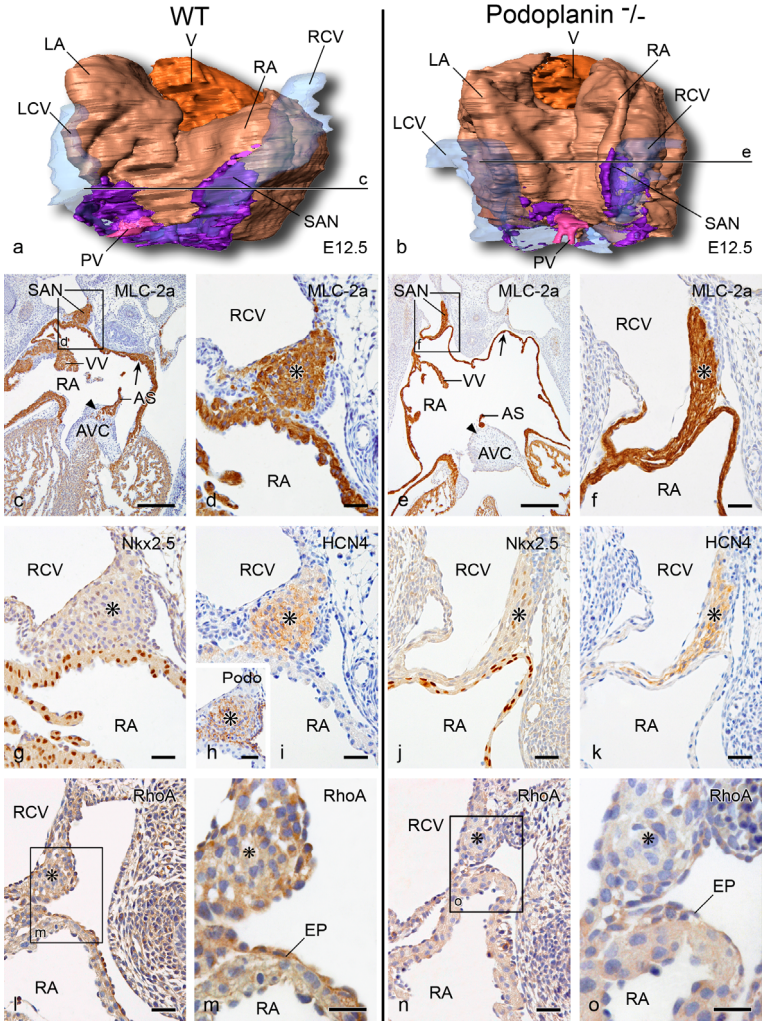

Figure 2.2 **Cranio-dorsal view of 3D reconstructions (a and b) and transverse sections (c-o) showing at E12.5 the hypoplasia of the sinoatrial nodal (SAN) region in *podoplanin* knockout (*podoplanin*$^{-/-}$) mouse embryos compared to the wildtype (WT) embryos.** The intersection line **c** refers to sections **c** and **d** and the intersection line **e** refers to sections **e** and **f**. In the SAN (asterisks) the expression level of MLC-2a (**c-f**), Nkx2.5 (**g** and **j**), and HCN4 (**i** and **k**) was unaltered in the WT (**c,d,g** and **i**) and *podoplanin*$^{-/-}$ embryos (**e,f,j** and **k**). Section **h** shows podoplanin (Podo) expression in the SAN of the WT heart. The SAN in the *podoplanin*$^{-/-}$ is thin and hypoplastic compared to the WT (compare **d** with **f**). In the mutants the venous valves (VV), the dorsal atrial wall (arrows in **c** and **e**) and the primary atrial septum (AS) were also small and hypoplastic (compare **c** with **e**). Because of the deficient AS the mutant hearts showed a large atrial septum defect (compare **c** with **e**) and the AS myocardium was not properly embedded in the atrioventricular cushion (AVC, arrow heads in **c** and **e**). The AVC was not fused properly with the ventricular septum resulting in a ventricular septum defect (compare **c** with **e**). In WT embryos, RhoA expression was seen in the coelomic mesenchyme,

the CE as well as in the SAN and epicardium (EP) (**l**,**m**). In the mutants, RhoA expression was downregulated in the SAN as well as in the CE and EP (**n**,**o**). Color codes: atrial myocardium: light brown, cardinal veins lumen: transparent blue, common pulmonary vein (PV) lumen: pink, sinus venosus myocardium: purple, ventricular myocardium (V): brown. LA: left atrium; LCV: left cardinal vein; RA: right atrium; RCV: right cardinal vein. Scale bars: c,e = 200µm; d,f-l,n = 30µm; m,o = 20µm.

Sinoatrial node and venous valves

In the sinoatrial node the MLC-2a positive (Figure 2.2c-f) and Nkx2.5 negative (Figure 2.2g, 2.2j) region were identical to the HCN4 (Figure 2.2i, 2.2k) and podoplanin (Figure 2.2h) positive areas. In contrast to the remaining sinus venosus myocardial structures, in the sinoatrial node HCN4 remained positive while Nkx2.5 negative staining was maintained. In the knockout mice the sinoatrial node was hypoplastic (Figure 2.2a, 2.2b, 2.2d, 2.2f) and the venous valves were shorter and thinner (Figure 2.2c, 2.2e), however, the expression pattern of MLC-2a, Nkx2.5 HCN4 and Cx43 (not shown) was not changed compared to the wildtype (Figure 2.2c-k). Comparable to E10.5 in wild type embryos, RhoA expression was seen in coelomic mesenchyme and epithelium as well as in sinoatrial node and epicardium (Figure 2.2l-m). In the mutants, RhoA expression was downregulated in the sinoatrial node as well as in the coelomic epithelium and the epicardium (Figure 2.2n-o).

Primary atrial septum and dorsal atrial wall

In both wildtype and *podoplanin* knockout embryos MLC-2a expression was present in the sinus venosus myocardium and the myocardium of the atrial and ventricular wall (Figure 2.2a-f and Figure 2.3a-c, 2.3e, 2.3l, 2.3n). Similar to the sinoatrial node and the venous valves, the expression pattern of the mentioned markers was unchanged in the mutants compared to the wildtype embryos. In the mutants, myocardial hypoplasia was seen of the dorsal atrial wall (Figure 2.2c-f). The atrial septum was thin (Figure 2.3c-f) and deficient (Figure 2.2c, 2.2e) with a large secondary foramen (Figure 2.2c, 2.2e). The myocardialization process at the base of the atrial septum was almost absent (Figure 2.2c, 2.2e). Additionally in the knockout embryos, the atrioventricular cushion was not fused properly to the top of the ventricular septum resulting in a persisting interventricular communication (Figure 2.2c, 2.2e). There is marked dilatation of the atria in the mutant embryos compared to the wildtype (Figure 2.2c, 2.2e).

Pulmonary and cardinal veins

In wildtype embryos the wall of the pulmonary and cardinal veins showed MLC-2a (Figure 2.3c, 2.3l) and HCN4 (Figure 2.3a, 2.3d, 2.3m) expression while the Nkx2.5 expression pattern was mosaic in the myocardium lining the pulmonary vein (Figure 2.3h, 2.3i) and negative in the wall of the cardinal veins (Figure 2.3h). The staining for

HCN4 was diminished at E15.5 compared to earlier stages whereas the initially Nkx2.5 negative myocardium of the cardinal veins and Nkx2.5 mosaic myocardium of the wall of the pulmonary vein became positive.

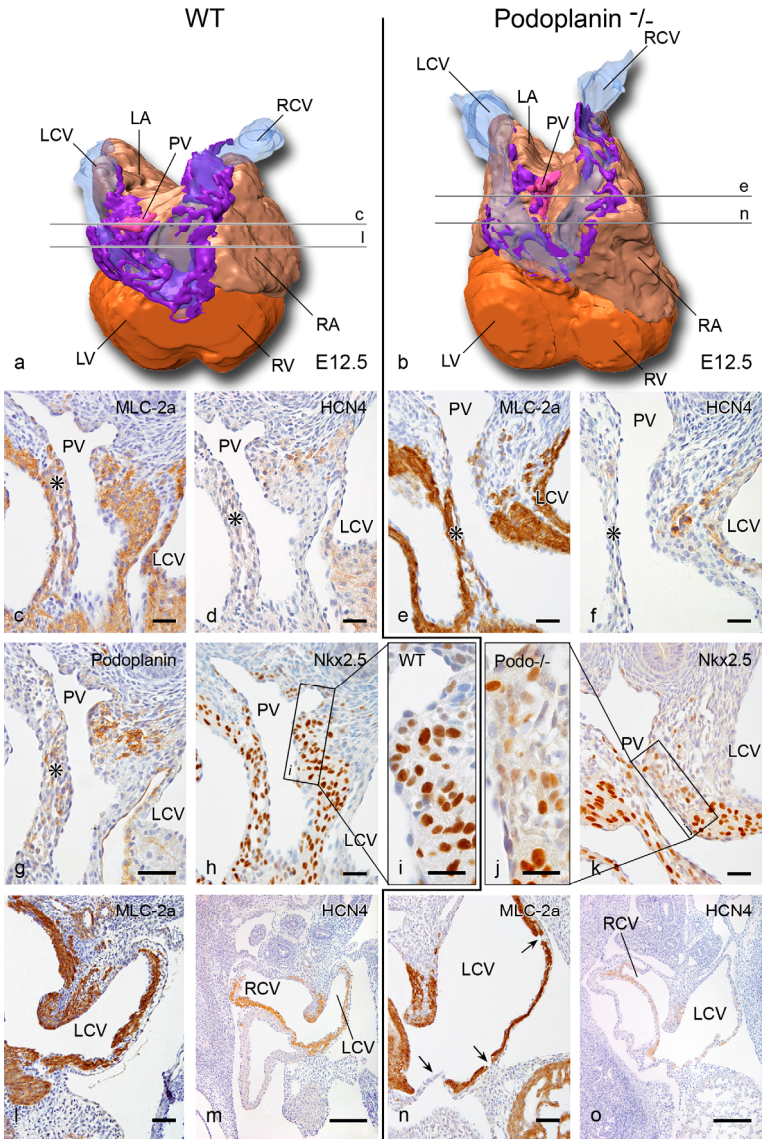

Figure 2.3 **Cranio-dorsal view of 3D reconstructions (a and b) and transverse sections (c-o) showing the myocardial hypoplasia of the common pulmonary vein (PV), atrial septum (asterisk) and the wall of the cardinal veins of E12.5 wildtype (WT) and *podoplanin* knockout (*podoplanin*$^{-/-}$) embryonic mouse hearts.** The intersection lines **c,l,e** and **n** refer to the sections **c,l,e** and **n** respectively. In the MLC-2a sections (**c,e**) the hypoplasia of the myocardium around the PV in the *podoplanin*$^{-/-}$ is clearly visible. Moreover, parts of myocardium around the PV which are

also positive for HCN4 (**d**) and podoplanin (**g**) are missing in the *podoplanin*$^{-/-}$ (compare **c,d** with **e,f**). This lack of myocardium around the PV is also seen in the sections stained with Nkx2.5 (**h-k**) where the Nkx2.5 mosaic myocardium of the PV is missing in the *podoplanin*$^{-/-}$ (**k,j**) compared to the WT (**h,i**). The hypoplasia of the atrial septum (asterisk) is seen in the *podoplanin*$^{-/-}$ (**e**) compared to the WT (**c**). Sections **l** and **n** are stained with MLC-2a and sections **m** and **o** show HCN4 expression of the same region demonstrating the hypoplasia and the perforations (arrows in **n**) of the myocardium of the cardinal veins in the *podoplanin*$^{-/-}$. Color codes: atrial myocardium: light brown, cardinal veins lumen: transparent blue, PV lumen: pink, sinus venosus myocardium: purple, ventricular myocardium: brown. LA: left atrium, LCV: left cardinal vein, LV: left ventricle, RA: right atrium, RCV: right cardinal vein, RV: right ventricle. Scale bars: c,e,l,n = 60µm; d,f,g,h,k = 30µm; i,j = 20µm, m,o = 200µm.

In the knockout embryos, the myocardium of the wall of the pulmonary vein was hypoplastic and almost absent compared to the wildtype (Figure 2.3c, 2.3e). The extent of hypoplasia and lack of myocardium of the pulmonary vein corresponded with the regions normally expressing HCN4 (Figure 2.3d, 2.3f) and podoplanin (Figure 2.3g). Comparable to the MLC-2a stained myocardium around the pulmonary vein as described above, the Nkx2.5 mosaic area was hypoplastic and almost absent in the knockout mice (compare Figure 2.3h-i with 2.3j-k).
The myocardium of the cardinal veins was also hypoplastic and showed several fenestrations (Figure 2.3l-o). Both the atrial lumen and the lumen of the cardinal veins were dilated. The myocardial volume of the sinus venosus (Figure 2.4a) and separately the sinoatrial node (Figure 2.4b), estimated by myocardial morphometry, were ($p<0.05$) decreased in the knockout embryos compared to the wildtype embryos.

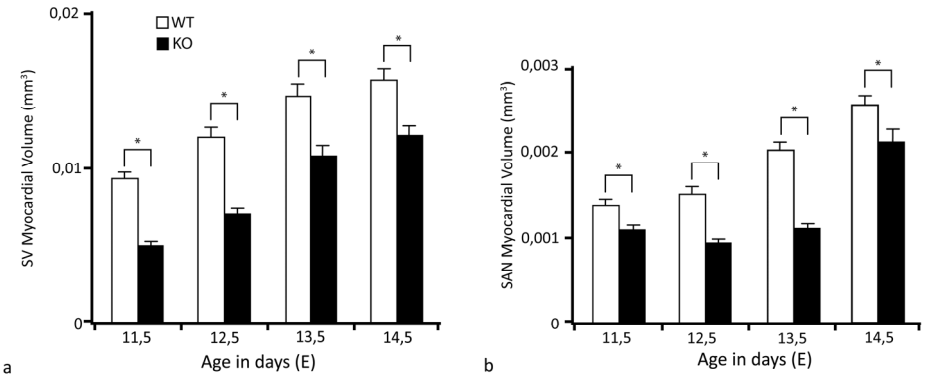

Figure 2.4 Sinus venosus (SV, **a**) and sinoatrial node (SAN, **b**) myocardial volume estimation of 12 wildtype (WT) mouse hearts of E11.5 (n=3), E12.5 (n=3), E13.5 (n=3) and E14.5 (n=3) and 12 podoplanin knockout (KO) mouse hearts E11.5 (n=3), E12.5 (n=3), E13.5 (n=3) and E14.5 (n=3). Podoplanin knockout embryos have a significant smaller SV and SAN myocardial volume (*P<0.05) compared to WT embryos.

Discussion

This study was conducted to elucidate the role of *podoplanin* in the development of the sinus venosus myocardium derived from the specific area of the second heart field which we have named PHF.[13,22] Our observations are based on the study of the *podoplanin* gene and its protein expression in different embryonic stages during cardiac development. We have generated *podoplanin* knockout mouse embryos and used several immunohistochemical markers to study the mutants and wildtypes. These findings have consequences for the development and contribution of the PHF to the sinus venosus myocardium.

Sinoatrial node and venous valves

The sinoatrial node is a complex structure that plays a fundamental role in cardiac pacemaker activity.[29] Despite its essential role in cardiac conduction the origin of the sinoatrial node is still not well understood. Recently the formation and differentiation of the sinoatrial node at the venous pole of the heart has been described from the novel Nkx2.5 negative and Tbx18 positive precursor cells[15] which were positive for podoplanin.[13] In the current study we report HCN4 expression in the podoplanin positive and Nkx2.5 negative sinoatrial node in accordance with observations in other studies.[15,31,41] The specific combination of Nkx2.5 negative and podoplanin and HCN4 positive expression in the sinoatrial node during early heart development is in contrast with the expression of these markers in the primary atrial myocardium. The latter suggests a different precursor for the sinoatrial node and the primary atrial myocardium. In contrast to the primary atrial myocardium, which derives from the primary heart field, the sinus venosus myocardium including the sinoatrial node originates from the second heart field, as concluded from Isl-1, Tbx3 and Tbx18 expression at the venous pole of the heart.[14,15,31,42] To clarify the functional role of *podoplanin* in the development of the sinus venosus myocardium we have studied *podoplanin* mutants and found a hypoplastic sinus venosus myocardium. Another interesting gene involved in the development of the sinus venosus myocardium is *Shox2.*[21] *Shox2* mutants show severe hypoplasia of the sinus venosus myocardium comparable to our observations in the *podoplanin* null mice. Moreover, the hypoplastic sinoatrial node in *Shox2* mutants showed aberrant expression of Cx43 combined with abnormal Nkx2.5 positivity. In contrast to the *Shox2* mutants, Nkx2.5 and Cx43 expression patterns remained unchanged in the *podoplanin* knockout mouse hearts suggesting a different role for *podoplanin* in the sinoatrial node pacemaking development than *Shox2*. Electrophysiological experiments will be carried out to investigate possible arrhythmias in these mutants to solve the mentioned neonatal death.

Primary atrial septum and dorsal atrial wall

Lineage tracing experiments studying *Isl1,*[14] *Fgf 10*[10] and *Tbx5,*[43,44] *Tbx18*[15] and *Shox2*[21] have demonstrated a contribution of the second heart field to the formation of the atrial myocardium which has a distinct molecular composition compared to the heart tube derived from the first heart field.[10,14,45]
Podoplanin is expressed in PHF as well and not only stains the derivatives of the proepicardial organ but also the Nkx2.5 negative myocardium in the dorsal mesocardium.[13] This myocardium is supposed to form part of the dorsal atrial wall as well as the atrial septum. In the *podoplanin* mutant mouse this myocardium is hypoplastic, probably due to diminished PHF-derived myocardial contribution. Another option, is that abnormal epicardial-myocardial interaction plays a role in development of deficient myocardium as is seen in *SP3* mutant mouse.[46] We already described the deficient EPDC contribution in the *podoplanin* mutant.[22,24] Therefore, both the hypoplasia of the atrial septum as well as the dorsal atrial wall observed in the current study, are related to the altered contribution of myocardial and epicardial cells from the PHF.

Pulmonary and cardinal veins

A controversy regarding the development of the venous pole concerns the origin of the pulmonary vein. The pulmonary pit develops either in the dorsal mesocardium at the midline,[47-49] at the left[50] or the right[50-52] side of the embryo as a solitary unpaired structure that arises from the sinus venosus[50-52] or primitive atrium.[45,47,53] Recently, Männer and Merkel[54] have described the pulmonary pit as a bilaterally paired structure. We have described that the early common pulmonary vein is surrounded by Nkx2.5 mosaic cells which are positive for MLC-2a and podoplanin.[13,23] Part of this myocardium has also been reported as 'mediastinal myocardium'.[53] The Nkx2.5 mosaic area forms a myocardial sleeve around the pulmonary vein extending to the atrial septum and Nkx2.5 negative cardinal veins in contrast to the primary atrial myocardium which is completely Nkx2.5 positive. These data support the formation of the wall of the pulmonary vein to be from the surrounding mesodermal precursor cells at the dorsal mesocardium postulated to be derived from the PHF.[13,23] Concomitant with the higher proliferation rate of the pulmonary vein myocardium,[55] the Nkx2.5 mosaic area became Nkx2.5 positive in contrast to the sinoatrial node and cardinal vein myocardium that remained Nkx2.5 negative but HCN4 positive. This suggests a distinct differentiation rate of the pulmonary vein myocardium compared to the sinoatrial node and cardinal vein myocardium. At E15.5 the cardinal vein myocardium became gradually positive for Nkx2.5, whereas the HCN4 expression was diminished suggesting the gradual completion of the differentiation process at the venous pole.
In the mutant embryos, the diminished myocardial contribution to the wall of the pulmonary vein and cardinal veins is evident. It is not clear whether MLC-2a and

Nkx2.5 are directly regulated by *podoplanin* or whether this is due to an altered addition of secondary myocardium from the PHF region by lack of *podoplanin*.

The role of *podoplanin* in EMT of the coelomic epithelium

An important feature of EMT is downregulation of E-cadherin[36,56,57] which is correlated with *podoplanin.*[37] We have observed upregulation of E-cadherin in the coelomic cavity epithelium of the *podoplanin* knockout embryos. Regarding the addition of myocardium from the second heart field, the observed hypoplasia at the sinus venosus region might be caused by upregulated E-cadherin in the *podoplanin* knockout embryos which causes abnormal EMT of the coelomic epithelium at specific sites of the sinus venosus myocardium.[22]

Moreover, *podoplanin* is involved in motility of cells where it colocalizes with the ezrin, radixin and moesin (ERM) protein family.[37,58] ERM proteins bind to the podoplanin ERM–binding site to activate RhoA, a member of the Rho GTPase protein family controlling a wide variety of cellular processes including proliferation, differentiation, cell morphology and motility.[59,60] The increased RhoA activity leads to '*podoplanin*-induced' EMT.[38] With regard to this mechanism, lack of *podoplanin* has resulted in diminished expression of RhoA protein which may prevent the '*podoplanin*-induced' EMT with subsequent myocardial abnormalities of the venous pole.

Taken together, we show severe hypoplasia and myocardial abnormalities of the sinus venosus myocardium by lack of *podoplanin*. In addition we postulate not only a common origin of the sinoatrial node, dorsal atrial wall, atrial septum, pulmonary and cardinal veins deriving from the PHF, but also provide a link between the pulmonary vein and sinus venosus myocardium rather than the pulmonary vein and primary atrial myocardium.

Clinical implications

Parts of the cardiac conduction system derive from the second heart field which may imply a role in the etiology of clinical syndromes. Several transgenic mice present with sick sinus syndrome, occurring in a familial form, are due to the lack of Ca^{2+} and other ion channels as well as gap junctions.[61] The dysfunctions include bradycardia, sinus dysrhythmia and sinus node exit block.[61] In our mutant embryos we have observed a hypoplastic sinoatrial node. Interestingly podoplanin is involved in water transport,[26] cationic, anionic and amino acid transport[62] and Ca^{2+} dependent cell adhesiveness[37]. Therefore it is relevant to perform functional studies in these hearts in the future to show dysfunctions such as bradycardia (sick sinus syndrome) comparable to *Shox2* mutants.[21]

Several studies suggested an embryonic background of atrial fibrillation originating from the pulmonary and caval veins and based on expression patterns of molecular and immunohistochemical markers.[49,63,64] In the current study we observed HCN4

expression in the sinoatrial node and in the myocardium of the wall of the cardinal veins and the pulmonary vein. In the mutant mice this population of HCN4 positive cells is diminished in the sinus venosus myocardium which may provide a developmental background for arrhythmias originating from this area.
Next to disturbances in cardiac conduction the observed deficient myocardial as well as epicardial contribution results in atrial and ventricular septal defects in addition to the already observed myocardial and coronary vascular abnormalities.[22]

References

1. DeRuiter MC, Poelmann RE, VanderPlas-de Vries I, Mentink MMT, Gittenberger-de Groot AC. The development of the myocardium and endocardium in mouse embryos. Fusion of two heart tubes? *Anat Embryol*. 1992;185:461-473.
2. Moreno-Rodriguez RA, Krug EL, Reyes L, Villavicencio L, Mjaatvedt CH, Markwald RR. Bidirectional fusion of the heart-forming fields in the developing chick embryo. *Dev Dyn*. 2006;235:191-202.
3. Linask KK. N-cadherin laclization in early development and polar expression of Na+, K+-ATpase, and integrin during pericardial coelom formation and epitheliazation of the differentiating myocardium. *Dev Biol*. 1992;151:213-224.
4. Linask KK, Knudsen KA, Gui YH. N-cadherin-catenin interaction: necessary component of cardiac cell compartmentalization during early vertebrate heart development. *Dev Biol*. 1997;185:148-164.
5. Stalsberg H, DeHaan RL. The precardiac areas and formation of the tubular heart in the chick embryo. *Dev Biol*. 1969;19:128-159.
6. Viragh S, Challice CE. Origin and differentiation of cardiac muscle cells in the mouse. *J Ultrastruct Res*. 1973;42:1-24.
7. De la Cruz MV, Gomez CS, Arteaga MM, Argüello C. Experimental study of the development of the truncus and the conus in the chick embryo. *J Anat*. 1977;123:661-686.
8. Waldo K, Kumiski DH, Wallis KT, Stadt HA, Hutson MR, Platt DH, Kirby ML. Conotruncal myocardium arises from a secondary heart field. *Development*. 2001;128:3179-3188.
9. Kelly RG, Brown NA, Buckingham ME. The arterial pole of the mouse heart forms from Fgf10-expressing cells in pharyngeal mesoderm. *Dev Cell*. 2001;1:435-440.
10. Kelly RG. Molecular inroads into the anterior heart field. *Trends Cardiovasc Med*. 2005;15:51-56.
11. Mjaatvedt CH, Nakaoka T, Moreno-Rodriguez R, Norris RA, Kern MJ, Eisenberg CA, Turner D, Markwald RR. The outflow tract of the heart is recruited from a novel heart-forming field. *Dev Biol*. 2001;238: 97-109.
12. Meilhac SM, Esner M, Kelly RG, Nicolas JF, Buckingham ME. The clonal origin of myocardial cells in different regions of the embryonic mouse heart. *Dev Cell*. 2004;6:685-698.
13. Gittenberger-de Groot AC, Mahtab EAF, Hahurij ND, Wisse LJ, DeRuiter MC, Wijffels MCEF, Poelmann RE. Nkx2.5 negative myocardium of the posterior heart field and its correlation with podoplanin expression in cells from the developing cardiac pacemaking and conduction system. *Anat Rec*. 2007;290:115-122.
14. Cai CL, Liang X, Shi Y, Chu PH, Pfaff SL, Chen J, Evans S. Isl1 identifies a cardiac progenitor population that proliferates prior to differentiation and contributes a majority of cells to the heart. *Dev Cell*. 2003;5:877-889.
15. Christoffels VM, Mommersteeg MT, Trowe MO, Prall OW, Gier-de Vries C, Soufan AT, Bussen M, Schuster-Gossler K, Harvey RP, Moorman AF, Kispert A. Formation of the venous pole of the heart from an Nkx2-5-negative precursor population requires Tbx18. *Circ Res*. 2006;98:1555-1563.
16. Saga Y, Miyagawa-Tomita S, Takagi A, Kitajima S, Miyazaki J, Inoue T. MesP1 is expressed in the heart precursor cells and required for the formation of a single heart tube. *Development*. 1999;126: 3437-3447.
17. Martinsen BJ, Frasier AJ, Baker CV, Lohr JL. Cardiac neural crest ablation alters Id2 gene expression in the developing heart. *Dev Biol*. 2004;272:176-190.
18. Dodou E, Verzi MP, Anderson JP, Xu SM, Black BL. Mef2c is a direct transcriptional target of ISL1 and GATA factors in the anterior heart field during mouse embryonic development. *Development*. 2004; 131:3931-3942.
19. Verzi MP, McCulley DJ, De Val S, Dodou E, Black BL. The right ventricle, outflow tract, and ventricular septum comprise a restricted expression domain within the secondary/anterior heart field. *Dev Biol*. 2005;287:134-145.
20. Xu H, Morishima M, Wylie JN, Schwartz RJ, Bruneau BG, Lindsay EA, Baldini A. Tbx1 has a dual role in the morphogenesis of the cardiac outflow tract. *Development*. 2004;131:3217-3227.

21. Blaschke RJ, Hahurij ND, Kuijper S, Just S, Wisse LJ, Deissler K, Maxelon T, Anastassiadis K, Spitzer J, Hardt SE, Schöler H, Feitsma H, Rottbauer W, Blum M, Meijlink F, Rappold GA, Gittenberger-de Groot AC. Targeted mutation reveals essential functions of the homeodomain transcription factor Shox2 in sinoatrial and pacemaking development. *Circulation*. 2007;115:1830-1838.
22. Mahtab EAF, Wijffels MCEF, van den Akker NMS, Hahurij ND, Lie-Venema H, Wisse LJ, DeRuiter MC, Uhrin P, Zaujec J, Binder BR, Schalij MJ, Poelmann RE, Gittenberger-de Groot AC. Cardiac malformations and myocardial abnormalities in podoplanin knockout mouse embryos: correlation with abnormal epicardial development. *Dev Dyn*. 2008;237:847-857.
23. Douglas YL, Mahtab EA, Jongbloed MR, Uhrin P, Zaujec J, Binder BR, Schalij MJ, Poelmann RE, DeRuiter MC, Gittenberger-de Groot AC. Pulmonary vein, dorsal atrial wall and atrial septum abnormalities in podoplanin knockout mice with disturbed posterior heart field contribution. *Pediatr Res*. 2009;65: 27-32.
24. Lie-Venema H, van den Akker NMS, Bax NAM, Winter EM, Maas S, Kekarainen T, Hoeben RC, DeRuiter MC, Poelmann RE, Gittenberger-de Groot AC. Origin, fate, and function of epicardium-derived cells (EPCDs) in normal and abnormal cardiac development. *ScientificWorldJournal*. 2007;7:1777-1798.
25. Wetterwald A, Hoffstetter W, Cecchini MG, Lanske B, Wagner C, Fleisch H, Atkinson M. Characterization and cloning of the E11 antigen, a marker expressed by rat osteoblasts and osteocytes. *Bone*. 1996;18:125-132.
26. Williams MC, Cao Y, Hinds A, Rishi AK, Wetterwald A. T1 alpha protein is developmentally regulated and expressed by alveolar type I cells, choroid plexus, and ciliary epithelia of adult rats. *Am J Respir Cell Mol Biol*. 1996;14:577-585.
27. Breiteneder-Geleff S, Matsui K, Soleiman A, Meraner P, Poczewski H, Kalt R, Schaffner G, Kerjaschki D. Podoplanin, novel 43-kd membrane protein of glomerular epithelial cells, is down-regulated in puromycin nephrosis. *Am J Pathol*. 1997;151:1141-1152.
28. Schacht V, Ramirez MI, Hong YK, Hirakawa S, Feng D, Harvey N, Williams M, Dvorak AM, Dvorak HF, Oliver G, Detmar M. T1alpha/podoplanin deficiency disrupts normal lymphatic vasculature formation and causes lymphedema. *EMBO J*. 2003;22:3546-3556.
29. Boyett MR, Honjo H, Kodama I. The sinoatrial node, a heterogeneous pacemaker structure. *Cardiovasc Res*. 2000;47:658-687.
30. Liu J, Dobrzynski H, Yanni J, Boyett MR, Lei M. Organisation of the mouse sinoatrial node: structure and expression of HCN channels. *Cardiovasc Res*. 2007;73:729-738.
31. Mommersteeg MT, Hoogaars WM, Prall OW, Gier-de Vries C, Wiese C, Clout DE, Papaioannou VE, Brown NA, Harvey RP, Moorman AF, Christoffels VM. Molecular pathway for the localized formation of the sinoatrial node. *Circ Res*. 2007;100:354-362.
32. Hay ED. The mesenchymal cell, its role in the embryo, and the remarkable signaling mechanisms that create it. *Dev Dyn*. 2005;233:706-720.
33. Moore AW, McInnes L, Kreidberg J, Hastie ND, Schedl A. YAC complementation shows a requirement for Wt1 in the development of epicardium, adrenal gland and throughout nephrogenesis. *Development*. 1999;126:1845-1857.
34. Perez-Pomares JM, Phelps A, Sedmerova M, Carmona R, Gonzalez-Iriarte M, Munoz-Chapuli R, Wessels A. Experimental Studies on the Spatiotemporal Expression of WT1 and RALDH2 in the Embryonic Avian Heart: A Model for the Regulation of Myocardial and Valvuloseptal Development by Epicardially Derived Cells (EPDCs). *Dev Biol*. 2002;247:307-326.
35. Carmona R, Gonzalez-Iriarte M, Perez-Pomares JM, Munoz-Chapuli R. Localization of the Wilm's tumour protein WT1 in avian embryos. *Cell Tissue Res*. 2001;303:173-186.
36. Cano A, Perez-Moreno MA, Rodrigo I, Locascio A, Blanco MJ, del Barrio MG, Portillo F, Nieto MA. The transcription factor snail controls epithelial-mesenchymal transitions by repressing E-cadherin expression. *Nat Cell Biol*. 2000;2:76-83.
37. Martin-Villar E, Scholl FG, Gamallo C, Yurrita MM, Munoz-Guerra M, Cruces J, Quintanilla M. Characterization of human PA2.26 antigen (T1alpha-2, podoplanin), a small membrane mucin induced in oral squamous cell carcinomas. *Int J Cancer*. 2005;113:899-910.
38. Martin-Villar E, Megias D, Castel S, Yurrita MM, Vilaro S, Quintanilla M. Podoplanin binds ERM proteins to activate RhoA and promote epithelial-mesenchymal transition. *J Cell Sci*. 2006;119:4541-4553.

39. Jongbloed MR, Wijffels MC, Schalij MJ, Blom NA, Poelmann RE, van der Laarse A, Mentink MM, Wang Z, Fishman GI, Gittenberger-de Groot AC. Development of the right ventricular inflow tract and moderator band: a possible morphological and functional explanation for Mahaim tachycardia. *Circ Res*. 2005;96:776-783.
40. Gundersen H.J., Jensen E.B. The efficiency of systematic sampling in stereology and its prediction. *J Microscopy*. 1987;147:229-263.
41. Garcia-Frigola C, Shi Y, Evans SM. Expression of the hyperpolarization-activated cyclic nucleotide-gated cation channel HCN4 during mouse heart development. *Gene Expr Patterns*. 2003;3:777-783.
42. Hoogaars WM, Engel A, Brons JF, Verkerk AO, de Lange FJ, Wong LY, Bakker ML, Clout DE, Wakker V, Barnett P, Ravesloot JH, Moorman AF, Verheijck EE, Christoffels VM. Tbx3 controls the sinoatrial node gene program and imposes pacemaker function on the atria. *Genes Dev*. 2007;21:1098-1112.
43. Bruneau BG, Logan M, Davis N, Levi T, Tabin CJ, Seidman JG, Seidman CE. Chamber-specific cardiac expression of Tbx5 and heart defects in Holt-Oram syndrome. *Dev Biol*. 1999;211:100-108.
44. Liberatore CM, Searcy-Schrick RD, Yutzey KE. Ventricular expression of tbx5 inhibits normal heart chamber development. *Dev Biol*. 2000;223:169-180.
45. Anderson RH, Brown NA, Moorman AF. Development and structures of the venous pole of the heart. *Dev Dyn*. 2006;235:2-9.
46. Van Loo PF, Mahtab EAF, Wisse LJ, Hou J, Grosveld F, Suske G, Philipsen S, Gittenberger-de Groot AC. Transcription Factor Sp3 knockout mice display serious cardiac malformations. *Mol Cell Biol*. 2007;27: 8571-8582.
47. Webb S, Brown N, Wessels A, Anderson RH. Development of the murine pulmonary vein and its relationship to the embryonic venous sinus. *Anat Rec*. 1998;250:325-334.
48. Wessels A, Anderson RH, Markwald RR, Webb S, Brown NA, Viragh S, Moorman AF, Lamers WH. Atrial development in the human heart: an immunohistochemical study with emphasis on the role of mesenchymal tissues. *Anat Rec*. 2000;259:288-300.
49. Jongbloed MRM, Schalij MJ, Poelmann RE, Blom NA, Fekkes ML, Wang Z, Fishman GI, Gittenberger-de Groot AC. Embryonic conduction tissue: a spatial correlation with adult arrhythmogenic areas? Transgenic CCS/lacZ expression in the cardiac conduction system of murine embryos. *J Cardiovasc Electrophysiol*. 2004;15:349-355.
50. Tasaka H, Krug EL, Markwald RR. Origin of the pulmonary venous orifice in the mouse and its relation to the morphogenesis of the sinus venosus, extracardiac mesenchyme (spina vestibuli), and atrium. *Anat Rec*. 1996;246:107-113.
51. DeRuiter MC, Gittenberger-de Groot AC, Wenink ACG, Poelmann RE, Mentink MMT. In normal development pulmonary veins are connected to the sinus venosus segment in the left atrium. *Anat Rec*. 1995;243:84-92.
52. Blom NA, Gittenberger-de Groot AC, Jongeneel TH, DeRuiter MC, Poelmann RE, Ottenkamp J. Normal development of the pulmonary veins in human embryos and formulation of a morphogenetic concept for sinus venosus defects. *Am J Cardiol*. 2001;87:305-309.
53. Soufan AT, van den Hoff MJ, Ruijter JM, de Boer PA, Hagoort J, Webb S, Anderson RH, Moorman AF. Reconstruction of the patterns of gene expression in the developing mouse heart reveals an architectural arrangement that facilitates the understanding of atrial malformations and arrhythmias. *Circ Res*. 2004;95:1207-1215.
54. Manner J, Merkel N. Early morphogenesis of the sinuatrial region of the chick heart: a contribution to the understanding of the pathogenesis of direct pulmonary venous connections to the right atrium and atrial septal defects in hearts with right isomerism of the atrial appendages. *Anat Rec (Hoboken)*. 2007;290:168-180.
55. Mommersteeg MT, Brown NA, Prall OW, de Gier-de Vries C, Harvey RP, Moorman AF, Christoffels VM. Pitx2c and Nkx2-5 Are Required for the Formation and Identity of the Pulmonary Myocardium. *Circ Res*. 2007;101:902-909.
56. Batlle E, Sancho E, Franci C, Dominguez D, Monfar M, Baulida J, Garcia de Herreros A. The transcription factor snail is a repressor of E-cadherin gene expression in epithelial tumour cells. *Nat Cell Biol*. 2000;2:84-89.
57. Carmona R, Gonzalez-Iriarte M, Macias D, Perez-Pomares JM, Garcia-Garrido L, Munoz-Chapuli R. Immunolocalization of the transcription factor Slug in the developing avian heart. *Anat Embryol*. 2000;201:103-109.

58. Scholl FG, Gamallo C, Vilaro S, Quintanilla M. Identification of PA2.26 antigen as a novel cell-surface mucin-type glycoprotein that induces plasma membrane extensions and increased motility in keratinocytes. *J Cell Sci*. 1999;112 (Pt 24):4601-4613.
59. Hall A. Small GTP-binding proteins and the regulation of the actin cytoskeleton. *Annu Rev Cell Biol*. 1994;10:31-54.
60. Van AL, Souza-Schorey C. Rho GTPases and signaling networks. *Genes Dev*. 1997;11:2295-2322.
61. Dobrzynski H, Boyett MR, Anderson RH. New insights into pacemaker activity: promoting understanding of sick sinus syndrome. *Circulation*. 2007;115:1921-1932.
62. Boucherot A, Schreiber R, Pavenstadt H, Kunzelmann K. Cloning and expression of the mouse glomerular podoplanin homologue gp38P. *Nephrol Dial Transplant*. 2002;17:978-984.
63. Blom NA, Gittenberger-de Groot AC, DeRuiter MC, Poelmann RE, Mentink MM, Ottenkamp J. Development of the cardiac conduction tissue in human embryos using HNK-1 antigen expression: possible relevance for understanding of abnormal atrial automaticity. *Circulation*. 1999;99:800-806.
64. Melnyk P, Ehrlich JR, Pourrier M, Villeneuve L, Cha TJ, Nattel S. Comparison of ion channel distribution and expression in cardiomyocytes of canine pulmonary veins versus left atrium. *Cardiovasc Res*. 2005;65:104-116.

Chapter 3

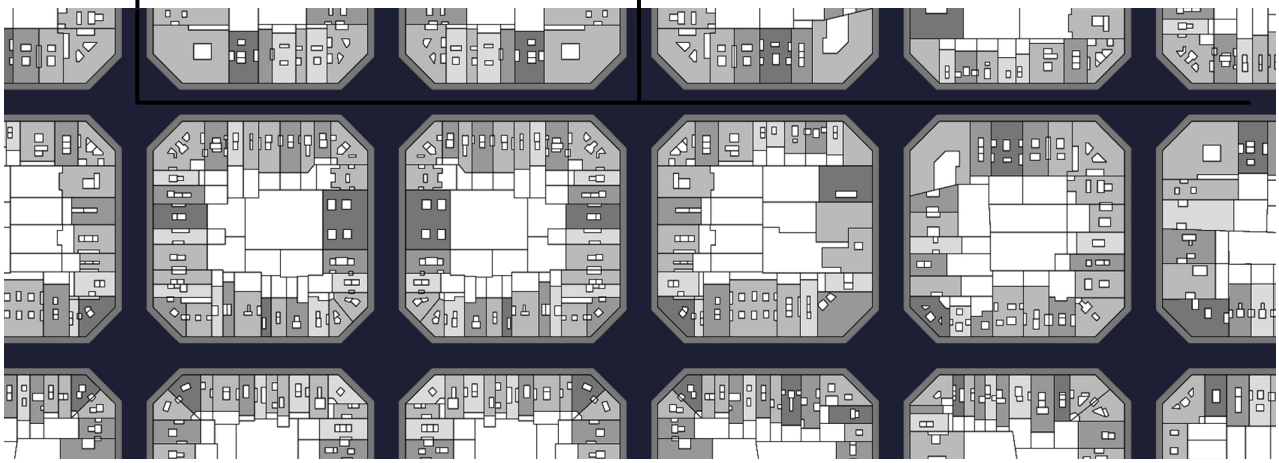

Electrical activation of sinus venosus myocardium and expression patterns of RhoA and Isl-1 in the chick embryo

Edris AF Mahtab, Rebecca Vicente-Steijn, Nathan D Hahurij, Monique RM Jongbloed, Lambertus J Wisse, Marco C DeRuiter, Pavel Uhrin, Jan Zaujec, Bernd R Binder, Martin J Schalij, Robert E Poelmann, Adriana C Gittenberger-de Groot

Modified after Developmental Dynamics 2009;238:183-193

Abstract

Introduction

Myocardium at the venous pole (sinus venosus) of the heart has gained clinical interest as arrhythmias can be initiated from this area. During development, sinus venosus myocardium is incorporated to the primary heart tube and expresses different markers than primary myocardium. We aimed to elucidate the development of sinus venosus myocardium, including the sinoatrial node (SAN), by studying expression patterns of RhoA in relation to other markers, and by studying electrical activation patterns of the developing sinus venosus myocardium.

Methods & Results

Expression of RhoA, myocardial markers cTnI and Nkx2.5, transcription factors Isl-1 and Tbx18, and cation channel *Hcn4*, were examined in sequential stages in chick. Electrical activation patterns were studied using micro-electrodes and optical mapping. Embryonic sinus venosus myocardium is cTnI and *Hcn4* positive, Nkx2.5 negative, complemented by distinct patterns of Isl-1 and Tbx18. During development, initial myocardium-wide expression of RhoA becomes restricted to right-sided sinus venosus myocardium, comprising the SAN. Electrophysiological measurements revealed initial capacity of both atria to show electrical activity that in time shifts to a right-sided dominance, coinciding with persistence of RhoA, Tbx18 and *Hcn4* and absence of Nkx2.5 expression in the definitive SAN.

Conclusion

Results show an initially bilateral electrical potential of sinus venosus myocardium evolving into a right-sided activation pattern during development, and suggest a role for RhoA in conduction system development. We hypothesize an initial sinus venosus wide capacity to generate pacemaker signals, becoming confined to the definitive SAN. Lack of differentiation towards a chamber phenotype would explain ectopic pacemaker foci.

Introduction

The venous pole or sinus venosus of the heart comprises the myocardium that surrounds the caval veins and the pulmonary veins, and also includes the sinoatrial node (SAN). The myocardium in this area has attracted the interest of those working in the field of clinical electrophysiology, by the discovery that this myocardium can be the source of ectopic pacemaker foci initiating clinical arrhythmias. Examples are atrial fibrillation originating from the myocardium surrounding the pulmonary veins and atrial arrhythmias originating from the myocardium of the ligament of Marshall, a remnant of the embryonic left cardinal vein.[1,2] The fact that the adult sinus venosus-derived myocardium is able to show ectopic activity whereas in the embryo this area contributes to the regular primary pacemaker of the heart, the SAN, prompted us to study the embryonic development and electrical activation patterns of this myocardium.

During embryonic development the heart tube is formed at the midline of the embryo by the fusion of the two bilateral cardiogenic plates.[3,4] The primary heart tube initially consists of a primitive left ventricle, atrioventricular canal, and part of the atria. The myocardium of the right ventricle and outflow tract at the arterial pole, and the sinus venosus myocardium at the venous pole, are progressively being incorporated during further development, via a process of epithelial-to-mesenchymal transformation from the mesodermal cells from the second heart field.[5-7] This implies that major parts of myocardium, including the sinus venosus myocardium, are being incorporated to the primary heart tube later during development from a mesenchymal progenitor population.

In mice, cells from the second heart field, including the putative sinus venosus cells, express the transcription factor *Islet-1* (Isl-1), whereas the myocardium of the primary heart tube does not express this marker.[5] In the mouse Isl-1 expressing cells are also observed at the site of the SAN and atrioventricular node (AVN), indicating a possible relation between second heart field-derived cells and formation of the cardiac conduction system (CCS).[8] In chick the cardiac progenitor population also shows Isl-1 expression.[9] There are however no data of a relation during the development to the future CCS.

In the early avian embryo (HH10), the first spontaneous action potentials are generated at the left posterior inflow-site of the heart (putative sinus venosus region).[10] Later on, the adult dominant pacemaker activity is located in the SAN at the entrance of the right cardinal vein in the right atrium. Therefore, a shift in atrial activation, generally referred to as pacemaker activity, from left to right is due to occur during development.

Recently, we described podoplanin, a 43kDa mucin-type transmembrane glycoprotein that is expressed in second heart field-derived structures at the venous pole of the heart (designated posterior heart field) and in the CCS in the mouse.[7,11] Interestingly, podoplanin expression is found initially at the left side of the embryo, followed by

expression in a U-shaped myocardial population surrounding the sinus venosus and the left and right cardinal veins including the SAN. This sinus venosus myocardium is further characterized by expression of the cation channel protein HCN4,[11,12] and lack of expression of the transcription factor Nkx2.5,[7,13] partially overlapping with expression of the transcription factor Tbx18.[13]

This sinus venosus myocardium has also been described to form a left-sided nodule of cells, referred to as a 'transient left' sinoatrial nodal area[7], that is continuous with the myocardium surrounding the pulmonary veins. *Podoplanin* knockout mice demonstrate a complex cardiac phenotype, encompassing a hypoplastic sinus venosus myocardium including the SAN[11] and the myocardium lining the pulmonary vein.[14] The absence of *podoplanin* is related to downregulation of RhoA expression observed in several structures including the SAN,[11] implying an interaction between podoplanin and RhoA, which is in accordance with previous studies.[15]

RhoA is a member of a family of small GTPases which act as molecular switches in a variety of processes such as cell migration, cytoskeletal reorganization, myogenic differentiation[16] and podoplanin-mediated epithelial-to-mesenchymal transformation.[15] Adult mice with an over- or underexpression of RhoA present phenotypes with atrial fibrillation and AV-block, indicating a possible role for RhoA in the function of specific ion channels in the CCS.[17,18] Our own studies support a possible role for both podoplanin and downstream RhoA in CCS development.[11] Thus far, studies to assess RhoA expression in the developing sinus venosus myocardium in the chick embryo are lacking.

Results of our own group and others indicated that the sinus venosus myocardium and components of the CCS are second heart field-derived, and can be distinguished from the myocardium of the primary heart tube by expression patterns of several immunohistochemical markers. In the current study we aim to elucidate the development of the sinus venosus myocardium including the SAN in chick by studying the expression patterns of RhoA, which was shown to be downstream of the second (posterior) heart field marker podoplanin, in relation to others markers expressed in the sinus venosus.

Furthermore, we performed electrophysiological recordings and optical mapping in chick embryonic hearts to assess the sequence of atrial activation during development, to determine the activation patterns in the sinus venosus as well as the time frame of the shift towards the definitive right-sided dominance of atrial activation.

Materials and Methods

Experimental preparation

Fertilized White Leghorn chicken eggs were incubated at 37°C. Animal experiments were performed in accordance to institutional guidelines of the Leiden University Medical Center. Embryos were extracted, staged according to standard (Hamburger and Hamilton 1951) criteria and euthanized by decapitation. For morphological analysis thoraxes were fixed in 4% paraformaldehyde for 24 hr, embedded in paraffin and serially sectioned (5μm).

Immunohistochemistry

Immunohistochemical stainings were conducted (HH15-HH35, n=35) as described[11] for primary antibodies: anti-cTnI (goat polyclonal antibody, sc-8118, Santa Cruz, 1/400), anti-Nkx2.5 (goat polyclonal antibody, sc-8697, Santa Cruz, 1/4000), anti-Isl-1 (mouse monoclonal antibody, clone 39.4D5, Developmental Studies Hybridoma Bank, 1/400), anti-Tbx18 (goat polyclonal, sc-17869, Santa Cruz, 1/800), and anti-RhoA (rabbit polyclonal, sc-179, Santa Cruz, 1/800). Slides were incubated with biotin-conjugated secondary antibodies specific to the appropriate species (goat-α-rabbit (BA-1000); horse-α-goat (BA-9500); horse- α-mouse (BA-2000), all from Vector Labs), visualized by incubation with 3-3'diaminobenzidin tetrahydrochloride (DAB, D5637, Sigma-Aldrich), and counterstained with haematoxylin (0.1%, Merck).

Nonradioactive in situ hybridization

Nonradioactive in situ hybridization analysis for *Hcn4* was conducted with digoxigenin-labeled antisense RNA probe in 10 μm embryo sections as described previously.[13,19] A cDNA fragment corresponding to HCN4 amino acids 400–602 was used as template and digoxigenin-labeled probes were generated. A sense RNA probe was used as a negative control.

3-D reconstructions

3-D reconstructions of the atrial and ventricular myocardium of cTnI-stained serial sections of HH17, HH22 and HH35 embryos were made as previously described[20] using the AMIRA v4.0 Software Package (Template Graphics Software, San Diego, USA). In the reconstructions of the HH17 and HH22 embryonic hearts based on cTnI expression, RhoA and Isl-1 positive and Nkx2.5 negative myocardium were superimposed. In the HH35 reconstruction RhoA positive and Nkx2.5 negative myocardium (cTnI positive) were inserted.

Ex-ovo extracellular micro-electrode recordings

Recordings were conducted in 67 embryonic hearts (HH20 to HH31) during superperfusion with oxygenated Tyrode solution as previously described.[21] Hearts were placed in a temperature-controlled fluid-heated superperfused tissue bath (35±0.1°C), fixed with a wire through non-cardiac tissue near the outflow tract and allowed to equilibrate for 10 min. Heart rates (bpm) below 60 or AV-intervals >100ms were not analyzed. Tungsten recording electrodes were placed on the right atrium (RA) (near the site of the definitive SAN), left atrium (LA) (near the site of the 'transient left-sided SAN'), on the left side of the ventricular apex (V), and a reference electrode in the tissue bath. The electrical activity was confirmed visually by mechanical activity (contraction) of the atria and ventricles. A difference of ≥1ms in local depolarization time between the recording electrodes was considered significant. The extracted hearts were grouped as follows: HH20-23 (A, n=25), HH24-27 (B, n=28), HH28-HH31 (C, n=14).

Optical mapping

Following micro-electrode mapping, a group of 10 hearts from group A (HH20-23) were used for additional optical mapping recordings. Hearts were submersed for 10 minutes in Tyrode's solution containing voltage-sensitive fluorescent dye Di-4-ANEPPS (8 μM, Invitrogen) and excitation-contraction inhibitor blebbistatin[22] (8,5 μM, Sigma-Aldrich, St. Louis, MO, USA) to reduce motion artifacts at 37° C.
Excitation light (λ=525±25 nm) was delivered by a halogen arc-lamp at 150W (MHAB-150W, Moritex Corporation). Fluorescent emission light (λ>590 nm) was passed through a camera lens (2x Planapo, WD=15 mm, Leica) and focused onto a 100 by 100 pixels (100 mm^2) CMOS camera (Ultima-L, SciMedia, Costa Mesa, CA, USA) viewing the posterior side of the heart, resulting in a total field of view of 25 mm^2 and a spatial resolution of 50 μm/pixel. Spontaneous activity was recorded at a sampling speed of 500, 1000 and 5000 frames s^{-1}, high-pass filtered and analyzed using Brain Vision Analyze (version 0904, Brainvision Inc, Tokyo, Japan). Activation time points were defined as dF/dt_{max}, which corresponds to the time point of maximum upstroke velocity. Atrioventricular conduction times were calculated by subtracting the average activation time point of a 5-by-5 pixel grid in the atrium of activation origin from the average activation time point of a similar sized grid in the ventricular apex.

Statistical analysis

Data was analyzed with SPSS software (SPSS, Inc, Chicago, Ill). HR, Atrial activation time and AV-intervals were compared between groups with a 2-tailed Student *t* test for normally distributed values. The comparison of categorical values (sequence of atrial activation) was done with the χ^2 test. A P value <0.05 (2-tailed) was considered significant. Results are presented as mean ±SD.

Results

Expression patterns of cTnI, RhoA, Isl-1, Tbx18 and Nkx2.5, as well as electrophysiological activity in chicken hearts in increasing stages of development (HH15-35) were studied. Figure 3.1 provides a schematic summary of the patterns for Isl-1, RhoA and Nkx2.5 expression. Data were correlated with RNA expression derived from in situ hybridization of *Hcn4*.

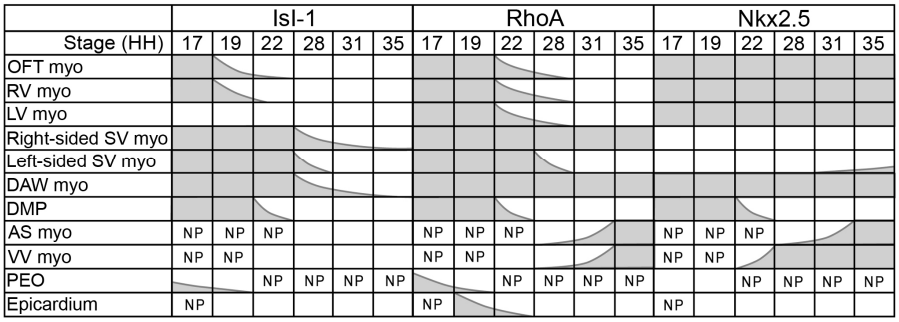

Figure 3.1 Schematic spatio-temporal representation of total protein expression patterns per area for Isl-1, RhoA and Nkx2.5 in the chick embryo. Filled squares represent maximum intensity at that stage for the specific area. Partially filled squares represent increase and decrease of expression. AS: atrial septum; DAW: dorsal atrial wall; DMP: dorsal mesocardial protrusion; LV: left ventricle; myo: myocardium; NP: not present; OFT: outflow tract; PEO: proepicardial organ; RV: right ventricle; SV: sinus venosus; VV: venous valves.

Expression patterns in the developing heart

HH15-19 (2-3 days of incubation)

Early looping of the heart is in progress but there is no septation between atria or ventricles and no venous valves are present, yet. Myocardialisation of the cardinal veins has barely started (Figure 3.2a-c). The myocardium of the heart is defined by expression of cTnI, overlapping in these stages with RhoA (Figure 3.1; 3.2a-b, 3.2d-e, 3.2j-k). At the arterial and venous pole the newly differentiating myocardium from the second heart field is positive for Isl-1 (Figure 3.1; 3.2a, 3.2f, 3.2l). In accordance with previous results in mouse,[7,13] Nkx2.5 is positive in the outflow tract but negative in the sinus venosus myocardium (Figure 3.1; 3.2c, 3.2g, 3.2m). This Nkx2.5 negative sinus venosus myocardium forms a U-shaped area at the venous pole of the heart (Figure 3.2c). In the myocardium at the borderline of the right cardinal vein and the right atrium, the site of the putative right (definitive) SAN is located (Figure 3.2d-i). This area is positive for the transcription factor Tbx18 (Figure 3.2h) and for the cation channel *Hcn4* (Figure 3.2i). Both RhoA and Isl-1 are expressed in the non-myocardial mesenchyme of the second heart field (Figure 3.2e-f).

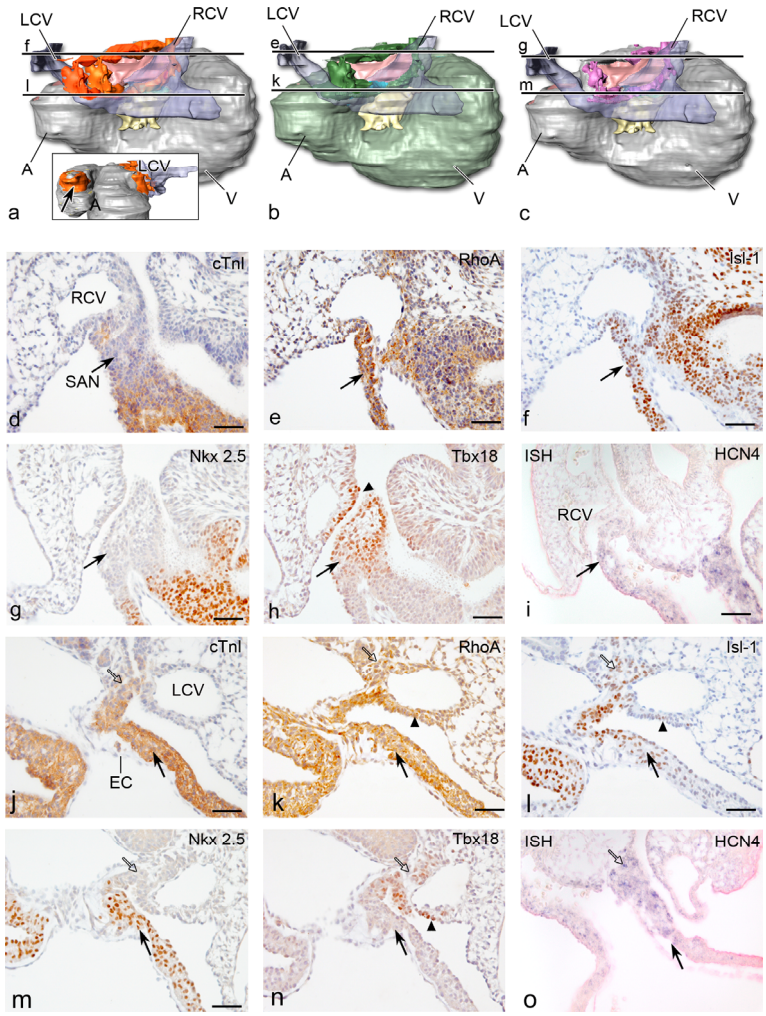

Figure 3.2 Expression of Isl-1 and RhoA and in the developing sinus venosus myocardium. **a-c** 3D reconstruction (dorsal view) of a HH17 heart. Atrial (A) and ventricular (V) myocardium (cTnI positive) are depicted in grey, the lumen of the left (LCV) and right (RCV) cardinal veins in transparent blue, atrial lumen in pale pink, and the proepicardial organ in yellow. **a** Isl-1 positive myocardium is superimposed in orange. Insert: left cranial view showing expression at the outflow tract (arrow). **b** RhoA positive myocardium is superimposed in green. **c** Nkx2.5 negative myocardium is purple. Intersection lines **f-g** and **k-m** refer to the respective sections. **d-i** Transverse sections showing expression of cTnI (**d**), RhoA (**e**), Isl-1 (**f**), no Nkx2.5 (**g**), Tbx18 (**h**) and *Hcn4* RNA (**i,** in situ hybridization (ISH), blue staining) in the right-sided sinoatrial node (SAN) (arrow). **j-o** Transverse sections showing a cluster of cells medial to the LCV (open arrow, 'transient left SAN' area),which expresses cTnI (**j**), RhoA (**k**), Isl-1 (**l**), no Nkx2.5 (**m**) but is positive for Tbx18 (**n**) and *Hcn4* (**o**). The dorsal atrial wall, above the atrioventricular canal (arrow **j-o**) shows cTnI (**j**), RhoA (**k**), Isl-1 (**l**) Nkx2.5 (**m**) and *Hcn4* (**o**) expression but no Tbx18 (**n**). Sporadic positive cells (arrowheads) lining the coelomic cavity show RhoA (**k),** Isl-1 (**l**) and Tbx18 expression (**h**, **n**). Scale bars d-o = 60 µm.

A similar patterning as described for the right side of the sinus venosus myocardium is found at the left side adjacent to the medial border of the left cardinal vein where there is overlap of cTnI and RhoA (Figure 3.2j-k). Comparable to the right side there is a small cTnI, RhoA and Isl-1 positive area (Figure 3.2j-l) that is negative for Nkx2.5 and positive for Tbx18 and *Hcn4* (Figure 3.2m-o). We regard this area as the site of a 'transient left SAN'. In close proximity the Isl-1 expressing cells show an interesting phenomenon in that they extend into the myocardium underneath the endocardial cushion tissue that lines the postero-inferior wall of the atrium (putative AVN area) (Figure 3.2l). There is patchy positivity of the coelomic wall for Isl-1 (Figure 3.2l), RhoA (Figure 3.2k) and Tbx18 (Figure 3.2h, 3.2n). RhoA is also found in the proepicardial organ (PEO) (Figure 3.1).

HH20-24 (3-4 days of incubation)

Looping of the heart has advanced and septation of the atria and ventricles has started. In the right atrium the left and right venous valves have become apparent. Details on the changes in the expression patterns are depicted in Figure 3.1. RhoA expression diminishes in the myocardium of the outflow tract, right and left ventricle. It remains prominently present in the U-shaped sinus venosus myocardium which now also extends around the anterior side of the cardinal veins (Figure 3.3d-e, 3.3j-k). On the right side, the definitive SAN area becomes more clear still showing Nkx2.5 negative and Tbx18 positive expression (Figure 3.3g-h) as well as Isl-1 positive cells (Figure 3.3f) and *Hcn4* expression (Figure 3.3i).
At the left side, the area of the transient left SAN remains present in the cTnI and RhoA overlapping expression medial of the left cardinal vein (Figure 3.3j-k). This myocardium is, like the regular SAN, negative for Nkx2.5 (Figure 3.3m) and positive for Isl-1, Tbx18 and *Hcn4* (Figure 3.3l, 3.3n-o).
The Isl-1 positive cells observed between the sinus venosus region and the dorsal atrial wall cranial to the underlying endocardial cushion tissue are no longer visible. The marked expression of Tbx18 in the coelomic wall (Figure 3.3h, 3.3n) is still obvious.

HH25-31 (4-6 days of incubation)

Atrial septation has advanced and the entire heart tube is now covered by epicardium. Ventricular septation is ongoing and components of the ventricular conduction system are becoming apparent. Covering of the pulmonary vein with a myocardial layer has been initiated. RhoA expression has been reduced in this stage to the sinus venosus myocardium including the myocardial sleeve surrounding the pulmonary vein, the right-sided SAN area, positive for Isl-1, and the dorsal atrial wall myocardium, which is now negative for Isl-1 and positive for Nkx2.5 (Figure 3.1).

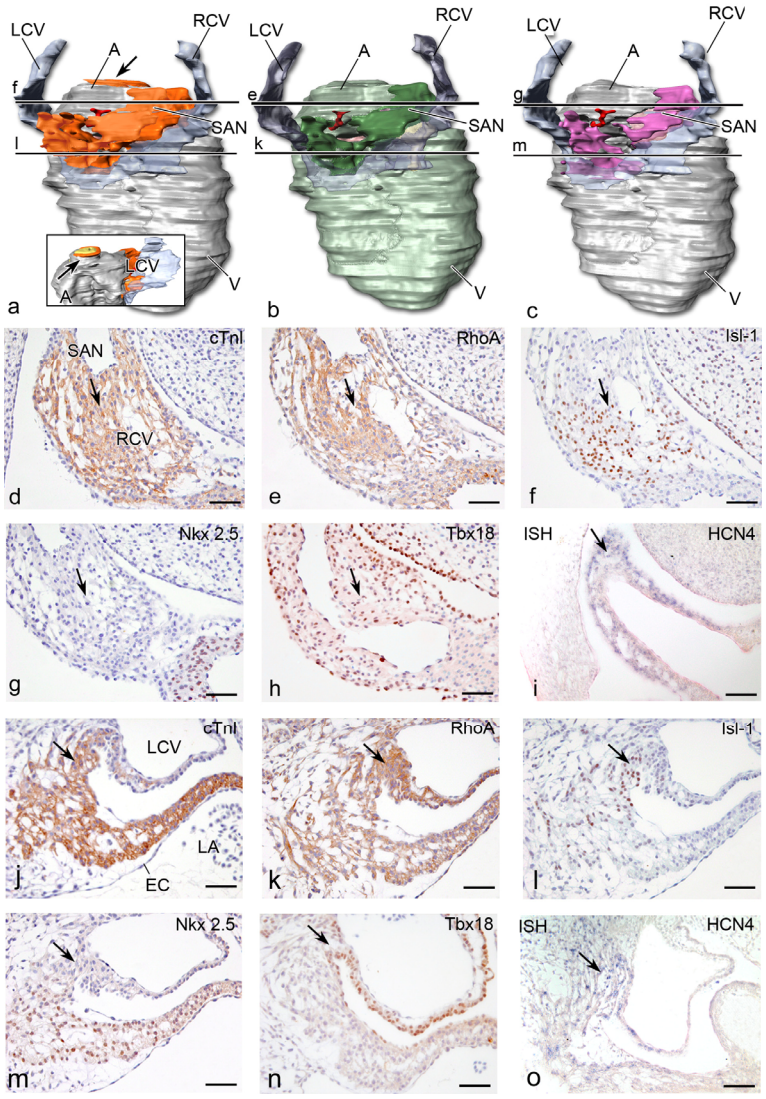

Figure 3.3 Sinus venosus myocardial areas still show Isl-1 and RhoA expression. 3D reconstruction (dorsal view) of a HH22 heart (**a-c**) in which atrial (A) and ventricular (V) myocardium is depicted in grey, the lumen of the pulmonary vein in red, the lumen of the left (LCV) and right (RCV) cardinal veins in transparent blue, and the atrial lumen in pale pink. The location of the sinoatrial node (SAN) has been indicated. **a** Isl-1 positive myocardium is superimposed in orange. Insert: left cranial view showing remaining expression at the outflow tract (arrow). **b** RhoA positive myocardium is superimposed in green. **c** Nkx2.5 negative myocardium is purple. The intersection lines **f-g** and **k-m** refer to the respective sections. **d-i** transverse sections show expression of cTnI (**d**), RhoA (**e**), Isl-1 (**f**), no Nkx2.5 (**g**), Tbx18 (**h**) and *Hcn4* RNA (**i,** in situ hybridization (ISH), blue staining) in the definitive right-sided SAN (arrow). **j-o** show the transverse sections of the cluster of cells medial to the LCV (arrow, 'transient left SAN' area), which expresses cTnI (**j**), RhoA (**k**), Isl-1 (**l**) no Nkx2.5 (**m**), Tbx18 (**m**) and *Hcn4* (**n**). LA, left atrium. Scale bar d-m = 60µm.

HH32-39 (7-13 days of incubation)

Ventricular septation is completed in these stages. In general, RhoA expression has been largely reduced to the right side of the sinus venosus myocardium (Figure 3.4a-b, 3.4d) including the SAN area, the venous valves as well as the dorsal wall of the right atrium (Figure 3.4b). The pulmonary vein is becoming entirely surrounded by a myocardial sleeve that has low expression of RhoA (Figure 3.4b). Part of the U-shaped sinus venosus myocardium is negative for Nkx2.5 including the right-sided SAN area (Figure 3.4c, 3.4f). Tbx18 and *Hcn4* are expressed in this area (Figure 3.4g-h) also extending in the left sinus venosus myocardium. Furthermore, we observed an area with a slightly higher RhoA expression in the cTnI and Nkx2.5 positive, Tbx18 negative and *Hcn4* positive myocardium (Figure 3.4i-m) at the right-sided base of the interatrial septum, where the developing AVN is expected.

Electrophysiological recordings to study atrial activation patterns

Embryonic chick hearts were recorded to study the atrial activation patterns during development. Data are summarized in Table 3.1. Micro-electrode recorded heart rates showed a regular rhythm of 178±51bpm (AV-interval 85±12ms). In group A (HH20-23) 56% of the hearts (14/25) presented a predominant right atrial (RA) activation pattern (definitive right-sided SAN, Figure 3.5a-b) but a considerable number of cases (8/25; 32%) presented a predominant left atrial (LA) activation pattern ('transient left-sided SAN', Figure 3.5c-d). Later in development the LA activation sequence in group B became less frequent (25%), and was almost negligible in group C (7%). Additionally, subsets of hearts presented an activation sequence in which the electrical impulse originated simultaneously from both atria (difference <1ms). There was no significant difference in AV-intervals between right (84±12ms; 42/67) or left (86±11ms;16/67) atrial activation patterns (p=0.572) or between the different groups throughout development. The left-sided activation sequence is visible up to HH28.

Optical mapping data in a set of 10 hearts from group A (previously measured with micro-electrodes) confirmed the results from the extracellular recordings. Hearts were observed with the first activation located at the junction of the right cardinal vein and the atrium (n=7; Figure 3.5e-i) but also hearts where it was located at the junction of the left cardinal vein and the atrium (n=3; Figure 3.5j-n). The atrial and AV-delay times were considerably different between the micro-electrode recordings and the optical mapping. A prolongation of the PQ interval has been reported as a result of the use of the voltage-sensitive dye Di-4-ANEPPS[23] and could explain the differences in conduction time we have observed.

Table 3.1 Activation sequences of electrophysiological recordings in chick hearts from HH20 to HH31.

Developmental Stage (HH)	n	LA	RA	LA=RA	AV-interval, ms, mean±SD (range)	HR, bpm, mean ± SD (range)
Group A	25	8(32%)	14(56%)	3(12%)	82±10 (72-92)	149±42(107-191)
HH20	3	-	3	-	88±5 (83-93)	131±49 (82-180)
HH21	8	2	5	1	81±10 (71-91)	145±37 (108-182)
HH22	8	2	5	1	77±7 (70-84)	147±41 (106-186)
HH23	6	4	1	1	82±6 (76-88)	177±41 (136-218)
Group B	28	7(25%)	15(54%)	6(21%)	83±10(73-93)	181±36(145-217)
HH24	7	1	4	2	85±6 (79-91)	174±43 (131-217)
HH25	4	1	2	1	88±14 (74-102)	159±35 (124-194)
HH26	8	3	4	1	78±8 (70-86)	189±26 (163-215)
HH27	9	2	5	2	82±12 (70-94)	190±38 (152-228)
Group C	14	1(7%)	12(86%)	1(7%)	94±14(80-108)	222±57(165-279)
HH28	1	1	-	-	97	171
HH29	5	-	4	1	92±18 (74-110)	176±30 (146-206)
HH30	6	-	6	-	94±15 (79-109)	258±47 (211-305)
HH31	2	-	2	-	99±3 (96-102)	259±62 (197-321)
Total	67	16(24%)	42(63%)	10(13%)	85±12 (73-97)	178±51 (127-229)

A left atrial activation pattern was observed up to HH28. AV, atrioventricular; HR, heart rate; LA, left atrium; RA, right atrium. No significant difference (Student *t* test; p<0.05) was observed between the values in de different groups.

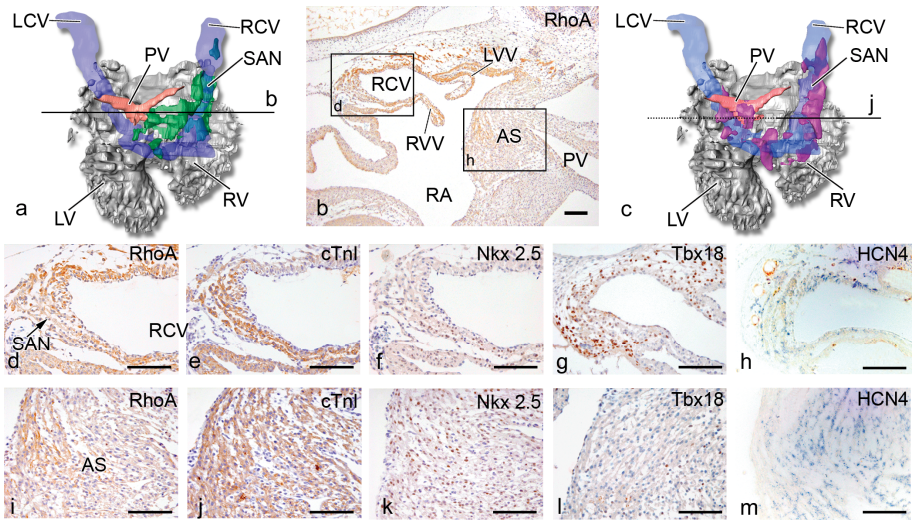

Figure 3.4 Remaining RhoA expression late in development. 3D reconstruction (dorsal view) of a HH35 heart (**a** and **c**). Atrial (left and right) and ventricular (left (LV) and right (RV)) lumens are depicted in grey, lumens of the left (LCV) and right (RCV) cardinal veins in transparent blue and the lumen of the pulmonary vein (PV) in pink. In **a** the RhoA positive myocardium is superimposed in green and in **c** the Nkx2.5 negative myocardium in purple. **b** Overview of RhoA expression in the RCV and atrial septum (AS) which represents transsection **b** in **a**. **d-h** are magnifications of the boxed area in **b** showing the definitive right-sided sinoatrial node (SAN) which expresses RhoA (**d**), cTnI (**e**), Tbx18(**g**) and *Hcn4* (**h,** in situ hybridization(ISH), blue staining) but no Nkx2.5 (**f**) . **i-m** are magnifications of the other boxed area in **b** showing the right-sided base of the AS which expresses RhoA (**i**), cTnI (**j**) and Nkx2.5 (**k**) and *Hcn4* (**m**) but no Tbx18 (**l**). LVV, left venous valve; RA, right atrium; RVV, right venous valve. Scale bars = b, d: 100µm; e-l: 60µm.

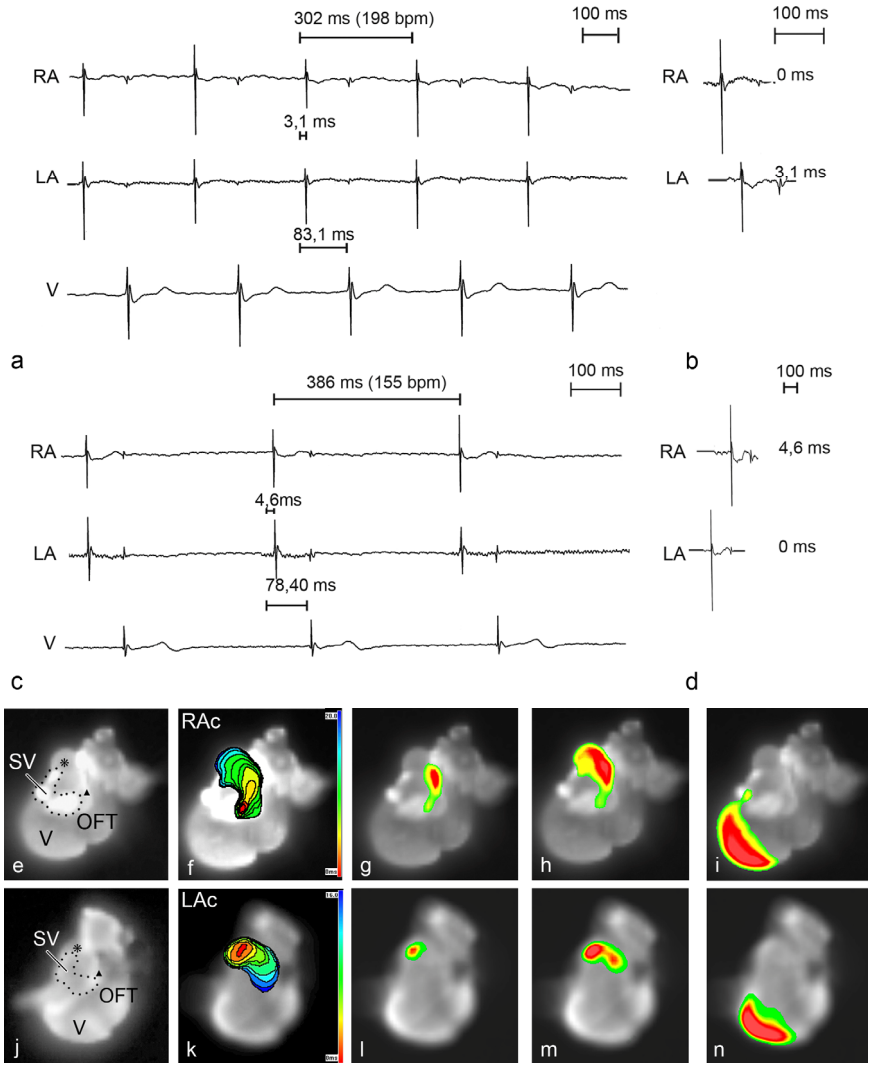

Figure 3.5 Electrophysiological measurement during development. **a** Representative example of electrocardiogram of a HH29 heart in which the electrical signal originates in the right atrium (RA) (heart rate (HR) 198 beats per minute (bpm), atrioventricular (AV)-interval 83,1 ms). **b** Magnification where we observe that the RA signal precedes the left atrial (LA) signal by 3,1 ms. **c** Representative example of a HH21 heart where the electrical signal originates in the LA and travels to the RA with a 4,6 ms delay (HR 155 bpm, AV-interval 78,4 ms). **d** shows a magnification of the delay between LA and RA. **e-n** Representative examples of the results obtained by optical mapping. **e-i** Right-sided activated HH22 heart, posterior view. **j-n.** Left-sided activated HH20 heart, posterior view. In **f** and **k**, isochrones are in 2ms interval and the earliest activated region is shown in red. **g-i** and **l-m** show individual frames of the sequence of activation of each heart respectively (from onset to ventricular propagation). Lac, left atrial activation; left atrium, asterisk (*); OFT, outflow tract; RAc, right atrial activation; right atrium, arrowhead (▲); SV, sinus venosus (dotted area in **e** and **j**); V, ventricle.

Discussion

During heart development, additional myocardial cells are incorporated from the second heart field into the linear heart tube through the arterial and the venous pole.[5,8] The sinus venosus myocardium differentiates from the mesodermal precursor population of the second heart field and forms a U-shaped myocardial structure comprising the definitive SAN area.[7,8,11] This special area of myocardium in the mouse is positive for Tbx18 and negative for Nkx2.5.[7,13] Other genes have also been described to be expressed in this myocardium like *podoplanin,*[7] *Shox2*[24] and *Hcn4,*[12] expression patterns being distinct from the non-second heart field-derived myocardium of the primary heart tube.

We have investigated specifically the sinus venosus myocardium in the chick embryo using most of the above described markers to correlate mouse and chick data and added the expression of *RhoA,* as this gene has been functionally linked to *podoplanin.*[11] Furthermore, RhoA is important for proper function of the CCS.[17,18]

As expected, Isl-1, considered in the stages concerned as a second heart field marker, was found in the mesenchyme of the second heart field as well as in the U-shaped sinus venosus myocardium. The current study shows in chick that initially sinus venosus wide Nkx2.5 negative and Tbx18 and Isl-1 positive expression persists in the right-sided sinus venosus in the area of the definitive right-sided SAN, as was previously demonstrated for mouse.[7,13] This expression thus disappears in the remainder of the U-shaped myocardium including the area of the transient left-sided SAN.

The expression of RhoA shows a specific spatio-temporal pattern that in part correlates with the already described patterns for Nkx2.5, Tbx18 and Isl-1. Initially, RhoA is found in the complete linear heart tube where it could be involved in Rho-mediated signaling essential for the migration of precardiac mesoderm and the proper looping of the heart.[16] RhoA expression is maintained in the right side of the sinus venosus myocardium including the SAN throughout development. A low remnant expression is observed in the myocardium with a more marked presence in the area of the putative AVN. Cardiac disruption in RhoA-signaling results in bradycardia, atrial fibrillation and AV-block,[17,18] suggesting a regulatory function for RhoA, although the exact mechanism remains to be elucidated.

Our electrophysiological recordings show that initially both atria have the potential to generate the first electrical activity, while later in development the activity becomes restricted to the right side, where the definitive adult pacemaker is located. Electrical activation originating at the left inflow portion has been demonstrated previously in the avian embryo.[10] However, the exact time point of the shift from a dominant left-sided electrical activation to an eventual right-sided pacemaker remained unspecified. Our study demonstrates the capacity of both sides of the sinus venosus myocardium to generate the first electrical activity until approximately HH28. This correlated with the disappearance of RhoA and Isl-1 positive cells and the gradual upregulation of

Nkx2.5 expression in the myocardium surrounding the left cardinal vein (transient left SAN area). Optical mapping confirmed the existence of hearts in which the first electrical activity was observed at the junction of the left cardinal vein and the atrium, as was also reported by Sedmera et al.[25] We hypothesize that this bilateral potential can be explained by a sinus venosus-wide capacity to generate pacemaker signals by the undifferentiated myocardium. During development the left-sided sinus venosus myocardium differentiates towards a chamber myocardium phenotype (and progressively looses the pacemaker potential), whereas the right side maintains the undifferentiated state and eventually remains as the definitive right-sided SAN. The occurrence of signals originating form both the left and right side, as well as simultaneous activation from both sides, progressively diminishing in time, could thus be explained. Preliminary optical mapping data in earlier developmental stages (HH14-16) confirm this phenomenon (data not shown). The shift in expression patterns of RhoA as observed in the current study, as well as an early sinus venosus wide expression of CCS markers, including *Hcn4*, that become confined to the definitive right SAN during development, support this hypothesis (current study and[12]).

In the right-sided dorsal atrial wall cranial to the atrioventricular junction (putative AVN area) a small population of Isl-1 positive cells was observed in early stages. The myocardium in this region is positive for Nkx2.5, RhoA and *Hcn4* and negative for Tbx18, differing as such from the SAN area and the chamber myocardium. The AVN has been hypothesized to originate partially from an embryonic counterpart of the SAN at the left sinus horn.[26] Given the proximity of the Isl-1 positive area of the left cardinal vein (transient left SAN) and the dorsal atrial wall a contribution of this left-sided sinus venosus myocardium to the AVN is hypothesized. These data are supported by recent Isl-1 tracing studies.[8]

Clinical implications

As described in the current study a bilateral electrical activity of the sinus venosus is transiently present during development, correlating with expression of markers that are also observed in elements of the definitive CCS, like the SAN. During development a shift in activation pattern towards a definitive right-sided activation origination from the SAN, concomitant with confinement of expression of markers to the area of the SAN, is due to occur. This means that the sinus venosus myocardium, with exception of the SAN that will keep a more primitive phenotype, will differentiate during development towards a chamber myocardium phenotype. Failure to differentiate into a chamber phenotype in these areas, or re-expression of the embryonic program may lead to potential arrhythmogenic substrates in the adult. This provides a plausible explanation for arrhythmias originating from ectopic pacemaker foci in the sinus venosus myocardium e.g. the myocardium surrounding the pulmonary veins and the ligament of Marshall.[1,2,20]

The possibility of a multicellular origin of the AVN is interesting in the light of AV nodal re-entry tachycardia, based on pathways within the AVN with distinctive electrophysiologic capacities providing the substrate for re-entry. Cell tracing-based proof of contribution of sinus venosus myocardium to the AVN area is necessary.

Conclusions

In conclusion we describe RhoA expression in both the left and right side of the embryonic sinus venosus myocardium, later persisting in the definitive SAN and less markedly in the AVN area. We have shown an early sinus venosus wide capacity to generate pacemaker signals, that later on becomes restricted to the definitive right SAN area, corresponding with restriction of RhoA (among other markers) expression to this region.

References

1. Haissaguerre M, Jais P, Shah DC, Takahashi A, Hocini M, Quiniou G, Garrigue S, Le MA, Le MP, Clementy J. Spontaneous initiation of atrial fibrillation by ectopic beats originating in the pulmonary veins. *N Engl J Med*. 1998;339:659-666.
2. Kurotobi T, Ito H, Inoue K, Iwakura K, Kawano S, Okamura A, Date M, Fujii K. Marshall vein as arrhythmogenic source in patients with atrial fibrillation: correlation between its anatomy and electrophysiological findings. *J Cardiovasc Electrophysiol*. 2006;17:1062-1067.
3. DeRuiter MC, Poelmann RE, VanderPlas-de Vries I, Mentink MMT, Gittenberger-de Groot AC. The development of the myocardium and endocardium in mouse embryos. Fusion of two heart tubes? *Anat Embryol*. 1992;185:461-473.
4. Moreno-Rodriguez RA, Krug EL, Reyes L, Villavicencio L, Mjaatvedt CH, Markwald RR. Bidirectional fusion of the heart-forming fields in the developing chick embryo. *Dev Dyn*. 2006;235:191-202.
5. Cai CL, Liang X, Shi Y, Chu PH, Pfaff SL, Chen J, Evans S. Isl1 identifies a cardiac progenitor population that proliferates prior to differentiation and contributes a majority of cells to the heart. *Dev Cell*. 2003;5:877-889.
6. Buckingham M, Meilhac S, Zaffran S. Building the mammalian heart from two sources of myocardial cells. *Nat Rev Genet*. 2005;6:826-835.
7. Gittenberger-de Groot AC, Mahtab EAF, Hahurij ND, Wisse LJ, DeRuiter MC, Wijffels MCEF, Poelmann RE. Nkx2.5 negative myocardium of the posterior heart field and its correlation with podoplanin expression in cells from the developing cardiac pacemaking and conduction system. *Anat Rec*. 2007;290:115-122.
8. Sun Y, Liang X, Najafi N, Cass M, Lin L, Cai CL, Chen J, Evans SM. Islet 1 is expressed in distinct cardiovascular lineages, including pacemaker and coronary vascular cells. *Dev Biol*. 2007;304:286-296.
9. Yuan S, Schoenwolf GC. Islet-1 marks the early heart rudiments and is asymmetrically expressed during early rotation of the foregut in the chick embryo. *Anat Rec*. 2000;260:204-207.
10. Kamino K, Hirota A, Fujii S. Localization of pacemaking activity in early embryonic heart monitored using voltage-sensitive dye. *Nature*. 1981;290:595-597.
11. Mahtab EA, Vicente-Steijn R, Hahurij ND, Jongbloed MR, Wisse LJ, DeRuiter MC, Uhrin P, Zaujec J, Binder BR, Schalij MJ, Poelmann RE, Gittenberger-de Groot AC. Podoplanin deficient mice show a Rhoa-related hypoplasia of the sinus venosus myocardium including the sinoatrial node. *Dev Dyn*. 2009;238:183-193.
12. Garcia-Frigola C, Shi Y, Evans SM. Expression of the hyperpolarization-activated cyclic nucleotide-gated cation channel HCN4 during mouse heart development. *Gene Expr Patterns*. 2003;3:777-783.
13. Christoffels VM, Mommersteeg MT, Trowe MO, Prall OW, Gier-de Vries C, Soufan AT, Bussen M, Schuster-Gossler K, Harvey RP, Moorman AF, Kispert A. Formation of the venous pole of the heart from an Nkx2-5-negative precursor population requires Tbx18. *Circ Res*. 2006;98:1555-1563.
14. Douglas YL, Mahtab EA, Jongbloed MR, Uhrin P, Zaujec J, Binder BR, Schalij MJ, Poelmann RE, DeRuiter MC, Gittenberger-de Groot AC. Pulmonary vein, dorsal atrial wall and atrial septum abnormalities in podoplanin knockout mice with disturbed posterior heart field contribution. *Pediatr Res*. 2009;65: 27-32.
15. Martin-Villar E, Megias D, Castel S, Yurrita MM, Vilaro S, Quintanilla M. Podoplanin binds ERM proteins to activate RhoA and promote epithelial-mesenchymal transition. *J Cell Sci*. 2006;119: 4541-4553.
16. Wei L, Roberts W, Wang L, Yamada M, Zhang S, Zhao Z, Rivkees SA, Schwartz RJ, Imanaka-Yoshida K. Rho kinases play an obligatory role in vertebrate embryonic organogenesis. *Development*. 2001;128:2953-2962.
17. Sah VP, Minamisawa S, Tam SP, Wu TH, Dorn GW, Ross J, Jr., Chien KR, Brown JH. Cardiac-specific overexpression of RhoA results in sinus and atrioventricular nodal dysfunction and contractile failure. *J Clin Invest*. 1999;103:1627-1634.
18. Wei L, Taffet GE, Khoury DS, Bo J, Li Y, Yatani A, Delaughter MC, Klevitsky R, Hewett TE, Robbins J, Michael LH, Schneider MD, Entman ML, Schwartz RJ. Disruption of Rho signaling results in progressive atrioventricular conduction defects while ventricular function remains preserved. *FASEB J*. 2004;18:857-859.

19. Kaarbo M, Crane DI, Murrell WG. RhoA is highly up-regulated in the process of early heart development of the chick and important for normal embryogenesis. *Dev Dyn*. 2003;227:35-47.
20. Jongbloed MRM, Schalij MJ, Poelmann RE, Blom NA, Fekkes ML, Wang Z, Fishman GI, Gittenberger-de Groot AC. Embryonic conduction tissue: a spatial correlation with adult arrhythmogenic areas? Transgenic CCS/lacZ expression in the cardiac conduction system of murine embryos. *J Cardiovasc Electrophysiol*. 2004;15:349-355.
21. Kolditz DP, Wijffels MCEF, Blom NA, Van der Laarse A, Markwald RR, Schalij MJ, Gittenberger-de Groot AC. Persistence of functional atrioventricular accessory pathways in post-septated embryonic avian hearts: implications for morphogenesis and functional maturation of the cardiac conduction system. *Circulation*. 2007;115:17-26.
22. Fedorov VV, Lozinsky IT, Sosunov EA, Anyukhovsky EP, Rosen MR, Balke CW, Efimov IR. Application of blebbistatin as an excitation-contraction uncoupler for electrophysiologic study of rat and rabbit hearts. *Heart Rhythm*. 2007;4:619-626.
23. Nygren A, Kondo C, Clark RB, Giles WR. Voltage-sensitive dye mapping in Langendorff-perfused rat hearts. *Am J Physiol Heart Circ Physiol*. 2003;284:H892-H902.
24. Blaschke RJ, Hahurij ND, Kuijper S, Just S, Wisse LJ, Deissler K, Maxelon T, Anastassiadis K, Spitzer J, Hardt SE, Schöler H, Feitsma H, Rottbauer W, Blum M, Meijlink F, Rappold GA, Gittenberger-de Groot AC. Targeted mutation reveals essential functions of the homeodomain transcription factor Shox2 in sinoatrial and pacemaking development. *Circulation*. 2007;115:1830-1838.
25. Sedmera D, Wessels A, Trusk TC, Thompson RP, Hewett KW, Gourdie RG. Changes in activation sequence of embryonic chick atria correlate with developing myocardial architecture. *Am J Physiol Heart Circ Physiol*. 2006;291:H1646-H1652.
26. James TN. Structure and function of the sinus node, AV node and His bundle of the human heart: part I - structure. *Progress in Cardiovascular Diseases*. 2002;45:235-267.

Chapter 4

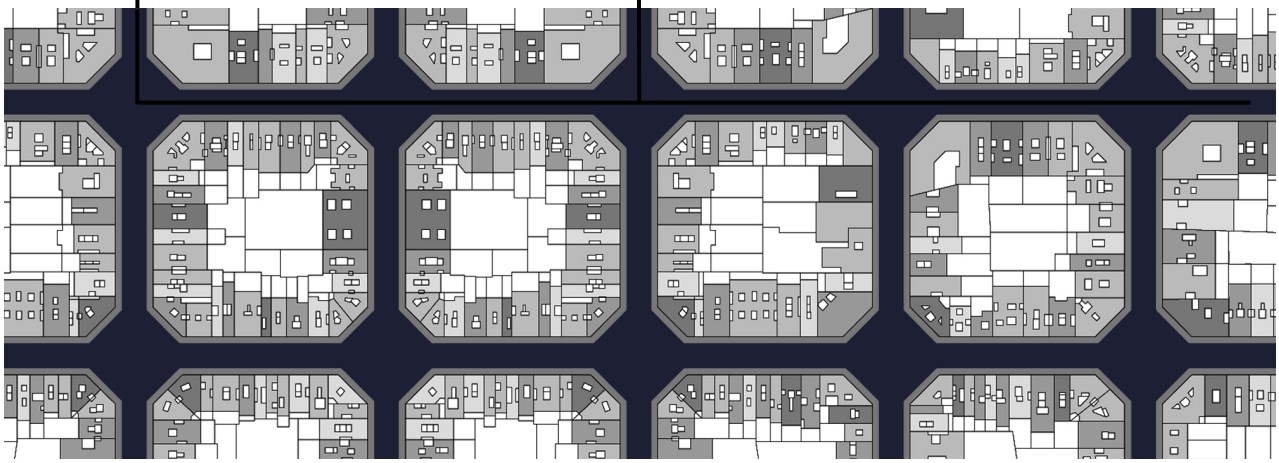

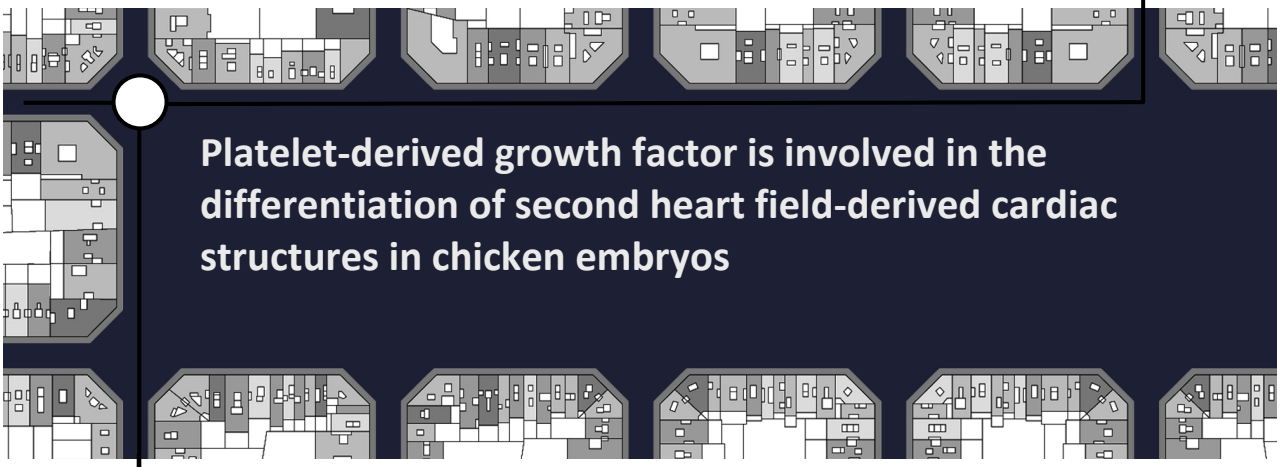

Platelet-derived growth factor is involved in the differentiation of second heart field-derived cardiac structures in chicken embryos

Noortje AM Bax, Heleen Lie-Venema, Rebecca Vicente-Steijn, Steven B Bleyl, Nynke MS van den Akker, Saskia Maas, Robert E Poelmann, Adriana C Gittenberger-de Groot

Modified after Developmental Dynamics 2009;238:2658-2669

Abstract

For the establishment of a fully functional septated heart, addition of myocardium from second heart field-derived structures is important. Platelet-derived growth factors (PDGFs) are known for their role in cardiovascular development. In this study, we aim to elucidate this role of PDGF-A, PDGF-C and their receptor PDGFR-α. We analyzed the expression patterns of PDGF-A, -C and their receptor PDGFR-α during avian heart development. A spatiotemporal pattern of ligands was seen with colocalization of the PDGFR-α. This was found in second heart field-derived myocardium as well as the proepicardial organ and epicardium. Mechanical inhibition of epicardial outgrowth as well as chemical disturbance of PDGFR-α support a functional role of the ligands and the receptor in cardiac development.

Introduction

The establishment of a fully septated heart is dependent on the addition of cells from a second heart cell lineage to the primary heart tube.[1-3] The second heart field or second lineage is located in the splanchnic mesoderm and can be divided into two fields related to the craniocaudal axis of the primary heart tube. From the second heart field myocardium is added at the outflow tract (OFT) or arterial pole (anterior heart field (AHF)).[2] Myocardium added to the inflow tract (IFT) or venous pole is also derived from the second heart field, and has been referred to as posterior heart field (PHF).[3,4] The outermost layer of the heart, the epicardium, develops initially as a cauliflower-like mesothelial primordium, the proepicardial organ (PEO), which is located near the sinus venosus.[5-7] In our view, the PEO is part of the PHF-derived structures.[4] Cells from the PEO traverse the pericardial cavity and spread out over the myocardial surface. Soon after the heart is covered, a subepicardial space develops between the epicardium and myocardium, which becomes populated by epicardium-derived cells (EPDCs). Subsequently, a subpopulation of EPDCs migrates into the myocardial interstitium to form interstitial fibroblasts, and smooth muscle cells and fibroblasts of the coronary vasculature.[8-10] Furthermore, EPDCs migrate into the atrioventricular (AV) endocardial cushions where they are involved in the differentiation of the atrioventricular valves.[9-11]

Proper outgrowth of the PEO and the epicardium, as well as normal interaction between EPDCs and developing cardiomyocytes are indispensable for normal cardiogenesis.[11-13] Several signalling pathways involved in epithelial-to-mesenchymal transformation (EMT), migration and differentiation of the epicardium and EPDCs in normal heart development have been described.[7] The initiation of EMT is regulated by many transcription factors, including Slug and Wilm's tumor supressor protein 1 (WT-1), and by retinoic acid (RA)-synthesizing enzyme RALDH2. These factors are also important for epicardial-myocardial interaction.[14-16] Recently a role for podoplanin and RhoA in this EMT process has been described.[17]

The platelet-derived growth factor (PDGF) family comprises regulators involved in epicardial-myocardial signalling and have been investigated in relation to coronary vascular development.[18,19] In our current study, we have extended this investigation to epicardial-myocardial interaction in pre-vascular stages. We also investigated the, in chicken cardiovascular development hitherto undescribed, PDGF-C expression and the expression of the ligand PDGF-A and their receptor PDGFR-α. The PDGF family consists of five dimeric isoforms, PDGF-AA, -AB, -BB, -CC and -DD. The PDGF receptor-α (PDGFR-α) and receptor-β (PDGFR-β), are receptor tyrosine kinases that can form homo- and heterodimers upon ligand binding.[20-23] Evidence for a functional role of PDGFs in avian heart development was provided by our description of the PDGF and PDGFR expression patterns in proepicardial quail/chicken chimeras. The spatiotemporal localization of PDGF-B and its receptors suggested that PDGF-B signalling through PDGFR-β was important for EPDC-related maturation of the

coronary system and atrioventricular valves.[18] Recent data in mice revealed that PDGFR-β is required for epicardial cell migration and development of coronary vascular smooth muscle cells.[24]

The localization of PDGF-A and its α-receptor showed that PDGF-A signalling through PDGFR-α was important for remodelling of the myocardium,[18] possibly, like in the mouse, through epicardial-myocardial interactions.[25,26] The role of PDGF-A and -C during development has been investigated in several null-mutant and over-expression mouse models. Phenotypical features of the *Pdgfc*$^{-/-}$ mice largely overlap with those of *Pdgfa*$^{-/-}$ mice, without a cardiac phenotype.[27-29] The hearts of the *Pdgfc*$^{-/-}$*Pdgfa*$^{-/-}$ double mutants, however showed lack of atrial septum formation.[28,29]

Patch mutants, with a spontaneous mutation of the PDGFR-α gene, showed severe heart malformations, including hypoplastic hearts and malformed valves. The number of adventitial fibroblasts in the coronary vessels was decreased and a locally thinned myocardium was observed in both models.[22,30,31] Thin compact myocardium is additionally observed in several models with defects in epicardial development. In these models there is disturbed or delayed outgrowth of the PEO, either by mechanical[12,13,32] or by genetic intervention.[4,14,33,34]

PDGF-C plays a role as a fibroblast mitogen. In the heart, it induced strong proliferation of myocardial interstitial fibroblasts.[29] Expansion of the cardiac interstitium in transgenic *Pdgfc* overexpression mice caused an altered myocardial architecture and an increased thickness of the ventricular walls.[35,36]

We hypothesize that PDGF-C, a recently discovered ligand for the PDGFR-α, is also involved in avian heart development. Therefore, we analysed the expression patterns during development of PDGF-A, PDGF-C and their receptor PDGFR-α in the avian heart. We observed that their expression was spatiotemporally related to the development of the second heart field-derived myocardium and to the proepicardium and epicardium. Analysis of embryos with mechanical inhibition of epicardial outgrowth as well as pharmaco-chemical disturbance of Pdgfrα-signalling support a functional role of the ligands and the receptor in development of proepicardial derivates and in cardiac development.

Materials and Methods

Chicken embryos

Fertilized eggs of White Leghorn chicken (*Gallus domesticus*) were incubated at 37^{o}C and 80% humidity. Embryos were isolated as described earlier[37] and staged according to Hamburger and Hamilton (HH[38]) criteria. Controls consisted of a developmental series of normal chicken embryos from stage HH17 to HH35 (n=3 per stage).

Inhibition of outgrowth of the proepicardial organ (PEO) in chicken embryos (HH15 to HH18) was achieved by placing a piece of egg shell membrane between the PEO and

the heart tube, as described earlier.[13,39] After reincubation, embryos were isolated at stages HH20 to HH28 (n=5 per stage). The embryos were fixed in 20% dimethylsulfoxide (DMSO) and 80% methanol for immunostaining with PDGFR-α or in 4% paraformaldehyde (PFA) for 24-48 hrs for all other staining protocols. Subsequently, they were embedded in paraffin and 5 µm serial sections were mounted on egg white/glycerine-coated microscope slides (Menzel-Gläser).

Pdgfra inhibition in chick

For PDGFR-α inhibition experiments,[40] the receptor tyrosine kinase (RTK) inhibitor Imatinib (STI571/Gleevec, Novartis Pharma AG, Switzerland) was used. Briefly, Imatinib tablets (100 mg) were dissolved in sterile saline with penicillin and streptomycin at room temperature, filtered and diluted to a 0.125 mg/ml working solution. Fertilized eggs were windowed at HH15 and treated with three doses of RTK inhibitors at 8-hour intervals. In separate experiments, 200 µl of Imatinib solution was added directly on top of the vitelline membrane at doses of 45, 75, 90, 150, 275 and 350 µg, while control embryos were treated with saline/antibiotic. For all *in ovo* inhibition experiments, embryos were inspected under a dissecting microscope at each dose for viability, assessing the correct stage of development and abnormalities. After treatment, embryos were reincubated for an additional 48-56 hours *in ovo* until 5 days of development (HH26-HH27). The embryos were fixated in modified Bodian's fixative at 4^{o}C overnight. Subsequently, they were sectioned and stained with Mayer's haematoxylin and eosin.

Western blotting

Previous performed Western blots of PDGF-A and PDGFR-α confirmed the specificity of these antibodies.[18] To confirm the specificity of the polyclonal antibody PDGF-C in chicken embryonic material, we also performed Western blots. In short, total protein was extracted from hearts of normal chicken embryos in 0.1 M Tris HCl with 0.1% Tween (pH7.5). The total protein content of the extracts was determined using the Ecl Advance Detection Kit (Amersham Biosciences). The results showed that the antibody specifically recognized the PDGF-C protein. Although PDGF-C can be secreted in a latent form and for activation cleavage of the N-terminal CUB domain by Tissue plasminogen activator (tPA) is necessary, we assume that regions with expression of PDGF-C are regions with potential activity.

Immunohistochemistry

Serial sections were subjected to standard immunohistochemical procedures.[4,18] Microwave antigen retrieval was applied for the PDGFR-α, cTnI, WT-1, Isl-1, Tbx18 and Nkx2.5 staining. Endogenous peroxidase was inactivated with 0.3% H_2O_2 in PBS. Before incubation with the primary antibodies, sections of chicken embryos selected

for the PDGF-C staining were blocked with 5% bovine serum albumin (BSA) in 0.05% Tween/PBS for 15 minutes. Sections were incubated overnight with rabbit-α-human PDGF-A (α-PDGF-A, 1:25; SC-128, Santa Cruz Biotechnology), goat-α-human PDGF-C (α-PDGF-C, 1:150, SC-18228, Santa Cruz Biotechnology), goat-α-human PDGFR-α (α-PDGFR-α, 1:50, P2110, Sigma-Aldrich), rabbit-α-human Wilm's tumor suppressor protein (α-WT-1, 1:500, CA1026, Calbiochem) goat-α-human Nkx2.5 (α-Nkx2.5, 1:6000, SC-8697 Santa Cruz Biotechnology), goat-α-human Tbx18 (α-Tbx18, 1:800, SC-17867, Santa Cruz Biotechnology), mouse-α-Isl-1 39.4D5 (α-Isl-1, 1:400, Developmental Studies Hybridoma Bank), goat-α-human cardiac Troponin I (cTnI, 1:400, SC-8118 Santa Cruz Biotechnology) or anti-atrial myosin light chain 2 (α-MLC-2a, 1:6000, which was kindly provided by S.W. Kubalak, Charleston, SC), followed by incubation with a secondary biotin-labelled antibody for 1 hr. Secondary antibodies used were biotin-labelled goat-α-rabbit (BA-1000, Vector Labs), horse-α-mouse (BA-2000, Vector Labs) and horse-α-goat (BA-9500, Vector Labs) in combination with normal goat serum (S-1000, Vector Labs) or normal horse serum (S-2000, Vector Labs), respectively. Subsequently, the sections were incubated with Vectastain ABC staining kit (PK-6100, Vector Labs) for 45 minutes. Slides were rinsed in PBS and Tris/Maleate (pH 7.6). 3-3'diaminobenzidine tetrahydrochloride (DAB) (D5637, Sigma-Aldrich) was used as chromogen and Mayer's haematoxylin as counterstaining. Finally, all slides were dehydrated and mounted with Entellan (Merck).

In situ hybridization

Sense and anti-sense digoxigenin-labeled riboprobes were used as previously described.[41,42] Probes were synthesized from chick *Pdgfr*α clones (ChEST55k2) and from chick *Pdgf*-α ligand clones (ChEST826l7). Sections were examined with a Nikon compound microscope using a QImaging CCD camera with QCapture software (QImaging, Burnaby, Canada).

Results

At subsequent stages of development expression patterns of PDGF-A, PDGF-C and their receptor PDGFR-α were analysed in the chicken heart (Figure 4.1). In addition, we examined embryos in which we mechanically inhibited epicardial outgrowth as well as embryos treated with Imantinib to block PDGF-signalling. In both experimental designs the role of epicardial-myocardial interaction in relation to PDGF was investigated.

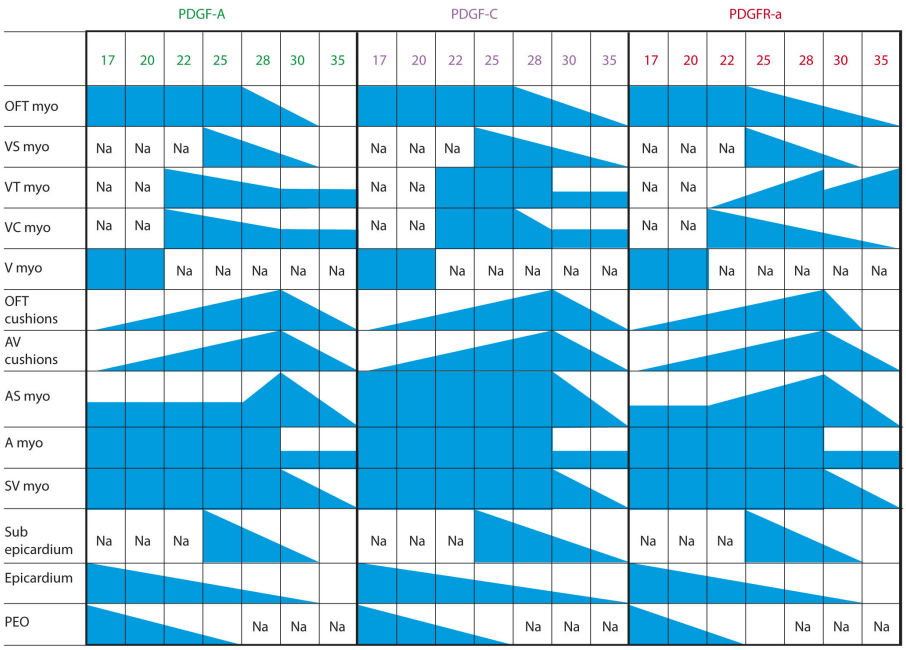

Figure 4.1 Summary of the spatiotemporal protein expression of platelet-derived growth factor (PDGF)-A, PDGF-C and their receptor PDGFR-α in the avian heart. This table displays alterations in protein expression per heart area at different Hamburger and Hamilton (HH) stages. Filled squares represent maximum intensity at that stage for the specific compartments. Partially filled squares represent increase and decrease of expression. A, atrial; AS, atrial septum; AV, atrioventricular; myo, myocardium; Na, not applicable; OFT, outflow tract; PEO, proepicardial organ; V, ventricular; VC, ventricular compact; VS, ventricular septum; VT, ventricular trabecular, SV, sinus venosus.

Expression of PDGF-A and PDGF-C

At HH17, staining of PDGF-A and PDGF-C was present in the complete myocardium of the heart, comprising the sinus venosus, the atrium, the ventricle, and the OFT (Appendix Figure 4.A1). The PEO as well as the villous protrusions of the PEO connecting to the myocardium were also positive for both ligands.

At stage HH20, the epicardium and the developing atrial septal myocardium had also become positive for PDGF-A and -C (Appendix Figure 4.A1). The expression levels in the PEO were decreased in comparison to HH17.

At HH22, the myocardial wall of the sinus venosus, including the sinoatrial node (SAN) region as well as a cluster of cells medial to the left cardinal vein (LCV), expressed both ligands comparable to stage HH20. In the AV cushions, the mesenchymal cell population contained positive and negative cells for both PDGF-A and -C. The expression pattern in the OFT cushions was comparable to that in the AV cushions.

The ventricular compact and trabecular myocardium could be discerned separately at this stage and both layers were positive for PDGF-A and -C. Less cells were positive in the epicardium and PEO compared to HH20.

At stage HH25, the trabecular myocardium of the ventricle showed more marked expression of PDGF-A and -C compared to the compact myocardium, especially in the inner part of the trabecular myocardium. This phenomenon was more distinct for PDGF-A than for PDGF-C (Appendix Figure 4.A1). This became clearer near the apex. The myocardium of the developing ventricular septum was positive for both ligands. The number of mesenchymal cells in the AV and OFT cushions that stained positive for both ligands was increased compared to previous stages, especially more cells in the subendocardial region of the cushions had become positive. The epicardial cells, fully covering the ventricular myocardium, and the EPDCs in the subepicardium showed a mosaic pattern for PDGF-A and -C expression. Compared to previous stages, there was an ongoing decrease in the number of positive cells in these two layers.

At HH28, the expression of both ligands in the atrial wall was comparable to earlier stages. There was a slightly more intense PDGF-A staining in the atrial septum (Fig. 2d), while the expression of PDGF-C was not altered (Figure 4.2a, 4.2g). The cell population of the AV and OFT cushion mesenchyme showed more positive cells near the subendocardial border compared to stage HH25. A more marked expression of PDGF-C in the ventricular trabecular myocardium was observed compared to the compact myocardium (Figure 4.2b, 4.2h). The expression of PDGF-A decreased in both layers of the myocardium, being still more distinct in the trabecular myocardium (Figure 4.2e). There was also a decrease in expression of both ligands in the OFT myocardium at HH28 (Figure 4.2c, 4.2f, 4.2i). The PEO had become negative for PDGF-A and -C. The subepicardium and epicardium, referred to hereafter as (sub)epicardium, showed less positive cells for both ligands compared to HH25.

At stage HH30, a clear decrease in PDGF-A and -C expression in the complete heart was observed. In the ventricular septal myocardium staining of PDGF-A had become weak in comparison to the ventricular compact and trabecular myocardium. In the AV and OFT cushion mesenchyme expression of both ligands was diminished. The majority of the cells of the (sub)epicardium were negative at this stage.

At the last stage we analysed, HH35, the expression of both ligands in the wall of the sinus venosus including the SAN region was decreased compared to HH30. The expression in the atrial wall was comparable to the previous stage, while the expression of both PDGF-A and -C was diminished in the atrial septum. The decrease of expression of both ligands in the AV and OFT cushion mesenchyme continued at this stage. The expression patterns of the ventricular compact and trabecular myocardium had not changed compared to stage HH30. The ventricular septum was negative for PDGF-A, while the expression of PDGF-C in the ventricular septum had decreased at this stage. A similar observation was made for the OFT myocardium. All the cells of the (sub)epicardium were negative for PDGF-A, while some cells were still positive for PDGF-C.

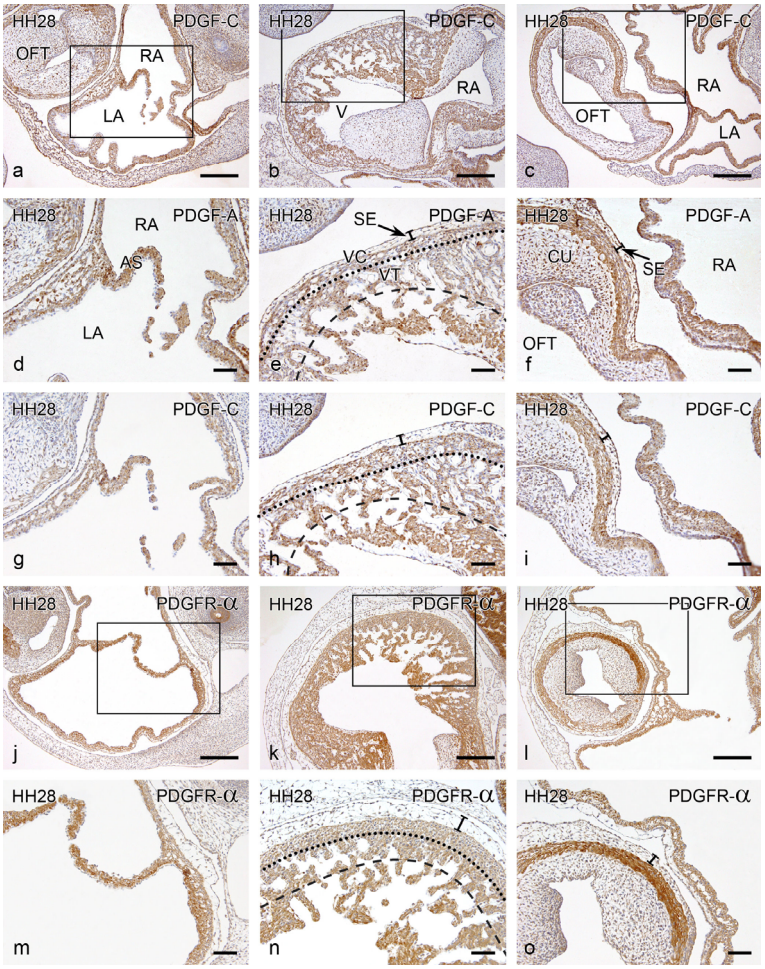

Figure 4.2 Expression of platelet-derived growth factor (PDGF)-A, -C and PDGFR-α in chicken hearts of Hamburger and Hamilton (HH) stage 28. Photomicrographs of representative transverse sections show expression of PDGF-A, -C and their receptor in the atrial wall and atrial septal (AS) myocardium (**a,d,g,j,m**). Boxed regions in lower magnification panels correlate to higher resolution images. The expression of PDGF-A and its receptor is more distinct in the AS myocardium compared to the myocardium of the atrial wall (**d,j,m**). PDGFR-α and its ligands are expressed more prominently in the ventricular trabecular (VT) myocardium compared to the ventricular compact myocardium (VC) (delineated with a dotted line) (**b,e,h,k,n**), especially in the inner part of the VT (delineated with a dashed line). Staining of PDGFR-α is more marked in the outflow tract (OFT) myocardium in comparison to the atrial myocardium (**l,o**). For the ligands the staining is comparable between the OFT and atrial myocardium (**c,f,i**). LA, left atrium; RA, right atrium; SE, subepicardium; CU, cushions. Scale bars: 200 µm (a-c, j-k), and (d-i, l-o) 60um.

Cardiac expression of PDGFR-α

To investigate the relation between PDGF-A and PDGF-C in heart development, we analyzed the protein expression of their common receptor PDGFR-α at the same developmental stages. At stage HH17 and HH20 the receptor colocalized with its ligands spatiotemporally in all previously described parts of the heart (Figure 4.1 and Appendix Figure 4.A1).

At stage HH22, colocalization of PDGFR-α with both ligands was seen in the myocardial wall of the sinus venosus including the SAN region, the atrial myocardium, the cells of the AV and OFT cushion mesenchyme, both the compact and trabecular myocardium of the ventricles and the OFT myocardium. At this stage, the expression of the receptor was increased in the atrial septum compared to HH20. In the PEO and the epicardium the expression of PDGFR-α colocalized to both PDGF-A and -C and was decreased in comparison to previous stages.

At HH25, receptor expression was further increased in the atrial septum (Appendix Figure 4.A1). The expression pattern of the receptor in the mesenchymal cells of the AV and OFT cushions was comparable to that of both ligands. In the ventricular myocardium, decreasing PDGFR-α levels in the compact myocardium coincided with increasing levels in the trabecular zone compared to HH22. The myocardium of the developing ventricular septum was positive. In general, the staining signal of the receptor was more dense in the OFT myocardium in comparison to that of the atrial myocardium, while for the ligands the staining levels were comparable between the OFT and atrial myocardium (Appendix Figure 4.A1). The expression of receptor-α was decreased in the OFT myocardium compared to HH22. At this stage, the PEO was negative for PDGFR-α. The (sub)epicardium showed both cells that were positive or negative like the staining for the ligands.

At stage HH28, the staining of PDGFR-α was comparable to HH25, as there was still a marked expression of receptor-α staining in the atrial septum compared to the atrial wall (Figure 4.2j, 4.2m). More cells in the subendocardial region of the AV and OFT cushion mesenchyme were positive compared to stage HH25. In the ventricular compact myocardium the expression of PDGFR-α decreased compared to the increasing expression in the trabecular myocardium (Figure 4.2k, 4.2n). There was also a decrease of expression in the OFT myocardium. The staining signal of the receptor was still more marked in the OFT myocardium in comparison to the atrial myocardium (Figure 4.2l, 4.2o), while for the ligands the expression levels were still comparable between the OFT and atrial myocardium at this stage (Figure 4.2c, 4.2f, 4.2i). In the (sub)epicardium less cells were positive for the receptor compared to HH25.

Comparable to the expression patterns of PDGF-A and -C at stage HH30, there was a decrease in PDGFR-α expression in the complete heart. The contrast between PDGFR-α expression in the OFT myocardium and atrial myocardium had disappeared. Furthermore, the contrast between ventricular septal myocardium and both layers of the ventricular myocardium was comparable to PDGF-A at this stage. In the AV and

OFT cushion mesenchyme the decrease in expression was comparable to both ligands. The majority of the cells of the (sub)epicardium were negative at this stage.
At stage HH35, the expression of PDGFR-α in the wall of the sinus venosus including the SAN region, AV and OFT cushion mesenchyme decreased compared to HH30. The expression pattern of the atrial wall and in the atrial septum was comparable to both ligands. In the (sub)epicardium PDGFR-α was absent at this stage, comparable to PDGF-A. The expression levels in the trabecular myocardium were increased compared to those of stage HH30, while the expression in the compact myocardium decreased. Furthermore, the ventricular septum was negative comparable to PDGF-A. A decrease in PDGFR-α staining was also observed in the OFT myocardium.

PDGF expression related to the developing venous pole

The expression of PDGFs in the OFT myocardium and in the myocardial wall of the sinus venosus suggested a role of PDGFs in the development of the second heart field. To further investigate expression in the SHF in more detail, we focussed on the expression of PDGFR-α and the ligands PDGF-A and -C, specifically in the venous pole region. As myocardium at the venous pole region was characterized by the presence of MLC-2a and absence of Nkx2.5, we stained serial sections of HH22 embryos with antibodies against these proteins. WT-1 staining was used to identify epicardium and EPDCs that are derived from the PEO, developing in this region in HH19 embryos. In the myocardial wall of the sinus venosus including the developing SAN, both ligands and their receptor were present in MLC-2a positive (Figure 4.3a-b, 4.3d-e, 4.3g-h), and Nkx2.5 (Figure 4,3j-k) negative areas. In the sinus venosus myocardium and in the wall of the cardinal veins including the developing SAN (data not shown), Isl-1 positive cells were also observed. The developing SAN also expressed Tbx18 (data not shown). WT-1 positive cells of the PEO were also positive for PDGFR-α and its ligands (Figure 4.3c, 4.3f, 4.3o). Furthermore, the cells of the PEO lack both the myocardial markers cTnI and Nkx2.5 (Figure 4.3i, 4.3l). In situ hybridization data show that the PEO and the outgrowing epicardium expressed higher levels of *Pdgf*-α and *Pdgfr*α compared to the surrounding tissues (Appendix Figure 4.A2).

Effect of mechanical inhibition of epicardial outgrowth on PDGF expression

The expression of PDGF-A and PDGF-C in the PEO and in the epicardium suggested a possible role in development of the compact myocardium of the ventricles. Therefore, we performed inhibition of epicardial outgrowth at stage HH15-HH18 embryos, to investigate the effect on the expression patterns of both ligands and the receptor at several timepoints (HH20-HH28). Investigation of the collected embryos revealed that there were no marked morphological differences between controls and embryos with inhibited epicardial outgrowth at all timepoints until HH25 (data not shown). At stage HH25 and HH28, subepicardium covering the ventricular myocardium was absent in

nine embryos. As the two stages were phenotypically comparable, we described the expression of PDGF-A, -C and their receptor PDGFR-α at stage HH28.

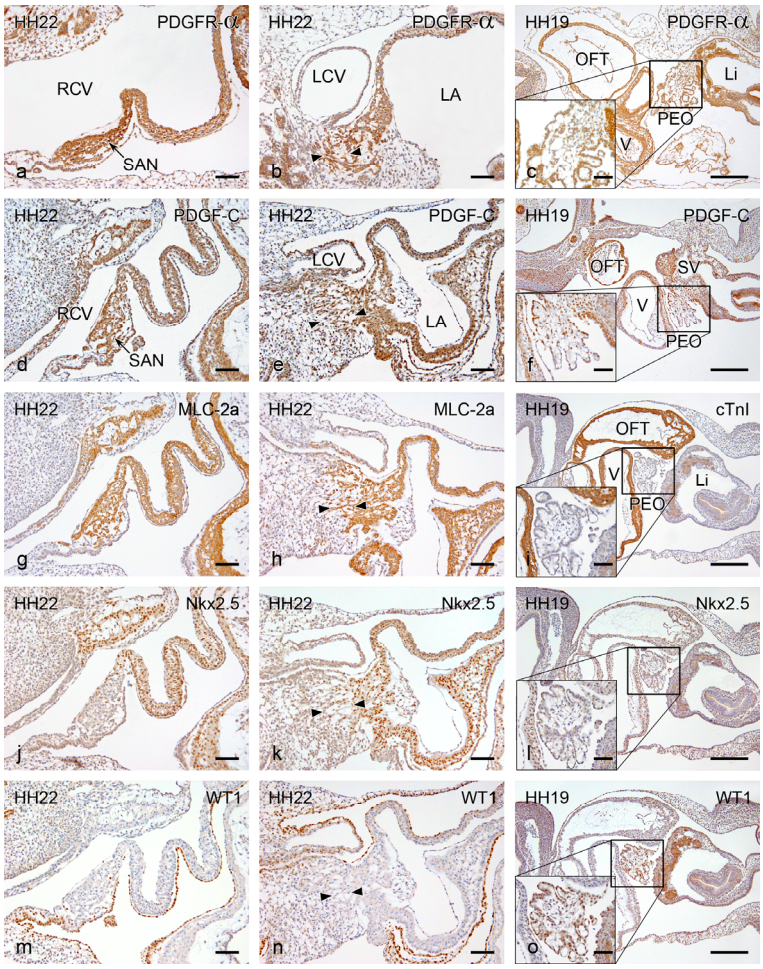

Figure 4.3 Platelet-derived growth factor (PDGF) is expressed in the myocardium at the venous pole of the heart. Photomicrographs show representative transverse sections of the left and right cardinal vein (LCV, RCV), sinoatrial node (SAN) region, proepicardial organ (PEO) and epicardium. Panels **d-f** show expression of PDGF-C and panels **a-c** the expression of its receptor PDGFR-α. Panels **g-h** show expression of MLC-2a in the myocardium surrounding the LCV, RCV, developing SAN and sinus venosus myocardium (marked by arrowheads). The PEO and epicardium are marked by WT-1 expression (**o**). There is no expression of the myocardial marker cTnI (**i**) and of Nkx2.5 in the PEO (**l**). At stage HH19 the PEO and epicardium (**c,f**) are positive for PDGFR-α and its ligand PDGF-C. Panels **j-l** show negative Nkx2.5 staining in the wall of the LCV, RCV and developing SAN. Arrowheads show the Nkx2.5 negative zone of the sinus venosus (SV) myocardium (**k**). OFT, outflow tract; V, ventricle; LA, left atrium; Li, liver. Scale bars: 60 µm (a-b,d-e,g-h,j-k,m-n), 20 µm in magnification box (c,f,i,l,o).

Partial inhibition of epicardial outgrowth was observed in 5 hearts. These hearts showed absence of subepicardium covering the ventricular myocardium, but have some subepicardium in the sulcus area (Figure 4.4b, 4.4e, 4.4h). Using immunohistochemistry, the expression of PDGFR-α was investigated in two hearts with partial inhibition of epicardial outgrowth. Expression of the receptor in the compact and trabecular layer of the ventricular myocardium of these embryos was less intense in comparison to the control embryos (Figure 4.4r-u),

Two hearts had a complete inhibition of epicardial outgrowth, as there was no subepicardium in the sulcus area (Figure 4.4c, 4.4f, 4.4i) and covering the ventricular myocardium, and these were used to investigate expression of the ligands. In the subendocardial region of the AV cushions of embryos with a complete inhibited outgrowth of epicardium, there was a decrease in number of cells that expressed PDGF-A and PDGF-C (Figure 4.4c, 4.4f, 4.4i). This decrease was more marked for PDGF-C compared to PDGF-A. In the AV cushions of hearts with a partial inhibition of epicardial outgrowth this decrease in expression was not observed (Figure 4.4b, 4.4e, 4.4h).

There was no subepicardium covering the ventricles of embryos with either partial or complete inhibition of epicardial outgrowth (Figure 4.4l-m, 4.4p-q). Expression of PDGF-A and -C in the compact and trabecular layer of the ventricular myocardium of these embryos was more intense in comparison to the control embryos (Figure 4.4j-q), showing also less cells forming the lining epicardium. The few remaining epicardial cells were mostly negative for the ligands, compared to controls presenting more positive epicardial cells (Figure 4.4k, 4.4m, 4.4o, 4.4q).

Pharmacochemical inhibition of PDGF-signaling

As PDGFs were expressed in the PEO and (sub)epicardium and PDGFs were altered with mechanical inhibition of epicardial outgrowth, we examined the effect of pharmaco-chemical inhibition of PDGF-signalling using Imantinib to elucidate a functional role of PDGFs in epicardial-myocardial interaction.

At stage HH25-27, Imantinib treated embryos demonstrated absence of subepicardium (33%) covering the ventricular myocardium, comparable with the embryos with inhibition of epicardial outgrowth (Appendix Figure 4.A3). The epicardial layer was in several areas not properly attached to the myocardium (Appendix Figure 4.A3). The dose-dependent incidence of other defects, comparable with defects in PDGFR-α deficient mice[22,43] including neural tube defects and subepidermal hemorrhages, in these Imantinib-treated embryos suggested that PDGF-signalling was being inhibited.

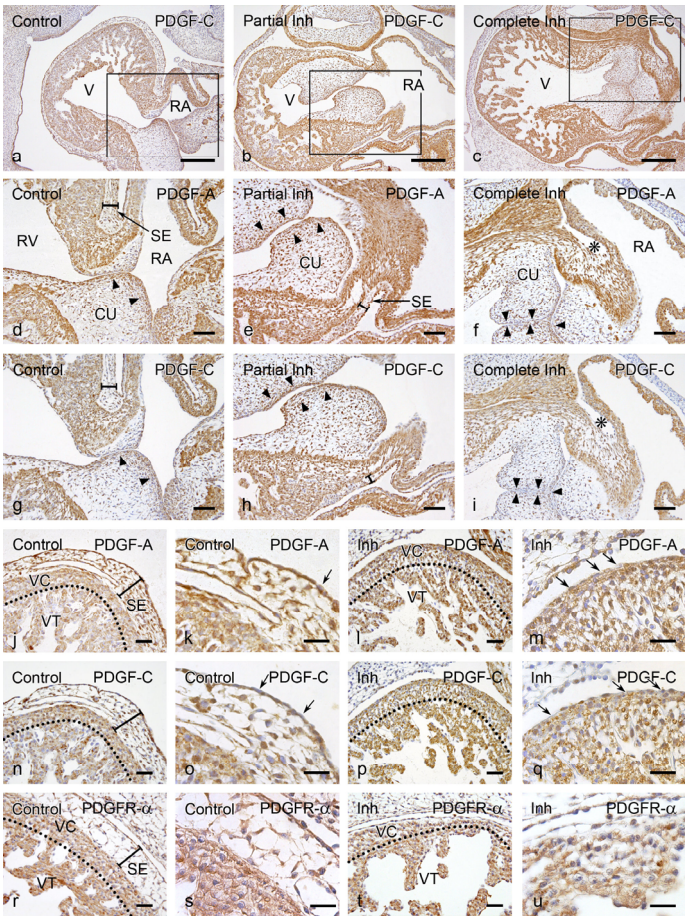

Figure 4.4 Expression of PDGF-A, and -C at stage HH28. Transverse sections show control chicken hearts (**a,d,g,j,n,r**) and hearts with partial (**b,e,h**) and complete inhibition of epicardial outgrowth at stage HH28 (**c,f,i-j,l-m,p-q,t-u**). Boxed areas in pictures **a-c** correlate to magnified areas in pictures **d-i**. Photomicrographs show representative sections of the atrioventicular (AV) groove, the atrioventricular cushions (CU), right ventricle (RV) and right atrium (RA). Subepicardium (SE) in the AV-groove is absent in the heart of embryos with a complete inhibited epicardial outgrowth (asterisk). In the control embryos and embryos with a partial inhibition of epicardial outgrowth the AV-groove is covered with SE (marked with thickness bar). The expression of PDGF-A (**e**) and -C (**b,h**) is located specifically in cells of the subendocardial region of the atrioventricular cushions mesenchyme in controls and embryos with a partial inhibition. In contrast, in the embryos with complete inhibition of epicardial outgrowth we observe a decrease in expression of PDGF-A (arrowheads in **e**) and PDGF-C (arrowheads in **k**) in this region. Subepicardium covering the ventricles is absent in embryos with either partial or complete inhibition of epicardial outgrowth (**l-m,p-q,t-u**). In these embryos less cells formed the lining epicardium and relatively fewer cells are positive for PDGF-A and -C (arrows in panels **m,q**). In the compact (VC) and trabecular (VT) layer of the ventricular myocardium, delineated with a dotted line, of the embryos with either partial or complete inhibition of epicardial outgrowth we observe a higher expression of PDGF-A (**l-m**) and -C (**p-q**) and less expression of PDGFR-α (**t-u**) compared to the control embryos (**j-k,n-o, r-s**). Scale bars: 200 µm (a-c), 60 µm (d-i), 30 µm (j,l,n,p,r,t) and 20 µm (k,m,o,q,s,u).

Discussion

We described cardiac expression patterns of PDGF-A, -C and their receptor PDGFR-α in the developing avian embryo, highlighting stages HH17-HH35. Furthermore, we have demonstrated that inhibition of epicardial outgrowth alters expression of both ligands and their receptor in the ventricular myocardium. We also showed abnormal epicardial development after PDGF inhibition supporting a functional role for PDGFs in epicardial development.

At the venous pole, the sinus venosus myocardium is derived from a specific area of the second heart field, for which we reserved the term posterior heart field (the PHF) as opposite to the arterial pole.[3] The myocardial component of this specific venous pole area is characterized by the expression of the myocardial marker MLC-2a combined with lack of staining for Nkx2.5.[3,44] The expression of MLC-2a colocalized with both ligands and their receptor in areas that were Nkx2.5 negative. An important role for PDGF in the development of the venous pole and the sinus venosus myocardium-derived structures is supported by the *Patch* (spontaneous mutation of the PDGFR-α gene) mutant mice showing abnormalities of the cardinal veins[18,43] and atrial septal defects.[30] Atrial septal defects are also observed in *Pdgfc*$^{-/-}$*Pdgfa*$^{-/-}$ double mutant mice.[30,45] We showed increase in expression of PDGFR-α in the developing atrial septum from stage HH22 onwards, further supporting the hypothesis that PDGFR-α is important herein.

A role for PDGFs in the development of the AV cushions is suggested by the staining for both of the ligands and their receptor in these structures. PDGFR-α is crucial, because *Patch* mutant mice fail to develop AV cushions.[43] We also see a diminished expression of PDGF-A and -C in the AV cushions of our embryos with complete inhibition of epicardial outgrowth. This is probably caused by impaired migration and subsequent impaired cell contribution of EPDCs to the AV cushions.[11] Normally, EPDCs invade the cushion mesenchyme directly and may influence EMT of the endocardium.[9-11,14] As embryos with partial inhibition of epicardial outgrowth have a subepicardium in the AV region and EPDCs are still present, this might explain why in these embryos the expression patterns of PDGF-A and -C are not affected.

The venous pole area not only provides myocardial progenitor cells to the heart, but most probably contributes mesenchymal progenitor cells to the PEO and subsequent epicardium and EPDCs.[4] Although the PEO and epicardium are positive for PDGF-A and -C, it is most likely that both ligands are not required for this contribution from the venous pole area as no alterations in PEO and epicardium development have been described or investigated in *Pdgfa*$^{-/-}$, *Pdgfc*$^{-/-}$ and *Pdgfc*$^{-/-}$*Pdgfa*$^{-/-}$ double mutants.[45] PDGFR-α was also expressed in the PEO and the epicardium until HH25. A role for PDGFR-α in epicardial development is supported by the finding that embryos treated with Imantinib have no subepicardium covering the ventricular myocardium. Furthermore, *Patch* mutants show a thin myocardium and malformed AV cushions.[30] Impaired PDGF-B/PDGFR-α-signalling could be at the basis of this altered epicardial

outgrowth, because PDGF-B mutants have extreme myocardial hypoplasia[19] and PDGF-B is able to induce epicardial EMT *in vitro.*[46] A role for PDGF-B/Pdgfrβ-signalling cannot be ruled out for altered epicardial outgrowth, because Imantinib also blocks other RTKs including PDGFR-β and the KIT proto-oncogene.[40]

The expression of PDGF-A, -C and receptor-α in the epicardium and the ventricular compact myocardium, supported by the fact that PDGF-A is an epicardial mitogen during heart development,[26] suggest that the ligands induce cardiomyocyte proliferation and proliferation of the epicardium in a paracrine and/or autocrine fashion. *Pdgfc*$^{-/-}$*Pdgfa*$^{-/-}$ double mutant mice revealed that PDGF-A and PDGF-C were not required for normal ventricular compact zone development.[45] In contrast, PDGFR-α knockout mice show hypoplastic hearts probably due to decreased proliferation-rate of cardiomyocytes possibly through the lack of PDGF-B/Pdgfrα-signalling.[19] Cardiomyocyte proliferation alone is probably insufficient for proper ventricular myocardial development, it is suggested that interstitial fibroblasts are necessary for establishing the myocardial architecture.[4,7,34] PDGF-A is a potent mitogen for cardiac fibroblasts[47] and overexpression of PDGF-C in mice at 3 months of age upregulated PDGFR-α mRNA and increased fibroblast proliferation leading to cardiac fibrosis and hypertrophy.[36] These data combined with the expression patterns of PDGF-A and -C and their receptor in the epicardium suggest a functional role for epicardium-dependent development of the ventricular myocardium for both ligands and their receptor. This is supported by our experimental data, in which the expression of both ligands and their receptor is altered in trabecular and compact ventricular myocardium of embryos with inhibited epicardial outgrowth as well as by the absence of subepicardium in Imantinib treated embryos.

We observed that both ligands and their receptor lose their subepicardial expression over time, during normal heart development when the subepicardium is formed between the epicardium and myocardium. In embryos with an inhibited epicardial outgrowth the subepicardium covering the ventricles was absent and a higher myocardial expression of ligand-A and -C and a lower myocardial expression of PDGFR-α was observed compared with control embryos. In the embryos treated with Imantinib there was no subepicardium. Therefore, in both experiments EPDCs were not able to migrate into the ventricular myocardium, resulting in abnormal interaction between epicardium and myocardium, which in turn could influence expression of both ligands and the receptor.

EPDCs that migrate into the myocardium are WT-1 positive[14] and transient transfection assays demonstrated a WT-1-mediated repression of PDGF-A. The absence of WT-1 positive EPDCs in the myocardium could therefore explain the increase of PDGF-A expression in embryos with inhibited epicardial outgrowth.[48] Recent data in mice showed that PDGFR-α is expressed by epicardial cells after they have migrated into the myocardium.[24] We suggest that in chicken embryos lacking subepicardium the altered expression of the receptor in the ventricular myocardium is caused by a markedly diminished number of EPDCs in the ventricle.

In the ventricular trabecular myocardium expression of PDGF-A and receptor-α became more restricted during subsequent stages.[18] Stimulation of trabecular formation by PDGF-A/PDGFR-α is suggested by impaired trabecular formation in the *Patch* mouse.[43] Expression of PDGF-A and -C in the ventricular septum suggests an activating role for PDGFR-α in the contribution of myocardium to the developing septum as *Patch* mice suffer from ventricular septal defects.[30]

The PDGF-expression patterns in the OFT myocardium and cushion mesenchyme indicate the recruitment of cells from the second heart field. These expression patterns correlate with preferential sites of cardiac malformations in the *Patch* mouse.[30,43] At chicken stage HH28 when expression of ligand-A and -C are decreased, we postulate that the addition of cells to the OFT myocardium and cushion mesenchyme from the second heart field seems to be completed. Alternatively, the role of PDGF in this contribution had become less important.

In conclusion, spatiotemporal expression patterns of PDGF-A and PDGF-C indicate that these ligands are overlapping and probably redundant in heart development. Expression of PDGF-A and PDGF-C and their receptor PDGFR-α suggests an activating role in remodelling of the myocardium of both outflow and inflow tract. Furthermore, PDGF-A, -C and PDGFR-α are involved in the remodelling of the ventricular compact and trabecular myocardium through epicardial-to-myocardial interaction. There might be an EPDC-related contribution of PDGF to the development of the AV cushions. As a consequence, PDGF-A, -C and their receptor PDGFR-α are important in several processes of cardiac tissue remodelling during heart development.

References

1. Cai CL, Liang X, Shi Y, Chu PH, Pfaff SL, Chen J, Evans S. Isl1 identifies a cardiac progenitor population that proliferates prior to differentiation and contributes a majority of cells to the heart. *Dev Cell*. 2003;5:877-889.
2. Kelly RG. Molecular inroads into the anterior heart field. *Trends Cardiovasc Med*. 2005;15:51-56.
3. Gittenberger-de Groot AC, Mahtab EAF, Hahurij ND, Wisse LJ, DeRuiter MC, Wijffels MCEF, Poelmann RE. Nkx2.5 negative myocardium of the posterior heart field and its correlation with podoplanin expression in cells from the developing cardiac pacemaking and conduction system. *Anat Rec*. 2007;290:115-122.
4. Mahtab EAF, Wijffels MCEF, van den Akker NMS, Hahurij ND, Lie-Venema H, Wisse LJ, DeRuiter MC, Uhrin P, Zaujec J, Binder BR, Schalij MJ, Poelmann RE, Gittenberger-de Groot AC. Cardiac malformations and myocardial abnormalities in podoplanin knockout mouse embryos: correlation with abnormal epicardial development. *Dev Dyn*. 2008;237:847-857.
5. Vrancken Peeters M-PFM, Gittenberger-de Groot AC, Mentink MMT, Poelmann RE. Smooth muscle cells and fibroblasts of the coronary arteries derive from epithelial-mesenchymal transformation of the epicardium. *Anat Embryol*. 1999;199:367-378.
6. Viragh S, Gittenberger-de Groot AC, Poelmann RE, Kalman F. Early development of quail heart epicardium and associated vascular and glandular structures. *Anat Embryol*. 1993;188:381-393.
7. Lie-Venema H, van den Akker NMS, Bax NAM, Winter EM, Maas S, Kekarainen T, Hoeben RC, DeRuiter MC, Poelmann RE, Gittenberger-de Groot AC. Origin, fate, and function of epicardium-derived cells (EPCDs) in normal and abnormal cardiac development. *ScientificWorldJournal*. 2007;7:1777-1798.
8. Dettman RW, Denetclaw W, Ordahl CP, Bristow J. Common epicardial origin of coronary vascular smooth muscle, perivascular fibroblasts, and intermyocardial fibroblasts in the avian heart. *Dev Biol*. 1998;193:169-181.
9. Gittenberger-de Groot AC, Vrancken Peeters M-PFM, Mentink MMT, Gourdie RG, Poelmann RE. Epicardium-derived cells contribute a novel population to the myocardial wall and the atrioventricular cushions. *Circ Res*. 1998;82:1043-1052.
10. Manner J, Perez-Pomares JM, Macias D, Munoz-Chapuli R. The origin, formation and developmental significance of the epicardium: a review. *Cells Tissues Organs*. 2001;169:89-103.
11. Lie-Venema H, Eralp I, Markwald RR, van den Akker NM, Wijffels M, Kolditz DP, Van der Laarse A, Schalij MJ, Poelmann RE, Bogers A, Gittenberger-de Groot AC. Periostin expression by epicardium-derived cells (EPDCs) is involved in the development of the atrioventricular valves and fibrous heart skeleton. *Differentiation*. 2008;76:809-819.
12. Gittenberger-de Groot AC, Vrancken Peeters M-PFM, Bergwerff M, Mentink MMT, Poelmann RE. Epicardial outgrowth inhibition leads to compensatory mesothelial outflow tract collar and abnormal cardiac septation and coronary formation. *Circ Res*. 2000;87:969-971.
13. Eralp I, Lie-Venema H, DeRuiter MC, van den Akker NM, Bogers AJ, Mentink MM, Poelmann RE, Gittenberger-de Groot AC. Coronary artery and orifice development is associated with proper timing of epicardial outgrowth and correlated Fas ligand associated apoptosis patterns. *Circ Res*. 2005;96:526-534.
14. Perez-Pomares JM, Phelps A, Sedmerova M, Carmona R, Gonzalez-Iriarte M, Munoz-Chapuli R, Wessels A. Experimental Studies on the Spatiotemporal Expression of WT1 and RALDH2 in the Embryonic Avian Heart: A Model for the Regulation of Myocardial and Valvuloseptal Development by Epicardially Derived Cells (EPDCs). *Dev Biol*. 2002;247:307-326.
15. Merki E, Zamora M, Raya A, Kawakami Y, Wang J, Zhang X, Burch J, Kubalak SW, Kaliman P, Belmonte JC, Chien KR, Ruiz-Lozano P. Epicardial retinoid X receptor alpha is required for myocardial growth and coronary artery formation. *Proc Natl Acad Sci U S A*. 2005;102:18455-18460.
16. Winter EM, Gittenberger-de Groot AC. Cardiovascular development: towards biomedical applicability: Epicardium-derived cells in cardiogenesis and cardiac regeneration. *Cell Mol Life Sci*. 2007;64:692-703.

17. Mahtab EA, Vicente-Steijn R, Hahurij ND, Jongbloed MR, Wisse LJ, DeRuiter MC, Uhrin P, Zaujec J, Binder BR, Schalij MJ, Poelmann RE, Gittenberger-de Groot AC. Podoplanin deficient mice show a Rhoa-related hypoplasia of the sinus venosus myocardium including the sinoatrial node. *Dev Dyn*. 2009;238:183-193.
18. van den Akker NMS, Lie-Venema H, Maas S, Eralp I, DeRuiter MC, Poelmann RE, Groot ACG. Platelet-derived growth factors in the developing avian heart and maturating coronary vasculature. *Developmental Dynamics*. 2005;233:1579-1588.
19. van den Akker NM, Winkel LC, Nisancioglu MH, Maas S, Wisse LJ, Armulik A, Poelmann RE, Lie-Venema H, Betsholtz C, Gittenberger-de Groot AC. PDGF-B signaling is important for murine cardiac development: Its role in developing atrioventricular valves, coronaries, and cardiac innervation. *Dev Dyn*. 2008;237:494-503.
20. Heldin CH, Westermark B. Mechanism of action and in vivo role of platelet-derived growth factor. *Physiol Rev*. 1999;79:1283-1316.
21. Hoch RV, Soriano P. Roles of PDGF in animal development. *Development*. 2003;130:4769-4784.
22. Soriano P. The PDGFa receptor is required for neural crest cell development and for normal patterning of the somites. *Development*. 1997;124:2691-2700.
23. Fredriksson L, Li H, Fieber C, Li X, Eriksson U. Tissue plasminogen activator is a potent activator of PDGF-CC. *EMBO J*. 2004;23:3793-3802.
24. Mellgren AM, Smith CL, Olsen GS, Eskiocak B, Zhou B, Kazi MN, Ruiz FR, Pu WT, Tallquist MD. Platelet-Derived Growth Factor Receptor {beta} Signaling Is Required for Efficient Epicardial Cell Migration and Development of Two Distinct Coronary Vascular Smooth Muscle Cell Populations. *Circ Res*. 2008.
25. Betsholtz C. Biology of platelet-derived growth factors in development. *Birth Defects Res*. 2003;69: 272-285.
26. Kang J, Gu Y, Li P, Johnson BL, Sucov HM, Thomas PS. PDGF-A as an epicardial mitogen during heart development. *Dev Dyn*. 2008;237:692-701.
27. Betsholtz C. Insight into the physiological functions of PDGF through genetic studies in mice. *Cytokine Growth Factor Rev*. 2004;15:215-228.
28. Ding H, Wu X, Bostrom H, Kim I, Wong N, Tsoi B, O'Rourke M, Koh GY, Soriano P, Betsholtz C, Hart TC, Marazita ML, Field LL, Tam PP, Nagy A. A specific requirement for PDGF-C in palate formation and PDGFR-alpha signaling. *Nat Genet*. 2004;36:1111-1116.
29. Reigstad LJ, Varhaug JE, Lillehaug JR. Structural and functional specificities of PDGF-C and PDGF-D, the novel members of the platelet-derived growth factors family. *FEBS J*. 2005;272:5723-5741.
30. Schatteman GC, Motley ST, Effmann EL, Bowen-Pope DF. Platelet-derived growth factor receptor alpha subunit deleted patch mouse exhibits severe cardiovascular dysmorphogenesis. *Teratology*. 1995; 51:351-366.
31. Betsholtz C, Karlsson L, Lindahl P. Developmental roles of platelet-derived growth factors. *BioEssays*. 2001;23:494-507.
32. Manner J, Schlueter J, Brand T. Experimental analyses of the function of the proepicardium using a new microsurgical procedure to induce loss-of-proepicardial-function in chick embryos. *Dev Dyn*. 2005;233:1454-1463.
33. Lie-Venema H, Gittenberger-de Groot AC, van Empel LJP, Boot MJ, Kerkdijk H, de Kant E, DeRuiter MC. Ets-1 and Ets-2 transcription factors are essential for normal coronary and myocardial development in chicken embryos. *Circ Res*. 2003;92:749-756.
34. Van Loo PF, Mahtab EAF, Wisse LJ, Hou J, Grosveld F, Suske G, Philipsen S, Gittenberger-de Groot AC. Transcription Factor Sp3 knockout mice display serious cardiac malformations. *Mol Cell Biol*. 2007;27:8571-8582.
35. Ponten A, Li X, Thoren P, Aase K, Sjoblom T, Ostman A, Eriksson U. Transgenic overexpression of platelet-derived growth factor-C in the mouse heart induces cardiac fibrosis, hypertrophy, and dilated cardiomyopathy. *Am J Pathol*. 2003;163:673-682.
36. Raines EW. PDGF and cardiovascular disease. *Cytokine Growth Factor Rev*. 2004;15:237-254.
37. Vrancken Peeters M-PFM, Gittenberger-de Groot AC, Mentink MMT, Hungerford JE, Little CD, Poelmann RE. The development of the coronary vessels and their differentiation into arteries and veins in the embryonic quail heart. *Dev Dyn*. 1997;208:338-348.
38. Hamburger V, Hamilton HL. A series of normal stages in the development of the chick embryo. *J Morphol*. 1951;88:49-92.

39. Manner J. Experimental study on the formation of the epicardium in chick embryos. *Anat Embryol (Berl)*. 1993;187:281-289.
40. Buchdunger E, Cioffi CL, Law N, Stover D, Ohno-Jones S, Druker BJ, Lydon NB. Abl protein-tyrosine kinase inhibitor STI571 inhibits in vitro signal transduction mediated by c-kit and platelet-derived growth factor receptors. *J Pharmacol Exp Ther*. 2000;295:139-145.
41. Sawitzke AL, Chapman SC, Bleyl SB, Schoenwolf GC. Improvements in histological quality and signal retention following in situ hybridization in early chick embryos using plastic resin and recolorization. *Biotech Histochem*. 2005;80:35-41.
42. Nomura M, Li E. Smad2 role in mesoderm formation, left-right patterning and craniofacial development. *Nature*. 1998;393:786-790.
43. Price RL, Thielen TE, Borg TK, Terracio L. Cardiac Defects Associated with the Absence of the Platelet-derived Growth Factor alpha Receptor in the Patch Mouse. *Microsc Microanal*. 2001;7:56-65.
44. Christoffels VM, Mommersteeg MT, Trowe MO, Prall OW, Gier-de Vries C, Soufan AT, Bussen M, Schuster-Gossler K, Harvey RP, Moorman AF, Kispert A. Formation of the venous pole of the heart from an Nkx2-5-negative precursor population requires Tbx18. *Circ Res*. 2006;98:1555-1563.
45. Ding H, Wu XL, Kim I, Tam PPL, Koh GY, Nagy A. The mouse Pdgfc gene: dynamic expression in embryonic tissues during organogenesis. *Mech Dev*. 2000;96:209-213.
46. Lu J, Landerholm TE, Wei JS, Dong XR, Wu SP, Liu XS, Nagata K, Inagaki M, Majesky MW. Coronary smooth muscle differentiation from proepicardial cells requires RhoA-mediated actin reorganization and p160 rho-kinase activity. *Dev Biol*. 2001;240:404-418.
47. Simm A, Nestler M, Hoppe V. Mitogenic effect of PDGF-AA on cardiac fibroblasts. *Basic Res Cardiol*. 1998;93 Suppl 3:40-43.
48. Ariyaratana S, Loeb DM. The role of the Wilms tumour gene (WT1) in normal and malignant haematopoiesis. *Expert Rev Mol Med*. 2007;9:1-17.

Appendix

Results

In the current study we have investigated the protein expression of PDGF-A, -C and their receptor PDGFR-α during several stages of development in the chicken heart (Appendix Figure 4.A1). Furthermore, we have performed in situ hybridizations of stage HH18 to show expression of PDGF-A and its receptor in the PEO and epicardium (Appendix Figure 4.A2). To elucidate the role of PDGFR-α in the development of the compact myocardium of the ventricles, PDGFR-α was inhibited with the use of the receptor tyrosine kinase (RTK) inhibitor Imantinib (ST1571) (Appendix Figure 4.A3).

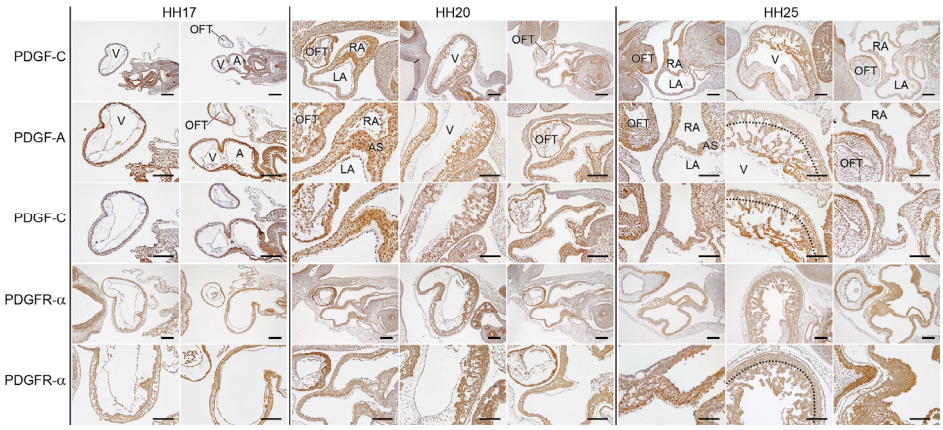

Figure 4.A1 Expression of PDGF-A, -C and PDGFR-α in chicken hearts of stage HH17, HH20 and HH25. Photomicrographs of representative transverse sections show expression of PDGF-A, -C and their receptor at the region of the atrial septum (AS) myocardium, the outflow tract (OFT) myocardium and in the ventricular myocardium. The dotted line in HH25 represents the boundary between ventricular compact and trabecular myocardium. A, atrium; AS, atrial septum LA, left atrium; RA, right atrium; V, ventricle. Scale bars: 200 µm (PDGF-C and PDGFR-α) and 60 µm (PDGF-A, PDGF-C, PDGFR-α).

Expression of PDGF-A, PDGF-C and PDGFR-α

Photomicroscopic representations of protein expression of PDGF-A, -C and PDGFR-α in chicken hearts of stages HH17, HH20 and HH25 (Appendix Figure 4.A1). These pictures support the summary of the spatiotemporal protein expression of both ligands and their receptor in the avian heart represented in Figure 4.1.

In Situ Hybridization

We examined expression of *Pdgfr*α and its ligand *Pdgf*-α in the PEO and epicardium of chicken embryos of stage HH18. Both *Pdgfr*α (Appendix Figure 4.A2a) as well as *Pdgf*-α (Appendix Figure 4.A2b) were expressed in the PEO and outgrowing epicardium.

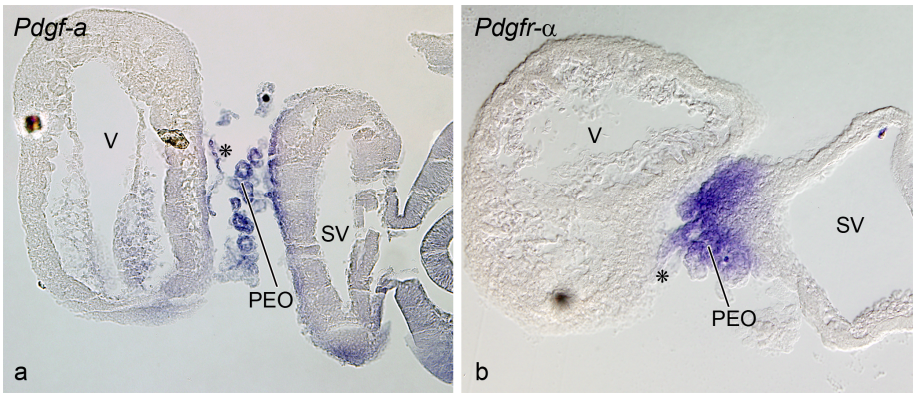

Figure 4.A2 PDGF-signalling in the PEO and epicardium. At stage HH18 the PEO and outgrowing epicardium (asterisk) express *Pdgf*-α (**a**) and *Pdgfrα* (**b**). PEO, proepicardial organ; V, ventricle; SV, sinus venosus. Scale bars: 50 µm.

PDGF-blockade is associated with altered epicardial development

Chicken embryos were treated with Imantinib to inhibit PDGFR-α during cardiac development. In 33% of the embryos treated with Imantinib the subepicardium covering the ventricular myocardium was absent. Also in several areas the epicardium was not attached properly to the myocardium compared to the controls (Appendix Figure 4.A3b, 4.A3d, 4.A3f, 4.A3h).

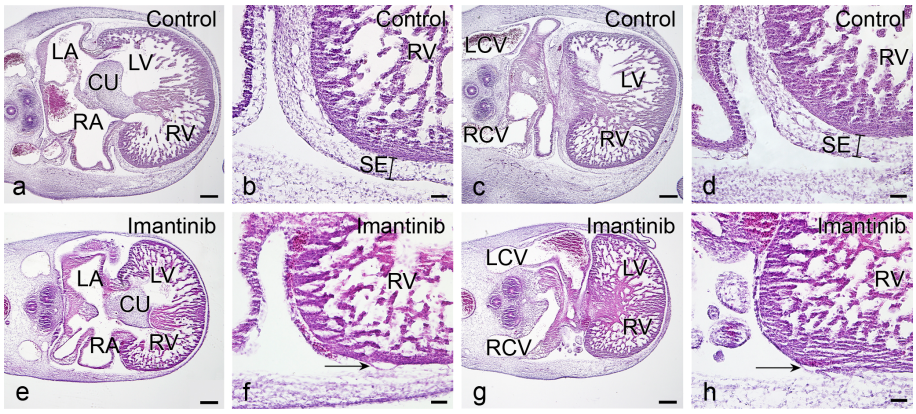

Figure 4.A3 Altered epicardial development with *Pdgfrα* blockade. *In ovo* blockade of *Pdgfrα* with Imantinib causes altered epicardial development in 33% of the embryos (**e-h**) compared to the controls (**a-d**). Altered epicardial development displays absence of subepicardium (SE) covering the ventricular myocardium and epicardium which is not properly attached to the myocardium (arrows). CU, cushions; LA, left atrium; LV, left ventricle; RA, right atrium; RV, right ventricle. Scale bars: 200 µm (a,c,e,g) and 50 µm (b,d,f,h).

92

Chapter 5

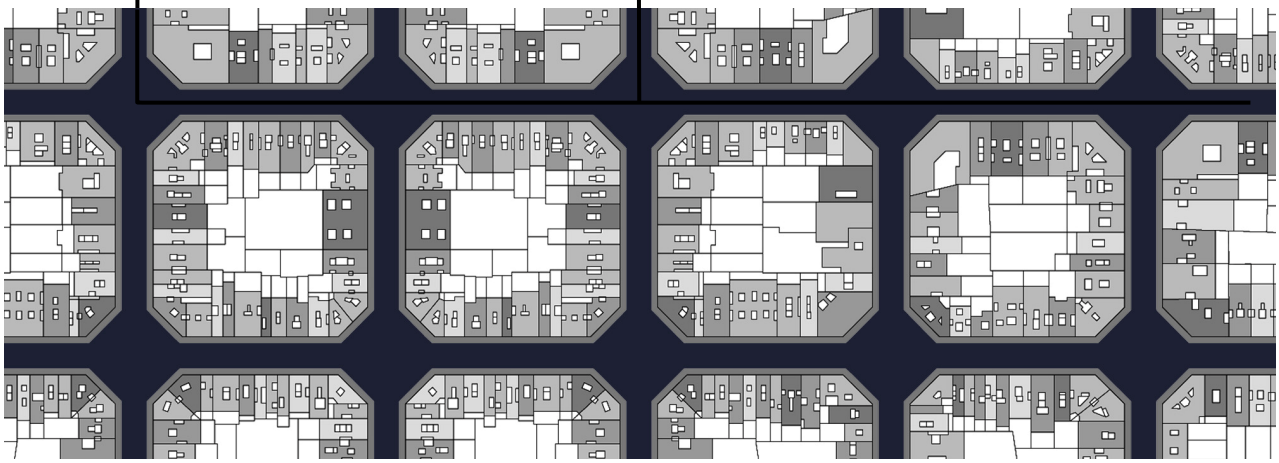

Expression of Id2 in the second heart field and cardiac defects in *Id2* knockout mice

Monique RM Jongbloed, Rebecca Vicente-Steijn, Y.L. Douglas, Lambertus J Wisse, K. Mori, Y. Yokota, Martin J Schalij, Edris AF Mahtab, Robert E Poelmann, Adriana C Gittenberger- de Groot

Submitted for publication

Abstract

The inhibitor of differentiation *Id2* is expressed in mesoderm of the second heart field, which contributes myocardial and mesenchymal cells to the primary heart tube. The role of *Id2* in cardiac development is insufficiently known. Heart development was studied in sequential developmental stages in *Id2* wildtype and knockout mouse embryos. Expression patterns of Id2, MLC-2a, Nkx2.5, HCN4 and WT-1 were analyzed. Id2 is expressed in myocardial progenitor cells at the inflow and outflow tract, in the endocardial and epicardial lineage, and in neural crest cells. *Id2* knockout embryos present with severe cardiac defects including abnormal orientation of systemic and pulmonary drainage, abnormal myocardialization of systemic and pulmonary veins, hypoplasia of the sinoatrial node, atrial and ventricular septal defects, double outlet right ventricle and myocardial hypoplasia. Our results indicate a role for *Id2* in the second heart field contribution at both the arterial and the venous poles of the heart.

Introduction

In vertebrates, the heart is the first organ that becomes functional during embryonic development, and is formed from the bilateral splanchnic mesoderm. This mesoderm, also referred to as the first heart field, contains the cardiac precursor cells that migrate towards the embryonic midline and fuse to form the cardiac crescent and subsequently the primary heart tube.[1,2] During further development, cells from the splanchnic mesoderm dorsal to the heart, the so-called second heart field (SHF), continue to contribute at both the arterial[3-5] and venous[6] poles. Cells of the SHF at the arterial pole contribute to the outflow tract and right ventricle. In contrast, cells of the first heart field give rise to most of the left ventricle, the atrioventricular canal, and part of the atrium. Although initially all cardiac precursor cells express Islet-1 (Isl-1),[7] cells from the first heart field loose this expression very early while the Isl-1 expressing SHF-derived cells incorporate into the heart later in development after which some cells are still recognized by Isl-1 expression.[6]

The SHF is also involved in incorporation of myocardium at the venous pole of the heart and cells from this population have been identified by the expression of several markers.[6,8-12] We have referred to this contribution as being derived from the posterior heart field (PHF),[9] as opposed to the anterior heart field recognized at the arterial pole. Myocardium derived from the PHF is characterized by the expression of several genes, including *podoplanin*,[9,13] its downstream factor *RhoA*,[14] *Hcn4*,[15] *Shox2*,[16] *Tbx5*[17] and *Tbx18*.[8] PHF-derived sinus venosus myocardium is furthermore characterized by the lack of expression of the transcription factor Nkx2.5.[8,9] Assessing the expression pattern of the coelomic and myocardial marker podoplanin, we postulated the addition of cells to the venous pole from two populations: a mesenchymal population, that gives an early contribution including the proepicardial organ and its derivatives,[18] and a myocardial population that will form the myocardium surrounding the cardinal veins, the pulmonary vein myocardium, the interatrial septum and parts of the cardiac conduction system.[9,13] A process of epithelial-to-mesenchymal transformation (EMT) from the coelomic epithelium as part of the SHF has been suggested as the underlying mechanism.

The role of the *Id2* gene (inhibitor of DNA binding 2/inhibitor of differentiation 2, a member of the *Id* gene family) in the second heart field has been described in chick and Xenopus.[19] Id proteins are negative regulators of basic helix-loop-helix proteins. They promote cell proliferation, have a possible role in control of cell differentiation and cell lineage commitment, and keep cells in an undifferentiated state.[20,21] Four *Id* family members, *Id1-4*, have been isolated in chick and mouse.[19,22] *Id2* is involved in many developmental processes including: myogenesis, neurogenesis, cell growth, and cell fate specification.[21] In chick, expression of Id2 was described in the cardiac neural crest, second heart field and anterior parasympathic plexus.[19] Neural crest ablation in chick results in structural defects of the outflow tract, such as common arterial trunk[19] and loss of Id2 expression in the outflow tract. It is not known whether this loss of Id2

expression is related to either a direct effect of neural crest cell ablation on Id2 expression, or alternatively an indirect effect, caused by defective signaling between cardiac neural crest and SHF.[23]

In mouse, expression of Id1, Id2 and Id3 is found in many sites associated with active EMT during organogenesis. In the heart Id2 is expressed in the atrioventricular canal, endocardial cushions, outflow tract, the cardiac valves, the epicardium and endocardium, but not the working myocardium.[22,24] Ablation of two *Id*-genes in any combination from *Id1, 2* or *3* results in severe cardiac defects including ventricular septal defects, thinning of the myocardium, and hypoplastic cushions in the atrioventricular canal and outflow tract.[24] In the latter study, no phenotype of single *Id2* ablation was observed. Interestingly, the phenotype could be rescued by injection of embryonic stem cells.[24] A recent study describes the expression of *Id2* specifically in the atrioventricular node (AVN) and ventricular cardiac conduction system, including the His bundle and bundle branches.[25] The expression of Id2 at the venous pole of the heart and the proximal cardiac conduction system, i.e. the sinoatrial node (SAN), has not been described to date.

In the current report, we have studied specifically the expression of Id2 in the PHF, where the SAN develops. We provide a detailed overview of Id2 expression in the heart in sequential developmental stages of the mouse embryo. Additionally, we have studied the congenital heart malformations in *Id2* knockout embryos, not only at the outflow tract but also at the inflow tract with specific interest in the PHF-derived SAN.

Materials and Methods

Generation of *Id2* knockout mice and harvesting of embryos

Generation of *Id2* wildtype and knockout mice was performed as described previously.[46] We studied the development of the heart in sequential developmental stages of 29 wild type embryos (E9.5: n=8, E10.5 n=4, E11.5: n=3, E12.5: n=3, E13.5: n=5 and E14.5: n=3) and 17 *Id2* knockout ($Id2^{-/-}$) embryos (E9.5: n=4, E11.5: n=3, E12.5: n=3, E13.5: n=5 and E14.5: n=2). The embryos were fixed in 4% paraformaldehyde (PFA) and routinely processed for paraffin immunohistochemical investigation. Sections (slice thickness 5 µm) were mounted onto eggwhite/glycerin coated glass slides in a 1 to 5 order, so that 5 different stainings from subsequent sections could be compared. Procedures followed were in accordance with institutional guidelines of the Leiden University Medical Center.

Immunohistochemistry

Routine immunohistochemical stainings were conducted for embryonic mouse hearts.[13] Briefly, after rehydration of the slides, inhibition of endogenous peroxidase

was performed with a solution of 0.3% H_2O_2 in PBS for 20 minutes. The slides were incubated overnight with the following primary antibodies: against MLC-2a (1/6000, kindly provided by S.W. Kubalak, Charleston, SC, USA), Nkx2.5 (1/4000, Santa Cruz Biotechnology, Inc., CA, USA, SC-8697), WT-1 (1/1000, Santa Cruz Biotechnology, Inc., CA, USA, sc-192) and Id2 (1/100, Zymed, CA, USA). Selected sections were also stained with the α-smooth muscle actin marker 1A4 (1/3000, Sigma Aldrich, A2547).
Primary antibodies were dissolved in phosphate buffered saline (PBS)-Tween-20 with 1% Bovine Serum Albumin (BSA, Sigma Aldrich, USA). Between subsequent incubation steps all slides were rinsed in PBS (2x) and PBS-Tween-20 (1x). The slides were incubated with the secondary antibody for 45 min: for MLC-2a, WT-1 and Id2 with 1/200 goat-anti-rabbit-biotin (Vector Laboratories, USA, BA-1000) and 1/66 goat serum (Vector Laboratories, USA, S1000) in PBS-Tween-20; for Nkx2.5 with 1/200 horse-anti-goat-biotin (Vector Laboratories, USA, BA-9500) and 1/66 horse serum (Brunschwig Chemie, Switserland, S-2000) in PBS-Tween-20 and for 1A4 with 1/250 rabbit-anti-mouse conjugated to horseradish peroxidase (P0260, DAKO).
The signal was amplified using the ABC staining kit (Vector Laboratories, USA, PK 6100) except for 1A4. For visualization the slides were incubated with 400 µg/ml 3-3'di-aminobenzidin tetrahydrochloride (DAB, Sigma-Aldrich Chemie, USA, D5637) dissolved in Tris-maleate buffer pH 7.6 to which 20 µl H_2O_2 was added: all antibodies for 10 min except MLC-2a which were incubated for 5 min. Counterstaining was performed with 0.1% haematoxylin (Merck, Darmstadt, Germany) for 5 sec, followed by rinsing with tap water for 10 min. All slides were dehydrated and mounted with Entellan (Merck, Darmstadt, Germany).

Morphological analysis and 3-D reconstructions

Slices were examined using classical light microscopy. Wildtype and knockout embryos ages E9.5, E12.5 and E14.5 were 3-D reconstructed to obtain optimal insight in cardiac morphology. Reconstructions were made of MLC-2a stained sections, on which stainings for Nkx2.5 were superimposed. Reconstruction were done using AMIRA v4.0 Software Package (Template Graphics Software, San Diego, USA) as previously described.[47] AMIRA™ is an advanced software system for 3D visualization, data analysis and geometry reconstruction from microscopic images.

Results

Expression patterns of Id2, MLC-2a, Nkx2.5, WT-1, HCN4 and cardiac morphology in mouse hearts in subsequent stages of development (E9.5-E14.5) were studied in *Id2* wildtype mouse embryos, and summarized in Figure 5.1. Additionally, expression patterns of MLC-2a, Nkx2.5, WT-1, HCN4 and cardiac morphology were studied in *Id2* knockout embryos.

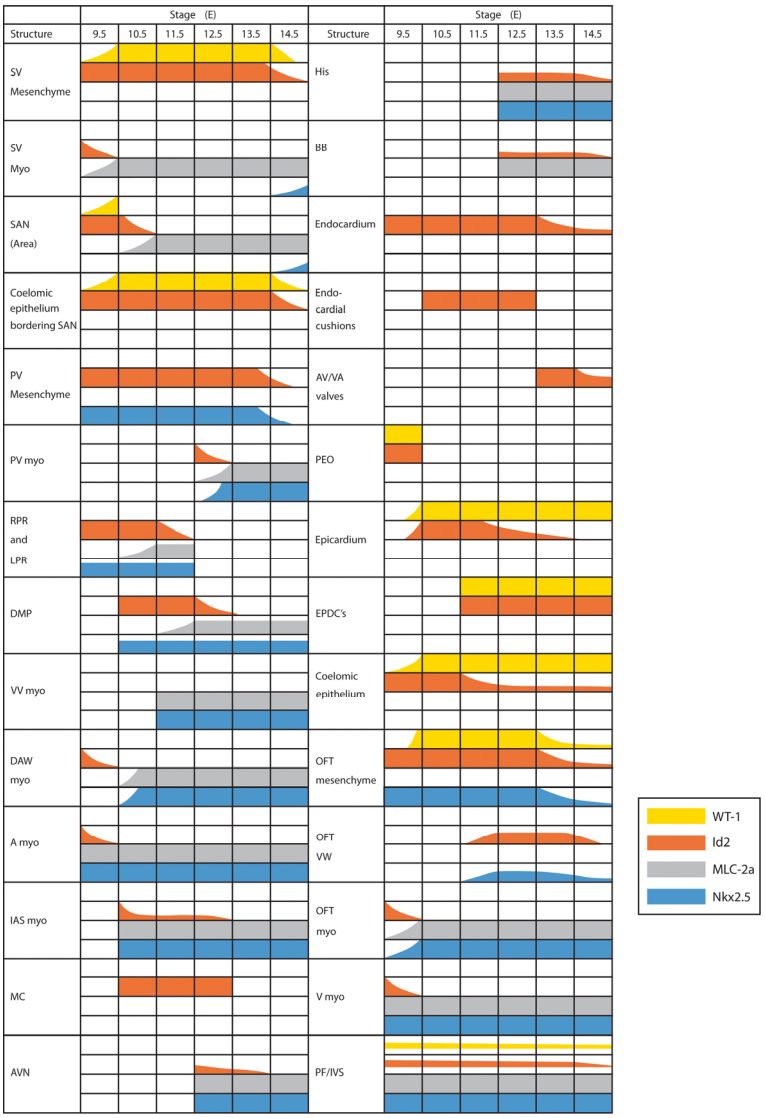

Figure 5.1 Qualitative overview of expression patterns per area of WT-1, Id2, MLC-2a and Nkx2.5 at sequential developmental stages. Filled squares represent maximum intensity at that stage for the specific area. Partially filled squares represent partial expression within a specific area, upslope and downslope represents increase and decrease of expression. A myo: atrial working myocardium, AV: atrioventricular, AVN: atrioventricular node, BB: bundle branches, DAW: dorsal atrial wall, DMP: dorsal mesenchymal protrusion, EPDC's: epicardium-derived cells, His: His bundle, IAS: interatrial septum, IVS: interventricular septum LPR: left pulmonary ridge, MC: mesenchymal cap, myo: myocardium, OFT: outflow tract, PEO: proepicardial organ, PF: primary fold, PV: pulmonary vein(s), RPR: right pulmonary ridge, SAN: sinoatrial node, SV: sinus venosus, VA: ventriculo-arterial, V myo: ventricular working myocardium, VV: venous valves, VW: vascular wall.

Stage E9.5

Wildtype embryos

Cardiac looping has not been completed. The atrioventricular canal is still situated entirely above the primitive left ventricle, whereas the outflow tract is positioned above the primitive right ventricle. Atrial and ventricular septation, as well as outflow tract septation have not been initiated.

Id2 expression is observed in the dorsal mesocardium and the coelomic wall epithelium, most markedly at the site bordering the pharyngeal endoderm, which also expresses Id2. The mesenchyme surrounding the proximal part of the cardinal veins expresses Id2. Interestingly, in the area of the putative SAN, an Id2 and WT-1 positive area is present at the right lateral border of the right cardinal vein, that is MLC-2a and Nkx2.5 negative (Figure 5.2a-e). The same phenomenon is observed at the left side (Figure 5.2f-j). The proepicardial organ (PEO) can easily be identified and stains positive for both Id2 and WT-1, whereas it shows no MLC-2a or Nkx2.5 expression (Figure 5.2k-o). An area of MLC-2a positive myocardium, that does not express Nkx2.5, Id2 or WT-1, is visible in the lower rim of the sinus venosus (Figure 5.2n-o, arrows) including the proximal part of the cardinal veins (green area in Figure 5,3a), indicating the first onset of formation of the sinus venosus myocardium. A pulmonary pit and strand is recognized in the dorsal mesocardium that, although not luminized yet, extends towards the common atrium. The left and right pulmonary ridges, located on either side of this putative pulmonary vein, highly express Id2 and Nkx2.5 but do not express MLC-2a or WT-1 (Figure 5.3a-f). There is no myocardial sleeve surrounding the primitive pulmonary vein yet.

The myocardium of the right and left atrial dorsal wall stains positive for Id2 (Fig. 3e), whereas MLC-2a expression is faint (Figure 5.3c). The myocardium of the inner curvature and primary fold i.e. the tissue between the primitive right and left ventricle also stains positive for Id2, as well as for MLC-2a and Nkx2.5. The remainder of the atrial and ventricular myocardium stains positive for Nkx2.5 and MLC-2a. Only a subset of these myocardial cells stains positive for Id2 in a mosaic pattern, i.e. a mixture of cells with positive and negative expression of Id2.

Other regions that show Id2 expression include the mesenchyme surrounding the outflow tract, the endocardium and the endocardial cushions of the atrioventricular canal and the outflow tract. Extracardiac areas of Id2 expression include the epithelium of the pulmonary bronchi, the foregut and the neural tube.

Id2 $^{-/-}$

In the *Id2* knockout, the inner curvature is wider compared to wildtype embryos. At the level of the primitive pulmonary vein, a distinct fine cellular pattern of cells in the mesocardium dorsal of the primitive vein is observed (Figure 5.3i, 5.3j, arrows).

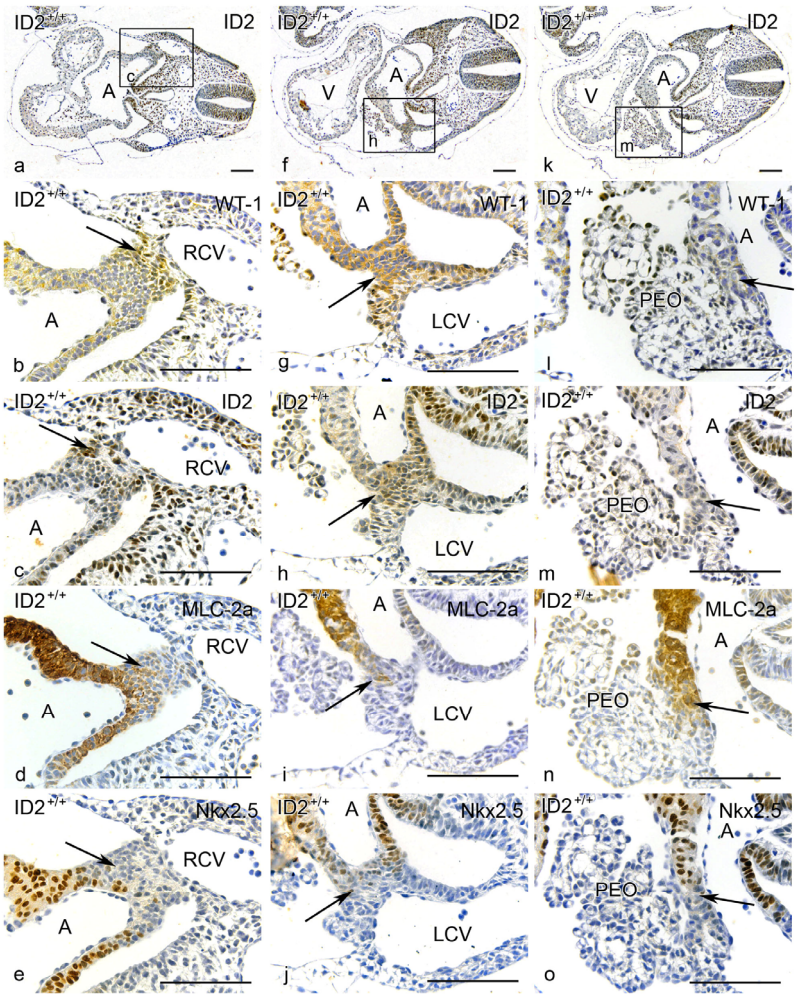

Figure 5.2 E9.5: Area of putative sinoatrial node and the proepicardial organ in wildtype embryos. **a-o**: Expression patterns in *Id2* wildtype($^{+/+}$) embryonic hearts. **b-e**, **g-j** and **l-o** are enlargements of the boxed areas in the overview sections in **a**, **f** and **k**, respectively. **a**. overview section. The boxed area indicates the level of the right cardinal vein (RCV) and putative right-sided sinoatrial node (SAN). **c**. Id2 is expressed in the area of the putative SAN (**c**, arrow). In this area, also WT-1 expression is observed (**b**), whereas MLC-2a and Nkx2.5 are not expressed (arrows in **d** and **e**). **f**. overview section. The boxed area indicates the level of the left cardinal vein (LCV) and putative transient left-sided SAN. Expression patterns of WT-1, Id2, MLC-2a and Nkx2.5 in the area of the transient left-sided SAN (arrows in **g-j**) are similar to the area of the right-sided SAN. **k**. overview section. The boxed area indicates the level of the proepicardial organ (PEO). The PEO expresses WT-1 (**l**), Id2 (**m**), but not MLC-2a (**n**) and Nkx2.5 (**o**). Note the small area of MLC-2a positive myocardium bordering the lumen of the atrium (arrow in **n**), that is WT-1, Id2 and Nkx2.5 negative (arrows in **l**,**m** and **o**) and indicates the first onset of formation of the sinus venosus myocardium. A: common atrium, V: common ventricle. Scale bars:100 µm.

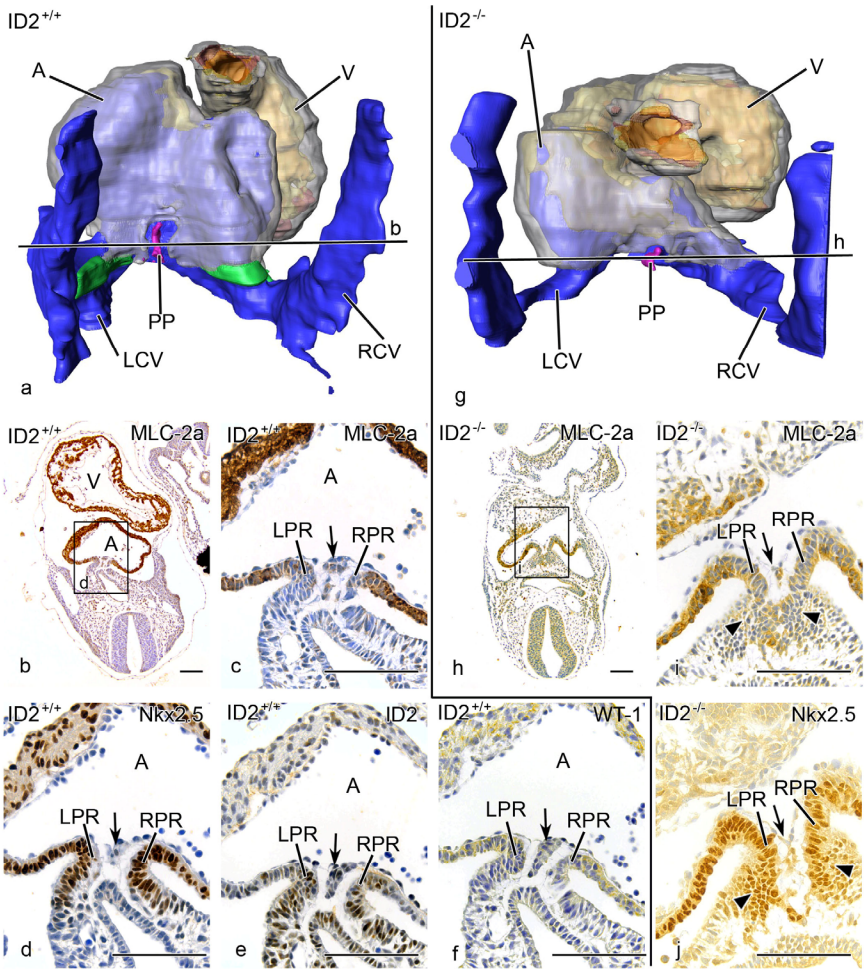

Figure 5.3 E9.5: Pulmonary pit and pulmonary ridges. Location of the systemic veins and of the pulmonary pit in wildtype ($^{+/+}$) versus knockout ($^{-/-}$) embryos. Expression patterns in *Id2* wild type (**a-f**) and knockout (**g-j**) embryonic hearts. **a**. 3D reconstruction of a wildtype heart, dorsal view. The horizontal line indicates the level of the section in **b**. Color coding: light blue/grey: myocardium, blue: lumen of the cardinal veins, orange: cushion tissue, green: MLC-2a positive and Nkx2.5 negative sinus venosus myocardium, pink: pulmonary pit (PP). **b**. overview section stained with MLC-2a. **c-f** are enlargements of the boxed area in the overview section in **b**, indicating the level of the PP (arrows) and right and left pulmonary ridges (RPR and LPR). Note the complementary expression patterns of MLC-2a (**c**) and Id2 (**e**) in the pulmonary ridges and the atrial wall. The RPR and LPR highly express Id2 and Nkx2.5 (**d**), whereas MLC-2a and WT-1 (**f**) are lacking. **g**. 3D reconstruction of a knockout heart, dorsal view. The horizontal line indicates the level of the sections in (**h-j**). Color coding is as in **a**. Note the absence of the (green) sinus venosus myocardium, as compared to **a**. **h**. overview section stained with MLC-2a. **i-j** are enlargements of the boxed area indicating the level of the PP (arrow) and RPR and LPR. Expression patterns of MLC-2a and Nkx2.5 do not differ from the wildtype. A fine cellular pattern in the dorsal mesocardium can be observed (arrowhead in **i** and **j**). Scale bars:100 µm.

The entrance of the cardinal veins in the sinus venosus is at a more caudal level compared to wildtype animals, and the myocardial covering of the sinus venosus and cardinal veins has not been initiated (Figure 5.3g). The pulmonary pit is situated more caudally. (Figure 5.3g). The structure of the PEO appears less compact than the PEO in wildtypes (not shown).

Stage E10.5

Wildtype embryos

Cardiac looping has advanced. Atrial and ventricular septation have started. Details on the changes in expression patterns for Id2, WT-1, MLC-2a, and Nkx2.5 are provided in Figure 5.1. Id2 expression is maintained in the same cardiac regions as before, as well as in the dorsal mesenchymal protrusion (DMP) and the mesenchymal cap on the developing interatrial septum, which become apparent at this stage. The formation of the sinus venosus myocardium is ongoing as recognized by the positive expression patterns of MLC-2a and HCN4, and no Nkx2.5. Id2 and WT-1 expressing cells are found surrounding the cardinal veins (putative sinus venosus myocardium). The putative SAN is recognized as a thickened area at the medial side of the right cardinal vein that expresses MLC-2a and is still positive for Id2 and negative for Nkx2.5. Cells in the coelomic wall bordering this region are cuboid in shape and WT-1 and Id2 positive, indicating active EMT at this site**.** The same phenomenon is observed on the left side medial to the left cardinal vein (transient left-sided SAN). As in the previous stage, profound Id2 expression is observed in the interventricular primary fold.
The epicardium, although not entirely continuous, can be distinguished as a WT-1 and Id2 positive layer covering the myocardium, but being negative for MLC-2a and Nkx2.5.

Stage E11.5

Wildtype embryos

Atrial and ventricular septation is ongoing. The dorsal atrial wall and the atrial myocardium are now Id2 negative (Figure 5.1). A few myocardial cells of the primary atrial septum show Id2 expression. Formation of the sinus venosus myocardium has progressed as shown by the presence of a larger area of MLC-2a and HCN4 positive, but Nkx2.5 and Id2 negative myocardium at the inflow region of the heart. The mesenchyme around the cardinal veins expresses Id2 and WT-1. The SAN has expanded and shows no Id2 expression at this stage, however, many cuboid shaped Id2 and WT-1 positive and MLC-2a negative cells are observed in the coelomic wall and mesoderm bordering the SAN (Figure 5.4a-f).
The ventricular myocardium is largely Id2 negative. Many Id2 positive cells are observed in the area of the primary fold, as well as in the inner curvature of the heart,

partially overlapping with WT-1 expression. Additionally, epicardial cells still show Id2 and WT-1 expression, although epicardial cells localized towards the apex of the heart stain negative.
The great arteries remain positioned mainly above the right ventricle (physiological double outlet right ventricle), but septation of the outflow tract has started. The outflow tract has gained length and Id2, being expressed in the mesenchyme and (less markedly) in the vascular wall, shows a complementary expression pattern to MLC-2a, expressed in the myocardium of the outflow tract (Figure 5.1).

Id2 $^{-/-}$

Knockout embryos show severe abnormalities. The cardiac compartments and the cardinal veins are dilated and progression of formation of sinus venosus myocardium is less advanced than in the wildtype. The atrial and ventricular myocardium, including the right en left venous valves, are hypoplastic**.** The SAN appears long-stretched and underdeveloped compared to the wildtype but maintains its expression pattern, i.e. MLC-2a and HCN4 positive and Nkx2.5 negative (Figure 5.4g-k). As observed in previous stages, the venous drainage pattern is different than in the wildtype, with the pulmonary veins draining at a more caudal level, below the entrance of the left cardinal vein in the coronary sinus. In contrast to the wildtype the primary atrial septum is severely hypoplastic and nearly absent. The ventricular myocardium is thin and less compact than in the wildtype. The epicardial layer is intact.

Stage E12.5

Wildtype embryos

Atrial and ventricular septation have further progressed. The atrial and ventricular myocardium express MLC-2a, with higher expression in the atria compared to the ventricles, staining largely negative for Id2. Formation of a myocardial sleeve surrounding the cardinal veins has progressed as shown by the presence of MLC-2a and HCN4, but no Nkx2.5 or Id2 in the proximal part of the myocardial sleeve covering the left and right cardinal veins (Figure 5.5a-d). The venous valves stain negative for Id2 but positive for HCN4, MLC-2a and Nkx2.5. The SAN can be distinguished at the entrance of the right superior cardinal vein in the atrium, as a large cluster of cells expressing MLC-2a and HCN4, but not Nkx2.5, WT-1 or Id2. As in previous stages, a cluster of cells is also observed at the left side, although this structure is significantly smaller in size. Id2 positive cells are observed in the myocardium in the basal part of the atrial septum, and in the mesenchymal cap. The DMP, located caudally between the sinus horns, also stains markedly positive for Id2, whereas expression of MLC-2a and Nkx2.5 is mosaic. This structure contains the intracardiac part of the primitive pulmonary vein. A myocardial sleeve is only just starting to form around extracardiac part of the pulmonary vein (Figure 5.5e, 5.5f).

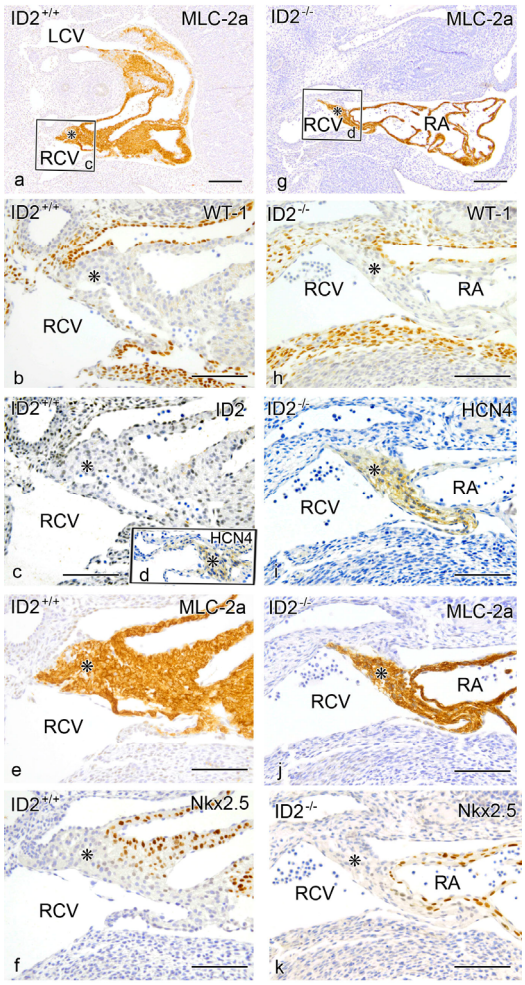

Figure 5.4 E11.5: Expression patterns in *Id2* wildtype ($^{+/+}$, **a-f**) and knockout ($^{-/-}$, **g-k**) embryonic hearts in the area of the developing sinoatrial node (SAN, asterisk). **b-f**, and **h-k** are enlargements of the boxed areas in the overview sections in **a** and **g**, respectively. **a**. overview section of MLC-2a expression in a wildtype embryo. The boxed area indicates the level of the right cardinal vein (RCV) and SAN (asterisk). **b**. expression of WT-1 in the coelomic epithelium. Epithelial cells bordering the SAN are characterized by a cuboid shape of the cells. **c**. Id2 expression in a wildtype embryo. The central part of the developing SAN does not express Id2, however, Id2 expressing cells are observed at the border of the SAN, in a pattern overlapping with WT-1-expression. The inset (**d**) demonstrates the expression of HCN4 in the SAN. The SAN is further characterized by expression of MLC-2a (**e**) and lack of expression of Nkx2.5 (**f**). **g**. overview section of MLC-2a expression in an *Id2* knockout embryo. The boxed area indicates the level of the RCV and SAN (asterisk). As in the wildtype, the coelomic epithelium expresses WT-1 (**h**). As compared to the wildtype, in knockout embryos the SAN (asterisks) is smaller in size and has a more stretched shape. As is the wildtype, the SAN is characterized by expression of HCN4 (**i**), MLC-2a (**j**) and is Nkx2.5 (**k**) negative. Scale bars:100 µm.

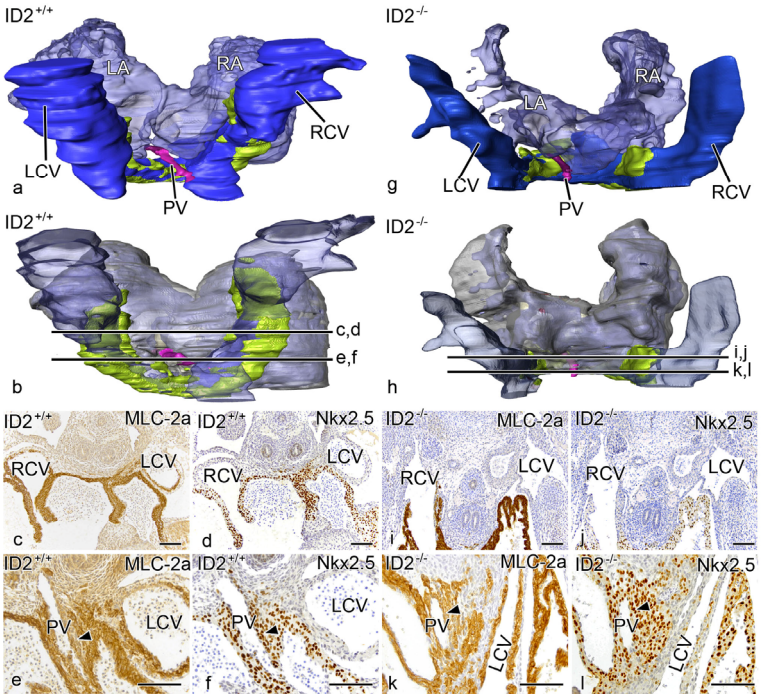

Figure 5.5 E12.5: Development of the cardinal veins and pulmonary vein (PV) in *Id2* wildtype ($^{+/+}$, **a-f**) versus knockout ($^{-/-}$, **g-l**) embryos. **a-b**: 3D reconstructions, dorsal views of *Id*$^{+/+}$ embryos. Color coding: grey: myocardium atria, blue: lumen of the cardinal veins, green: MLC-2a positive and Nkx2.5 negative sinus venosus myocardium, pink: pulmonary vein. In **b** and **h** the lumen of the right cardinal vein (RCV) and left cardinal vein (LCV) has been made transparent to allow optimal visualization of the (green) sinus venosus myocardium. The horizontal bars in **b** indicate the levels of the sections depicted in **c-f**. At this stage, the formation of a myocardial sleeve surrounding the RCV and LCV has progressed, as indicated by the presence of a cuff of MLC-2a positive and Nkx2.5 negative myocardium (green area in **a-b**, and sections **c** and **d**). **e-f**: The intracardiac PV runs in the dorsal mesenchymal protrusion, that is partly. The major part of the PV outside the dorsal mesenchymal protrusion is not yet surrounded by a MLC-2a positive sleeve (**e**). Note that the (MLC-2a negative) mesoderm of the dorsal mesenchymal protrusion surrounding the PV is Nkx2.5 positive. (arrowheads in e and f). **g-h**: 3D reconstructions, dorsal views of *Id*$^{-/-}$ embryos. Color coding is as described for **a** and **b**. The horizontal bars in **h** indicate the levels of the sections depicted in **i-l**. Note the different orientation of the RCV, LCV and PV as compared to the wildtype embryos. The formation of a myocardial sleeve surrounding the RCV and LCV is less advanced compared to wildtype as indicated by a shorter cuff of MLC-2a positive and Nkx2.5 negative myocardium (compare the green area in **a** and **b** with the green area in **g** and **h**). This is also indicated in sections **i** and **j**, where a sleeve of myocardium surrounding the RCV and LCV is lacking, (compare sections in **i** and **j**, with wildtype sections in **c** and **d**). **k-l**: In the knockout embryos, the intracardiac part of the PV, running in the dorsal mesenchymal protrusion, is already completely surrounded by MLC-2a positive and Nkx2.5 positive myocardium (arrowheads in **k** and **l**). Scale bars:100 µm.

Separation of the outflow tract has progressed, although the aorta and pulmonary trunk are still positioned partly above the right ventricle. In accordance with the previous stage, Id2 expression in the outflow tract is complementary to MLC-2a. The mesenchyme and vascular wall of the outflow tract show no MLC-2a expression but stain positive for Nkx2.5 and Id2.

Id2 $^{-/-}$

Knockout mice show major abnormalities. Atrial and ventricular myocardium is hypoplastic, and the atrial myocardium lacks trabeculation. There are large interatrial communications in accordance with a less developed interatrial septum than expected at this stage. Likewise, the progression of ventricular septation is less advanced as compared to the wildtype. The SAN still appears smaller and slightly elongated in shape, although the difference with the wildtype is less marked than in the previous stage. Staining patterns for MLC-2a and Nkx2.5 remain unchanged. In contrast to wildtype, hardly any myocardial formation around the cardinal veins is present (Figure 5.5g-j). As in previous stages, the more caudal drainage of cardinal veins and the pulmonary veins to the heart is observed (Figure 5.5g-h). In knockout embryos the intracardiac part of the pulmonary vein is already completely surrounded by MLC-2a positive and Nkx2.5 positive myocardium (Figure 5.5k-l, arrowheads), whereas the extracardiac part, similar to the cardinal veins, lacks myocardium.
At the level of the outflow tract the position of the aorta and pulmonary trunk is abnormal, located side-to-side above the right ventricle.

Stage E13.5

Wildtype embryos

Atrial septation has been completed but ventricular septation is not finished, as there is still an open communication between the right and left ventricle in most hearts. A great part of the atrial septum is negative for Id2, although positive cells are observed at the base of the atrial septum in the region of the AVN. The myocardial sleeve surrounding the cardinal veins is now well developed, with positive MLC-2a and HCN4 expression and lacking Id2 expression. A well developed sleeve of myocardium is present surrounding the proximal extracardiac part of the pulmonary vein, but does not extend distally to the peripheral part of the veins. This myocardial sleeve in the proximity of the left atrium is markedly positive for MLC-2a and Nkx2.5, whereas more peripheral where MLC-2a is still faint less Nkx2.5 positive cells are observed. Id2 expression is observed in the mesenchyme in the peripheral area of the pulmonary veins.
Many Id2 positive cells are observed at the inner curvature of the heart. Id2 positive cells are observed in a subpopulation of epicardial cells and in the subepicardial layer, probably representing epicardium-derived cells (EPDCs).[26] Id2 positive components of

the cardiac conduction system, including the His bundle and right and left bundle braches, are recognized as reported previously.[25]

The outflow tract has completely separated. The position of the aorta and pulmonary trunk is normal, with the aorta connected to the left ventricle. Expression of Id2 is complementary to MLC-2a in the outflow tract (Figure 5.6a-d).

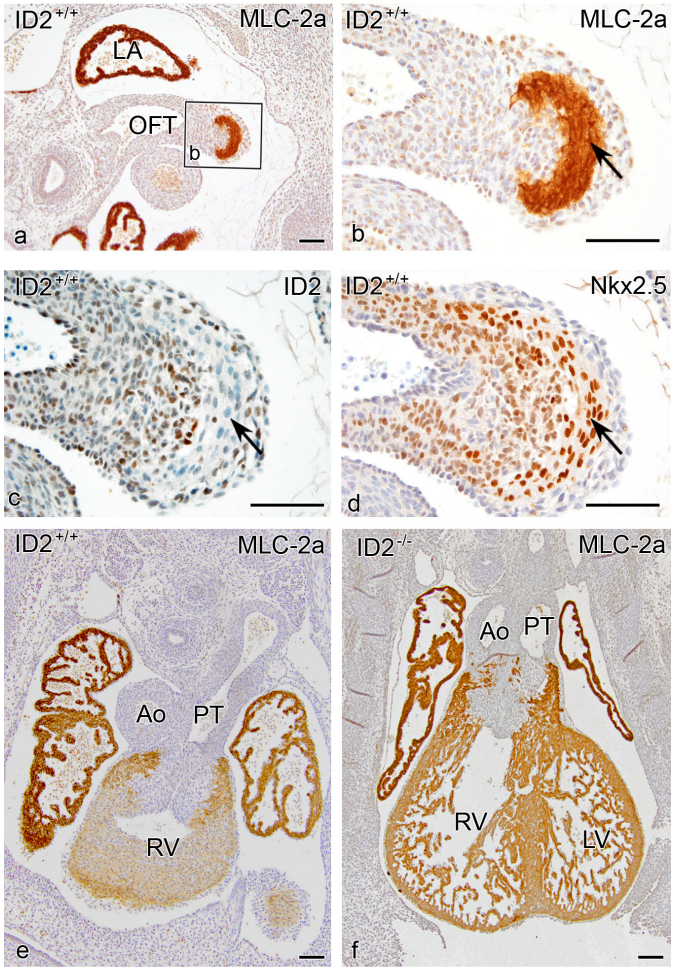

Figure 5.6 E13.5: Expression patterns in the outflow tract of *Id2* wildtype ($^{+/+}$) embryos and outflow tract abnormalities in knockout ($^{-/-}$) embryos. **a**. Overview section of MLC-2a expression. The boxed area indicates the level of the proximal outflow tract (OFT). **b**, **c** and **d** are enlargements of the boxed area in **a**. Expression of MLC-2a (**b**) is complementary to expression of Id2 (**c**) in the proximal outflow tract (arrows). MLC-2a and Id2 expression are overlapping with expression of Nkx2.5 (**d**) that is expressed in both mesenchymal and myocardial components of the OFT. **e**. Normal position of the aorta (Ao) and pulmonary trunk (PT) in a wildtype embryo. **f**. Double outlet right ventricle in a knockout embryo. LA: left atrium, LV: left ventricle, RV: right ventricle. Scale bars:100 µm.

Id2 $^{-/-}$

The atrial myocardium is hypoplastic and the left atrium appears smaller than in the wildtype. In several specimen, fenestrations in the atrial myocardium are observed, which are discontinuities in the myocardial wall allowing epicardial-endocardial contact. The SAN appears normal in size although slightly more stretched in shape. The myocardium surrounding the cardinal veins is thin especially on the dorsal side and the myocardial sleeves are shorter than in wildtype. Myocardialization of the intracardiac part of the pulmonary veins however, does not appear diminished in the knockouts. As in previous stages, the cardinal and pulmonary veins drain into the atria at a more caudal level than in the wildtype.
In all knockout embryos the position of the vessels of the outflow tract is abnormal, with a parallel position of the aorta and the pulmonary trunk, dextraposition of the aorta with evident overriding over the ventricular septum (>50%), causing a double outlet right ventricle (compare Figure 5.6e and 5.6f).

Stage E14.5

Wildtype embryos

Overall Id2 expression has diminished at this stage (Figure 5.1). Atrial and ventricular septation have been completed, although the interatrial communication of the foramen ovale remains present before birth (Figure 5.7a-b). The mesenchymal cap and DMP have myocardialized and express MLC-2a, Nkx2.5, and scattered Id2.
The myocardial sleeve covering the right and left cardinal veins is fully developed and lacks Id2. In contrast to previous stages, mosaic Nkx2.5 expression is observed in the myocardium surrounding the cardinal veins and coronary sinus, being the cardiac continuation of the left cardinal vein. The right SAN has fully developed and expresses MLC-2a, HCN4 and now contains a few Nkx2.5 expressing cells. As observed before, a smaller left SAN is recognized and shares the same expression pattern as the right SAN. The SAN is no longer bordered by Id2 and WT-1 positive cells at this stage. The pulmonary veins are surrounded by myocardium that is MLC-2a and Nkx2.5 positive and Id2 negative. Id2 expression in the ventricular conduction system has decreased (Figure 5.1).
Epicardial Id2 expression has been lost with exception of the epicardial cells of the distal outflow tract. Id2 positive cells are still present in the subepicardial layer. Id2 expression is observed in the semilunar valves and in the aortopulmonary septum, between the aorta and pulmonary trunk.

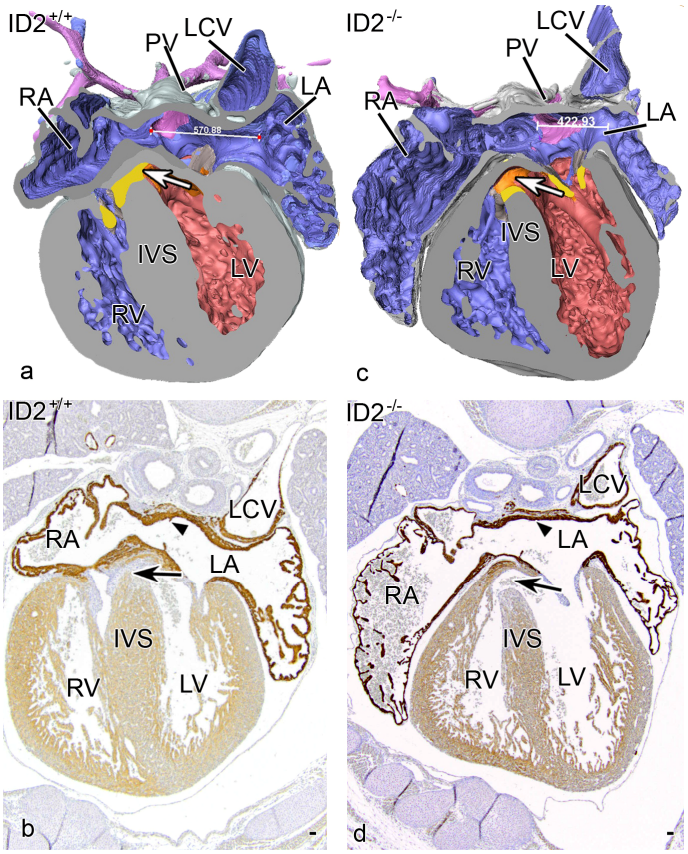

Figure 5.7 E14.5: 3D reconstructions of *Id2* wildtype ($^{+/+}$) and knockout ($^{-/-}$) embryos. **a**. 3D reconstruction, anterior view of a E14.5 $Id^{+/+}$ embryo. Color coding: grey: myocardium atria and ventricles, light blue: lumen of the atria and cardinal veins, pink: pulmonary veins (PV), yelllow: tissue of the fibrous heart skeleton, that includes the membranous part of the interventricular septum (IVS), red: lumen left ventricle (LV), dark blue: lumen right ventricle (RV). **b**. Corresponding section of the wildtype embryo. Atrial and ventricular septation have been completed, although the foramen ovale is still open. The arrowhead indicates part of the primary atrial septum. **c**. 3D reconstruction of a knockout embryo, frontal view. Color coding is as indicated in a. **d**. Corresponding section of the knockout embryo. There is a ventricular septal defect (arrow in **c** and **d**). Also, the primary atrial septum is lacking (arrowhead). Note the thin atrial and ventricular myocardium, and the small size of the left atrium (LA) as compared to the wildtype embryo (compare the white lines in the reconstructions in **a** and **c**). LCV: left cardinal vein, RA: right atrium, RCV: right cardinal vein, Scale bars:100 µm.

Id2 $^{-/-}$

Phenotypes range from a generally normal appearance to grossly abnormal. In the most severely affected embryo, the atria and atrial appendages are dilated, and the myocardial wall as well as the interatrial septum is thin. As in the previous stage, the

left atrium appears smaller than in the wildtype (compare Figure 5.7a-b to 5.7c-d) although the lining with smooth muscle cells of the body of the left atrium is undisturbed. The venous valves are thin and the cardinal veins are dilated and covered by hypoplastic myocardium that stains positive for MLC-2a and mosaic for Nkx2.5. The well developed SAN stains positive for MLC-2a and although mainly negative for Nkx2.5, some positive cells are becoming visible. Ventricular and atrial septation is disturbed as indicated by the presence of atrial and ventricular septal defects (Figure 5.7c-d). There is an abnormal position of the great vessels, although dextraposition is less extreme than observed in previous stages.

Discussion

In this paper, the expression of the Id2 in the heart is described, as well as cardiovascular consequences of deficiency of *Id2*. The role of *Id2* in heart development[22,24] and cardiac conduction system development[25] has been previously recognized, but detailed reports on expression patterns of Id2 in the heart, specifically at the venous pole and proximal cardiac conduction system in subsequent embryonic stages, are lacking. Key findings in the current study are 1. The expression of Id2 in cardiac progenitor cells not only at the arterial but also at the venous pole of the heart, including the area of the putative SAN. 2. A severe cardiac phenotype in *Id2* knockout embryos with abnormal drainage patterns at the arterial pole (double outlet right ventricle) as well as at the venous pole (abnormal level of drainage of systemic and pulmonary veins) of the heart. 3. Congenital heart malformations related to anterior and posterior second heart field deficiency in *Id2* knockout embryos.

Expression of Id2 was observed in multiple cell lines in the cardiovascular system. Throughout embryological development Id2 expression is observed in the endocardium and endocardial cushions as well as in the PEO and epicardium in early stages, whereas epicardial expression is largely lost during further development. In early stages Id2 expression is observed in myocardium and myocardial progenitor cells at both the inflow and outflow tract of the heart, whereas after full differentiation of the myocardium, Id2 expression is lost. These results indicate that Id2 is expressed in pre-differentiation stages of the myocardium, and is no longer present in fully differentiated cells of the working myocardium. This pattern was also observed in the coelomic epithelium bordering the SAN, where marked Id2 expression was observed during SAN development, whereas the myocardial SAN itself did not show expression. A similar phenomenon was observed in the outflow tract of the heart, where complementary expression patterns of the myocardial markers MLC-2a and Id2 were observed. Furthermore, Id2 is expressed in neural crest cell areas, as previously reported in chick.[19] Remarkably, expression of several other genes involved in heart development is observed in both myocardial and neural crest lineages, including *Isl-1*[6]

and *Tbx3.*[27] Additionally, Id2 was observed in components of the ventricular cardiac conduction system, as described previously.[25]

Abnormalities observed in *Id2* knockout embryos

Id2 knockout embryos demonstrate a broad spectrum of abnormalities, which may be attributed to the extensive expression pattern observed in the wildtype. Both abnormalities of the inflow tract as well as of the outflow tract were observed.

Venous pole abnormalities. All *Id2* knockout embryos presented an abnormal orientation of the venous drainage pattern, with the pulmonary and systemic veins draining into the heart at a significantly more caudal level as compared to the wild type. This drainage pattern resembles the pattern observed in platelet derived growth factor-receptor alpha (*Pdgfr-α*) knockout embryos.[28,29] Interestingly, expression patterns of Id2 resemble that of PDGFR-α, that is expressed both in myocardium of the primary heart tube, as well as in SHF-derived myocardium and mesenchyme.[30,31,31] *Pdgfr-α* knockout embryos are further characterized by hypoplasia of the SAN, probably due to an accelerated rate of differentiation. Also, Nkx2.5 was upregulated in the SAN of *Pdgfr-α* knockout embryos.[29] In *Id2* knockout embryos, hypoplasia of the SAN was also observed during early developmental stages, although this was not evident any more in more advanced stages. In contrast to the *Pdgfr-α* knockout embryos, Nkx2.5 expression was not altered in the knockout, confirming previous results that place *Nkx2.5* upstream of *Id2*.[32]

The presence of Id2 in the cuboid coelomic cells bordering the SAN, suggesting an active EMT state of these cells, may be related to the proliferation and maintenance of an undifferentiated state of the progenitor population contributing to the SAN, after which Id2 is switched off allowing these cells to further differentiate to a SAN phenotype.

Id2 knockout embryos demonstrated hypoplasia of the atrial myocardium and larger interatrial communications than observed in wildtype animals, a phenotype that was also observed in other models with impaired myocardial contributions from the PHF, including mice lacking *podoplanin*, *Pdgfr-α* and *Shox2*.[16,29,33] However, in contrast to observations in *podoplanin* and *Pdgfr-α* knockout embryos, atrioventricular septal defects were not observed in *Id2* knockouts. This is in line with the fact that the DMP was not affected in the *Id2* knockout. An interesting observation was the small left atrium in the *Id2* knockout embryos, with a normally differentiated vascular smooth muscle lining, as described by Douglas et al.[33] These findings are in contrast with the phenotype in the *podoplanin* knockout mouse, with a normal sized left atrium but a deficient left atrial vascular smooth muscle wall.[33] We hypothesize that in the *podoplanin* knockout, the phenotype is determined by a disturbed smooth muscle cell contribution from the SHF, and in the *Id2* knockouts, by a deficient incorporation of the pulmonary veins, in line with the abnormal drainage pattern observed. The intracardiac part of the pulmonary vein runs in the DMP, itself PHF-derived,[34] that

expresses Id2 throughout development. Remarkably in the *Id2*-knockout embryos, the myocardialization of the DMP appeared more advanced than in the wildtype, which may indicate an accelerated rate of differentiation of the DMP after loss of Id2 expression. Myocardialization of the systemic veins was diminished. *Id2* is known to maintain the progenitor population in an undifferentiated state. We hypothesize that in knockout embryos, the balance between undifferentiated and differentiated cells is disturbed. This may result in diminished formation of the cardinal vein myocardium. The milder phenotype observed in *Id2* knockout embryos at advanced developmental stages may result from the fact that embryos with the most severe phenotype have a higher rate of embryonic mortality.

Arterial pole abnormalities. In the *Id2* knockout embryos outflow tract abnormalities were consistently observed, from dextroposition of the aorta to full blown double outlet right ventricle. In chick outflow tract abnormalities were also observed after deletion of neural crest cells, resulting in decreased expression of Id2 in the heart.[19] The latter implies that presence of neural crest cells is required for Id2 expression in the heart. Alternatively, an interaction between Id2 positive SHF cells and neural crest might underlie the outflow tract anomalies, as was suggested previously.[5] We postulate that in the *Id2* knockout embryos a disturbed recruitment of myocardium from the SHF may also contribute to an abnormal position of the outflow tract.

Epicardium-related abnormalities. The ventricular myocardium, being thin, resembled ventricular non-compaction. The wide inner curvature in early stages and abnormal position of the outflow tract suggest looping abnormalities. These findings resemble a disturbed epicardial contribution from the PHF, as described previously in mouse after mutation of *podoplanin*[18] and *Pdgfr-α*[29] and in chick after epicardial ablation.[35]

Furthermore, we observed membranous ventricular septal defects in the *Id2* knockout embryos, which may be related to the prominent expression of Id2 in the endocardial cushions.

The co-occurrence of both inflow and outflow tract anomalies in *Id2* knockout embryos may be of clinical interest for understanding the complex cardiac phenotype sometimes observed in congenital heart disease. Indeed, the co-occurrence of both inflow and outflow tract anomalies has been reported.[36] These phenotypes might (partly) be explained by the deficiency of genes with functional roles in both the anterior and posterior part of the SHF. Here we propose *Id2* as one of the culprit genes. Several upstream regulators of *Id2* have been suggested including Smad4, nmyc, cyclin D1 and D2, BMP, TGFβ, GATA4,[20,37-39] and finally Tbx5 and Nkx2.5.[25] The Smad-Id2 pathway appears to be particularly relevant in the etiology of the observed congenital malformations as *Smad7* mutant mice have a cardiovascular phenotype that includes ventricular septal defects, ventricular noncompaction and outflow tract malformation[40] and myocardial specific inactivation of *Smad4* causes myocardial hypoplasia.[38] These phenotypes resemble the phenotype observed in *Id2* knockout embryos observed in the current study, and is supported by a recent study that describes the activation of *Id2* by *Gata4* and *Smad4* in the heart.[41] However, less

information is available about downstream targets of *Id2*. *Id*-genes negatively regulate basic helix-loop-helix proteins. bHLH proteins with (partially) overlapping expression pattern with *Id*-genes include E2A, M-twist, paraxis, Screraxis and Hes1.[22,42,43] For many of these genes, a functional pathway in heart development has not been shown yet. Interestingly, Hes1 has recently been described in the SHF and neural crest cells and in the pharyngeal endoderm and mesoderm of the SHF. *Hes1* mutant hearts demonstrate outflow tract alignment defects including ventricular septal defects and overriding aorta.[44] As expressions patterns and phenotype of *Hes* deficiency resemble observations in the *Id2* mouse, we hypothesize that *Hes1* is a downstream target of *Id2* in the heart, as has been described for neural stem cells.[42] Another downstream candidate for Id2 is *Vegf*, which is completely absent in *Id2* knockout neuroblastoma cells.[45] A specific relation between *Id2* and *Vegf* in the heart is not known.

In conclusion, we provide expression patterns of Id2 in the heart in sequential developmental stages of the mouse embryo. Id2 is expressed in cardiac progenitor cells of both the arterial and venous poles during cardiovascular development. At the venous pole, Id2 is expressed in myocardial progenitor cells of the sinus venosus, and in the coelomic epithelium directly bordering the SAN, which implies a role for Id2 in SAN development. Abnormalities observed in *Id2* knockout embryos indicate a disturbed contribution of the second heart field at both the arterial and venous pole. The pathways in which *Id2* is involved and downstream targets warrant further investigation.

References

1. DeRuiter MC, Poelmann RE, VanderPlas-de Vries I, Mentink MMT, Gittenberger-de Groot AC. The development of the myocardium and endocardium in mouse embryos. Fusion of two heart tubes? *Anat Embryol*. 1992;185:461-473.
2. Moreno-Rodriguez RA, Krug EL, Reyes L, Villavicencio L, Mjaatvedt CH, Markwald RR. Bidirectional fusion of the heart-forming fields in the developing chick embryo. *Dev Dyn*. 2006;235:191-202.
3. Mjaatvedt CH, Nakaoka T, Moreno-Rodriguez R, Norris RA, Kern MJ, Eisenberg CA, Turner D, Markwald RR. The outflow tract of the heart is recruited from a novel heart-forming field. *Dev Biol*. 2001;238: 97--109.
4. Waldo K, Kumiski DH, Wallis KT, Stadt HA, Hutson MR, Platt DH, Kirby ML. Conotruncal myocardium arises from a secondary heart field. *Development*. 2001;128:3179-3188.
5. Kelly RG, Brown NA, Buckingham ME. The arterial pole of the mouse heart forms from Fgf10-expressing cells in pharyngeal mesoderm. *Dev Cell*. 2001;1:435-440.
6. Cai CL, Liang X, Shi Y, Chu PH, Pfaff SL, Chen J, Evans S. Isl1 identifies a cardiac progenitor population that proliferates prior to differentiation and contributes a majority of cells to the heart. *Dev Cell*. 2003;5:877-889.
7. Laugwitz KL, Moretti A, Caron L, Nakano A, Chien KR. Islet1 cardiovascular progenitors: a single source for heart lineages? *Development*. 2008;135:193-205.
8. Christoffels VM, Mommersteeg MT, Trowe MO, Prall OW, Gier-de Vries C, Soufan AT, Bussen M, Schuster-Gossler K, Harvey RP, Moorman AF, Kispert A. Formation of the venous pole of the heart from an Nkx2-5-negative precursor population requires Tbx18. *Circ Res*. 2006;98:1555-1563.
9. Gittenberger-de Groot AC, Mahtab EAF, Hahurij ND, Wisse LJ, DeRuiter MC, Wijffels MCEF, Poelmann RE. Nkx2.5 negative myocardium of the posterior heart field and its correlation with podoplanin expression in cells from the developing cardiac pacemaking and conduction system. *Anat Rec*. 2007;290:115-122.
10. Kelly RG, Buckingham ME. The anterior heart-forming field: voyage to the arterial pole of the heart. *Trends Genet*. 2002;18:210-216.
11. Kelly RG. Molecular inroads into the anterior heart field. *Trends Cardiovasc Med*. 2005;15:51-56.
12. Snarr BS, O'Neal JL, Chintalapudi MR, Wirrig EE, Phelps AL, Kubalak SW, Wessels A. Isl1 expression at the venous pole identifies a novel role for the second heart field in cardiac development. *Circ Res*. 2007;101:971-974.
13. Mahtab EA, Vicente-Steijn R, Hahurij ND, Jongbloed MR, Wisse LJ, DeRuiter MC, Uhrin P, Zaujec J, Binder BR, Schalij MJ, Poelmann RE, Gittenberger-de Groot AC. Podoplanin deficient mice show a Rhoa-related hypoplasia of the sinus venosus myocardium including the sinoatrial node. *Dev Dyn*. 2009;238:183-193.
14. Vicente-Steijn R, Kolditz DP, Mahtab EA, Askar SF, Bax NA, van der Graaf LM, Wisse LJ, Passier R, Pijnappels DA, Schalij MJ, Poelmann RE, Gittenberger-de Groot AC, Jongbloed MR. Electrical activation of sinus venosus myocardium and expression patterns of RhoA and Isl-1 in the chick embryo. *J Cardiovasc Electrophysiol*. 2010;21:1284-1292.
15. Garcia-Frigola C, Shi Y, Evans SM. Expression of the hyperpolarization-activated cyclic nucleotide-gated cation channel HCN4 during mouse heart development. *Gene Expr Patterns*. 2003;3:777-783.
16. Blaschke RJ, Hahurij ND, Kuijper S, Just S, Wisse LJ, Deissler K, Maxelon T, Anastassiadis K, Spitzer J, Hardt SE, Schöler H, Feitsma H, Rottbauer W, Blum M, Meijlink F, Rappold GA, Gittenberger-de Groot AC. Targeted mutation reveals essential functions of the homeodomain transcription factor Shox2 in sinoatrial and pacemaking development. *Circulation*. 2007;115:1830-1838.
17. Puskaric S, Schmitteckert S, Mori AD, Glaser A, Schneider KU, Bruneau BG, Blaschke RJ, Steinbeisser H, Rappold G. Shox2 mediates Tbx5 activity by regulating Bmp4 in the pacemaker region of the developing heart. *Hum Mol Genet*. 2010;19:4625-4633.
18. Mahtab EAF, Wijffels MCEF, van den Akker NMS, Hahurij ND, Lie-Venema H, Wisse LJ, DeRuiter MC, Uhrin P, Zaujec J, Binder BR, Schalij MJ, Poelmann RE, Gittenberger-de Groot AC. Cardiac malformations and myocardial abnormalities in podoplanin knockout mouse embryos: correlation with abnormal epicardial development. *Dev Dyn*. 2008;237:847-857.

19. Martinsen BJ, Frasier AJ, Baker CV, Lohr JL. Cardiac neural crest ablation alters Id2 gene expression in the developing heart. *Dev Biol*. 2004;272:176-190.
20. Lim JY, Kim WH, Kim J, Park SI. Induction of Id2 expression by cardiac transcription factors GATA4 and Nkx2.5. *J Cell Biochem*. 2008;103:182-194.
21. Yokota Y, Mori S, Narumi O, Kitajima K. In vivo function of a differentiation inhibitor, Id2. *IUBMB Life*. 2001;51:207-214.
22. Jen Y, Manova K, Benezra R. Expression patterns of Id1, Id2, and Id3 are highly related but distinct from that of Id4 during mouse embryogenesis. *Dev Dyn*. 1996;207:235-252.
23. Kelly RG, Jerome-Majewska LA, Papaioannou VE. The del22q11.2 candidate gene Tbx1 regulates branchiomeric myogenesis. *Hum Mol Genet*. 2004;13:2829-2840.
24. Fraidenraich D, Stillwell E, Romero E, Wilkes D, Manova K, Basson CT, Benezra R. Rescue of cardiac defects in id knockout embryos by injection of embryonic stem cells. *Science*. 2004;306:247-252.
25. Moskowitz IP, Kim JB, Moore ML, Wolf CM, Peterson MA, Shendure J, Nobrega MA, Yokota Y, Berul C, Izumo S, Seidman JG, Seidman CE. A molecular pathway including Id2, Tbx5, and Nkx2-5 required for cardiac conduction system development. *Cell*. 2007;129:1365-1376.
26. Gittenberger-de Groot AC, Vrancken Peeters M-PFM, Mentink MMT, Gourdie RG, Poelmann RE. Epicardium-derived cells contribute a novel population to the myocardial wall and the atrioventricular cushions. *Circ Res*. 1998;82:1043-1052.
27. Mesbah K, Harrelson Z, Theveniau-Ruissy M, Papaioannou VE, Kelly RG. Tbx3 is required for outflow tract development. *Circ Res*. 2008;103:743-750.
28. Bleyl SB, Saijoh Y, Bax NA, Gittenberger-de Groot AC, Wisse LJ, Chapman SC, Hunter J, Shiratori H, Hamada H, Yamada S, Shiota K, Klewer SE, Leppert MF, Schoenwolf GC. Dysregulation of the PDGFRA gene causes inflow tract anomalies including TAPVR: integrating evidence from human genetics and model organisms. *Hum Mol Genet*. 2010;19:1286-1301.
29. Bax NA, Bleyl SB, Gallini R, Wisse LJ, Hunter J, Van Oorschot AA, Mahtab EA, Lie-Venema H, Goumans MJ, Betsholtz C, Gittenberger-de Groot AC. Cardiac malformations in Pdgfralpha mutant embryos are associated with increased expression of WT1 and Nkx2.5 in the second heart field. *Dev Dyn*. 2010;239:2307-2317.
30. van den Akker NMS, Lie-Venema H, Maas S, Eralp I, DeRuiter MC, Poelmann RE, Groot ACG. Platelet-derived growth factors in the developing avian heart and maturating coronary vasculature. *Developmental Dynamics*. 2005;233:1579-1588.
31. Bax NA, Lie-Venema H, Vicente-Steijn R, Bleyl SB, van den Akker NM, Maas S, Poelmann RE, Gittenberger-de Groot AC. Platelet-derived growth factor is involved in the differentiation of second heart field-derived cardiac structures in chicken embryos. *Dev Dyn*. 2009;238:2658-2669.
32. Moskowitz IP, Pizard A, Patel VV, Bruneau BG, Kim JB, Kupershmidt S, Roden D, Berul CI, Seidman CE, Seidman JG. The T-Box transcription factor Tbx5 is required for the patterning and maturation of the murine cardiac conduction system. *Development*. 2004;131:4107-4116.
33. Douglas YL, Mahtab EA, Jongbloed MR, Uhrin P, Zaujec J, Binder BR, Schalij MJ, Poelmann RE, DeRuiter MC, Gittenberger-de Groot AC. Pulmonary vein, dorsal atrial wall and atrial septum abnormalities in podoplanin knockout mice with disturbed posterior heart field contribution. *Pediatr Res*. 2009;65: 27-32.
34. Snarr BS, Wirrig EE, Phelps AL, Trusk TC, Wessels A. A spatiotemporal evaluation of the contribution of the dorsal mesenchymal protrusion to cardiac development. *Dev Dyn*. 2007;236:1287-1294.
35. Lie-Venema H, van den Akker NMS, Bax NAM, Winter EM, Maas S, Kekarainen T, Hoeben RC, DeRuiter MC, Poelmann RE, Gittenberger-de Groot AC. Origin, fate, and function of epicardium-derived cells (EPCDs) in normal and abnormal cardiac development. *ScientificWorldJournal*. 2007;7:1777-1798.
36. Bajolle F, Zaffran S, Losay J, Ou P, Buckingham M, Bonnet D. Conotruncal defects associated with anomalous pulmonary venous connections. *Arch Cardiovasc Dis*. 2009;102:105-110.
37. Valcourt U, Kowanetz M, Niimi H, Heldin CH, Moustakas A. TGF-beta and the Smad signaling pathway support transcriptomic reprogramming during epithelial-mesenchymal cell transition. *Mol Biol Cell*. 2005;16:1987-2002.
38. Song L, Yan W, Chen X, Deng CX, Wang Q, Jiao K. Myocardial smad4 is essential for cardiogenesis in mouse embryos. *Circ Res*. 2007;101:277-285.
39. Nakahiro T, Kurooka H, Mori K, Sano K, Yokota Y. Identification of BMP-responsive elements in the mouse Id2 gene. *Biochem Biophys Res Commun*. 2010;399:416-421.

40. Chen Q, Chen H, Zheng D, Kuang C, Fang H, Zou B, Zhu W, Bu G, Jin T, Wang Z, Zhang X, Chen J, Field LJ, Rubart M, Shou W, Chen Y. Smad7 is required for the development and function of the heart. *J Biol Chem*. 2009;284:292-300.
41. Moskowitz IP, Wang J, Peterson MA, Pu WT, Mackinnon AC, Oxburgh L, Chu GC, Sarkar M, Berul C, Smoot L, Robertson EJ, Schwartz R, Seidman JG, Seidman CE. Cardiac-specific transcription factor genes Smad4 and Gata4 cooperatively regulate cardiac valve development. *Proc Natl Acad Sci U S A*. 2011;108:4006-4011.
42. Bai G, Sheng N, Xie Z, Bian W, Yokota Y, Benezra R, Kageyama R, Guillemot F, Jing N. Id sustains Hes1 expression to inhibit precocious neurogenesis by releasing negative autoregulation of Hes1. *Dev Cell*. 2007;13:283-297.
43. Jogi A, Persson P, Grynfeld A, Pahlman S, Axelson H. Modulation of basic helix-loop-helix transcription complex formation by Id proteins during neuronal differentiation. *J Biol Chem*. 2002;277:9118-9126.
44. Rochais F, Dandonneau M, Mesbah K, Jarry T, Mattei MG, Kelly RG. Hes1 is expressed in the second heart field and is required for outflow tract development. *PLoS One*. 2009;4:e6267.
45. Lasorella A, Rothschild G, Yokota Y, Russell RG, Iavarone A. Id2 mediates tumor initiation, proliferation, and angiogenesis in Rb mutant mice. *Mol Cell Biol*. 2005;25:3563-3574.
46. Yokota Y, Mansouri A, Mori S, Sugawara S, Adachi S, Nishikawa S, Gruss P. Development of peripheral lymphoid organs and natural killer cells depends on the helix-loop-helix inhibitor Id2. *Nature*. 1999;397:702-706.
47. Jongbloed MR, Wijffels MC, Schalij MJ, Blom NA, Poelmann RE, van der Laarse, Mentink MM, Wang Z, Fishman GI, Gittenberger-de Groot AC. Development of the right ventricular inflow tract and moderator band: a possible morphological and functional explanation for Mahaim tachycardia. *Circ Res*. 2005;96:776-783.

Chapter 6

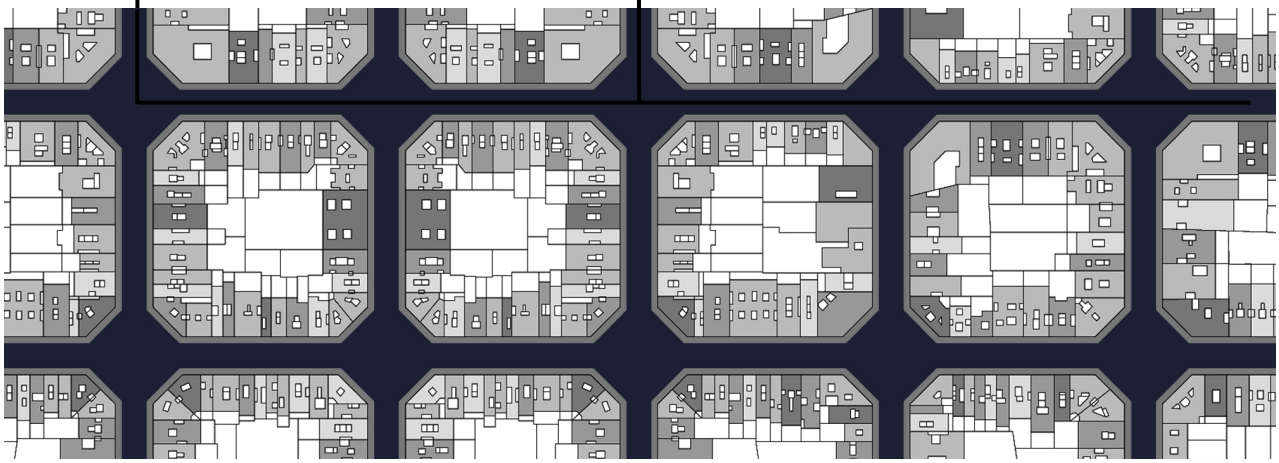

The funny current channel HCN4 delineates the developing cardiac conduction system in the chicken heart

Rebecca Vicente-Steijn, Robert Passier, Lambertus J Wisse, Martin J Schalij, Robert E Poelmann, Adriana C Gittenberger-de Groot, Monique RM Jongbloed

Heart Rhythm 2011 in press

Abstract

Background
Hyperpolarization-activated cyclic nucleotide-gated channel 4 (HCN4) in the mouse is expressed in the developing cardiac conduction system (CCS). In the sinoatrial node (SAN), HCN4 is the predominant isoform responsible for the funny current. To date no data is available on HCN4 expression during chicken CCS development.

Objective
To provide the full-length sequence of *Hcn4* and describe its expression pattern during development in relation to the CCS in the chicken embryo.

Methods
Hcn4 RNA expression was studied by in situ hybridization in sequential chick developmental stages (HH11-HH35) and immunohistochemical stainings were conducted for the myocardial protein cTnI and the cardiac transcription factor Nkx2.5.

Results
We obtained the full-length sequence of *Hcn4* in chick. *Hcn4* expression was observed early in development in the primary heart tube. At later stages, expression became restricted to transitional zones flanked by working myocardium , comprising the sinus venosus myocardium where the SAN develops, the atrioventricular canal myocardium, the primary fold (a myocardial zone between the developing ventricles), and the developing outflow tract. Further in development, *Hcn4* expression was restricted to the SAN, the atrioventricular node, the common bundle, the bundle branches and the internodal and atrioventricular ring myocardium.

Conclusion
We have identified *Hcn4* as a marker of the developing CCS in the chick. The primary heart tube expresses *Hcn4*, which is later restricted to the transitional zones and eventually the elements of the mature CCS. Furthermore, we hypothesize that expression patterns during development may delineate potential arrhythmogenic sites in the adult heart.

Introduction

In the adult heart, the cardiac conduction system (CCS) is responsible for initiating and propagating the cardiac electrical impulse. This impulse originates in the SAN, located at the entrance of the right caval vein into the right atrium (RA) and is conducted via Bachmann's bundle to the left atrium (LA) and through the atrial muscle to the atrioventricular node (AVN), where it is delayed. The impulse is then propagated through the common bundle and the left and right bundle branches to the Purkinje fiber network, which will conduct it rapidly to the working ventricular myocardium allowing the ventricles to contract in an apex to base manner. Cardiac arrhythmias can be initiated from anatomical predilection sites in the heart that are not part of the adult CCS. Known arrhythmogenic areas are the myocardium surrounding the caval veins and the coronary sinus in the RA, and the pulmonary veins in the LA.[1] Interestingly, this myocardium expresses several markers that are also found in elements of the developing CCS.[2,3]

In the early embryo the heart starts out as a single myocardial tube that will incorporate myocardium at the arterial and venous[3,4] poles from a cell population dorsal to the heart, the second heart field.[3-6] In recent years, it has become clear that the sinus venosus myocardium including the SAN is also derived from this second heart field, while the contribution of the second heart field to AVN is still a matter of debate.[7,8] Molecular genetic studies in the mouse have demonstrated that a complex network of transcription factors is required for the formation of the CCS.[9] However, the molecular pathways guiding the cells towards either a working or pacemaking myocardium are not clear and several models have been postulated.[10,11] Specific transitional zones can be identified after looping of the heart has started, which are interposed between the developing cardiac segments that consist of working myocardium. These zones have a different expression profile compared to the working myocardium and have been identified based on the expression patterns of several immunohistochemical and molecular markers, e.g. the transcriptional repressor *Tbx3,*[12] HNK-1,[13] MinK,[14] engrailed-2-LacZ/CCS-LacZ,[2] and podoplanin.[3] The transitional zones include the sinus venosus myocardium (i.e. the myocardium surrounding the embryonic cardinal veins) where the SAN will develop. Furthermore, the atrioventricular canal where the AVN will form, the primary fold, which is the myocardium between the primitive right ventricle (RV) and left ventricle (LV) where the common bundle and the bundle branches will develop, and finally regions of the outflow tract.[2,12]

Previously, we have shown in chicken embryos that the entire sinus venosus myocardium including the developing SAN is initially formed by myocardium with a different phenotype compared to the working myocardium of the developing chambers. Additionally, this myocardium expresses the pacemaker channel *Hcn4* and this entire area has the potential to generate the initial electrical impulse.[6] HCN4 is a member of the hyperpolarization-activated cyclic nucleotide-gated (HCN) channel

gene family (HCN1-4). In the adult heart, these channels are expressed in nodal, atrial and ventricular tissues. In the adult SAN of lower mammals and humans, the HCN4 isotype is the predominant channel responsible for the funny current,[15] although HCN1 and HCN2 have also been detected at lower levels in some species.[16] In the mouse *Hcn4* has been reported as a marker for pacemaker tissues of the sinus venosus[17] being expressed in the embryo as early as embryonic day (E)7.5 in the cardiac mesoderm followed by expression in the sinus venosus myocardium, and eventually the SAN.[18] Currently, no data on *Hcn4* expression in chicken is available, although the chicken embryo is frequently used as experimental model for cardiovascular development.
In the current study we provide the full-length coding sequence of the chick *Hcn4.* We analyzed *Hcn4* mRNA expression and localization during sequential developmental stages in the chick embryo and provide an overview of the expression patterns during chick CCS development.

Materials and Methods

Animal preparation

Fertilized White Leghorn chicken eggs were incubated at 37°C. Animal experiments were performed in accordance to institutional guidelines of the Leiden University Medical Center. Embryos were extracted and staged according to standard (Hamburger&Hamilton 1951) criteria and fixed in 4% paraformaldehyde for 24h.

RNA isolation, cDNA synthesis and Reverse Transcriptase PCR

RNA was isolated from embryonic chicken hearts (HH11-12, n=18; HH16-17, n=7; HH27, n=2 and HH31, n=2) using Trizol reagent (Invitrogen, Carlsbad, CA) and reversely transcribed into cDNA using Superscript II reverse transcription-polymerase and random primers (Invitrogen). To cover the full-length of the predicted *Hcn4* sequence (XM_425050) overlapping primers were designed using Primer3 software. The full-length was obtained by reverse transcriptase-PCR (RT-PCR) using AccuPrime GC Rich DNA polymerase (Invitrogen) according to protocol as well as RACE-methods. In the RACE-method, 3'-RACE cDNA was synthesized following the manufacturer's protocol (TaKaRa, Dalian, China). The 3' region of *Hcn4* was obtained in 3'-RACE reactions using the SMART RACE cDNA Amplification Kit (TaKaRa, Dalian, China) with two gene specific primers (5'-CCGGCTCATCCGCTATATT-3' and 5'-CATGCCACTCTTTGCCAAC-3') and the universal primer mix (UPM) provided by the manufacturer. The products obtained with the AccuPrime DNA polymerases were directly sequenced; 3'RACE amplified cDNA fragments were first cloned into the pCRII-TOPO vector (Invitrogen), followed by sequencing.

Real time qPCR

Chicken specific primers for *Hcn4* (forward 5'-AAAAGGCTCCAGTCCCTGAT-3', reverse 5'-CACCGCTCAGTCCCTGCT-3') and *Hcn1* (forward 5'-CTGCACCCAAGAATGAGGTT-3', reverse 5'-ATCAGGGTGGAAATCTCGTG-3') were designed. Each reaction contained 10µl of SybrGreen Mastermix (Bio-Rad, Hercules, CA), 0.5mM forward and reverse primer, and 1µl of cDNA in a final volume of 20µl. Reactions were carried out in triplicate for each sample. Negative controls were reactions containing H_2O instead of cDNA. PCR was run on a Bio-Rad CFX96 Real Time System and a melting curve was produced to verify single PCR product amplification. Efficiency of the PCR reaction was tested using a standard curve synthesized from a dilution series of cDNA. Chicken *Gapdh* (forward: 5′-CTAAGGCTGTGGGGAAGGT-3′, reverse: 5′-GTTGTTGACCTGACCTGCC-3′) was used as the reference standard for normalization and relative quantification of differences in mRNA expression was determined.

Whole mount and tissue sections for non-radioactive in situ hybridization (ISH)

Whole mount ISH was performed according to protocol.[19] A *Hcn4* cDNA template was generated using chicken *Hcn4* specific primers (forward: 5'-GTGTCACTGGGATGGCTGCCT-3', reverse:5'-GCCAATGGTGCCCTCCCGAA-3'). These primers produced a purified cDNA fragment corresponding to amino acids 400-602 of the chicken predicted *Hcn4* sequence (XM_425050). Additionally, ISH on 10µm transversal sections from chicken embryos ranging from HH15-HH35 (n=22) was performed as described previously.[4,6] Five embryos per probe (sense/αsense) were used for the whole mount ISH.

Immunohistochemistry

Immunohistochemical stainings were conducted as described previously[20] on sister sections from the *Hcn4* ISH stained sections (HH15-HH35). The stainings were conducted using the primary antibody cardiac Troponin I (cTnI, goat polyclonal antibody, sc-15368, Santa Cruz, 1/400) and Nkx2.5 (goat polyclonal antibody, sc-8697, Santa Cruz, 1/4000). Slides were incubated with a biotin-conjugated secondary antibody (horse-α-goat(BA-9500), from Vector Labs), visualized by incubation with 3-3'diaminobenzidin tetrahydrochloride (DAB, D5637, Sigma-Aldrich), and counterstained with haematoxylin (0.1%, Merck).

3-D reconstructions

3-D reconstructions of atrial and ventricular myocardium of cTnI-stained serial sections of HH24 and HH32 embryos were made as previously described[2] using the

AMIRA v4.0 Software Package (Template Graphics Software, San Diego, USA). *Hcn4* RNA expression observed in immediate sister sections was superimposed.

Results

Identification of *Hcn4* and expression levels in the chick

To obtain the full-length coding sequence of HCN4, overlapping primers were designed based on the predicted sequence XM_425050 as found on NCBI. Several PCRs using chicken heart cDNA as template were conducted. The obtained consensus sequence encodes a 1208 amino acid protein which when aligned to mouse and human HCN4 sequences shows a 71 % and 70% homology respectively (Figure 6.1).
To study the expression patterns of *Hcn4* during chick heart development, a RNA probe was designed based on the predicted sequence. To confirm that the probe was specific for *Hcn4* (and did not cross-react with the other family members) a homology search of nucleotide and amino acid sequences was conducted using the BLAST algorithm. We confirmed that the sequence of the probe was identical to *Hcn4*, although it also displayed an 88% homology to a 149bp fragment (of the 606bp) which belonged to the HCN1 channel in chick. Therefore, we conducted quantitative real-time PCR for *Hcn4* and *Hcn1* on embryonic hearts from consecutive stages to determine their expression levels. The results confirmed that *Hcn4* mRNA is the dominant isoform expressed (Figure 6.2), specifically it is 10-20-fold higher than *Hcn1*. Interestingly, a distinct peak of *Hcn4* mRNA expression is visible in HH16/17 hearts compared to the other stages.

Expression patterns of *Hcn4* during development

Expression patterns of cTnI, Nkx2.5 and *Hcn4* (ISH) in chicken hearts in sequential stages of development (HH11-35) were studied (Figures 6.3-6.6).

HH11-17 (~2 days of incubation)

Looping of the heart has barely started as only a slightly C-shaped heart tube is present (Figure 6.3a-b). This heart tube consists of a single ventricle with an outflow part and an inflow part with a sinus venosus and a primitive atrium. On whole mount ISH *Hcn4* expression was observed in HH11-12 embryos throughout the entire developing heart tube (Figure 6.3a-b) with a slightly more marked staining at the inflow portion (sinus venosus) and the atrioventricular canal. The control sense probe did not show this pattern, indicating that the staining observed was specific (Figure 6.3c-d). Later in development (around HH13-14) the heart transforms from a C-shape to a S-shaped loop in which *Hcn4* expression is still observed throughout the entire heart tube (Figure 6.3e-g) exclusively in the myocardial layer as delineated by cardiac

Troponin I (cTnI) expression (Figure 6.3h-j), being absent from the endocardium and cardiac jelly.

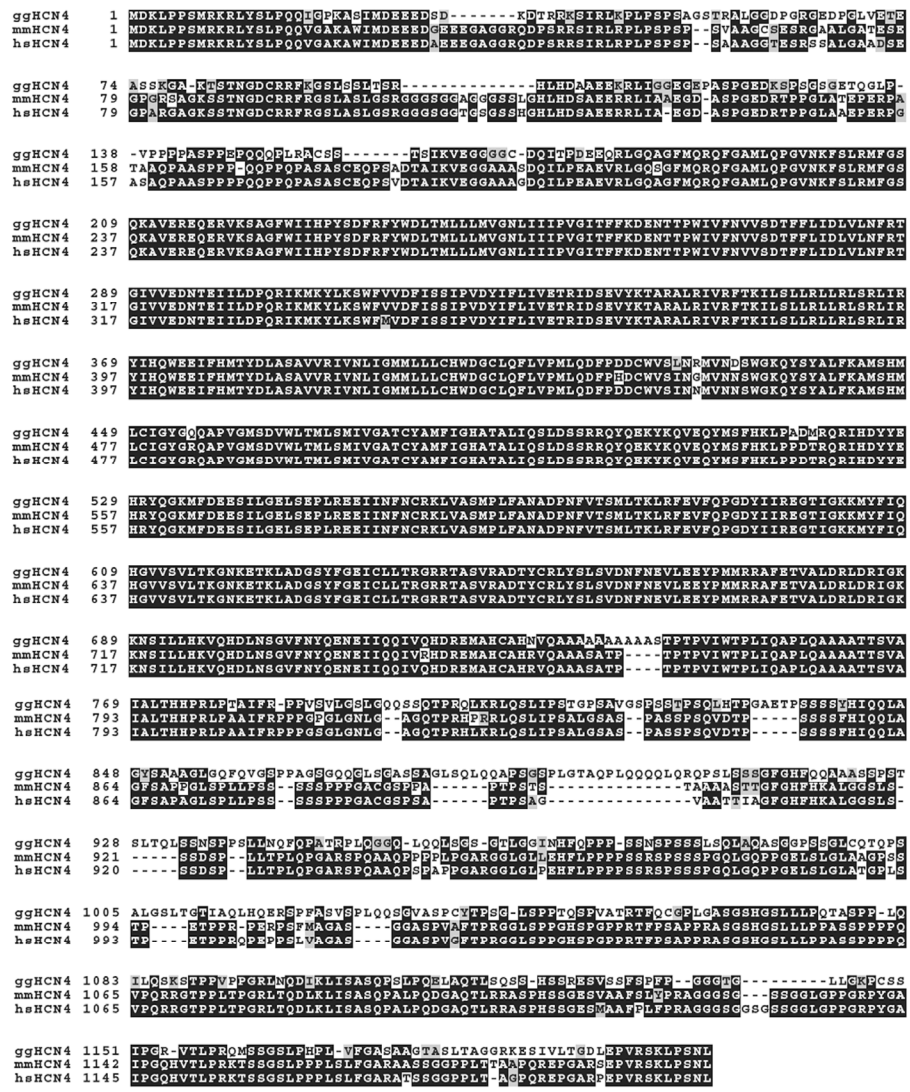

Figure 6.1 *Hcn4* sequence in chick based on the predicted ATG site. Alignment and amino acid sequence between different vertebrates. Similar residues are shaded in grey while identical ones are shaded in black. Positions in the amino acid sequence are given by numbers and gaps are indicated by a dash. gg: *Gallus gallus;* hs: *Homo sapiens;* mm: *Mus musculu*s.

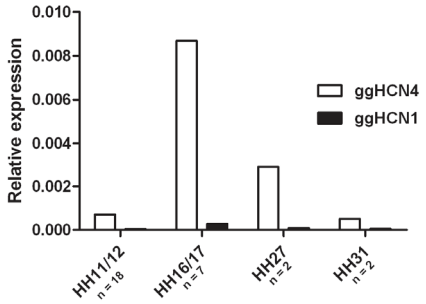

Figure 6.2 *Hcn4* and *Hcn1* mRNA expression in chicken embryonic hearts at different developmental stages (HH11/12-HH31). Expression levels were normalized to *Gapdh*. gg: *Gallus gallus.*

HH18- 24 (2-4 days of incubation)

Heart looping continues and the sinus venosus is shifted from its initial location caudal to the atria to its final location dorsal to the atria. Both atria are still connected to the primitive LV. During these stages, expansion of both atria and ventricles becomes apparent as they start to balloon out from the linear heart tube. *Hcn4* expression becomes restricted to specific sites in the myocardium. A 3D-representation of the expression pattern is shown in Figure 6.4a-b. Expression is observed in the so-called transitional zones of the heart that comprise at the venous pole the myocardium of the entire sinus venosus, i.e. the myocardium surrounding both cardinal veins including the SAN (Figure 6.4c-f), as well as in the myocardium surrounding the region where the pulmonary vein (pulmonary pit) has become apparent (Figure 6.4g-j). This region contains already differentiated myocardium as shown by cTnI expression (Figure 6.4e, 6.4g and 6.4i) and is characterized by lack of Nkx2.5 expression (Figure 6.4f). The developing pulmonary pit has a limited myocardial sleeve (Figure 6.4i-j) that shows *Hcn4* expression (Figure 6.4c and 6.4h). The venous valves are starting to develop at the entrance of the right cardinal vein into the RA. The right venous valve expresses *Hcn4* (Figure 6.4c-d) whereas the left venous valve shows a lower expression level. *Hcn4* is also found in the atrioventricular transition encompassing the myocardium of the complete atrioventricular canal (Figure 6.4k-l) as well as in the primary fold, situated between the LV and the developing RV (Figure 6.4m). Intenser local staining in the trabeculations is observed (not shown). Additionally, *Hcn4* is observed at the proximal part of the outflow tract (Figure 6.4n). The ballooning part of the myocardium of both atria and ventricles does not express *Hcn4* mRNA.

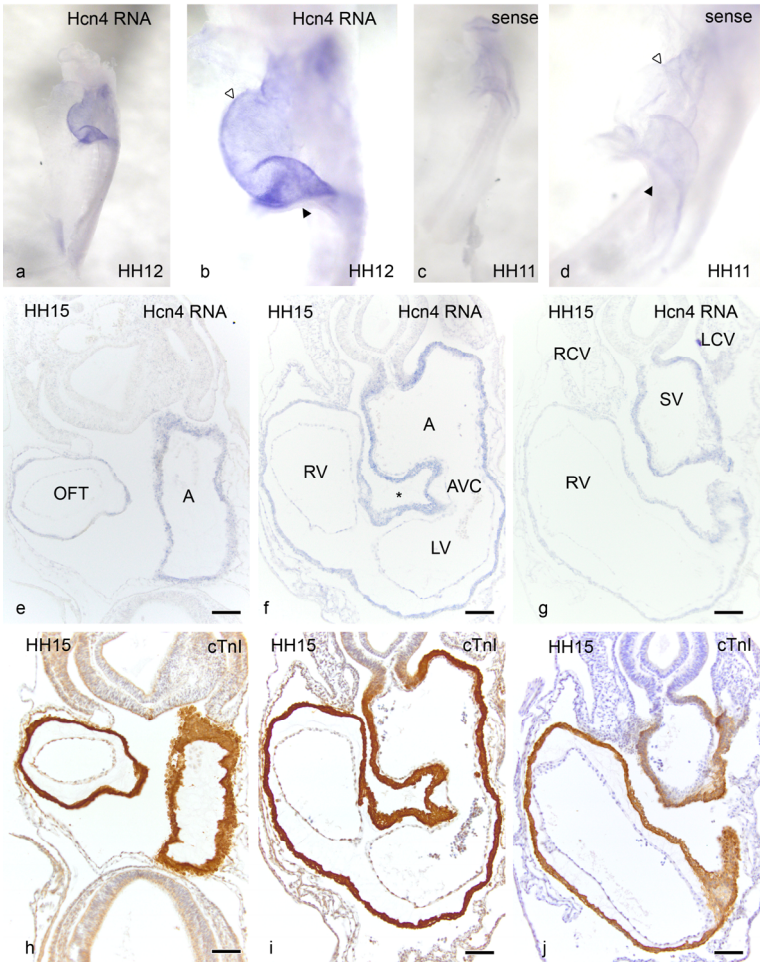

Figure 6.3 *Hcn4* mRNA expression in the entire heart tube in early stages. **a-b**. Whole mount in situ hybridization on HH12 embryos, showing positive signal in the embryonic heart tube (arrowhead). **b**. magnification in which the venous (arrowhead) and arterial (open arrowhead) poles are visible. **c**. Hybridization with the sense probe revealed no signal in the embryo including the heart. **d**. Magnification of the heart in **c**. Transverse sections of a stage HH15 chick heart showing *Hcn4* mRNA expression at different levels from cranial(**e**) to caudal(**g**), and cTnI expression in sister sections of the same heart from cranial(**h**) to caudal(**j**). A:common atrium; AVC:atrioventricular canal; IC:inner curvature; LCV:left cardinal vein; LV:primitive left ventricle; OFT:outflow tract; RCV:right cardinal vein; RV:primitive right ventricle; SV:sinus venosus lumen. Scale bars=100µm.

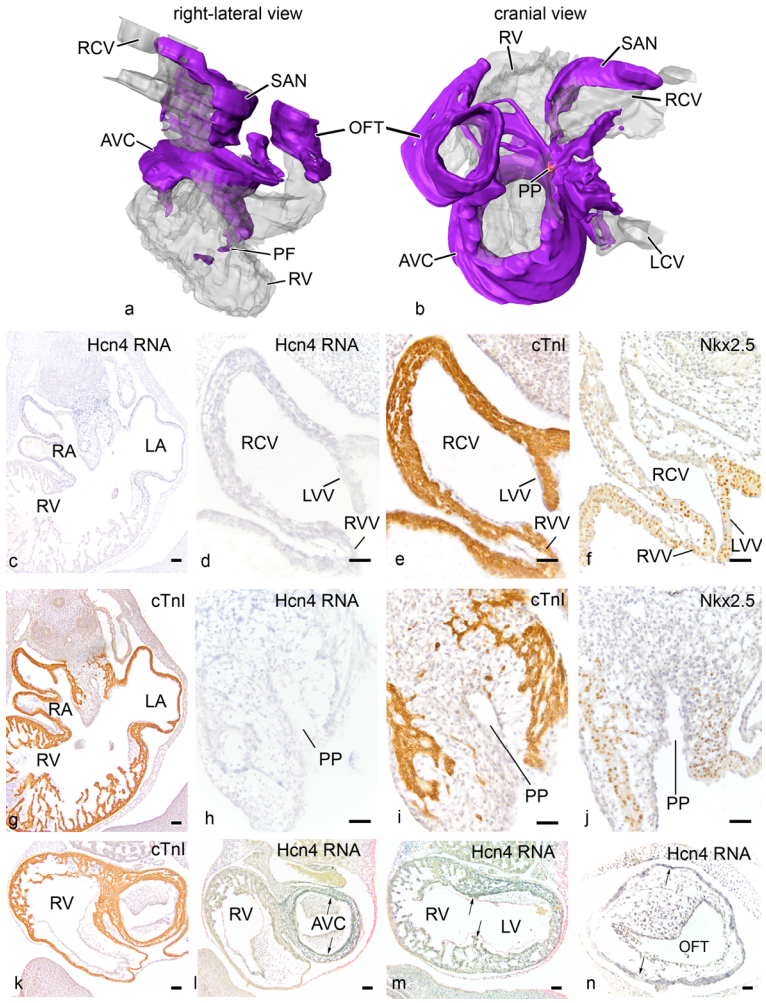

Figure 6.4 *Hcn4* mRNA expression in transitional zones. **a-b** 3D reconstruction of stage HH24. (**a**) right-lateral and (**b**) cranial view. *Hcn4* mRNA expression in depicted in purple, outflow tract (OFT), right ventricle (RV) and right and left cardinal vein (R/LCV) lumens in grey, and the pulmonary pit (PP) in pink. **c**. Transverse section showing *Hcn4* expression in myocardium surrounding the RCV where the sinoatrial node (SAN) is located, and myocardium surrounding the developing pulmonary vein (PP). **d-f**. Transverse sections depicting the SAN which expresses *Hcn4* (**d**), cTnI (**e**) but no Nkx2.5(**f**). **g-j**. Transverse sections depicting the developing PP surrounded by myocardium expressing HCN4(**h**),cTnI(**i**) and Nkx2.5(**j**). **k-l**. Transverse sections of the atrioventricular canal showing cTnI(**k**) and *Hcn4* expression(**l**, arrows). **m**. Transverse section showing *Hcn4* expression in the primary fold (arrows in **m**). **n**. Transverse section showing *Hcn4* expression in the developing OFT depicted by the arrows. LA:left atrium; LV:left ventricle, LVV:left venous valve; RA:right atrium; RVV:right venous valve. Scale bars d,h,l-o=100µm, e-g and i-k=50µm.

HH25-29 (4,5-6 days of incubation)

Looping of the heart is completed and the mature position of the chambers is achieved. After development of the RV inflow tract and the connection of the LV with the aorta, both atria are situated above each corresponding ventricle and the outflow portion of the heart is ventral to the chambers. Cardiac septation is ongoing and from HH28 onwards atrioventricular valve formation starts. *Hcn4* expression is visible in the same restricted areas as described before except for the outflow tract, where the expression has disappeared.

HH30-35 (6,5-9 days of incubation)

Cardiac septation is finalized and atrioventricular valve maturation is ongoing. A 3D-reconstruction of a stage HH32 heart shows the spatial expression pattern of *Hcn4* (Figure 6.5a-c). The myocardium surrounding left and right cardinal veins (sinus venosus myocardium) including the SAN still expresses *Hcn4* (Figure 6.5d-e) and cTnI (Figure 6.5f), but no Nkx2.5 (Figure 6.5g). A myocardial pulmonary sleeve has developed in which myocardial (i.e. cTnI (Figure 6.5j) and Nkx2.5 positive (Figure 6.5k)) *Hcn4* expressing cells are still visible (Figure 6.5h-i). At the base of the atrial septum, at the expected location of the AVN, *Hcn4* expression is present in the myocardium (Figure 6.6a-f). *Hcn4* expression is observed throughout the entire atrioventricular ring (i.e. right and left-sided), is continuous with the *Hcn4* positive myocardium that runs in a retro-aortic position from the RA to the LA and is observed in the internodal myocardium in the right atrium that connects the SAN and the AVN (Figure 6.5a-b and 6.5d). The anterior region of the ventricular septum, where the common bundle is located (Figure 6.5a-c and Figure 6.6a-c, 6.6g-i) also shows *Hcn4* expression. This myocardium expresses both cTnI (Figure 6.6h) and Nkx2.5 (Figure 6.6i). Additionally, the myocardium on both sides of the ventricular septum, where the bundle branches are found shows expression of *Hcn4*, (Figure 6.5a-b and 6.6a), cTnI (Figure 6.6b) and Nkx2.5 (Figure 6.6c).

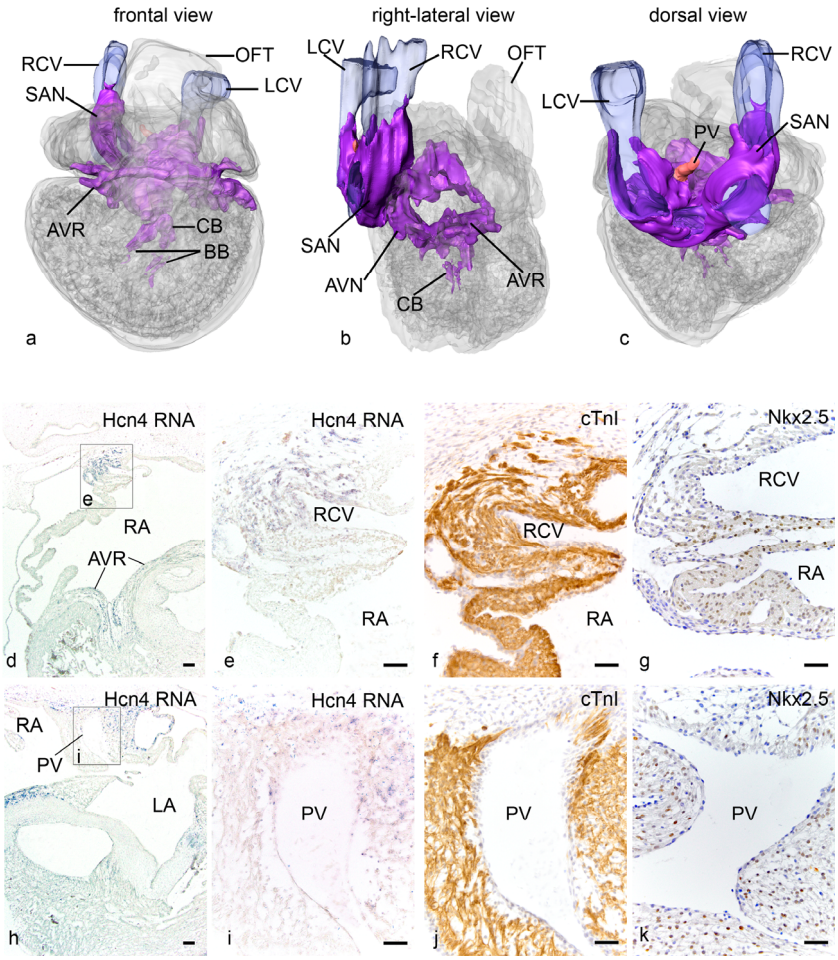

Figure 6.5 *Hcn4* expression in sinus venosus myocardium. **a-c.** 3D reconstruction of stage HH35. (**a**)frontal, (**b**)right lateral and (**c**)dorsal view. *Hcn4* mRNA expression in depicted in purple, atrial and ventricular myocardium and lumen, and outflow tract (OFT) myocardium and lumen are depicted in grey, lumen of the left (LCV) and right (RCV) cardinal veins in transparent blue and lumen of the pulmonary vein (PV) in pink. **d** *Hcn4* expression in the myocardium of the sinoatrial node (SAN) and atrioventricular ring (AVR). **e-g.** Magnifications of the boxed area in **d** showing the definitive SAN which expresses *Hcn4*(**e**) and cTnI(**f**) but lacks Nkx2.5 expression(**g**). **h.** *Hcn4* expression surrounding the PV. **i-k**. Magnifications of the boxed area in **h** showing the myocardium surrounding the PV expressing *Hcn4* (**i**), cTnI(**j**) and Nkx2.5(**k**) at this stage. AVN:atrioventricular node, BB:bundle branches, CB:common bundle, LA:left atrium, RA:right atrium. Scale bars d,h=100µm, e-g, i-k=50µm.

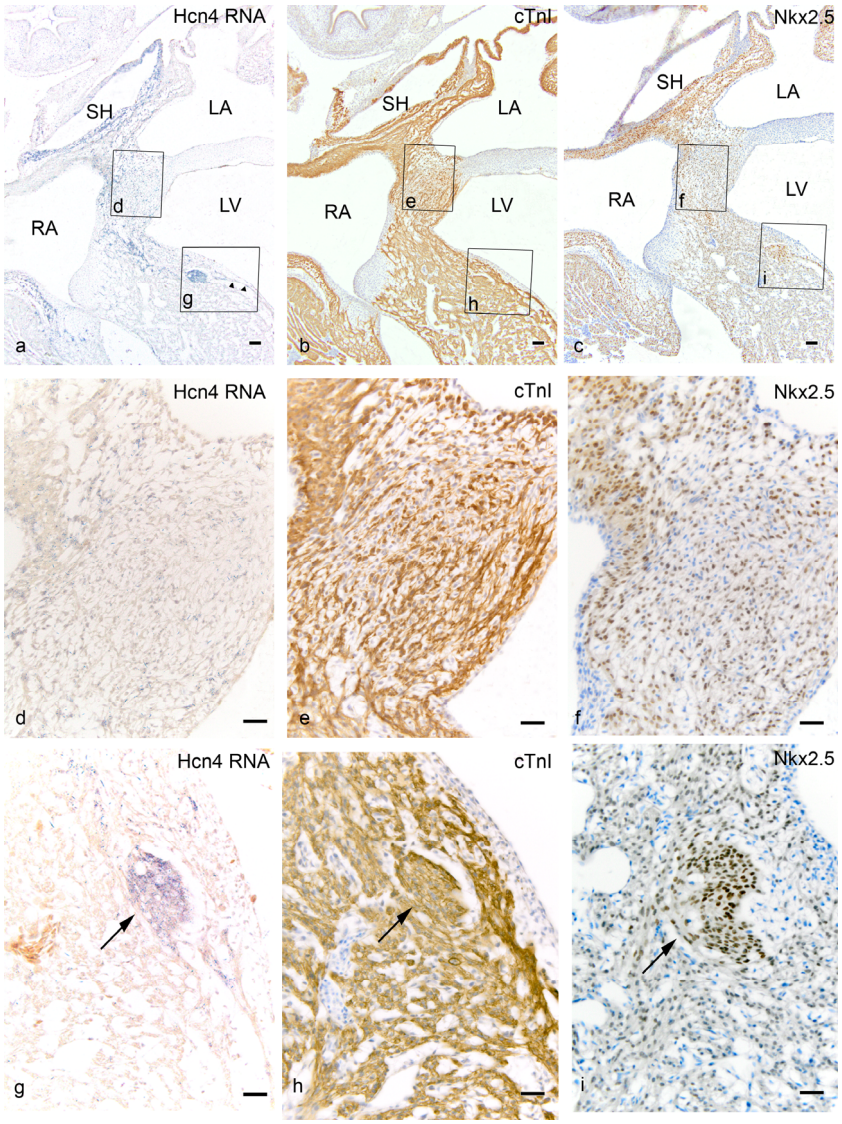

Figure 6.6 *Hcn4* expression in the atrioventricular conduction axis. **a-c**. *Hcn4* (**a**), cTnI(**b**) and Nkx2.5(**c**) expression in the atrioventricular node area, common bundle and bundle branches (arrowheads in **a**). **d-f.** Magnifications of boxed areas in **a-c** showing the atrioventricular node region which shows *Hcn4*(**d**), cTnI(**e**) and Nkx2.5(**f**) expression. **g-i.** Magnifications of the other boxed areas in **a-c** showing the common bundle (arrow) which expresses *Hcn4*(**g**), cTnI(**h**) and Nkx2.5(**i**). Scale bars a-c=100µm, d-i=50µm.

Discussion

Understanding the development of the CCS may help elucidate mechanisms that explain the occurrence of arrhythmias observed in the adult. In this study, we provide the full-length coding sequence of *Hcn4* in the chick, which could be clearly distinguished from the closely related *Hcn1* family member. Further, we describe for the first time the expression of the funny current channel *Hcn4* in the developing CCS in chick. The *Hcn4* mRNA expression data in the chick differ slightly from the described mRNA patterns in mouse.[8,18,21] Our first noteworthy finding is the presence of *Hcn*4 mRNA in the complete linear heart tube at stage HH11/12 in the chicken embryo, which has not been reported for *Hcn4* in the mouse embryo.[18] Only a few genes that are linked to myocardial and CCS development have been described in the early heart tube, e.g. the transcription factors *Nkx2.5,*[22] *Gata4*[23] and *Tbx5.*[24] Other transcription factors, such as *Tbx2* and *Tbx3,*[12,25] implicated in CCS formation and function, are expressed upon ballooning of the cardiac chambers. The MinK protein, implicated in CCS function and expressed in the developing CCS,[14] has also not been reported in the primary heart tube. Thus far, to our knowledge, no functional genes involved in CCS formation and function have been described in the primary heart tube. It has already been reported that the primary heart tube presents a nodal-like functional phenotype in that it shows automaticity, slow conduction of the electrical signal and a peristaltic-like contraction pattern.[11,26] Given the functional relevance of the ion channel HCN4, the primary heart tube wide expression suggests that the entire myocardium has the capacity to generate the electrical impulse necessary for the peristaltic contractions at this stage.[26]

During looping, septation and chamber formation *Hcn4* mRNA becomes restricted to the transitional zones of the heart. The expression pattern overlaps with that of *Tbx2* and *Tbx3,*[12,25,27] that play a role in CCS formation and remain expressed in the transitional zones where they prevent chamber formation. An especially important zone for the development of the CCS is the sinus venosus myocardium at the venous pole, which is derived from the second heart field mesoderm.[5] Studies in both mouse[3,4,21] and chicken[6] describe the sinus venosus myocardium as a progenitor for the development of the pacemaking myocardium. This includes a transient left SAN and ultimately the definitive right-sided SAN.[3,6] Other second heart field-derived myocardium in this area includes the internodal myocardium, encompassing the right venous valve (the future terminal crest) and the left venous valve, as well as the myocardium that will develop around the pulmonary veins. These structures express *Hcn4* mRNA in the chicken. During maturation, expression diminishes but persists in the definitive SAN. This characteristic is shared with a number of sinus venosus myocardium expressed transcriptional factors including *Shox2,*[28] *Tbx18,*[4,21] the protein podoplanin[3,20] and RhoA.[6,20] The transcriptional pathways that influence *Hcn4* expression are not well understood. Recently, *Hcn4* was reported downstream of *Shox2* indicated by reduced expression in *Shox2* knock out mice,[17] although a direct

regulation still needs to be confirmed. In the SAN, *Hcn4* is critical for proper electrical impulse generation[29] whereas *Shox2* is necessary for establishing SAN identity, as the lack of *Shox2* results in a hypoplastic SAN and ectopic Nkx2.5 and Cx40 expression.[17,28] Interestingly, deficiency of *Tbx3* does not affect *Hcn4* expression or SAN formation.[27] Based on the expression of *Hcn4* in the developing CCS, we suggest that several key transcriptional players are involved in the differentiation of components of the CCS and possible additional players remain to be identified.

In the fully septated heart *Hcn*4 expression is confined to the SAN, the AVN, the common bundle and the bundle branches. It is also still expressed in the internodal myocardium, in a ring bundle encircling the atrioventricular canal and in a retro-aortic band running from the RA to the LA. These areas are indicative of the developing CCS and suggest a broader function for HCN4 in the CCS, as has also been reported by others.[8,30-33]

Limitations of the study

It is evident from the studies of *Hcn*4 expression that it can not be indicated as a lineage marker, since both first and second heart field-derived myocardium are involved. *Hcn4* seems more a functional marker that distinguishes the potential CCS myocardium from the working myocardium. Our results, however, are based on mRNA expression and not protein expression, making functional conclusions difficult. No data on mRNA expression patterns of other HCN-channel family member has been studied, so we cannot exclude that other isotypes are also expressed during chick CCS development. Although we have observed low levels of *Hcn1* mRNA during development, *Hcn4* remains the dominant isotype (this study and[31]). An interaction between HCN1 and HCN4 resulting in the funny current of the rabbit SAN has been hypothesized.[34]

Clinical implications

The embryonic expression pattern of *Hcn4* might relate to the occurrence of arrhythmias at specific predilection sites in the adult heart. In line with previous studies,[2-4,6,13] the expression of *Hcn4* in the myocardial sleeve surrounding the pulmonary veins and the sinus venosus myocardium (putative sleeves surrounding the caval veins), well known predilection sites for the initiation of arrhythmias,[1] is interesting. We propose that either re-expression of the embryonic program or remnants of embryonic tissue could explain the arrhythmogenic potential of these sites. Studies in human show an elevated funny current due to increased HCN4 and HCN2 expression during heart failure.[35] Although the mechanism is certainly more complex, this suggests that during pathophysiological remodeling the embryonic program can be re-activated. This may shed new light on the frequent co-occurrence of atrial fibrillation and heart failure.

In conclusion, this report provides a description of *Hcn4* mRNA expression during chicken heart development, being expressed in the entire developing CCS, which supports the concept that CCS components during development can share the same transcriptional regulatory network.

References

1. Haissaguerre M, Jais P, Shah DC, Takahashi A, Hocini M, Quiniou G, Garrigue S, Le MA, Le MP, Clementy J. Spontaneous initiation of atrial fibrillation by ectopic beats originating in the pulmonary veins. *N Engl J Med*. 1998;339:659-666.
2. Jongbloed MRM, Schalij MJ, Poelmann RE, Blom NA, Fekkes ML, Wang Z, Fishman GI, Gittenberger-de Groot AC. Embryonic conduction tissue: a spatial correlation with adult arrhythmogenic areas? Transgenic CCS/lacZ expression in the cardiac conduction system of murine embryos. *J Cardiovasc Electrophysiol*. 2004;15:349-355.
3. Gittenberger-de Groot AC, Mahtab EAF, Hahurij ND, Wisse LJ, DeRuiter MC, Wijffels MCEF, Poelmann RE. Nkx2.5 negative myocardium of the posterior heart field and its correlation with podoplanin expression in cells from the developing cardiac pacemaking and conduction system. *Anat Rec*. 2007;290:115-122.
4. Christoffels VM, Mommersteeg MT, Trowe MO, Prall OW, Gier-de Vries C, Soufan AT, Bussen M, Schuster-Gossler K, Harvey RP, Moorman AF, Kispert A. Formation of the venous pole of the heart from an Nkx2-5-negative precursor population requires Tbx18. *Circ Res*. 2006;98:1555-1563.
5. Cai CL, Liang X, Shi Y, Chu PH, Pfaff SL, Chen J, Evans S. Isl1 identifies a cardiac progenitor population that proliferates prior to differentiation and contributes a majority of cells to the heart. *Dev Cell*. 2003;5:877-889.
6. Vicente-Steijn R, Kolditz DP, Mahtab EA, Askar SF, Bax NA, van der Graaf LM, Wisse LJ, Passier R, Pijnappels DA, Schalij MJ, Poelmann RE, Gittenberger-de Groot AC, Jongbloed MR. Electrical activation of sinus venosus myocardium and expression patterns of RhoA and Isl-1 in the chick embryo. *J Cardiovasc Electrophysiol*. 2010;21:1284-1292.
7. Sun Y, Liang X, Najafi N, Cass M, Lin L, Cai CL, Chen J, Evans SM. Islet 1 is expressed in distinct cardiovascular lineages, including pacemaker and coronary vascular cells. *Dev Biol*. 2007;304:286-296.
8. Aanhaanen WT, Mommersteeg MT, Norden J, Wakker V, de Gier-de Vries C, Anderson RH, Kispert A, Moorman AF, Christoffels VM. Developmental Origin, Growth, and Three-Dimensional Architecture of the Atrioventricular Conduction Axis of the Mouse Heart. *Circ Res*. 2010;107:728-736.
9. Srivastava D, Olson EN. A genetic blueprint for cardiac development. *Nature*. 2000;407:221-226.
10. Cheng G, Litchenberg WH, Cole GJ, Mikawa T, Thompson RP, Gourdie RG. Development of the cardiac conduction system involves recruitment within a multipotent cardiomyogenic lineage. *Development*. 1999;126:5041-5049.
11. Moorman AFM, Christoffels VM. Cardiac chamber formation: Development, genes and evolution. *Physiol Rev*. 2003;83:1223-1267.
12. Hoogaars WM, Tessari A, Moorman AF, de Boer PA, Hagoort J, Soufan AT, Campione M, Christoffels VM. The transcriptional repressor Tbx3 delineates the developing central conduction system of the heart. *Cardiovasc Res*. 2004;62:489-499.
13. Blom NA, Gittenberger-de Groot AC, DeRuiter MC, Poelmann RE, Mentink MM, Ottenkamp J. Development of the cardiac conduction tissue in human embryos using HNK-1 antigen expression: possible relevance for understanding of abnormal atrial automaticity. *Circulation*. 1999;99:800-806.
14. Kondo RP, Anderson RH, Kupershmidt S, Roden DM, Evans SM. Development of the cardiac conduction system as delineated by minK-lacZ. *J Cardiovasc Electrophysiol*. 2003;14:383-391.
15. DiFrancesco D. The cardiac hyperpolarizing-activated current, if. Origins and developments. *Prog Biophys Mol Biol*. 1985;46:163-183.
16. Ishii TM, Takano M, Xie LH, Noma A, Ohmori H. Molecular characterization of the hyperpolarization-activated cation channel in rabbit heart sinoatrial node. *J Biol Chem*. 1999;274:12835-12839.
17. Espinoza-Lewis RA, Yu L, He F, Liu H, Tang R, Shi J, Sun X, Martin JF, Wang D, Yang J, Chen Y. Shox2 is essential for the differentiation of cardiac pacemaker cells by repressing Nkx2-5. *Dev Biol*. 2009;327:376-385.
18. Garcia-Frigola C, Shi Y, Evans SM. Expression of the hyperpolarization-activated cyclic nucleotide-gated cation channel HCN4 during mouse heart development. *Gene Expr Patterns*. 2003;3:777-783.
19. Nieto MA, Bennett MF, Sargent MG, Wilkinson DG. Cloning and developmental expression of Sna, a murine homologue of the Drosophila snail gene. *Development*. 1992;116:227-237.

20. Mahtab EA, Vicente-Steijn R, Hahurij ND, Jongbloed MR, Wisse LJ, DeRuiter MC, Uhrin P, Zaujec J, Binder BR, Schalij MJ, Poelmann RE, Gittenberger-de Groot AC. Podoplanin deficient mice show a Rhoa-related hypoplasia of the sinus venosus myocardium including the sinoatrial node. *Dev Dyn*. 2009;238:183-193.
21. Wiese C, Grieskamp T, Airik R, Mommersteeg MT, Gardiwal A, de Gier-de Vries C, Schuster-Gossler K, Moorman AF, Kispert A, Christoffels VM. Formation of the sinus node head and differentiation of sinus node myocardium are independently regulated by Tbx18 and Tbx3. *Circ Res*. 2009;104:388-397.
22. Harvey RP. NK-2 homeobox genes and heart development. *Dev Biol*. 1996;178:203-216.
23. Heikinheimo M, Scandrett JM, Wilson DB. Localization of transcription factor GATA-4 to regions of the mouse embryo involved in cardiac development. *Dev Biol*. 1994;164:361-373.
24. Bruneau BG, Logan M, Davis N, Levi T, Tabin CJ, Seidman JG, Seidman CE. Chamber-specific cardiac expression of Tbx5 and heart defects in Holt-Oram syndrome. *Dev Biol*. 1999;211:100-108.
25. Christoffels VM, Hoogaars WM, Tessari A, Clout DE, Moorman AF, Campione M. T-box transcription factor Tbx2 represses differentiation and formation of the cardiac chambers. *Dev Dyn*. 2004;229: 763-770.
26. de Jong F, Opthof T, Wilde AA, Janse MJ, Charles R, Lamers WH, Moorman AF. Persisting zones of slow impulse conduction in developing chicken hearts. *Circ Res*. 1992;71:240-250.
27. Hoogaars WM, Engel A, Brons JF, Verkerk AO, de Lange FJ, Wong LY, Bakker ML, Clout DE, Wakker V, Barnett P, Ravesloot JH, Moorman AF, Verheijck EE, Christoffels VM. Tbx3 controls the sinoatrial node gene program and imposes pacemaker function on the atria. *Genes Dev*. 2007;21:1098-1112.
28. Blaschke RJ, Hahurij ND, Kuijper S, Just S, Wisse LJ, Deissler K, Maxelon T, Anastassiadis K, Spitzer J, Hardt SE, Schöler H, Feitsma H, Rottbauer W, Blum M, Meijlink F, Rappold GA, Gittenberger-de Groot AC. Targeted mutation reveals essential functions of the homeodomain transcription factor Shox2 in sinoatrial and pacemaking development. *Circulation*. 2007;115:1830-1838.
29. Stieber J, Herrmann S, Feil S, Loster J, Feil R, Biel M, Hofmann F, Ludwig A. The hyperpolarization-activated channel HCN4 is required for the generation of pacemaker action potentials in the embryonic heart. *Proc Natl Acad Sci U S A*. 2003;100:15235-15240.
30. Plotnikov AN, Bucchi A, Shlapakova I, Danilo P, Jr., Brink PR, Robinson RB, Cohen IS, Rosen MR. HCN212-channel biological pacemakers manifesting ventricular tachyarrhythmias are responsive to treatment with I(f) blockade. *Heart Rhythm*. 2008;5:282-288.
31. Schweizer PA, Yampolsky P, Malik R, Thomas D, Zehelein J, Katus HA, Koenen M. Transcription profiling of HCN-channel isotypes throughout mouse cardiac development. *Basic Res Cardiol*. 2009;104: 621-629.
32. Yanni J, Boyett MR, Anderson RH, Dobrzynski H. The extent of the specialized atrioventricular ring tissues. *Heart Rhythm*. 2009;6:672-680.
33. Sarre A, Pedretti S, Gardier S, Raddatz E. Specific inhibition of HCN channels slows rhythm differently in atria, ventricle and outflow tract and stabilizes conduction in the anoxic-reoxygenated embryonic heart model. *Pharmacol Res*. 2010;61:85-91.
34. Altomare C, Terragni B, Brioschi C, Milanesi R, Pagliuca C, Viscomi C, Moroni A, Baruscotti M, DiFrancesco D. Heteromeric HCN1-HCN4 channels: a comparison with native pacemaker channels from the rabbit sinoatrial node. *J Physiol*. 2003;549:347-359.
35. Stillitano F, Lonardo G, Zicha S, Varro A, Cerbai E, Mugelli A, Nattel S. Molecular basis of funny current (If) in normal and failing human heart. *J Mol Cell Cardiol*. 2008;45:289-299.

Chapter 7

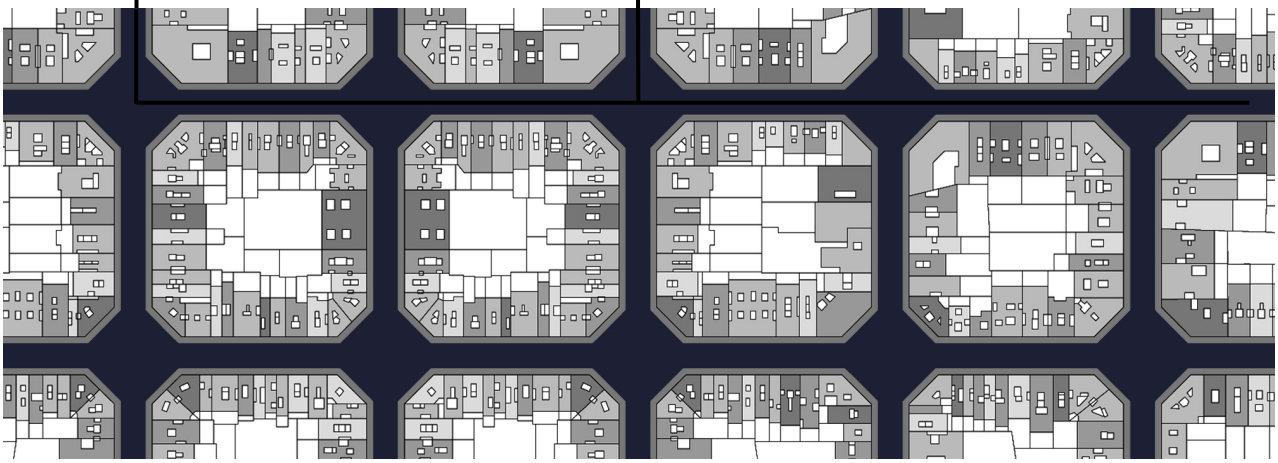

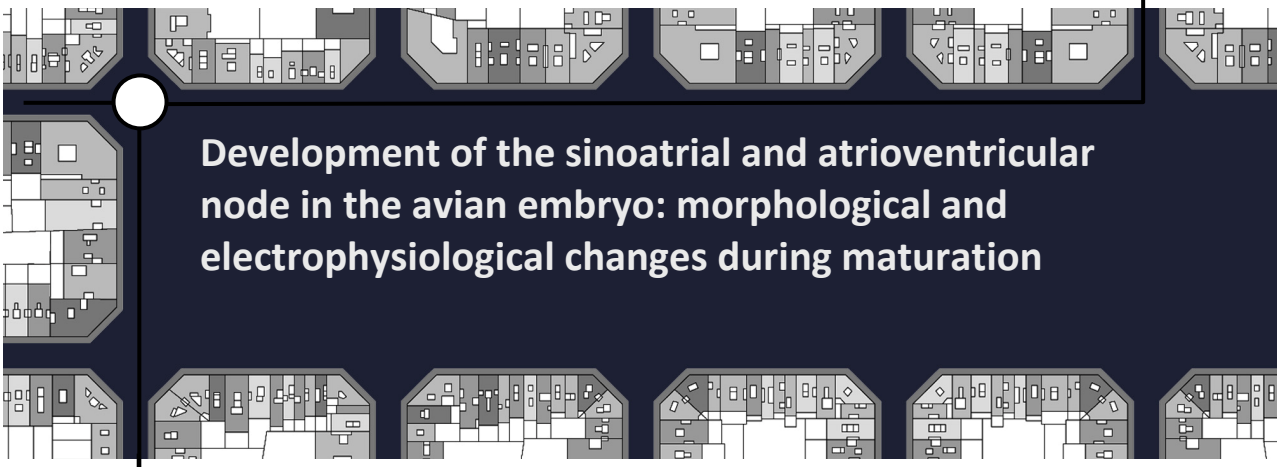

Development of the sinoatrial and atrioventricular node in the avian embryo: morphological and electrophysiological changes during maturation

Rebecca Vicente-Steijn, Denise P Kolditz, Antoine AF de Vries, Robert E Poelmann, Martin J Schalij, Adriana C Gittenberger-de Groot, Monique RM Jongbloed

Submitted for publication

Abstract

Background

To understand the mechanisms of specific arrhythmias, the morphological and electrophysiological changes that occur during sinoatrial (SAN) and atrioventricular (AVN) nodal differentiation and maturation in avian heart development were analyzed.

Methods & Results

The developing SAN and AVN areas were characterized by studying expression patterns of the cardiac markers cTnI, Nkx2.5, the gap junction protein Cx43 and the cation channel *Hcn4*. The periodic acid Schiff reaction was used to detect glycogen. The developing electrogram and atrial activation patterns were studied by *ex ovo* electrophysiological recordings. Early in development, the entire sinus venosus myocardium, including the right-sided SAN and a transient left-sided SAN, expresses cTnI, *Hcn4*, but not Nkx2.5. This myocardium has the potential to initiate the electrical activity. Eventually, cTnI and *Hcn4* expression and the initial electrical activation become restricted to the definitive right-sided SAN. Similarly, the early atrioventricular canal and at later stages the atrioventricular ring myocardium and AVN area display a common expression pattern of cardiac markers. These morphological changes coincide with a significant increase in heart rate and atrioventricular delay during development. Lineage tracing experiments reveal a potential sinoatrial contribution to the AVN area.

Conclusion

Significant developmental changes occur in morphology and electrical characteristics of avian sinus venosus and atrioventricular ring myocardium during development, where respectively the SAN and AVN will form. The initially broad electrical potential and gene expression patterns of these structures may relate to predilection sites for arrhythmias in the adult.

Introduction

Supraventricular tachycardias are the most common cardiac arrhythmias in adults and children.[1] Both components of, as well as myocardial structures that do not belong to the adult cardiac conduction system (CCS), can be involved in arrhythmogenesis. Arrhythmias associated with adult CCS components include sinoatrial (SAN) and atrioventricular (AVN) nodal re-entrant tachycardias.[2,3] Arrhythmias occurring elsewhere include ectopic foci in the atria that tend to occur at anatomical predilection sites, such as the crista terminalis in the right atrium (RA),[4] and the myocardial sleeves of the pulmonary veins in the left atrium (LA).[5] The mechanism facilitating these arrhythmias remains elusive. Embryonic remnants of the CCS or re-expression of embryonic genes could provide an explanation.[6,7]

During development, the heart starts off as a primary heart tube and expands through continuous incorporation of cells from the mesoderm dorsal to the heart, the so-called second heart field, at the arterial and venous pole.[8,9] The primary heart tube has a nodal-like functional phenotype showing automaticity, slow conduction, and a peristaltic contraction for blood propulsion.[10,11] The initial pacemaker signal originates from the sinus venosus myocardium, i.e. the myocardium at the inflow part of the heart, covering the cardinal veins (putative caval veins), where the SAN will develop. From the onset, this sinus venosus myocardium shows a different gene expression pattern compared to the atrial working myocardium. It expresses podoplanin,[9] RhoA,[7] Shox2,[12] Tbx18,[8] Tbx3[13] and *Hcn4*[14] and lacks Nkx2.5 expression.[8,9] An atrioventricular (AV)-delay can already be recorded at early stages in the atrioventricular canal (AVC), which is a myocardial band between the developing atria and ventricles with a slow-conducting phenotype.[10,15,16] Later in development, the AVN, consisting of a compact node bordered by transitional cells, will develop and become responsible for the AV-delay.[14,20] Simultaneously, the common bundle and bundle branches will develop and conduct the impulse rapidly to the ventricular working myocardium, and the initial base-to-apex activation pattern of the heart will shift to the mature apex-to-base activation pattern.[17] The exact origin of cells contributing to the SAN and AVN is still unclear. An origin of the SAN from the coelomic epithelium by a process of epithelial-to-mesenchymal transformation has been hypothesized,[9] although confirmation by lineage tracing experiments is required. The compact part of the murine AVN most probably is derived form the atrioventricular ring (AVR) myocardium[18] although a partial atrial contribution to the AVN has also been reported.[19] Whether the avian system has an AVN is still a matter of debate. Some state that the AVR myocardium functions as the AVN,[15] while others describe the AVN at the right side of the base of the interatrial septum (~HH29-31),[20] at the antero-inferior margin of the orifice of the left superior vena cava (putative coronary sinus in humans).[21,22]

As access to human embryonic and fetal tissues to study the development of the CCS is limited, animal models have been widely used over the past decades. Although structural developmental differences exist, both mouse and chicken are considered

useful models to study the developing CCS as results largely comply with observations made in humans. The avian system has the advantage of *in ovo* manipulation which cannot be done in the *in utero* murine system. Although knowledge on the morphological development of the avian heart is available, reference values for heart rate or AV-intervals during cardiac development in the chick related to the morphology of the CCS are lacking. This may complicate the interpretation of results during experimental manipulations.
In the current study, we provide a morphological and functional series of SAN and AVN development in the avian embryo. To study cellular contributions from the second heart field to the SAN and AVN, lineage tracing experiments were carried out.

Materials and Methods

A detailed description of the methods used in this study is provided in the expanded methods appendix.

Experimental preparations

All animal experiments were approved by the Committee on Animal Welfare of the Leiden University Medical Center (LUMC), Leiden, the Netherlands and in compliance with the Guide for the Care and Use of Laboratory Animals (NIH Publication No.85-23, revised 1996).

Immunohistochemistry and nonradioactive *in situ* hybridization

Immunohistochemical stainings were conducted[7,23] for 36 chick and 28 quail hearts (HH12-HH42) for the myocardial protein cardiac troponin I (cTnI; goat polyclonal antibody, sc-8118, Santa Cruz, 1/400), the cardiac transcription factor Nkx2.5 (goat polyclonal antibody, sc-8697, Santa Cruz, 1/4000) and the gap junction subunit connexin (Cx)43 (rabbit polyclonal antibody, Abcam, ab-407, 1/200), which is the dominant subunit expressed in the working myocardium in both mouse and chicken. The periodic acid Schiff (PAS) reaction was used to detect glycogen, which is virtually absent in the avian CCS, while the atrial and ventricular myocardium have a high glycogen content.[24] Nonradioactive *in situ* hybridization analysis of *Hcn4* expression was conducted with a digoxigenin-labeled antisense RNA probe in 10-µm-thick embryo sections.[7,9]

Labeling of the pericardial mesothelium for lineage tracing

To label the cells lining the pericardial cavity of chick embryos, we used Endorem (Guerbet, Gorinchem, the Netherlands) (HH25-35, n=18), a superparamagnetic iron oxide (SPIO) nanoparticle, used for short-term (<72 hours) tracing experiments. For

long-term follow-up a vesicular stomatitis virus G-protein-pseudotyped self-inactivating lentiviral vector designated LV.hUbiC.TurboFP635. WHVPRE, encoding the far-red fluorescent protein Katushka (HH31-37, n=12) was used.

Ex ovo extracellular electrogram recordings

Extracellular electrograms were recorded during superperfusion with oxygenated Tyrode[7,17] in wildtype embryonic chick (n=60) and quail (n=22) hearts (HH20-31). The excised hearts were grouped as follows: A (HH20-24, n=31), B (HH24-28, n=38) and C (HH28-31, n=13). Unipolar extracellular electrograms were recorded by positioning 3 tungsten recording electrodes on the LA, RA and common ventricle(CV), respectively. A reference electrode was placed in the tissue bath.

Results

The morphogenesis of the SAN and AVN was studied by expression of key genes for myocardial and CCS development. *Ex ovo* local electrocardiograms were recorded during a regular rhythm of 177±41 bpm (AV-interval 84±12ms).

HH11-23 (~2-3 days of incubation)

Development of the sinus venosus myocardium including the SAN

At stage HH11 looping of the heart has started as shown by the C-shape of the primary heart tube consisting of a single ventricle with an outflow part, and an inflow part. The latter consists of a sinus venosus receiving the venous blood from the cardinal veins (putative caval veins) and a primitive atrium. At this stage the entire primary heart tube including the sinus venosus expresses *Hcn4* mRNA as shown previously.[25] The SAN develops within the sinus venosus myocardium characterized by the expression of cTnI and not Nkx2.5. The onset of development of this sinus venosus myocardium can be observed (Figure 7.1a, 7.1c-h) ventrally of the cardinal veins and in continuity with two small clusters of cells at the entrance of each cardinal vein into the common atrium. The cluster situated at the entrance of the right cardinal vein (superior caval vein in the adult) is the putative right-sided SAN (Figure 7.1c-e), whereas the cluster at the left side corresponds to the left-sided SAN (Figure 7.1f-h), a temporary structure.

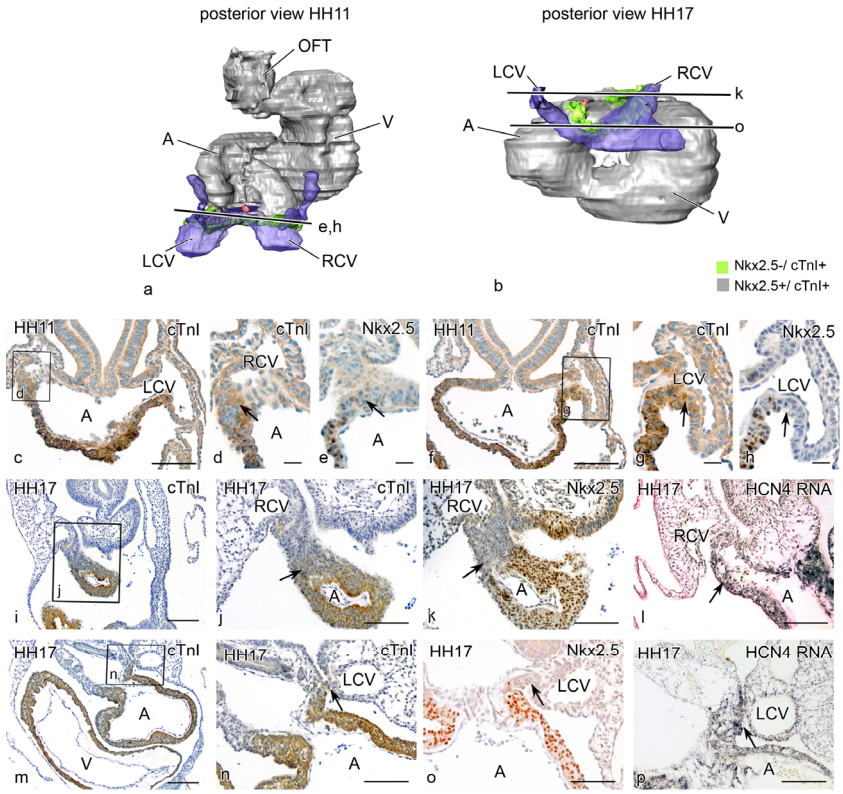

Figure 7.1 Early development of the sinus venosus myocardium. Posterior view of 3D reconstructions of HH11(**a**) and HH17(**b**) embryonic chicken hearts. Nkx2.5-negative myocardium is depicted in lime green, Nkx2.5-positive myocardium is depicted in grey, right and left cardinal vein (R/LCV) lumen in blue and the pulmonary pit (PP) in pink. The intersection lines **e**,**h**,**k** and **o** refer to the respective transverse sections. **c-e** HH11 heart showing cTnI(**c,d**) but no Nkx2.5(**e**) expression in the myocardium surrounding the RCV (arrow, prospective sinoatrial node (SAN)). **f-h** Caudal sections showing a cluster of cells medial to the LCV (arrow, 'transient left SAN' area) expressing cTnI(**f,g**) and no Nkx2.5(**h**). **i-l** HH17 heart showing cTnI(**i-j**), no Nkx2.5(**k**) and *Hcn4*(**l**) expression in the SAN (arrow). **m-p** Transverse sections showing cTnI (**m,n**), no Nkx2.5(**o**) and *Hcn4*(**p**) expression in the transient left-sided SAN (arrow). A:atrium; OFT:outflow tract; V:ventricle. Scale bars:100 µm.

After looping into an S-shape the common atrium and AVC are positioned cranially to the primitive left ventricle, while the outflow tract is situated above the primitive right ventricle. The U-shaped sinus venosus myocardium is characterized by expression of cTnI (Figure 7.1b, 7.1i-j, 7.1m-n) and *Hcn4* (Figure 7.1l, 7.1p) but not Nkx2.5 (Figure 7.1k, 7.1o). This area still encompasses a distinct cluster of cTnI-positive but Nkx2.5-

negative cells surrounding the antero-ventral wall of the proximal right cardinal vein (the right-sided SAN) (Figure 7.1i-l) as well as a second cluster located in the ventral myocardial part of the left cardinal vein (left-sided SAN) (Figure 7.1m-p), which at this stage appears larger in size than its right-sided counterpart.

Development of the AV canal myocardium

During these stages, the common atrium, AVC and ventricle express cTnI, Cx43, and Nkx2.5 and are characterized by a high glycogen content as determined by PAS staining (not shown).

Electrophysiological characteristics

An overview of the electrophysiological measurements is provided in Table 7.1. Early in development, the mean heart rate for group A (<HH24) is 156±30bpm (range 122-186 bpm) and the average AV-interval is 79±8ms (range 71-85 ms). A high variability in atrial activation sequences (Table 7.2) was observed. While in the majority (17/31;55%) of hearts, right atrial activation preceded left atrial activation, a relatively large number (11/31;35%) of hearts showed the first atrial activation originating in the LA, indicating a left-sided dominant pacemaker (Figure 7.2a-b). Additionally, concurrent activation (time difference <1 ms) of the right and left atrium (RA=LA) was found in 10% (3/31) of the hearts.

Table 7.1 Electrophysiological measurements and atrial activation patterns during development.

Atrial Activation Pattern	n	HR, bpm, mean±SD (range)	AV-interval, ms, mean±SD (range)
Group A	31	156±30 (122-186)	79±8 (71-85)
RA	17	157±32 (125-189)	77±7 (70-84)
LA	11	152±22 (130-174)	81±11 (70-92)
RA=LA	3	167±55 (112-222)	83±5 (78-88)
Group B	38	175±25 (150-200)	83±11 (71-93)
RA	22	167±22 (145-189)	79±11 (68-90)
LA	8	193±18 (175-211)	91±11 (80-102)
RA=LA	8	181±31(150-212)	84±8 (76-94)
Group C	13	231±52 (179-283)	96±12 (84-108)
RA	12	235±51 (184-286)	95±11 (84-106)
RA=LA	1	177	112
Total	**82**	**177±41 (136-218)**	**84±12 (72-96)**

HH24-30 (~4-6 days of incubation)

Development of the sinus venosus myocardium including the SAN

At these stages, looping of the heart progresses and the sinus venosus becomes positioned dorsal to the atria. The venous valves become apparent on the right side of the atrium. The myocardium of the sinus venosus continues to expand and the right-

sided SAN becomes larger (Figure 7.3a-b, 7.3c-f) expressing cTnI (Figure 7.3c, 7.3d) and *Hcn4* (Figure 7.3f) but lacking Nkx2.5 (Figure 7.3e). The area of the transient left-sided SAN shows a similar expression pattern of these markers (Figure 7.3a, 7.3g-j). Additionally, the sinus venosus, including both nodal structures, shows low Cx43 expression (Figure 7.4c, 7.4f) as well as a low level of glycogen (Figure 7.4a-b, 7.4d-e) when compared to the working myocardium.

Table 7.2 Atrial activation sequences in groups A, B, C with corresponding location of the first atrial activation.

Developmental Stage (HH)	n	RA (%)	LA (%)	RA=LA (%)
Group A (<HH24)				
HH20	4	4		
HH21	10	6	3	1
HH22	10	5	3	2
HH23	7	2	5	
Subtotal	31	17 (55%)	11 (35%)	3 (10%)
Group B (HH24-28)				
HH24	8	5	1	2
HH25	7	4	1	2
HH26	10	7	2	1
HH27	9	4	3	2
HH28	4	2	1	1
Subtotal	38	22 (58%)	8 (21%)	8 (21%)
Group C (>HH28)				
HH29	4	3		1
HH30	7	7		
HH31	2	2		
Subtotal	13	12 (92%)		1 (8%)
Total	**82**	**51 (62%)**	**19 (23%)**	**12 (15%)**

Development of the AV canal myocardium and AVN area

The AVC myocardium now displays specific morphological and immunohistological features, including enlargement of the intercellular spaces and a lower glycogen content (Figure 7.4g, 7.4h). The AVC myocardium expresses cTnI and Nkx2.5 (Figure 7.3a) and shows an increase in the expression pattern of Cx43 (Figure 7.4i) and *Hcn4* (Figure 7.3k). Additional *Hcn4* expression is observed at the base of the atrial septum, the putative AVN area, (Figure 7.3k, 7.3l) which expresses cTnI (Figure 7.3m) and shows a mosaic expression pattern (positive and negative cells) for Nkx2.5 (Figure 7.3n).

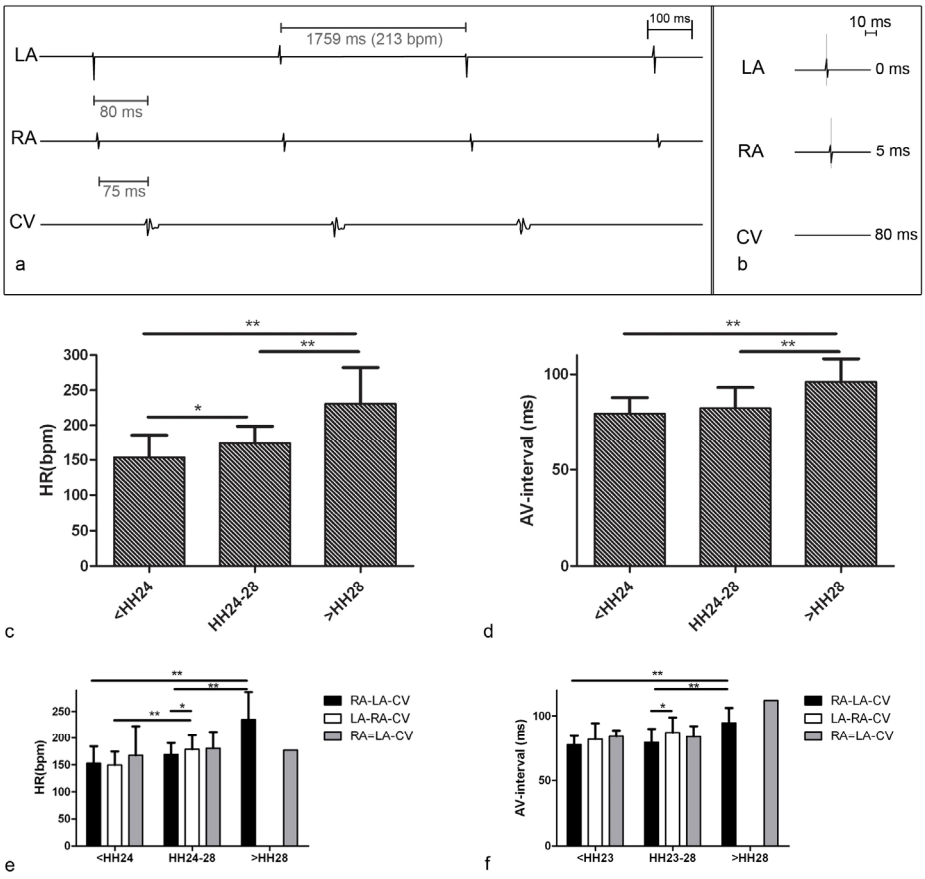

Figure 7.2 Electrophysiological changes during development. **a** Representative example of a recording of a chicken heart at HH24, showing pacemaking dominance in the left atrium (LA). **b** Magnification of the LA signal. **c-d** Changes in heart rate (HR) in beats per minute (bpm)(**c**) and atrioventricular (AV) interval in milliseconds (ms)(**d**) during development. **e-f** Changes in HR and AV interval for the different atrial activation patterns. CV: common ventricle; LA-RA-CV:left-sided dominant pacemaker; RA: right atrium; RA-LA-CV:right-sided dominant pacemaker; RA=LA-CV:concurrent activation. *p<0.05; **p<0.005.

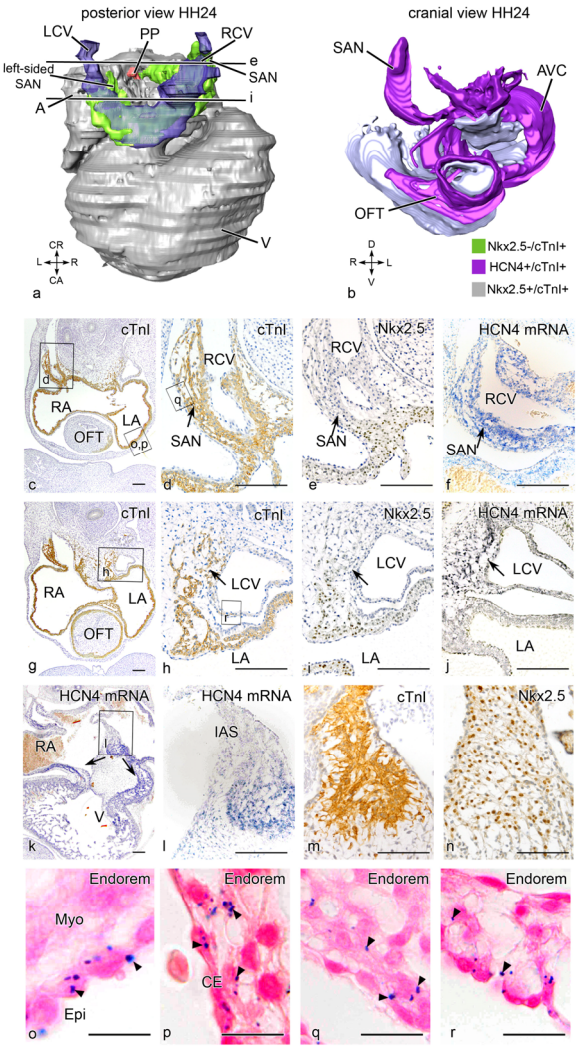

Figure 7.3 Development of the putative sinoatrial and atrioventricular nodes. Posterior(**a**) and cranial(**b**) view of a HH24 heart 3D reconstruction. Lime green depicts the Nkx2.5-negative myocardium, purple the *Hcn4*-positive myocardium, grey the Nkx2.5-positive myocardium, light blue the outflow tract (OFT) and atrioventricular canal (AVC) cushion, blue the right and left cardinal vein (R/LCV) lumen and pink the pulmonary pit (PP). Intersection lines **e** and **i** refer to the respective transverse sections. **c-f** cTnI(**c,d**), no Nkx2.5(**e**) and *Hcn4*(**f**) expression in the right-sided sinoatrial node (SAN). **g-j** Cluster of cells medial to the LCV (arrow, transient left-sided SAN) expressing cTnI(**g,h**), no Nkx2.5(**i**) and *Hcn4*(**j**). **k** Overview of *Hcn4* expression in the base of the interatrial septum (IAS; boxed area) as well as in the AVC (arrows). **l-n** Transverse sections of the putative area of the atrioventricular node showing *Hcn4*(**l**), cTnI(**m**) and less marked (mosaic) Nkx2.5(**n**) expression. **o-r** Prussian blue-stained HH24 embryo showing Endorem labelling (arrowheads) in the epicardium (Epi)(**p**)(arrowheads), the coelomic epithelium (CE)(**q**)(arrowheads) and the SAN (**q,r**). L/RA:left/right atrium; Myo:myocardium; V:ventricle. Scale bars:**c-n:**100µm,**o-r**:50µm.

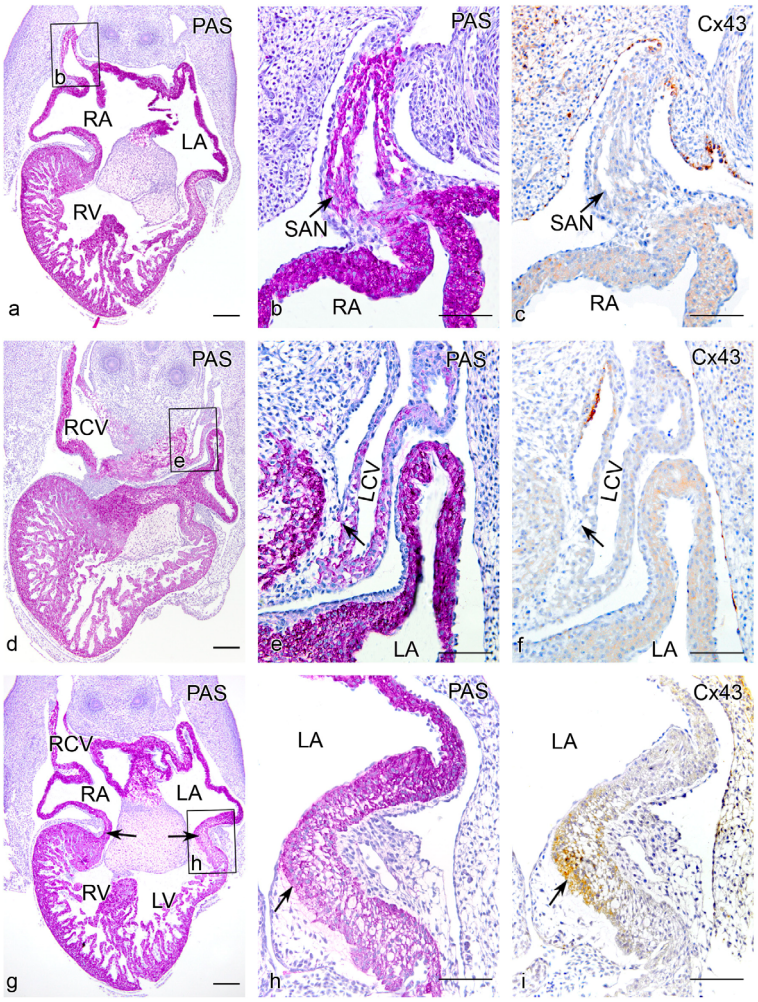

Figure 7.4 Glycogen and Cx43 levels in the avian heart. **a-c** Transverse sections showing low amounts of glycogen(**a,b**) and Cx43(**c**) content in the right-sided sinoatrial node (SAN, arrow). **d-f** Transverse sections showing low glycogen(**d,e**) and Cx43(**f**) levels in the transient left-sided SAN (arrow). Additional low glycogen(**g,h**) content but slightly more marked Cx43(**i**) expression is visible in the atrioventricular canal (arrows). L/RA:left/right atrium; L/RCV: left/right cardinal vein; L/RV: left/right ventricle. Scale bars:100µm.

Lineage tracing of the SAN and AVN

Cell tracing experiments were performed to study the origin of cells contributing to the developing SAN and AVN. Endorem was injected in the pericardial cavity, and uptake was seen 24-48 hours after injection in the majority of cells of the coelomic epithelium including in the epicardial cells covering the heart (Figure 7.3o-p). 24 to 48 hours post-injection, the sinus venosus region showed Endorem-labeled cells throughout the coelomic epithelium covering both cardinal veins, as well as in the SAN region (Figure 7.3q-r), indicating that cells from this epithelium or the underlying mesoderm could contribute to the SAN region as proposed previously.[9,19]

Electrophysiological changes

There was a small but significant increase in heart rate compared to the previous stage (group A (<HH24, 156±30 bpm, range 122-186 bpm); group B (HH24-28, 175±25 bpm, range 150-200 bpm; p=0.0054)). Heart rates below 145 bpm were no longer observed. A slight increase in AV-interval was observed in group B (HH24-28, 83±11 ms, range 71-93 ms; p=0.1507) compared to group A (<HH24, 79±8ms, range 71-85 ms). LA-activated hearts were still visible (8/38;21%) as well as concurrent activation (8/38;21%). LA-activated hearts showed a significant increase in heart rate (p=0.015) and a slight increase in AV-interval (p=0.058) (Figure 7.2e-f) when compared to the RA-activated hearts.

HH31-35 (~7-9 days of incubation)

Development of the sinus venosus myocardium including the SAN

The sinus venosus myocardium expands dorsally to cover a great part of the cardinal veins, still lacking Nkx2.5 expression (Figure 7.5a). *Hcn4* expression overlaps with Nkx2.5 negativity in this region (Figure 7.5a-b). Additional *Hcn4* expression is observed in the internodal myocardium in the RA that connects the SAN and the AVN (Figure 7.5b). This myocardium runs along the terminal crest (formed by the embryonic right venous valve in the posterior atrial wall) and part of the interatrial septum (partly formed by the embryonic left venous valve). *Hcn4* is also expressed in the Bachmann's bundle, a myocardial bundle connecting the RA and LA. The right-sided SAN can be recognized as a comma-shaped compact structure covering the right cardinal vein (Figure 7.5a) and maintains the expression pattern for the reported cardiac markers as previously. A transient left-sided SAN can still be recognized in close proximity to the orifice of the pulmonary vein. cTnI-positive and Nkx2.5-negative cells cover parts of the pulmonary veins. At the right side, scattered cTnI-positive/Nkx2.5-negative cells can be followed section-by-section from the right-sided SAN towards the pulmonary vein (Figure 7.5c-e). Similarly, the left pulmonary vein is in contact with the transient left-sided SAN (Figure 7.5g-i). These myocardial cells show *Hcn4* expression (Figure 7.5f-j).

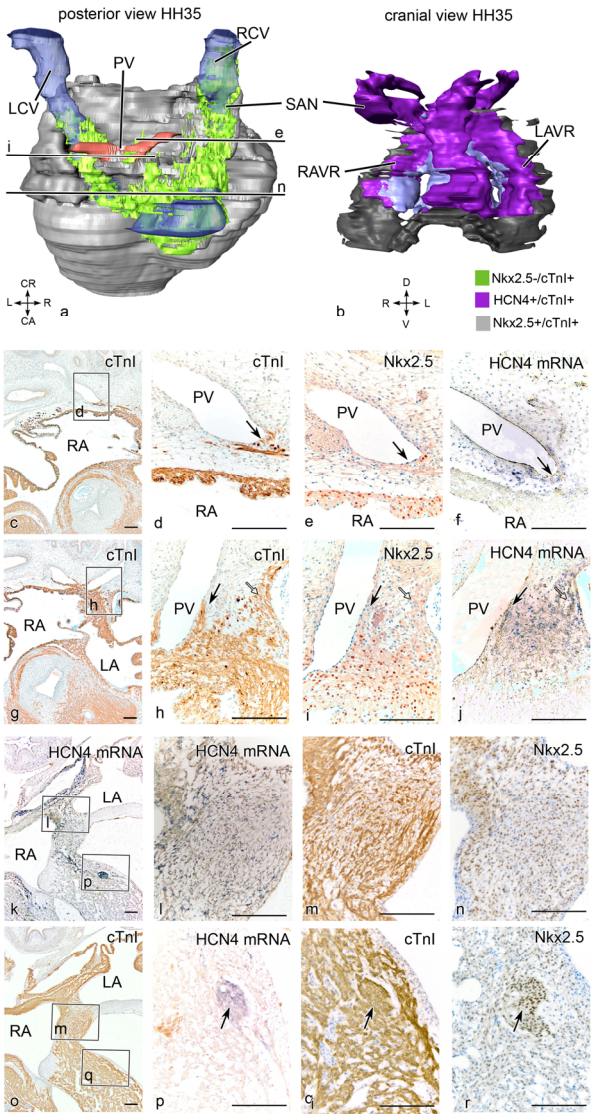

Figure 7.5 Sinoatrial and atrioventricular nodes in the mature heart. Posterior(**a**) and cranial(**b**) view of a HH35 heart 3D reconstruction. Nkx2.5-negative myocardium is depicted in lime green, *Hcn4*-positive myocardium in purple, Nkx2.5-positive myocardium in grey, right and left cardinal vein (R/LCV) lumen in blue, fibrotic tissue in dark grey, valve tissue in light blue and the pulmonary vein (PV) lumen in pink. The sinoatrial node (SAN) is indicated. The intersection lines **e,i** and **n** refer to the respective transverse sections. **c-f** The myocardium covering the right pulmonary vein (PV) expresses cTnI(**c,d**), no Nkx2.5(**e**) and *Hcn4*(**f**)(arrows). **g-j** The myocardium covering the left PV at the level of the transient left-sided SAN (open arrow) expresses cTnI(**g,h**), no Nkx2.5(**i**) and *Hcn4*(**j**) (arrows). **k-n** The atrioventricular node area expresses *Hcn4*(**k,l**), cTnI(**m**) and less marked (mosaic) Nkx2.5(**n**). **o-r** The common bundle expresses *Hcn4*(**p**), cTnI(**o,q**) and Nkx2.5(**r**). L/RA:left/right atrium; L/RAVR: left/right atrioventricular ring. Scale bars: 100µm.

Development of the AV ring myocardium and AVN area

Around HH32, formation of the isolating annulus fibrosus is largely completed bringing the AVR myocardium to the lower atrial rim and the developing AVN to the atrial level. *Hcn4*-expressing cells are observed in this AVR myocardium surrounding the orifices of the tricuspid and mitral valves. At the left side, the *Hcn4* expression pattern forms a complete ring (Figure 7.5b). However, the right-sided *Hcn4*-expressing AVR is scattered, and the adjacent fibrous annulus is discontinuous with multiple atrioventricular myocardial *Hcn4*-expressing connections. *Hcn4* is also expressed at the base of the atrial septum, the AVN area, above the annulus of the tricuspid orifice and adjacent to the orifice of the left cardinal vein (putative coronary sinus) (Figure 7.5k and 7.5l). This myocardium expresses cTnI (Figure 7.5m) and shows a mosaic expression pattern for Nkx2.5 (Figure 7.5n). The common bundle is easily recognized and expresses *Hcn4*, cTnI and Nkx2.5 (Figure 7.5o-r).

Lineage tracing of the SAN and AVN

Katushka-labeled embryos were studied at these progressed developmental stages (3-7 days post-injection). Immunohistological analysis of expression of the cardiac protein α-actinin, which resembles that of cTnI, was used to determine the myocardial identity of the labeled cells. These results confirmed the previous Endorem experiments, showing Katushka-specific labeling of the coelomic epithelium, epicardium and subepicardium as well as scattered Katushka-labeled cells in the wall of the sinus venosus (not shown). Katushka-labeled α-actinin positive myocardial cells were found in the SAN region and in both venous valves (Figure 7.6a-d), as well as, interestingly, the AVN area at the right side of the base of the atrial septum (Figure 7.6e-h). Although cells of the coelomic epithelium surrounding the left cardinal vein were labeled, no myocardial cells from this source were found in the heart.

Electrophysiological changes

Throughout development the average heart rate increased, being significantly higher in the oldest group (Figure 7.2c) (>HH28, 230±52bpm, range 179-283 bpm; $p<0.0001$) when compared to the younger groups. The average AV-interval also increased throughout development (Figure 7.2d) and was significantly higher in group C (>HH28, 96±12 ms, range 84-108 ms; $p<0.0001$ and $p=0.0007$) when compared to groups A and B respectively. In contrast to previous stages, none of the hearts in group C (>HH28) showed left atrial activation patterns, whereas concurrent activation was still observed in one heart (1/12;8%).

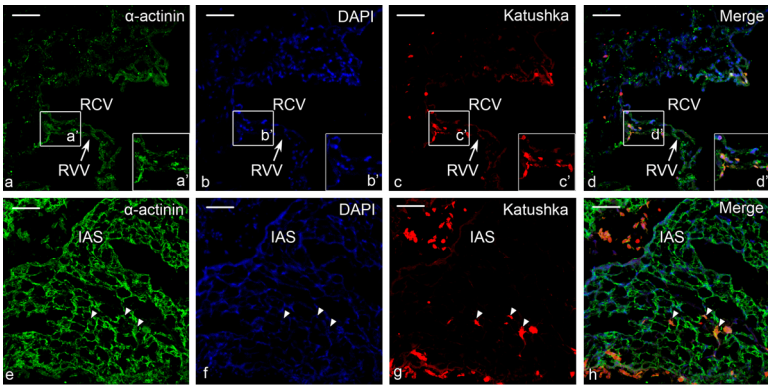

Figure 7.6 Katushka-labeled cells in long-term tracing experiments. Transverse sections of α-actinin–stained, Katushka-labeled HH35 embryos. **a-d** Katushka-labeled myocardial (i.e α-actinin positive) cells in the right venous valve (RVV, white arrow). **a'-d'** Magnification of these labeled cells. **e-h** Katushka-labeled myocardial cells (white arrowheads) at the base of the interatrial septum (IAS), being the atrioventricular node region. RCV:right cardinal vein. Scale bars:50µm.

>HH35-hatching

During these last stages of development the heart further matures, growing in size. In contrast to previous stages, the majority of the sinus venosus myocardium expresses Nkx2.5, whereas *Hcn4* is decreased. The fully developed right-sided SAN shows cTnI and *Hcn4* expression (Figure 7.7a-b, 7.7d), and no Nkx2.5 (Figure 7.7c). However, the transient left-sided SAN, which is no longer functional, shows cTnI (Figure 7.7e-f) and Nkx2.5 (Figure 7.7g) expression but no *Hcn4* (Figure 7.7h).

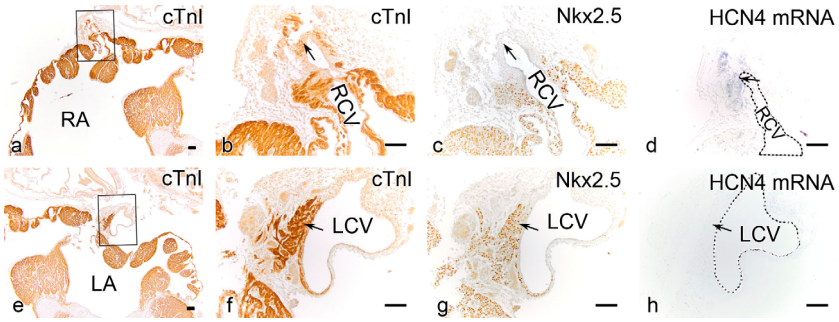

Figure 7.7 Terminal differentiation of the sinus venosus myocardium except for the right-sided sinoatrial node (SAN). **a-d** Transverse sections of a HH42 chicken embryo depicting the right-sided SAN expressing cTnI(**a,b**), no Nkx2.5(**c**) and *Hcn4*(**d**). **e-h** The left-sided SAN expresses cTnI(**e,f**), Nkx2.5 (**g**) and no *Hcn4*(**h**). L/RA:left/right atrium; LCV: left cardinal vein. Scale bars:100µm.

Discussion

in this study the development of the SAN and AVN in the avian embryo were analyzed and related to the development of the electrogram.

SAN development: from broad pacemaking to a definitive right-sided SAN

The developing sinus venosus myocardium includes the right-sided and a transient left-sided SAN. This myocardium is characterized by the lack of Nkx2.5 and is initially observed ventral to the cardinal veins, expanding dorsally throughout development (Figure 7.8). During development, regions of the sinus venosus myocardium including the left-sided SAN start expressing Nkx2.5 and loosing *Hcn4*, differentiating towards working myocardium. Additionally, the dominant pacemaker activity becomes restricted to the right-sided SAN. These findings support previous studies that show that genes essential for establishing a pacemaker phenotype are initially expressed throughout the developing sinus venosus myocardium,[8,9,12,13,26] reinforcing the broad pacemaker capacity of this myocardium. A group of key players in SAN development have been identified as well as their regulatory function in the pacemaking transcriptional program (e.g. Tbx3[27], *Hcn4* [14]and Shox2[12,26]). How the definitive right-sided SAN maintains its phenotype while the left side of the sinus venosus differentiates into working myocardium, loosing its pacemaker potential, is largely unknown. *Pitx2c*, essential in the embryonic control of left/right asymmetry, might play an important role, as mice lacking this gene show right atrial isomerism, resulting in the formation of two similar SANs.[27] At stages HH24-28, the LA-activated hearts showed a significantly faster heart rate than the RA-activated hearts, which is expected as the “fastest” pacemaker determines the heart rate. Given that the left-sided SAN appears earlier in development and is initially larger in size than the right-sided SAN, it is plausible that the left-sided SAN functions as the primary pacemaker at a developmental time point at which the right-sided SAN is not fully mature yet.

The developmental origin of the myocardial sleeves surrounding the pulmonary veins is a matter of continuous discussion.[9,28] Initial studies suggested an atrial contribution[29] but more recent studies indicate a second heart field contribution.[9,28] The current study shows that during development Nkx2.5-negative/*Hcn4*-positive myocardium temporarily forms part of the myocardial sleeves of the pulmonary vein. Several markers expressed during development in the sinus venosus myocardium including the SAN, are also expressed in the myocardium surrounding the pulmonary veins, e.g. HNK-1,[30] podoplanin,[9] *Hcn4* and PDGFR-α.[31] This is interesting in the light of the arrhythmogenic potential that has been attributed to the myocardial sleeves of the pulmonary veins.[5]

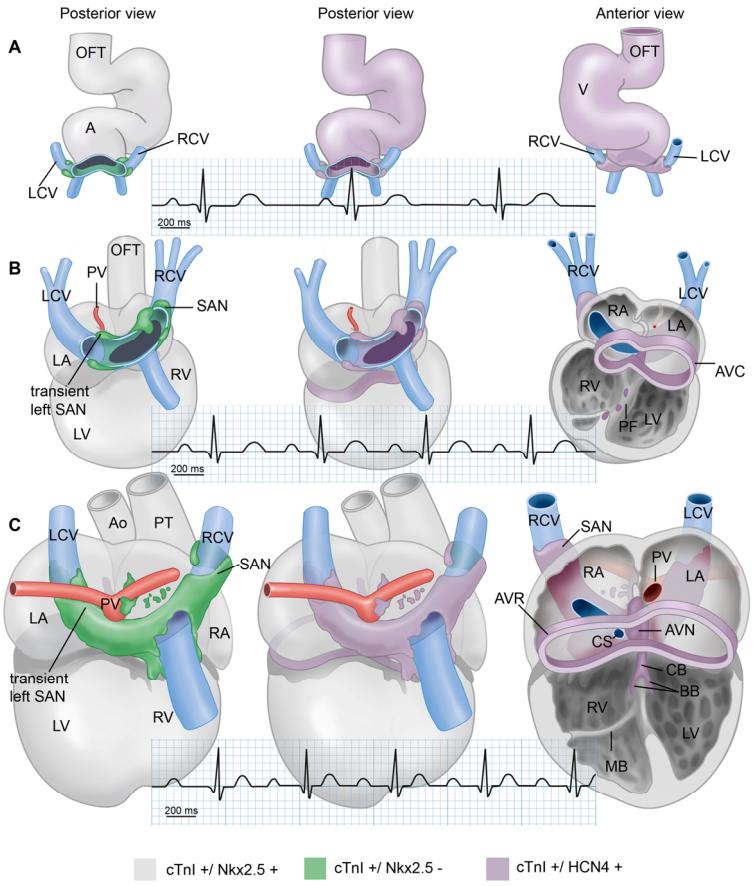

Figure 7.8 Schematic representation of the development of the sinoatrial (SAN) and atrioventricular (AVN) nodes in the avian embryo. **A** The sinus venosus myocardium where the SAN will develop is located ventrally to the cardinal veins (A1) and characterized by expression of cTnI but the lack of Nkx2.5 (green). The myocardium of the entire primary heart tube including this sinus venosus myocardium expresses *Hcn4* (purple) (A2-3). A schematic electrocardiographic (ECG) representation based on measurements of <HH24 hearts is added. **B** Later in development the area covered by the sinus venosus myocardium (green) has expanded and covers the dorsal side of the cardinal veins (B1). Both right-sided SAN and a transient left-sided SAN are recognized. *Hcn4* expression (B2-3) becomes restricted to specific regions in the heart which include the sinus venosus myocardium where the SAN is developing, the atrioventricular canal (AVC) myocardium where the atrioventricular node (AVN) will develop and parts of the primary fold (PF) which is situated between the developing ventricles (purple). A schematic ECG representation based on measurements of HH24-HH28 hearts is added. **C** At late stages of development the sinus venosus myocardium (green) has entirely covered the cardinal veins including the right-sided SAN and the transient left-sided SAN (C1). Additional Nkx2.5-negative/cTnI-positive cells cover the pulmonary vein (PV). *Hcn4* expression (C2-3) is found in the sinus venosus myocardium, in the atrioventricular ring (AVR) myocardium, the AVN, the common bundle (CB) and part of the bundle branches (BB) (purple). A schematic ECG representation based on measurements of >HH28 hearts is added. Ao: Aorta; CS: coronary sinus; L/RA: left/right atrium (A); L/RCV: left/right cardinal vein; L/RV: left/right ventricle (V); MB: moderator band; OFT: outflow tract; PT: pulmonary trunk.

Development of the AVN: AV ring versus AV node

In humans and lower mammals, the adult AVN consists of a compact node, surrounded by transitional cells.[18] The existence of an AVN in the avian system is still a matter of discussion. In the current study we were unable to distinguish these structures in the chicken AVN area. Rather, the AVN contained loose cells and large intercellular spaces when compared to the working myocardium.

In mouse, the AVN expresses HCN4, Tbx3 and Cx45 and lacks Cx40 and Cx43.[18] In chicken, we observed *Hcn4* expression throughout the AVC and the lower part of the atrial septum accompanied by specific Cx43 and PAS staining patterns. Later on, *Hcn4* was expressed in the AVN area as well as throughout the AVR myocardium, the common bundle and the bundle branches (Figure 7.8). An AV-delay is already detected early in development before the AVN has fully developed and has been attributed to the slow conducting AVC myocardium.[10,15] Throughout development we observed an AV-delay which increased significantly and could be related to the developing AVN as this area markedly expands late in development.

The AV myocardial continuity present around the entire circumference of the slow-conducting AVC disappears as a result of annulus fibrosus formation.[17,32] The common bundle is eventually the only myocardial continuity between the AVN at the atrial level and the bundle branches at the ventricular level. Evidence in chicken and human shows the persistence of accessory pathways until late developmental stages,[17,33] causing ventricular pre-excitation. In the current study, we observed *Hcn4* expression in these accessory AV connections at late embryonic stages. Additionally, a better isolation of the left-sided AVR compared to the scattered right-sided AVR was confirmed,[17] suggesting local differences in completion of the AVR isolation which correlates with findings in humans.[34]

Lineage tracing analysis: atrial contribution through the internodal pathways?

Recent discoveries in heart development show cellular contributions from the second heart field to components of the CCS.[7,19] A second heart field origin of the SAN has been demonstrated[19], supporting the idea that the SAN originates from the coelomic epithelium by a process of epithelial-to-mesenchymal transformation.[9] The compact part of the AVN in mouse is probably derived from the AVR myocardium[18], although a partial atrial contribution to the AVN has also been found.[19] Endorem labeling results showed labeled cells in the sinus venosus myocardium, supporting a cellular contribution from the coelomic epithelium. Longer-term tracing experiments with Katushka-labeled coelomic cells revealed myocardial cells in the SAN, in the right venous valve, but also at the base of the atrial septum, where the AVN is located. Although these studies need to be expanded, we hypothesize that cells from the atrial myocardium provide a cellular contribution to the AVN through the internodal myocardium.

Conclusions and clinical implications

During development, significant changes occur both in morphology and electrical properties of chick sinus venosus and AVR myocardium where the SAN and AVN will develop, respectively. Results of the current study may be useful as baseline measurements for the avian system.

An interesting finding relates to the myocardial sleeves surrounding the pulmonary vein, which shows cells expressing *Hcn4,* also expressed in the sinus venosus myocardium. Failure of differentiation into chamber myocardium, or re-expression of the embryonic phenotype may be a plausible mechanism for the ectopic arrhythmogenic foci reported in sinus venosus related structures in the RA and pulmonary venous myocardium in the LA in adult patients.[4,5] The AVR myocardium and the base of the atrial septum, the putative AVN area, also express *Hcn4*. Electrical isolation will occur by fibrosis of the AVR, which is more complete on the left than on the right side, resulting in predominantly right sided *Hcn4* expressing AV connections. This might explain the higher frequency of right-sided accessory pathways observed in the adult.[17,34]

Cellular contributions to the AVN from multiple sources as suggested by the results of the lineage tracing experiments might be interesting in the light of occurrence of re-entry within the AV node.

References

1. Ko JK, Deal BJ, Strasburger JF, Benson DW, Jr. Supraventricular tachycardia mechanisms and their age distribution in pediatric patients. *Am J Cardiol*. 1992;69:1028-1032.
2. Gomes JA, Mehta D, Langan MN. Sinus node reentrant tachycardia. *Pacing Clin Electrophysiol*. 1995;18:1045-1057.
3. Lee PC, Chen SA, Hwang B. Atrioventricular node anatomy and physiology: implications for ablation of atrioventricular nodal reentrant tachycardia. *Curr Opin Cardiol*. 2009;24:105-112.
4. Shah DC, Jais P, Haissaguerre M, Chouairi S, Takahashi A, Hocini M, Garrigue S, Clementy J. Three-dimensional mapping of the common atrial flutter circuit in the right atrium. *Circulation*. 1997;96:3904-3912.
5. Haissaguerre M, Jais P, Shah DC, Takahashi A, Hocini M, Quiniou G, Garrigue S, Le MA, Le MP, Clementy J. Spontaneous initiation of atrial fibrillation by ectopic beats originating in the pulmonary veins. *N Engl J Med*. 1998;339:659-666.
6. Jongbloed MRM, Schalij MJ, Poelmann RE, Blom NA, Fekkes ML, Wang Z, Fishman GI, Gittenberger-de Groot AC. Embryonic conduction tissue: a spatial correlation with adult arrhythmogenic areas? Transgenic CCS/lacZ expression in the cardiac conduction system of murine embryos. *J Cardiovasc Electrophysiol*. 2004;15:349-355.
7. Vicente-Steijn R, Kolditz DP, Mahtab EA, Askar SF, Bax NA, van der Graaf LM, Wisse LJ, Passier R, Pijnappels DA, Schalij MJ, Poelmann RE, Gittenberger-de Groot AC, Jongbloed MR. Electrical activation of sinus venosus myocardium and expression patterns of RhoA and Isl-1 in the chick embryo. *J Cardiovasc Electrophysiol*. 2010;21:1284-1292.
8. Christoffels VM, Mommersteeg MT, Trowe MO, Prall OW, Gier-de Vries C, Soufan AT, Bussen M, Schuster-Gossler K, Harvey RP, Moorman AF, Kispert A. Formation of the venous pole of the heart from an Nkx2-5-negative precursor population requires Tbx18. *Circ Res*. 2006;98:1555-1563.
9. Gittenberger-de Groot AC, Mahtab EAF, Hahurij ND, Wisse LJ, DeRuiter MC, Wijffels MCEF, Poelmann RE. Nkx2.5 negative myocardium of the posterior heart field and its correlation with podoplanin expression in cells from the developing cardiac pacemaking and conduction system. *Anat Rec*. 2007;290:115-122.
10. de Jong F, Opthof T, Wilde AA, Janse MJ, Charles R, Lamers WH, Moorman AF. Persisting zones of slow impulse conduction in developing chicken hearts. *Circ Res*. 1992;71:240-250.
11. Moorman AFM, Christoffels VM. Cardiac chamber formation: Development, genes and evolution. *Physiol Rev*. 2003;83:1223-1267.
12. Blaschke RJ, Hahurij ND, Kuijper S, Just S, Wisse LJ, Deissler K, Maxelon T, Anastassiadis K, Spitzer J, Hardt SE, Schöler H, Feitsma H, Rottbauer W, Blum M, Meijlink F, Rappold GA, Gittenberger-de Groot AC. Targeted mutation reveals essential functions of the homeodomain transcription factor Shox2 in sinoatrial and pacemaking development. *Circulation*. 2007;115:1830-1838.
13. Hoogaars WM, Tessari A, Moorman AF, de Boer PA, Hagoort J, Soufan AT, Campione M, Christoffels VM. The transcriptional repressor Tbx3 delineates the developing central conduction system of the heart. *Cardiovasc Res*. 2004;62:489-499.
14. Garcia-Frigola C, Shi Y, Evans SM. Expression of the hyperpolarization-activated cyclic nucleotide-gated cation channel HCN4 during mouse heart development. *Gene Expr Patterns*. 2003;3:777-783.
15. Lieberman M, Paes de CA. The Electrophysiological Organization of the Embryonic Chick Heart. *J Gen Physiol*. 1965;49:351-363.
16. Arguello C, Alanis J, Pantoja O, Valenzuela B. Electrophysiological and ultrastructural study of the atrioventricular canal during the development of the chick embryo. *J Mol Cell Cardiol*. 1986;18:499-510.
17. Kolditz DP, Wijffels MCEF, Blom NA, Van der Laarse A, Markwald RR, Schalij MJ, Gittenberger-de Groot AC. Persistence of functional atrioventricular accessory pathways in post-septated embryonic avian hearts: implications for morphogenesis and functional maturation of the cardiac conduction system. *Circulation*. 2007;115:17-26.
18. Aanhaanen WT, Mommersteeg MT, Norden J, Wakker V, de Gier-de Vries C, Anderson RH, Kispert A, Moorman AF, Christoffels VM. Developmental Origin, Growth, and Three-Dimensional Architecture of the Atrioventricular Conduction Axis of the Mouse Heart. *Circ Res*. 2010;107:728-736.

19. Sun Y, Liang X, Najafi N, Cass M, Lin L, Cai CL, Chen J, Evans SM. Islet 1 is expressed in distinct cardiovascular lineages, including pacemaker and coronary vascular cells. *Dev Biol*. 2007;304:286-296.
20. Arguello C, Alanis J, Valenzuela B. The early development of the atrioventricular node and bundle of His in the embryonic chick heart. An electrophysiological and morphological study. *Development*. 1988;102:623-637.
21. Lu Y, James TN, Yamamoto S, Terasaki F. Cardiac conduction system in the chicken: Gross anatomy plus light and electron microscopy. *Anat Rec*. 1993;236:493-510.
22. Anderson RH, Becker AE, Brechenmacher C, Davies MJ, Rossi L. The human atrioventricular junctional area. A morphological study of the AV mode and bundle. *Eur J Cardiol*. 1975;3:11-25.
23. Mahtab EA, Vicente-Steijn R, Hahurij ND, Jongbloed MR, Wisse LJ, DeRuiter MC, Uhrin P, Zaujec J, Binder BR, Schalij MJ, Poelmann RE, Gittenberger-de Groot AC. Podoplanin deficient mice show a Rhoa-related hypoplasia of the sinus venosus myocardium including the sinoatrial node. *Dev Dyn*. 2009;238:183-193.
24. Allen H.J. Glycogen in the chick embryo. *Biological Bulletin*. 1919;36:63-U66.
25. Vicente-Steijn R, Passier R, Wisse LJ, Schalij MJ, Poelmann RE, Gittenberger-de-Groot AC, Jongbloed MRM. The funny current channel HCN4 delineates the developing cardiac conduction system in the chicken heart. *Heart Rhythm in press*. 2011 (Chapter 6 of this thesis).
26. Espinoza-Lewis RA, Yu L, He F, Liu H, Tang R, Shi J, Sun X, Martin JF, Wang D, Yang J, Chen Y. Shox2 is essential for the differentiation of cardiac pacemaker cells by repressing Nkx2-5. *Dev Biol*. 2009;327:376-385.
27. Mommersteeg MT, Hoogaars WM, Prall OW, Gier-de Vries C, Wiese C, Clout DE, Papaioannou VE, Brown NA, Harvey RP, Moorman AF, Christoffels VM. Molecular pathway for the localized formation of the sinoatrial node. *Circ Res*. 2007;100:354-362.
28. Mommersteeg MT, Brown NA, Prall OW, de Gier-de Vries C, Harvey RP, Moorman AF, Christoffels VM. Pitx2c and Nkx2-5 Are Required for the Formation and Identity of the Pulmonary Myocardium. *Circ Res*. 2007;101:902-909.
29. Saito T, Waki K, Becker AE. Left atrial myocardial extension onto pulmonary veins in humans: anatomic observations relevant for atrial arrhythmias. *J Cardiovasc Electrophysiol*. 2000;11:888-894.
30. Blom NA, Gittenberger-de Groot AC, DeRuiter MC, Poelmann RE, Mentink MM, Ottenkamp J. Development of the cardiac conduction tissue in human embryos using HNK-1 antigen expression: possible relevance for understanding of abnormal atrial automaticity. *Circulation*. 1999;99:800-806.
31. Bax NA, Bleyl SB, Gallini R, Wisse LJ, Hunter J, Van Oorschot AA, Mahtab EA, Lie-Venema H, Goumans MJ, Betsholtz C, Gittenberger-de Groot AC. Cardiac malformations in Pdgfralpha mutant embryos are associated with increased expression of WT1 and Nkx2.5 in the second heart field. *Dev Dyn*. 2010;239:2307-2317.
32. Rothenberg F, Watanabe M, Eloff B, Rosenbaum D. Emerging patterns of cardiac conduction in the chick embryo: waveform analysis with photodiode array-based optical imaging. *Dev Dyn*. 2005;233:456-465.
33. Hahurij ND, Gittenberger-de Groot AC, Kolditz DP, Bokenkamp R, Schalij MJ, Poelmann RE, Blom NA. Accessory atrioventricular myocardial connections in the developing human heart: relevance for perinatal supraventricular tachycardias. *Circulation*. 2008;117:2850-2858.
34. Becker AE, Anderson RH, Durrer D, Wellens HJ. The anatomical substrates of Wolff-Parkinson-White syndrome. A clinicopathologic correlation in seven patients. *Circulation*. 1978;57:870-879.

APPENDIX

Expanded Methods

Experimental preparations

All animal experiments were approved by the Committee on Animal Welfare of the Leiden University Medical Center (LUMC), Leiden, the Netherlands. Animal experiments were conducted in compliance with the Guide for the Care and Use of Laboratory Animals (NIH Publication No.85-23, revised 1996). Fertilized eggs of the Japanese quail (*Coturnix coturnix japonica*) and white leghorn chick (*Gallus domesticus*) were incubated at 37.5°C and 80% humidity. Embryos were staged according to the Hamburger-Hamilton (HH) criteria.[1]

Immunohistochemistry

After completion of the extracellular electrogram recordings, the hearts were removed from the Tyrode's solution and fixed in a 4% paraformaldehyde in phosphate-buffered saline (PBS) at 4°C for 24 hours and embedded in paraffin. Subsequently, 36 chick and 28 quail (HH12-42) hearts were serially sectioned in the frontal plane at 5-μm intervals and transferred to albumin/glycerin-coated objective slides. After deparaffinization and rehydration, the sections were prepared for standard periodic acid Schiff (PAS) staining or for immunohistochemical staining by treatment with 0.3% H_2O_2 in PBS for 20 minutes to block endogenous peroxidase activity.

Routine immunohistochemical staining was subsequently performed by overnight incubation of the sections in a humidified chamber with antibodies specific for the sarcomeric protein cardiac troponin I (cTnI; goat polyclonal antibody; sc-8118; Santa Cruz, Santa Cruz, CA; 1/400), the cardiac transcription factor Nkx2.5 (goat polyclonal antibody; sc-8697; Santa Cruz; 1/4.000) or the gap junction subunit connexin (Cx)43 (rabbit polyclonal antibody; Abcam, Cambridge, United Kingdom; ab-407; 1/200), which is the dominant Cx in the working myocardium in both mouse[2] and chicken.[3] The antibodies were diluted in PBS with 1% bovine serum albumin (BSA; Sigma-Aldrich, St. Louis, MO).

After rinsing in PBS and PBS-0.05% Tween-20 (PBST), the sections were incubated for 60 minutes with appropriate biotin-conjugated secondary antibodies (goat anti-rabbit IgG (BA-1000; Vector Laboratories, Burlingame, CA) or horse anti-goat IgG (BA-9500; Vector Laboratories) diluted 1:200 in a 1:66 dilution of normal goat (S1000, Vector Laboratories) or horse serum (S2000; Brunschwig Chemie) in PBST. The normal goat/horse serum served to block a-specific binding of the secondary antibodies. After rinsing in PBS and PBST, the sections were incubated with ABC-reagent (Vector Laboratories; PK 6100) for 45 minutes. After rinsing with PBS and tris/maleate (0.05M,

pH 7.6) the sections were incubated for 10 minutes with 3,3'-diaminobenzidine (DAB; Sigma-Aldrich; D5637) in a concentration of 400 mg/l with 4 droplets of H_2O_2 acting as catalyst. After incubation with DAB, the sections were rinsed with demineralized water and counterstained with 0.1% hematoxylin solution (Merck, Darmstadt, Germany) for 10 seconds. Finally, the sections were rinsed with tap water for 10 minutes, dehydrated and mounted in Entellan (Merck).

Nonradioactive *in situ* hybridization

Nonradioactive *in situ* hybridization analysis for *Hcn4* was conducted with digoxigenin-labeled antisense RNA probe in 10-µm-thick embryo sections as described previously.[4-6] A cDNA fragment corresponding to positions 1198 through 1804 of the *Hcn4* open reading frame was used as template and digoxigenin-labeled probes were generated using chicken Hcn4 specific primers (forward: 5'-GTGTCACTGGGATGGCTGCCT-3', reverse:5'-GCCAATGGTGCCCTCCCGAA-3'). A sense RNA probe derived from the same part of the *Hcn4* gene was used as a negative control.

3-D reconstructions

3-D reconstructions of the myocardium were made using cTnI-stained serial sections of HH12, HH17, HH24 and HH35 embryos. The Nkx2.5 negative myocardium and the Hcn4-positive myocardium were superimposed on the reconstructions as previously described[7,8] with the aid of the AMIRA v4.0 software package (Template Graphics Software, San Diego, CA).

Lentiviral vectors

The production of vesicular stomatitis virus G protein-pseudotyped self-inactivating human immunodeficiency virus type 1-based vectors (SIN-LVs) was carried out in 293T cells using the packaging constructs psPAX2 (Addgene, Cambridge, MA) and pLP/VSVG (Invitrogen, Breda, the Netherlands) as previously described.[9] SIN-LV particles were purified by filtration of the culture supernatant of the producer cells through 0.45-µm pore-sized HT Tuffryn membrane syringe filters (Pall, Mijdrecht, the Netherlands) and the subsequent centrifugation of the vector particles through 20% (wt/vol) sucrose (Merck, Nottingham, United Kingdom) cushions.[9] The monocistronic SIN-LV LV.hUbiC.TurboFP635.WHVPRE, which codes for a far red-shifted mutant of the red fluorescent protein of the sea anemone *Entacmaea quadricolor* (designated TurboFP635 or Katushka[10]), was made with the aid of shuttle construct pLV.hUbiC.TurboFP635.WHVPRE. The shuttle plasmid pLV.hUbiC.TurboFP635.WHVPRE contains the human *ubiquitin C* gene promoter coupled to the coding sequence of TurboFP635 and the woodchuck hepatitis virus post-transcriptional regulatory element. pLV.hUbiC.TurboFP635.WHVPRE was generated by ligation of the 743-bp BstUI fragment from pTurboFP635-N (Evrogen, Moscow, Russia) to the 9.1-kb Klenow

polymerase-treated XbaI fragment of pFugW.[11] The gene transfer activity of the LV.hUbiC.TurboFP635.WHVPRE stock was determined by end-point titration on HeLa indicator cells using flow cytometric analysis of *Katushka* expression as read-out. The titer is thus of the LV.hUbiC.TurboFP635.WHVPRE expressed in HeLa cell-transducing units (HTUs) per ml.

Labeling of pericardial mesothelium

To label the pericardial mesothelium of chick embryos, we used two different labeling agents: Endorem and a SIN-LV containing the far-red fluorescent protein Katushka.[10,12] Endorem (Guerbet, Gorinchem, the Netherlands) is a superparamagnetic iron oxide (SPIO) nanoparticle which has been widely used as a contrast agent to label and track cells. SPIOs are nontoxic and biodegradable, the uptake occurs naturally because of the dextran coating and they have no effect on the proliferation and differentiation of cells.[13] Katushka is a novel far-red fluorescent protein that is 7-10-fold brighter than other far-red fluorescent proteins (e.g. mPlum, HcRed[10]).
For labeling the pericardial cavity, white leghorn chick (*Gallus domesticus*) embryos were incubated and staged as previously mentioned. After incubation for approximately 3 days, a small window was cut into the egg shell and the extraembryonic membranes were carefully opened around the heart. A glass micropipette mounted on a micromanipulator was positioned into the pericardial cavity and Endorem (approximately 0,33µl) or LV.hUbiC.TurboFP635.WHVPRE particles (0,33µl of the SIN-LV preparation, which corresponds to ± 3 x 10^4 HTUs) were injected into the pericardial cavity using a programmable microinjector (IM-300, Narishige, Japan).[14] Leakage was restricted by leaving the needle in the cavity for a couple of minutes before withdrawal. After injection, eggs were sealed and returned to the incubator for further development.

Iron oxide staining

After Endorem labeling of the pericardial cavity, embryos were extracted from stages HH25 (n=5), HH28 (n=4), HH30 (n=3), HH32 (n=3) and HH35 (n=3), fixed in 4% paraformaldehyde in PBS at 4°C for 24 hours, embedded in paraffin and sectioned at 5-µm intervals. To identify cells that had incorporated the iron particles, Prussian blue staining was performed.

Immunofluorescence

After lentiviral transduction of the pericardial mesothelium, chick embryos were extracted from stages HH31-32 (n=4), HH34-35 (n=5), HH36-37 (n=3), fixed in 2% paraformaldehyde and 0.25% glutaraldehyde in PBS for 2 hours, embedded in Tissue Tek (OCT compound, Sakura Finetek, Zoeterwoude, the Netherlands) and sectioned at 8-µm intervals. To identify the myocardial Katushka-labeled cells, immunostainings

were performed for cTnI and α-actinin (mouse monoclonal antibody, EA-53, Sigma-Aldrich, 1/600). Appropriate secondary antibodies (fluorescein isothiocyanate-labeled donkey anti-goat IgG [sc-2024, Santa Cruz] for cTnI and Alexa Fluor 488-conjugated goat-anti-mouse IgG (H+L) highly cross-absorbed [A11029, Invitrogen-Molecular Probes, Breda, the Netherlands] for α-actinin) were used for visualization of the signal using a Leica TCS SPE confocal microscope (Leica Microsystems).

Ex ovo extracellular electrode recordings - technical features & recording protocol

Extracellular electrograms were recorded in wildtype embryonic chick (n=60) and quail (n=22) hearts ranging from stages HH20 to HH31 as previously described.[8,15] The excised hearts were grouped as follows: <HH24 (HH20-24, group A, n=31), HH24-28 (group B, n=38) and >HH28 (HH28-31, group C, n=13). The experimental preparations were placed in a custom-build, fluid-heated, temperature-controlled tissue bath and superfused with carbogenated (95% O_2 and 5% CO_2) Tyrode's solution (35 ± 0.5°C) of the following composition (mmol/l): NaCl 130, KCl 4, KH_2PO_4 1.2, $MgSO_4$ 0.6, $NaHCO_3$ 20, $CaCl_2$ 1.5, glucose 10 (pH 7.35).
Unipolar extracellular electrogram recording was subsequently performed using an established method[8,15,16] by consistently positioning 3 tungsten-recording electrodes (tip:1-2 µm; impedance 0.5-1.0MΩ, WPI, Berlin, Germany) on the left atrium (LA), right atrium (RA) and common ventricle (CV) . A silver reference electrode was placed in the tissue bath.
In short, the experimental preparations were allowed to equilibrate for 10 minutes before starting the recording protocol. Recordings in embryonic hearts with a spontaneous heart rate of <60 beats per minute were considered non-physiological and excluded from the present study.

Definitions

In extracellular electrogram recordings, a mean difference in local depolarization time between two recording electrodes of ≥1 ms was considered significant.[15,16] In all experiments, a stable 1:1 relation between atrial and ventricular activation was assured to be present. The time difference between atrial activation and the earliest ventricular activation was denominated as the atrioventricular (AV)-interval.

Statistical analysis

Heart rates and AV-intervals were compared between groups using the 2-tailed Student *t* test for normally distributed values. For comparison of categorical variables (atrial activation sequences), the χ^2-test was applied. A p value <0.05 (2-tailed) was considered statistically significant. All analyses were performed using the Statistical Package for Social Studies version 12.0 (SPSS, Chicago, IL).

References List Appendix

1. Hamburger V, Hamilton HL. A series of normal stages in the development of the chick embryo. *J Morphol*. 1951;88:49-92.
2. Miquerol L, Dupays L, Théveniau-Ruissy M, Alcoléa S, Jarry-Guichard T, Abran P, Gros D. Gap junctional connexins in the developing mouse cardiac conduction system. *Novartis Found Symp*. 2003;250:80-109.
3. Minkoff R, Rundus VR, Parker SB, Beyer EC, Hertzberg EL. Connexin expression in the developing avian cardiovascular system. *Circ Res*. 1993;73:71-78.
4. Kaarbo M, Crane DI, Murrell WG. RhoA is highly up-regulated in the process of early heart development of the chick and important for normal embryogenesis. *Dev Dyn*. 2003;227:35-47.
5. Christoffels VM, Mommersteeg MT, Trowe MO, Prall OW, Gier-de Vries C, Soufan AT, Bussen M, Schuster-Gossler K, Harvey RP, Moorman AF, Kispert A. Formation of the venous pole of the heart from an Nkx2-5-negative precursor population requires Tbx18. *Circ Res*. 2006;98:1555-1563.
6. Vicente-Steijn R, Passier R, Wisse LJ, Schalij MJ, Poelmann RE, Gittenberger-de-Groot AC, Jongbloed MRM. The funny current channel HCN4 delineates the developing cardiac conduction system in the chicken heart. *Heart Rhythm in press*. 2011.
7. Mahtab EA, Vicente-Steijn R, Hahurij ND, Jongbloed MR, Wisse LJ, DeRuiter MC, Uhrin P, Zaujec J, Binder BR, Schalij MJ, Poelmann RE, Gittenberger-de Groot AC. Podoplanin deficient mice show a Rhoa-related hypoplasia of the sinus venosus myocardium including the sinoatrial node. *Dev Dyn*. 2009;238:183-193.
8. Vicente-Steijn R, Kolditz DP, Mahtab EA, Askar SF, Bax NA, van der Graaf LM, Wisse LJ, Passier R, Pijnappels DA, Schalij MJ, Poelmann RE, Gittenberger-de Groot AC, Jongbloed MR. Electrical activation of sinus venosus myocardium and expression patterns of RhoA and Isl-1 in the chick embryo. *J Cardiovasc Electrophysiol*. 2010;21:1284-1292.
9. van TJ, Pijnappels DA, de Vries AA, de V, I, van der Velde-van Dijke, Knaan-Shanzer S, Van der Laarse A, Schalij MJ, Atsma DE. Fibroblasts from human postmyocardial infarction scars acquire properties of cardiomyocytes after transduction with a recombinant myocardin gene. *FASEB J*. 2007;21:3369-3379.
10. Shcherbo D, Merzlyak EM, Chepurnykh TV, Fradkov AF, Ermakova GV, Solovieva EA, Lukyanov KA, Bogdanova EA, Zaraisky AG, Lukyanov S, Chudakov DM. Bright far-red fluorescent protein for whole-body imaging. *Nat Methods*. 2007;4:741-746.
11. Lois C, Hong EJ, Pease S, Brown EJ, Baltimore D. Germline transmission and tissue-specific expression of transgenes delivered by lentiviral vectors. *Science*. 2002;295:868-872.
12. Hoffman RM. A better fluorescent protein for whole-body imaging. *Trends Biotechnol*. 2008;26:1-4.
13. Amsalem Y, Mardor Y, Feinberg MS, Landa N, Miller L, Daniels D, Ocherashvilli A, Holbova R, Yosef O, Barbash IM, Leor J. Iron-oxide labeling and outcome of transplanted mesenchymal stem cells in the infarcted myocardium. *Circulation*. 2007;116:I38-I45.
14. Boot MJ, Gittenberger-de Groot AC, van Iperen L, Poelmann RE. The myth of ventrally emigrating neural tube (VENT) cells and their contribution to the developing cardiovascular system. *Anat Embryol*. 2003;206:327-333.
15. Kolditz DP, Wijffels MCEF, Blom NA, Van der Laarse A, Markwald RR, Schalij MJ, Gittenberger-de Groot AC. Persistence of functional atrioventricular accessory pathways in post-septated embryonic avian hearts: implications for morphogenesis and functional maturation of the cardiac conduction system. *Circulation*. 2007;115:17-26.
16. Kolditz DP, Wijffels MC, Blom NA, Van der Laarse A, Hahurij ND, Lie-Venema H, Markwald RR, Poelmann RE, Schalij MJ, Gittenberger-de Groot AC. Epicardium-derived cells in development of annulus fibrosis and persistence of accessory pathways. *Circulation*. 2008;117:1508-1517.

166

Chapter 8

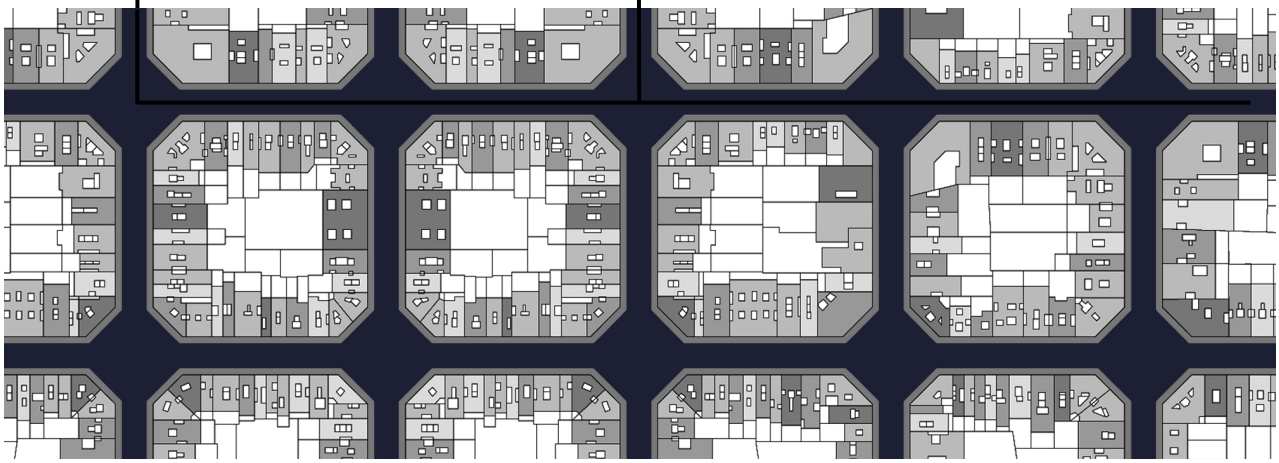

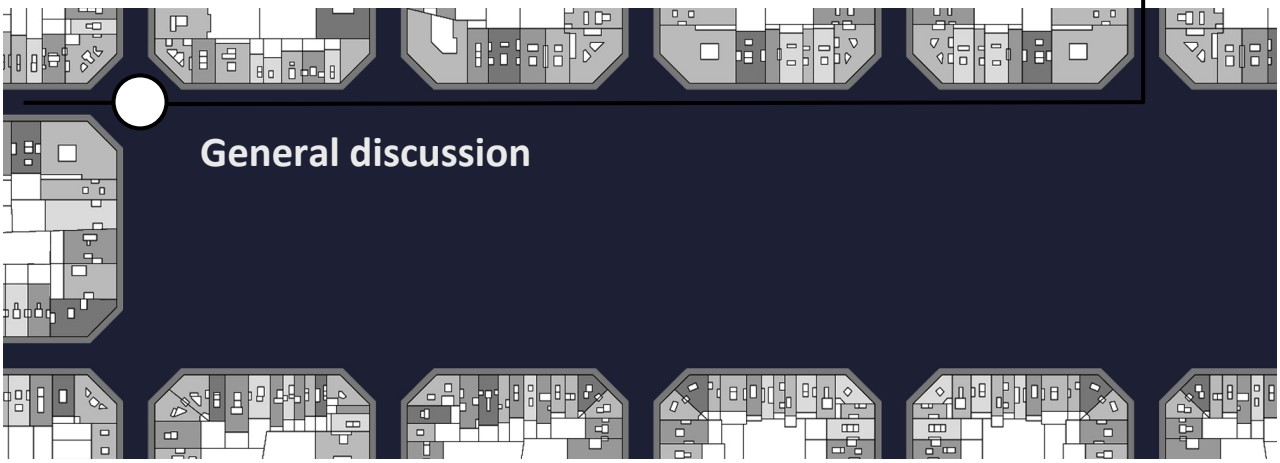
General discussion

Introduction

In the human population almost 1% of newborn children have some form of congenital heart defects, and probably 30% of embryonic or fetal loss is due to cardiac malformations.[1] With the discovery of the first and second heart field (SHF) lineages contributing to the heart[2-5] several concepts on heart development were better understood and needed to be revised. Many studies help shed light into the mechanisms leading to specific cardiac malformations and the genes involved in those processes.
In this thesis we have studied the contribution of the SHF-derived cells to the developing heart, focusing on both the morphological as well as functional development of the sinus venosus myocardium and the components of the central cardiac conduction system (CCS), specifically the sinoatrial (SAN) and atrioventricular (AVN) node. In this chapter we will discuss our findings and place them in perspective with novel findings in the field. Finally, we comment on the consequences of our results to the better understanding of the etiology of arrhythmias.

The role of second heart field in cardiac development

As we described in Chapter 1, the heart starts off as a linear heart tube and additional cells will be incorporated from the SHF at the arterial and venous pole. The contribution at the arterial pole (anterior or secondary heart field) is of importance for the proper development of the outflow tract and the right ventricle, while the contribution at the venous pole (posterior heart field) is necessary for normal development of the sinus venosus myocardium which comprises the myocardium surrounding the cardinal veins including the SAN and the pulmonary veins. As discussed earlier in this thesis, *Islet-1*(*Isl-1*) is a transcription factor expressed throughout the entire SHF population, and lack of expression of this factor results in abnormal development of both the arterial and venous pole of the heart.[5] Recent studies have shown Islet-1 protein expression in the cardiac crescent, or first heart field, and more importantly, in the absence of Nkx2.5 expression, differentiating myocardial cells of the crescent maintain Islet-1 expression throughout development, suggesting that Islet-1 is expressed in both heart fields.[6] Nevertheless, *Isl-1* mutant embryos still form a primitive heart tube which shows abnormal SHF contribution to the heart and states the importance of this gene within the SHF population.[5] It is questionable whether the heart fields can be seen as two separate lineages or more like a spatiotemporal continuum of progenitor cells that are added at different time points during heart development. The evidence of the existence of subdomains within the SHF is increasing. In addition to *Isl-1*, a number of genes have now been characterized like platelet-derived growth factor receptor α (*Pdgfr-α*)[6,7](Chapter 4) or the inhibitor of differentiation *Id2*[8,9](Chapter 5). In this thesis we have shown that

both genes are important for the arterial and venous pole development of the heart and these will be discussed for each separate population.

Anterior Heart Field

The cellular addition at the arterial pole contributes to the formation of the outflow tract i.e where the pulmonary trunk and the aorta will develop[2-4] and the right ventricle.[10] In *Pdgfr-α* mutant embryos, several outflow tract abnormalities have been reported like persistent truncus arteriorsus, double outlet right ventricle (DORV) and dextraposition of the aorta which have been attributed to the interaction between the neural crest cell population and the myocardium at the outflow tract.[11] Id2 expression has been observed in the cardiac neural crest cells, the splanchnic mesoderm dorsal to the heart (SHF) and the anterior parasympathetic plexus.[8] *Id2* knockout mice show outflow tract abnormalities ranging from dextraposition of the aorta to DORV. These malformations have been related to anomalies of the cardiac neural crest cell population as ablation of this population in *Xenopus* and chick results in reduced Id2 expression and outflow tract abnormalities[8] (Chapter 5). However, it is not clear whether the loss of Id2 expression is due to a direct effect of neural crest cells on Id2 expression or an indirect effect caused by defective signalling between the neural crest cells and the SHF.[12] Given the potential function of *Id2* on the SHF population a possible explanation for the outflow tract abnormalities in these mice could be that alteration of SHF recruitment or expansion eventually can lead to DORV.

Posterior Heart Field

As already stated by our lab, the venous pole progenitor population referred to as posterior heart field (PHF) can be divided into a mesenchymal and a myocardial component.[13] Genes like *Tbx18, podoplanin, RhoA, Pdgfr-α* or *Id2* (this thesis and[7,13-15]) are important for proper development of both PHF-derived components. Interestingly we have not found a gene exclusive to one of the subpopulations within the PHF, suggesting that this population has the potential to differentiate into any of the components early in development and that they share the same initial molecular pathways[16](this thesis). We propose that this population is derived from the mesodermal lining of the coelomic cavity through a process of epithelial-to-mesenchymal transition (EMT) which is supported by the abnormal EMT observed in the *podoplanin* knockout model (Chapter 2).

Dorsal mesenchymal protrusion

Atrial and ventricular septation are complex processes that involve multiple cell populations. In the case of atrial septation, an atrioventricular (AV) mesenchymal complex is formed by fusion of the mesenchymal cap which is cushion tissue attached to the primary atrial septum and the dorsal mesenchymal protrusion (DMP). The

latter is a mesenchymal population derived from the PHF that will undergo myocardial differentiation. These structures will further fuse to the superior and inferior AV cushions. If one of these cell populations is affected, given the complexity of this process, atrial septal defects (ASDs) could develop. More interestingly, mice lacking a PHF-specific gene (Chapters 2, 5 and[7]) show ASDs or AV septal defects (AVSDs) which strongly supports the role of PHF in atrial septation. Specifically, the mutant *Pdgfr-α* mice show a reduced mesenchymal cap that does not fuse with the AV mesenchymal complex and a hypoplastic DMP, which eventually results in AVSD.[7] Podoplanin expression was also observed in the dorsal mesocardium and the DMP extending into the heart[13] and mice lacking this gene show an ASD and lack myocardialisation at the base of the atrial septum (Chapter 2), suggesting an abnormal development of the DMP. Both mouse models show a reduced contribution of PHF-derived myocardial cells to the embryonic heart which results in generalized myocardial hypoplasia and eventually in ASD or AVSD. *Id2* knockout mice present ASDs (Chapter 5) although we have not observed abnormalities in the DMP or the mesenchymal cap that could explain these defects. A possible explanation for the ASD in this model is that the SHF-derived myocardial differentiation is altered resulting in hypoplasia due to a reduced number of cells at a specific developmental time point.

Proepicardial organ and derivatives

The proepicardial organ (PEO) and its derivatives the epicardium and the epicardium-derived cells (EPDCs) are very important as structural as well as inductive contributors to the developing heart.[17-19] Several models involving defective epicardial development have resulted in severe hypoplasia of the compact myocardium and looping disorders.[20-25] The PEO and its derivatives develop by EMT from the coelomic mesothelium. During this process, epithelial cells become mobile mesenchymal cells[26] loosing E-cadherin expression which results in loss of all epithelial features.[27] *In vitro* studies have shown podoplanin-mediated RhoA-associated EMT in human cells.[28,29] Although expression of RhoA, studied in Chapter 3, was observed in the PEO and its derivatives, no specific epicardial phenotype can be linked to this protein in relation to PHF development. Interestingly, podoplanin expression has been observed in the PEO, the epicardium and the EPDCs by our group.[13] *Podoplanin* mutant embryos show upregularion of E-cadherin resulting in abnormal epicardial adhesion and myocardial hypoplasia of the compact myocardium with atrioventricular and ventricular septal abnormalities.[15] Similar abnormalities were observed in the *Pdgfr-α* mutant mice.[7] One of the hypotheses regarding the development of ventricular myocardial hypoplasia states that abnormal epicardial lining or blebbing leads to impaired epicardial-myocardial signalling. The abnormal signalling results in hypoplastic compact myocardium in part due to the lack of myocardial remodelling in which interstitial fibroblasts, derived from EPDCs, are essential for proper myocardial proliferation and maturation.[30] The platelet-derived growth factor family has been associated with epicardial-myocardial signalling in relation to coronary vasculature

development.[31,32] In this thesis we have investigated the expression patterns of PDGF-A, -C and PDGFR-α during chicken heart development (Chapter 4). These factors and the receptor were expressed in SHF-derived structures and in the ventricular myocardium. Inhibition of epicardial outgrowth resulted in abnormal expression of both ligands and their receptor, whereas pharmacological inhibition of PDGFR-α signalling resulted in abnormal epicardial development. These findings suggest that PDGF-A, -C and PDGFR-α are involved in cardiac remodelling during development, specifically related to the ventricular compact and trabecular myocardium through epicardial-myocardial interactions.

Myocardial population

The myocardial component of the PHF is essential for the proper development at the venous pole of the heart that will encompass the myocardium of structures like the cardinal veins, the pulmonary veins and the SAN. We have already proposed that other components of the CCS could be related to the PHF, like part of the AVN and the internodal tracts (Chapters 3, 6-7). The origin of these structures will be discussed later. The initial focus of this thesis was to analyse the myocardial recruitment at the inflow portion of the heart and its consequences for heart development. Provided the normal expression patterns of the PHF-associated protein podoplanin, we concentrated on the myocardial cardiac phenotype of mice lacking this protein (Chapter 2). Absence of *podoplanin* during development results in hypoplasia of the SAN, dorsal atrial wall as well as the atrial septum. The myocardium surrounding both cardinal and pulmonary veins is thin and discontinuous. With respect to the function of podoplanin in EMT[29] and its expression in active epithelium of the coelomic cavity,[13] we suggest that the impaired myocardial formation is correlated to the abnormal EMT of the coelomic epithelium due to up-regulated E-cadherin and down-regulated RhoA (Chapter 2).

Podoplanin knockout embryos also show diminished smooth muscle cell extension in the pulmonary veins. The developmental origin of the myocardium lining the pulmonary veins is a matter of continuous discussion.[33-36] Initial studies have suggested that the myocardialisation of the pulmonary vein is accomplished by a process of migration of atrial cardiomyocytes into the extracardiac mesenchyme extending towards the pulmonary vein.[37,38] However recent studies have proven that the mesodermal population of the SHF contributes to the development of the pulmonary vein.[13,33] Our most recent studies show that during development Nkx2.5 negative myocardium temporarily covers parts of the myocardial sleeves of the pulmonary vein suggesting a possible relation between this myocardial population and the sinus venosus myocardium, known to lack Nkx2.5 expression (Chapter 7 and[13]). Several markers related to the PHF-derived myocardium are also expressed in the myocardium surrounding the pulmonary vein including HNK-1,[39] podoplanin,[13] HCN4 (Chapters 2 and 6) and PDGFR-α.[7] Additionally, mouse models lacking genes involved in SHF development like *podoplanin*, *PDGFR-α* or *Id2* show abnormal

pulmonary vein development. The abnormalities can vary from myocardial hypoplasia and diminished smooth muscle cell population[34] to abnormal incorporation of the pulmonary vein[7,40](Chapter 5). The extent of the abnormalities is based on the function of the affected gene in the SHF population and indicates the close proximity of the pulmonary vein to the developing venous pole, independent of the developmental relationship. Embryos with abnormalities in the DMP, like the *Pdgfr-α* mutant[7] also show hypoplastic pulmonary vein myocardium. Given the anatomical location of these structures it is possible that defects of one structure could result in abnormalities in the other without any developmental relationship or that they share signalling pathways involved in proper myocardial differentiation. Nevertheless, the *Id2* knockout mouse does not show abnormalities in the DMP but does show an abnormal incorporation of the pulmonary vein. Further research is imperative to understand the different processes involved in pulmonary vein development.[35]

The sinus venosus myocardium differentiates from the mesodermal precursor population of the SHF and forms a U-shaped myocardial structure comprising the definitive SAN area.[13,41] This special area of myocardium in the mouse is positive for Tbx18 and negative for Nkx2.5.[13,14] Other genes have also been described to be expressed here like *podoplanin,*[13] *Shox2*[42] and *Hcn4,*[43] their expression patterns being distinct from working myocardium. As commented above, *podoplanin* knockout embryos show a RhoA-related hypoplasia of this myocardium, finally resulting in a hypoplastic SAN (Chapter 2). A hypoplastic SAN was also observed in the *Id2* knockout mice (Chapter 5). Ectopic expression of working myocardium-related genes like Nkx2.5 or Cx43 in the SAN has been observed in other mouse models lacking PHF-related genes like the *Shox2*[42] or the *Pdgfr-α*[7] model. This suggests that although the initial transcriptional framework in which these genes are found might be the same, the functional repercussions might differ. One set of genes seems involved in the proper incorporation of cell from the SHF to the developing SAN, while the other seems related to the proper patterning of the SAN towards a functional structure (repressing the working myocardium phenotype). The next step regarding these models could be to analyse the electrophysiological properties of these hearts and investigate whether there are any differences in phenotypes or whether the resulting phenotype remains the same.

Development of the CCS: Tools for a better comprehension of clinical arrhythmias

Arrhythmias can occur due to many reasons including congenital malformations of the heart, aging or dysfunctional gene expression and can result in dysfunction of the pacemaker tissues.[44-47] Even though many studies have been conducted to unravel the electrophysiological and cellular composition of the nodes (SAN and AVN)[48-51] the pathologies involving the SAN and AVN are not understood.

Origin of CCS cells

As already stated in Chapter 1, CCS cells are of myocardial origin.[52,53] Markers also associated with neuronal development or function have been identified in components of the CCS, like the antigen HNK-1 which, in the embryo, was initially identified as a marker of neural crest cells,[39,54] the neural tissue antigen Gln2,[55] EAP-300, a protein expressed in the neural cells of the chicken retina,[56] the transcriptional repressor Tbx3[57] and the recently discovered Purkinje fiber marker Contactin-2, a cell adhesion molecule involved in axonal patterning and ion clustering.[58] The neural crest population provides the majority of cells of the autonomic nervous system, which play an important role in the regulation of cardiac function.[59] During development, cardiac ganglia will form partly from the neural crest population and although they can vary in number and distribution between species, they are mostly found within the subepicardial layer.[60] In mammals, they are predominantly located around the atria where the caval and pulmonary veins enter the heart. From there nerves extend into the heart to reach the SAN and AVN.[59,61,62] These nodes are surrounded by a large number of neuronal cells and are thus thoroughly under the control of the autonomic nervous system, which can vary the heart rate or cardiac output. Based on the overlapping expression of neuronal markers in CCS tissue and the abundance of neuronal tissue surrounding CCS structures, additional research is needed to unravel the interactions between the neural cell population and the patterning of the CCS.

CCS development

Three models for CCS development were used to study the mechanism behind the pathways that guide cells towards a working myocardium or pacemaking phenotype[53,63,64] as reviewed in Chapter 1. In Chapter 6 we describe for the first time the expression of the funny current channel *Hcn4* in the developing CCS in chick. The *Hcn4* mRNA expression data in the chick differ slightly from the described mRNA patterns in mouse.[43,65,66] A noteworthy finding is the presence of *Hcn*4 mRNA in the complete linear heart tube at stage HH11/12 in the chicken embryo, which has not been reported for *Hcn4* in the mouse embryo.[43] Only a few genes that are linked to myocardial and CCS development have been described in the early heart tube, e.g. the transcription factors *Nkx2.5,*[67] *Gata4*[68] and *Tbx5.*[69] Other transcription factors, such as *Tbx2* and *Tbx3*, implicated in CCS formation and function, are expressed upon ballooning of the cardiac chambers.[70,71] The MinK protein, implicated in CCS function and expressed in the developing CCS,[72] has also not been reported before in the primary heart tube. To our knowledge no functional genes involved in CCS formation and function have been described in the primary heart tube. It has already been reported that the primary heart tube presents a nodal-like functional phenotype as it shows automaticity, slow conduction of the electrical signal and a peristaltic-like contraction pattern.[64,73] Based on the functional relevance of the ion channel HCN4, the primary heart tube wide expression suggests that the entire myocardium has the

capacity to generate the electrical impulse necessary for the peristaltic contractions at this stage.[73]

During looping, septation and chamber formation *Hcn4* mRNA becomes restricted to the transitional zones of the heart. The expression pattern overlaps with that of *Tbx2* and *Tbx3*[70,71,74] that play a role in CCS formation and remain expressed in the transitional zones where they prevent chamber formation. Based on our own and others' results, a model emerges in which the primary heart tube tissue has automaticity and pacemaker potential. As the heart further develops and the SHF population is being added, this initial myocardium will become positioned in the already described transitional zones of the heart which can be linked to developing CCS structures. Late in development, parts of these zones will further differentiate into working myocardium while the remainder will become part of the mature CCS. Taking the different models into account a starting point is proposed involving recruitment of myocardial progenitors into the primary heart tube (recruitment step) followed by specification of these cells towards a nodal phenotype (early specification step) based on a specific transcriptional network and the confinement of this myocardium to specific areas in the developing heart (transitional zones) which can be traced to the mature CCS. In this concept, cells that will form the CCS repress the working myocardial genetic program rather than differentiating into a CCS phenotype[75] reinforcing the idea that the primary heart tube possesses a nodal phenotype.

Development of the Pacemaker of the heart (SAN)

Functionally, the first spontaneous action potentials are generated at the left posterior inflow-site of the heart which is the putative sinus venosus region.[76] Our electrophysiological recordings show that at later stages both atria have the potential to generate the first electrical activity, while later in development the activity becomes restricted to the right side, where the definitive adult pacemaker is located (Chapters 3 and 7). However, the exact time point of the shift from a dominant left-sided electrical activation to an eventual right-sided pacemaker remained unspecified. This shift is correlated with the disappearance of RhoA and Isl-1 positive cells and the gradual upregulation of Nkx2.5 expression in the myocardium surrounding the left cardinal vein which is where the transient left SAN is located (Chapters 3 and 7). This bilateral potential can be explained by a sinus venosus-wide capacity to generate pacemaker signals by this myocardium that shows a nodal-like phenotype. During development the left-sided sinus venosus myocardium differentiates towards working myocardium and progressively loses the pacemaker potential, whereas the right side maintains the initial expression pattern, persisting as the definitive right-sided SAN (Chapter 7). The origin of signals from both the left and right side, as well as simultaneous activation from both sides, progressively diminishing in time, could thus be explained.

The SAN at later stages of development is recognized as a comma shaped compact structure with a “head” at the border between the superior caval vein and the atrium and a “tail” along the terminal crest.[77] The area of the developing sinus venosus myocardium includes the primordium of the SAN at the right side and a cluster of cells at the left side, the transient left-sided SAN, where the left cardinal vein enters the atrium. The lack of Nkx2.5 is the main characteristic of this myocardium, which is initially located ventral of the cardinal veins and expands to the dorsal side during development. Later in development parts of this myocardium upregulate Nkx2.5 expression coinciding with the dominant pacemaker activity persisting at the right side of the sinus venosus. In the last years a panel of molecular markers and other relevant proteins has established the specific expression pattern of this tissue. The newly added myocardium at the venous pole of the heart where the SAN will develop expresses Tbx18, podoplanin but not Nkx2.5.[13,14] HCN4 expression is mandatory for proper SAN function and the transcriptional pathways that regulate this channel are still being investigated. Additionally, the SAN primordium also expresses the transcriptional repressor *Tbx3*[71] which has been demonstrated to inhibit differentiation of cells into working myocardium.[65,74] Recent findings show that the head and tail of the SAN present different gene programs in which *Tbx18* is essential for head establishment and *Tbx3* for proper differentiation.[77] Proper SAN differentiation also requires Shox2 expression[42] which regulates HCN4 expression through repression of *Nkx2.5.*[78] However, our own results (Nathan Hahurij, unpublished data) do not confirm these interpretations. Shox2 expression is part of a retinoic acid-Tbx5[79,80] axis which confines Shox2 expression to the sinus venosus. The HCN4 isotype, which is the predominant channel responsible for the 'funny' current (an inward current activated on hyperpolarization) in SAN cardiomyocytes, has been related to the spontaneous activity of pacemaker cells and the control of heart rate.[81] *Tbx3*-deficient mice show normal expression of HCN4[75] but *Nkx2.5* deficient embryos show ectopic expression of both HCN4 and Tbx3 in the heart tube[65] and ectopic pacemaker activity originating from the embryonic ventricle,[82] suggesting a repressive role for *Nkx2.5* in the pacemaking transcriptional program. Many of the genes described have been found essential but not sufficient in establishing the pacemaker phenotype.[42,74] Supporting our own findings (Chapter 6 and 7), these genes are expressed throughout the developing sinus venosus compartment,[13,14,42,71,78] reinforcing the concept of a broad pacemaker capacity of this myocardium. A question that remains unanswered is how the definitive right-sided SAN maintains its phenotype while the left side of the sinus venosus further differentiates into working myocardium (i.e. expressing Nkx2.5 and Cx43), slowly losing the ability to initiate electrical activity. The transcription factor *Pitx2* controls left/right asymmetry in the embryo including the heart, and more interestingly, *Pitx2c* deficient mice show right atrial isomerism resulting in the formation of two SAN that show similar expression patterns.[65] A recent study has detected a correlation between familial atrial fibrillation and variability in the *Pitx2* locus in humans,[83] suggesting an important role for *Pitx2* in

repressing the SAN program on the left side of the heart. An alternative could be of functional relevance. As the right-sided SAN becomes the dominant pacemaker and shows the highest intrinsic firing rate, the left-sided SAN becomes obsolete and ceases to function, finally differentiating towards chamber myocardium. However, the exact mechanism that couples the functional redundancy and the onset of working myocardium differentiation is not known. A third alternative, requiring further study is that the left-sided SAN is incorporated into the AVN region where the inferior nodal extension is located, potentially contributing to the slow conducting pathway of the AVN (see below).

Development of the AVN

The adult AVN is a complex and heterogeneous structure that consists of multiple components and different cell types with differential gene expression profiles[50,84] and it was first described in 1906 by Sunao Tawara as the only myocardial structure that crossed the insulating annulus fibrosus at the AV junction.[85] The AVN is located in a triangular region known as the triangle of Koch,[86] and is deliniated by three anatomical landmarks: the superior border is occupied by the Tendon of Todaro, a fibrous structure bordering the opening of the coronary sinus and the inferior caval vein; the inferior border is occupied by the septal leaflet of the tricuspid valve; and finally the base by the ostium of the coronary sinus.

Several structures form a part of the AV nodal area and have been identified at the AV junction of the heart showing differential expression patterns. These structures include an inferior nodal extension, a compact AVN and lower nodal cells that connect to the common bundle.[50,66,87,88] From the AVN region, nodal-like myocytes extend towards the tricuspid valve (right AV ring bundle) and the mitral valve (left AV ring bundle) to contact anteriorly and form the retroaortic node.[89] An AV-delay is present early in development and has been initially attributed to the myocardium of the atrioventricular canal (AVC) with a slow conducting phenotype.[73,90-95] This myocardium shows structural and functional characteristics of nodal-like myocardium and overlapping expression patterns with the SAN like expression of Tbx3[71] or *Hcn4*[66](Chapters 6 and 7). Whether the avian system has an AVN is still a matter of debate. Some studies have stated that the AV ring (AVR) myocardium functions as the AVN in the chicken, at least until late stages of development.[90] Others have described the adult chicken AVN at the right side of the base of the interatrial septum, at the antero-inferior margin of the orifice of the left superior caval vein which corresponds to the ostium of the coronary sinus in the human heart,[96] coinciding with the location of the AVN in human.[97] Additional studies in embryonic chicken hearts have distinguished an AVN at 5-6 days of development (~HH29-31) at the lower dorsal segment of the interatrial septum.[94] Several theories postulate on the origin of the AVN from the AVR myocardium,[63,98] the lowest and dorsal part of the interatrial segment,[94] the dorsal atrial wall[99] or as a counterpart of the left sinus horn.[100,101] The

hypothesis of multiple cellular contributions to the AVN is also based on electrophysiological data.[102] The compact part of the AVN in mouse is most probably derived form the AVR myocardium,[66] although a partial atrial contribution to the AVN has also been found.[41] In chicken (Chapters 3, 6 and 7) we have observed similarities in expression profiles between the AVC myocardium early in development and the AVR (right and left) and the AVN at later stages as well as a possible sinoatrial contribution to the base of the atrium septum (AVN area). The location of these cells coincides with the location of the inferior nodal extension in the adult AVN. Our tracing experiments with Katushka-labelled coelomic cells show myocardial cells not only in the SAN, but also in the right venous valve and at the base of the atrial septum, where the AVN is located (Chapter 7). Although these results need to be expanded, we hypothesize that cells from the atrial myocardium provide a cellular contribution to the AVN through the internodal myocardium (i.e. the internodal tracts) located between the SAN and AVN. These tracts run in the right atrium between the SAN and the AVN. Specifically they run along the terminal crest (formed by the embryonic right venous valve in the posterior atrial wall) and part of the interatrial septum (partly formed by the embryonic left venous valve). Although the existence of preferential atrial conduction tracts has been demonstrated,[103] controversy exists in whether these tracts are exclusively developmental structures or actually have functional properties postnatally. In Chapters 6 and 7 we demonstrated that these tracts contain Hcn4 mRNA, while other studies have revealed the expression of CCS markers like Tbx3,[71,104] CCS-LacZ[105] or HNK-1,[39] suggesting that they have a nodal phenotype in embryonic stages. In view of the phenotypical similarities between the SAN and the AVN, a possible cellular contribution cannot be excluded in which the internodal tracts serve as pathways. However, additional lineage tracing experiments are needed to confirm this hypothesis. An alternative cellular contribution to the AVN involves the transient left-sided SAN, a cluster of cells that disappears both functionally and morphologically during development. Based on the final anatomical location of this structure near the ostium of the coronary sinus combined with the nodal phenotype we hypothesize that it could contribute to the formation of the slow pathway of the AVN.

Coinciding with completion of ventricular septation the AV myocardial continuity, present around the entire circumference of the slow conducting AVC, disappears as a result of annulus fibrosus formation.[106-108] The myocardium of the AVR, expressing *Hcn4*, is incorporated in the atrial myocardium, specifically in the lower atrial rim. Normally, the His bundle is the only myocardial continuity between the AVN at the atrial level and the bundle branches at the ventricular level. Recent evidence has shown the persistence of accessory pathways until late developmental stages[108] causing ventricular pre-excitation. These pathways were suggested to derive from the primitive AVC myocardium and therefore show slow conduction.[91] Our own *Hcn4* results suggest that this myocardium still expresses *Hcn4*. Additionally, we confirm that the left-sided AVR shows a better isolation than the fibrous scattering in the

right-sided AVR.[108] This suggests a developmental time-difference in completion of the AVR isolation which is in line with previous findings in humans.[109]

Clinical implications

Supraventricular tachycardias are the most common cardiac arrhythmias in both adults and children.[110] Components of the adult CCS as well as myocardial structures outside the adult CCS can be involved in arrhythmogenesis. Examples of the first group include rhythm disturbances related to the SAN and AVN, such as inappropriate sinustachycardia, and SAN and AVN re-entrant tachycardias.[111,112] Examples of the last group include ectopic foci in the atria that can initiate atrial arrhythmias.

As described in this thesis a bilateral electrical activity of the sinus venosus is transiently present during development, correlating with expression of markers that are also observed in elements of the definitive CCS, like the SAN. During development a shift in activation pattern towards a definitive right-sided activation from the SAN, concomitant with confinement of expression of markers to the area of the SAN, is due to occur. This means that the sinus venosus myocardium, with exception of the SAN that will keep a more primitive nodal-like phenotype, will differentiate during development towards working myocardium. Failure to differentiate into working myocardium in these areas, or re-expression of the embryonic program may lead to potential arrhythmogenic substrates in the adult. This provides a plausible explanation for arrhythmias originating from ectopic pacemaker foci in the sinus venosus myocardium e.g. the myocardium surrounding the pulmonary veins (Chapters 6 and 7) and the ligament of Marshall.[105,113,114] Previous studies in human have shown an elevated funny current during heart failure,[115] suggesting that during pathophysiological remodeling, the embryonic program can be re-activated, a well known mechanism in heart failure. This may shed new light on the frequent co-occurrence of atrial fibrillation and heart failure.[116] A recent study provides evidence that heart failure increases ectopic pacemaker activity by activating the pacemaking potential of the lower crista terminalis.[117]

The compact AVN is derived from the AVC myocardium.[66,118] However, a contribution from the SHF to the AVN has also been hypothesized.[41] Re-entry requires the presence of two tracts with distinct electrical characteristics, the so-called “fast” and “slow” pathways. The possibility of a multicellular origin of the AVN is interesting in the light of AV nodal re-entry tachycardia, based on pathways within the AVN with distinctive electrophysiologic capacities providing the substrate for re-entry. Cell tracing-based proof of contribution of sinus venosus myocardium to the AVN area is necessary.

The AVR myocardium expresses *Hcn4*, and already in early stages an accumulation of *Hcn4* positive cells is detected at the base of the atrial septum, the putative AVN area. During development an increase in AV-delay occurs. Electrical isolation will occur by fibrosis of the AVR, which is completed earlier on the left than on the right side

(Chapter 7). This is in accordance with findings in human, and may explain the more frequent occurrence of right-sided accessory pathways,[108,109] substrate for AV re-entrant tachycardia if present postnatally.

Future perspectives

Most of the data presented in this thesis shows expression patterns of specific markers of the CCS or working myocardium throughout development. The results obtained from the expression patterns are not indicative of lineage relationships and are not considered as such. To evaluate the function of specific proteins during heart development we have evaluated the cardiac malformation resulting from mice lacking the gene of interest. We have investigated potential mechanisms, but additional experiments are required for solid conclusions. Additionally, we have not found a single marker that is unique either for the SAN or the AVN, being unable to make any distinctions between the cell types in each of these structures. In the near future we intend to conduct lineage tracing analysis in both chicken and mouse embryos to unravel the cellular contributions to each of these structures. We will also be conducting RNA profiling and functional assays to study the cells that contribute to the SAN and AVN.

References

1. Bruneau BG. The developmental genetics of congenital heart disease. *Nature*. 2008;451:943-948.
2. Kelly RG, Brown NA, Buckingham ME. The arterial pole of the mouse heart forms from Fgf10-expressing cells in pharyngeal mesoderm. *Dev Cell*. 2001;1:435-440.
3. Mjaatvedt CH, Nakaoka T, Moreno-Rodriguez R, Norris RA, Kern MJ, Eisenberg CA, Turner D, Markwald RR. The outflow tract of the heart is recruited from a novel heart-forming field. *Dev Biol*. 2001;238:97-109.
4. Waldo K, Kumiski DH, Wallis KT, Stadt HA, Hutson MR, Platt DH, Kirby ML. Conotruncal myocardium arises from a secondary heart field. *Development*. 2001;128:3179-3188.
5. Cai CL, Liang X, Shi Y, Chu PH, Pfaff SL, Chen J, Evans S. Isl1 identifies a cardiac progenitor population that proliferates prior to differentiation and contributes a majority of cells to the heart. *Dev Cell*. 2003;5:877-889.
6. Prall OW, Menon MK, Solloway MJ, Watanabe Y, Zaffran S, Bajolle F, Biben C, McBride JJ, Robertson BR, Chaulet H, Stennard FA, Wise N, Schaft D, Wolstein O, Furtado MB, Shiratori H, Chien KR, Hamada H, Black BL, Saga Y, Robertson EJ, Buckingham ME, Harvey RP. An Nkx2-5/Bmp2/Smad1 negative feedback loop controls heart progenitor specification and proliferation. *Cell*. 2007;128:947-959.
7. Bax NA, Bleyl SB, Gallini R, Wisse LJ, Hunter J, Van Oorschot AA, Mahtab EA, Lie-Venema H, Goumans MJ, Betsholtz C, Gittenberger-de Groot AC. Cardiac malformations in Pdgfralpha mutant embryos are associated with increased expression of WT1 and Nkx2.5 in the second heart field. *Dev Dyn*. 2010;239:2307-2317.
8. Martinsen BJ, Frasier AJ, Baker CV, Lohr JL. Cardiac neural crest ablation alters Id2 gene expression in the developing heart. *Dev Biol*. 2004;272:176-190.
9. Moskowitz IP, Kim JB, Moore ML, Wolf CM, Peterson MA, Shendure J, Nobrega MA, Yokota Y, Berul C, Izumo S, Seidman JG, Seidman CE. A molecular pathway including Id2, Tbx5, and Nkx2-5 required for cardiac conduction system development. *Cell*. 2007;129:1365-1376.
10. Zaffran S, Kelly RG, Meilhac SM, Buckingham ME, Brown NA. Right ventricular myocardium derives from the anterior heart field. *Circ Res*. 2004;95:261-268.
11. Schatteman GC, Motley ST, Effmann EL, Bowen-Pope DF. Platelet-derived growth factor receptor alpha subunit deleted patch mouse exhibits severe cardiovascular dysmorphogenesis. *Teratology*. 1995;51:351-366.
12. Yelbuz TM, Waldo KL, Kumiski DH, Stadt HA, Wolfe RR, Leatherbury L, Kirby ML. Shortened outflow tract leads to altered cardiac looping after neural crest ablation. *Circulation*. 2002;106:504-510.
13. Gittenberger-de Groot AC, Mahtab EAF, Hahurij ND, Wisse LJ, DeRuiter MC, Wijffels MCEF, Poelmann RE. Nkx2.5 negative myocardium of the posterior heart field and its correlation with podoplanin expression in cells from the developing cardiac pacemaking and conduction system. *Anat Rec*. 2007;290:115-122.
14. Christoffels VM, Mommersteeg MT, Trowe MO, Prall OW, Gier-de Vries C, Soufan AT, Bussen M, Schuster-Gossler K, Harvey RP, Moorman AF, Kispert A. Formation of the venous pole of the heart from an Nkx2-5-negative precursor population requires Tbx18. *Circ Res*. 2006;98:1555-1563.
15. Mahtab EAF, Wijffels MCEF, van den Akker NMS, Hahurij ND, Lie-Venema H, Wisse LJ, DeRuiter MC, Uhrin P, Zaujec J, Binder BR, Schalij MJ, Poelmann RE, Gittenberger-de Groot AC. Cardiac malformations and myocardial abnormalities in podoplanin knockout mouse embryos: correlation with abnormal epicardial development. *Dev Dyn*. 2008;237:847-857.
16. Kruithof BP, van Wijk B, Somi S, Kruithof-de Julio M, Perez Pomares JM, Weesie F, Wessels A, Moorman AF, van den Hoff MJ. BMP and FGF regulate the differentiation of multipotential pericardial mesoderm into the myocardial or epicardial lineage. *Dev Biol*. 2006;295:507-522.
17. Gittenberger-de Groot AC, Vrancken Peeters M-PFM, Mentink MMT, Gourdie RG, Poelmann RE. Epicardium-derived cells contribute a novel population to the myocardial wall and the atrioventricular cushions. *Circ Res*. 1998;82:1043-1052.
18. Gittenberger-de Groot AC, Vrancken Peeters M-PFM, Poelmann RE. EPDC participate in formation of cardiac valves and coronary vascular wall and initiate purkinje fiber differentiation. 2000;247-250.

19. Lie-Venema H, van den Akker NMS, Bax NAM, Winter EM, Maas S, Kekarainen T, Hoeben RC, DeRuiter MC, Poelmann RE, Gittenberger-de Groot AC. Origin, fate, and function of epicardium-derived cells (EPCDs) in normal and abnormal cardiac development. *ScientificWorldJournal*. 2007;7:1777-1798.
20. Yang JT, Rayburn H, Hynes RO. Cell adhesion events mediated by alpha 4 integrins are essential in placental and cardiac development. *Development*. 1995;121:549-560.
21. Tevosian SG, Deconinck AE, Tanaka M, Schinke M, Litovsky SH, Izumo S, Fujiwara Y, Orkin SH. FOG-2, a cofactor for GATA transcription factors, is essential for heart morphogenesis and development of coronary vessels from epicardium. *Cell*. 2000;101:729-739.
22. Lie-Venema H, Gittenberger-de Groot AC, van Empel LJP, Boot MJ, Kerkdijk H, de Kant E, DeRuiter MC. Ets-1 and Ets-2 transcription factors are essential for normal coronary and myocardial development in chicken embryos. *Circ Res*. 2003;92:749-756.
23. Watt AJ, Battle MA, Li J, Duncan SA. GATA4 is essential for formation of the proepicardium and regulates cardiogenesis. *Proc Natl Acad Sci U S A*. 2004;101:12573-12578.
24. Eralp I, Lie-Venema H, DeRuiter MC, van den Akker NM, Bogers AJ, Mentink MM, Poelmann RE, Gittenberger-de Groot AC. Coronary artery and orifice development is associated with proper timing of epicardial outgrowth and correlated Fas ligand associated apoptosis patterns. *Circ Res*. 2005;96:526-534.
25. Merki E, Zamora M, Raya A, Kawakami Y, Wang J, Zhang X, Burch J, Kubalak SW, Kaliman P, Belmonte JC, Chien KR, Ruiz-Lozano P. Epicardial retinoid X receptor alpha is required for myocardial growth and coronary artery formation. *Proc Natl Acad Sci U S A*. 2005;102:18455-18460.
26. Hay ED. The mesenchymal cell, its role in the embryo, and the remarkable signaling mechanisms that create it. *Dev Dyn*. 2005;233:706-720.
27. Cano A, Perez-Moreno MA, Rodrigo I, Locascio A, Blanco MJ, del Barrio MG, Portillo F, Nieto MA. The transcription factor snail controls epithelial-mesenchymal transitions by repressing E-cadherin expression. *Nat Cell Biol*. 2000;2:76-83.
28. Martin-Villar E, Scholl FG, Gamallo C, Yurrita MM, Munoz-Guerra M, Cruces J, Quintanilla M. Characterization of human PA2.26 antigen (T1alpha-2, podoplanin), a small membrane mucin induced in oral squamous cell carcinomas. *Int J Cancer*. 2005;113:899-910.
29. Martin-Villar E, Megias D, Castel S, Yurrita MM, Vilaro S, Quintanilla M. Podoplanin binds ERM proteins to activate RhoA and promote epithelial-mesenchymal transition. *J Cell Sci*. 2006;119: 4541-4553.
30. Weeke-Klimp A, Bax NA, Bellu AR, Winter EM, Vrolijk J, Plantinga J, Maas S, Brinker M, Mahtab EA, Gittenberger-de Groot AC, van Luyn MJ, Harmsen MC, Lie-Venema H. Epicardium-derived cells enhance proliferation, cellular maturation and alignment of cardiomyocytes. *J Mol Cell Cardiol*. 2010;49:606-616.
31. van den Akker NMS, Lie-Venema H, Maas S, Eralp I, DeRuiter MC, Poelmann RE, Groot ACG. Platelet-derived growth factors in the developing avian heart and maturating coronary vasculature. *Developmental Dynamics*. 2005;233:1579-1588.
32. van den Akker NM, Winkel LC, Nisancioglu MH, Maas S, Wisse LJ, Armulik A, Poelmann RE, Lie-Venema H, Betsholtz C, Gittenberger-de Groot AC. PDGF-B signaling is important for murine cardiac development: Its role in developing atrioventricular valves, coronaries, and cardiac innervation. *Dev Dyn*. 2008;237:494-503.
33. Mommersteeg MT, Brown NA, Prall OW, de Gier-de Vries C, Harvey RP, Moorman AF, Christoffels VM. Pitx2c and Nkx2-5 Are Required for the Formation and Identity of the Pulmonary Myocardium. *Circ Res*. 2007;101:902-909.
34. Douglas YL, Mahtab EA, Jongbloed MR, Uhrin P, Zaujec J, Binder BR, Schalij MJ, Poelmann RE, DeRuiter MC, Gittenberger-de Groot AC. Pulmonary vein, dorsal atrial wall and atrial septum abnormalities in podoplanin knockout mice with disturbed posterior heart field contribution. *Pediatr Res*. 2009;65:27-32.
35. Douglas YL, Jongbloed MR, DeRuiter MC, Gittenberger-de Groot AC. Normal and abnormal development of pulmonary veins: State of the art and correlation with clinical entities. *Int J Cardiol*. 2011; 147:13-24.
36. Sizarov A, Anderson RH, Christoffels VM, Moorman AF. Three-dimensional and molecular analysis of the venous pole of the developing human heart. *Circulation*. 2010;122:798-807.

37. Saito T, Waki K, Becker AE. Left atrial myocardial extension onto pulmonary veins in humans: anatomic observations relevant for atrial arrhythmias. *J Cardiovasc Electrophysiol*. 2000;11:888-894.
38. Ho SY, Anderson RH, Sanchez-Quintana D. Atrial structure and fibres: morphologic bases of atrial conduction. *Cardiovasc Res*. 2002;54:325-336.
39. Blom NA, Gittenberger-de Groot AC, DeRuiter MC, Poelmann RE, Mentink MM, Ottenkamp J. Development of the cardiac conduction tissue in human embryos using HNK-1 antigen expression: possible relevance for understanding of abnormal atrial automaticity. *Circulation*. 1999;99:800-806.
40. Bleyl SB, Saijoh Y, Bax NA, Gittenberger-de Groot AC, Wisse LJ, Chapman SC, Hunter J, Shiratori H, Hamada H, Yamada S, Shiota K, Klewer SE, Leppert MF, Schoenwolf GC. Dysregulation of the PDGFRA gene causes inflow tract anomalies including TAPVR: integrating evidence from human genetics and model organisms. *Hum Mol Genet*. 2010;19:1286-1301.
41. Sun Y, Liang X, Najafi N, Cass M, Lin L, Cai CL, Chen J, Evans SM. Islet 1 is expressed in distinct cardiovascular lineages, including pacemaker and coronary vascular cells. *Dev Biol*. 2007;304:286-296.
42. Blaschke RJ, Hahurij ND, Kuijper S, Just S, Wisse LJ, Deissler K, Maxelon T, Anastassiadis K, Spitzer J, Hardt SE, Schöler H, Feitsma H, Rottbauer W, Blum M, Meijlink F, Rappold GA, Gittenberger-de Groot AC. Targeted mutation reveals essential functions of the homeodomain transcription factor Shox2 in sinoatrial and pacemaking development. *Circulation*. 2007;115:1830-1838.
43. Garcia-Frigola C, Shi Y, Evans SM. Expression of the hyperpolarization-activated cyclic nucleotide-gated cation channel HCN4 during mouse heart development. *Gene Expr Patterns*. 2003;3:777-783.
44. Wolf CM, Berul CI. Inherited conduction system abnormalities--one group of diseases, many genes. *J Cardiovasc Electrophysiol*. 2006;17:446-455.
45. Dobrzynski H, Boyett MR, Anderson RH. New insights into pacemaker activity: promoting understanding of sick sinus syndrome. *Circulation*. 2007;115:1921-1932.
46. Jongbloed MR, Mahtab EAF, Blom NA, Schalij MJ, Gittenberger-de Groot AC. Development of the cardiac conduction system and the possible relation to predilection sites of arrhythmogenesis. *ScientificWorldJournal*. 2008;8:239-269.
47. Christoffels VM, Moorman AF. Development of the cardiac conduction system: why are some regions of the heart more arrhythmogenic than others? *Circ Arrhythm Electrophysiol*. 2009;2:195-207.
48. Tellez JO, Dobrzynski H, Greener ID, Graham GM, Laing E, Honjo H, Hubbard SJ, Boyett MR, Billeter R. Differential expression of ion channel transcripts in atrial muscle and sinoatrial node in rabbit. *Circ Res*. 2006;99:1384-1393.
49. Boyett MR, Inada S, Yoo S, Li J, Liu J, Tellez J, Greener ID, Honjo H, Billeter R, Lei M, Zhang H, Efimov IR, Dobrzynski H. Connexins in the sinoatrial and atrioventricular nodes. *Adv Cardiol*. 2006;42: 175-197.
50. Li J, Greener ID, Inada S, Nikolski VP, Yamamoto M, Hancox JC, Zhang H, Billeter R, Efimov IR, Dobrzynski H, Boyett MR. Computer three-dimensional reconstruction of the atrioventricular node. *Circ Res*. 2008;102:975-985.
51. Greener ID, Tellez JO, Dobrzynski H, Yamamoto M, Graham GM, Billeter R, Boyett MR. Ion channel transcript expression at the rabbit atrioventricular conduction axis. *Circ Arrhythm Electrophysiol*. 2009;2:305-315.
52. Gourdie RG, Mima T, Thompson RP, Mikawa T. Terminal diversification of the myocyte lineage generates purkinje fibers of the cardiac conduction system. *Development*. 1995;121:1423-1431.
53. Cheng G, Litchenberg WH, Cole GJ, Mikawa T, Thompson RP, Gourdie RG. Development of the cardiac conduction system involves recruitment within a multipotent cardiomyogenic lineage. *Development*. 1999;126:5041-5049.
54. Bronner-Fraser M. Perturbation of cranial neural crest migration by the HNK-1 antibody. *Dev Biol*. 1987;123:321-331.
55. Wessels A, Vermeulen JL, Verbeek FJ, Virágh Sz, Kalman F, Lamers WH, Moorman AFM. Spatial distribution of "tissue-specific" antigens in the developing human heart and skeletal muscle. III. An immunohistochemical analysis of the distribution of the neural tissue antigen G1N2 in the embryonic heart; implications for the development of the atrioventricular conduction system. *Anat Rec*. 1992;232:97-111.
56. McCabe CF, Gourdie RG, Thompson RP, Cole GJ. Developmentally regulated neural protein EAP-300 is expressed by myocardium and cardiac neural crest during chick embryogenesis. *Dev Dyn*. 1995;203:51-60.

57. Mesbah K, Harrelson Z, Theveniau-Ruissy M, Papaioannou VE, Kelly RG. Tbx3 is required for outflow tract development. *Circ Res*. 2008;103:743-750.
58. Pallante BA, Giovannone S, Fang-Yu L, Zhang J, Liu N, Kang G, Dun W, Boyden PA, Fishman GI. Contactin-2 expression in the cardiac Purkinje fiber network. *Circ Arrhythm Electrophysiol*. 2010;3:186-194.
59. Hildreth V, Anderson RH, Henderson DJ. Autonomic innervation of the developing heart: origins and function. *Clin Anat*. 2009;22:36-46.
60. Rickenbacher J, Müller E. The development of cholinergic ganglia in the chick embryo heart. *Anat Embryol*. 1979;155:253-258.
61. Verberne ME, Gittenberger-de Groot AC, Poelmann RE. Lineage and development of the parasympathetic nervous system of the embryonic chicken heart. *Anat Embryol*. 1998;198:171-184.
62. Poelmann RE, Gittenberger-de Groot AC. A subpopulation of apoptosis-prone cardiac neural crest cells targets to the venous pole: multiple functions in heart development? *Dev Biol*. 1999;207: 271-286.
63. Wenink ACG. Development of the human cardiac conducting system. *J Anat*. 1976;121/3:617-631.
64. Moorman AFM, Christoffels VM. Cardiac chamber formation: Development, genes and evolution. *Physiol Rev*. 2003;83:1223-1267.
65. Mommersteeg MT, Hoogaars WM, Prall OW, Gier-de Vries C, Wiese C, Clout DE, Papaioannou VE, Brown NA, Harvey RP, Moorman AF, Christoffels VM. Molecular pathway for the localized formation of the sinoatrial node. *Circ Res*. 2007;100:354-362.
66. Aanhaanen WT, Mommersteeg MT, Norden J, Wakker V, de Gier-de Vries C, Anderson RH, Kispert A, Moorman AF, Christoffels VM. Developmental Origin, Growth, and Three-Dimensional Architecture of the Atrioventricular Conduction Axis of the Mouse Heart. *Circ Res*. 2010;107:728-736.
67. Harvey RP. NK-2 homeobox genes and heart development. *Dev Biol*. 1996;178:203-216.
68. Heikinheimo M, Scandrett JM, Wilson DB. Localization of transcription factor GATA-4 to regions of the mouse embryo involved in cardiac development. *Dev Biol*. 1994;164:361-373.
69. Bruneau BG, Logan M, Davis N, Levi T, Tabin CJ, Seidman JG, Seidman CE. Chamber-specific cardiac expression of Tbx5 and heart defects in Holt-Oram syndrome. *Dev Biol*. 1999;211:100-108.
70. Christoffels VM, Hoogaars WM, Tessari A, Clout DE, Moorman AF, Campione M. T-box transcription factor Tbx2 represses differentiation and formation of the cardiac chambers. *Dev Dyn*. 2004;229: 763-770.
71. Hoogaars WM, Tessari A, Moorman AF, de Boer PA, Hagoort J, Soufan AT, Campione M, Christoffels VM. The transcriptional repressor Tbx3 delineates the developing central conduction system of the heart. *Cardiovasc Res*. 2004;62:489-499.
72. Kondo RP, Anderson RH, Kupershmidt S, Roden DM, Evans SM. Development of the cardiac conduction system as delineated by minK-lacZ. *J Cardiovasc Electrophysiol*. 2003;14:383-391.
73. de Jong F, Opthof T, Wilde AA, Janse MJ, Charles R, Lamers WH, Moorman AF. Persisting zones of slow impulse conduction in developing chicken hearts. *Circ Res*. 1992;71:240-250.
74. Hoogaars WM, Engel A, Brons JF, Verkerk AO, de Lange FJ, Wong LY, Bakker ML, Clout DE, Wakker V, Barnett P, Ravesloot JH, Moorman AF, Verheijck EE, Christoffels VM. Tbx3 controls the sinoatrial node gene program and imposes pacemaker function on the atria. *Genes Dev*. 2007;21:1098-1112.
75. Hoogaars WM, Engel A, Brons JF, Verkerk AO, de Lange FJ, Wong LY, Bakker ML, Clout DE, Wakker V, Barnett P, Ravesloot JH, Moorman AF, Verheijck EE, Christoffels VM. Tbx3 controls the sinoatrial node gene program and imposes pacemaker function on the atria. *Genes Dev*. 2007;21:1098-1112.
76. Kamino K, Hirota A, Fujii S. Localization of pacemaking activity in early embryonic heart monitored using voltage-sensitive dye. *Nature*. 1981;290:595-597.
77. Wiese C, Grieskamp T, Airik R, Mommersteeg MT, Gardiwal A, de Gier-de Vries C, Schuster-Gossler K, Moorman AF, Kispert A, Christoffels VM. Formation of the sinus node head and differentiation of sinus node myocardium are independently regulated by Tbx18 and Tbx3. *Circ Res*. 2009;104:388-397.
78. Espinoza-Lewis RA, Yu L, He F, Liu H, Tang R, Shi J, Sun X, Martin JF, Wang D, Yang J, Chen Y. Shox2 is essential for the differentiation of cardiac pacemaker cells by repressing Nkx2-5. *Dev Biol*. 2009;327:376-385.
79. Niederreither K, Vermot J, Messaddeq N, Schuhbaur B, Chambon P, Dolle P. Embryonic retinoic acid synthesis is essential for heart morphogenesis in the mouse. *Development*. 2001;128:1019-1031.

80. Puskaric S, Schmitteckert S, Mori AD, Glaser A, Schneider KU, Bruneau BG, Blaschke RJ, Steinbeisser H, Rappold G. Shox2 mediates Tbx5 activity by regulating Bmp4 in the pacemaker region of the developing heart. *Hum Mol Genet*. 2010;19:4625-4633.
81. DiFrancesco D. The role of the funny current in pacemaker activity. *Circ Res*. 2010;106:434-446.
82. Dupays L, Jarry-Guichard T, Mazurais D, Calmels T, Izumo S, Gros D, Theveniau-Ruissy M. Dysregulation of connexins and inactivation of NFATc1 in the cardiovascular system of Nkx2-5 null mutants. *J Mol Cell Cardiol*. 2005;38:787-798.
83. Wang J, Klysik E, Sood S, Johnson RL, Wehrens XH, Martin JF. Pitx2 prevents susceptibility to atrial arrhythmias by inhibiting left-sided pacemaker specification. *Proc Natl Acad Sci U S A*. 2010;107: 9753-9758.
84. Mangoni ME, Nargeot J. Genesis and regulation of the heart automaticity. *Physiol Rev*. 2008;88: 919-982.
85. Tawara S. Das reizleitungssystem des saugetierherzens. Eine anatomisch-histologische studie uber das atrioventrikularbundel und die Purkinjeschen faden. 1906.
86. Koch W. Ueber die Blutversorgung der Sinusknotens und etwaige Beziehungen des Letzteren zum Atrioventrikularknoten. *Munch Med Wochenschr*. 1909;56:2362-2364.
87. Yoo S, Dobrzynski H, Fedorov VV, Xu SZ, Yamanushi TT, Jones SA, Yamamoto M, Nikolski VP, Efimov IR, Boyett MR. Localization of Na+ channel isoforms at the atrioventricular junction and atrioventricular node in the rat. *Circulation*. 2006;114:1360-1371.
88. Anderson RH, Ho SY, Becker AE. Anatomic boundaries between the atrioventricular node and the atrioventricular bundle. *J Cardiovasc Electrophysiol*. 1998;9:225-228.
89. Yanni J, Boyett MR, Anderson RH, Dobrzynski H. The extent of the specialized atrioventricular ring tissues. *Heart Rhythm*. 2009;6:672-680.
90. Lieberman M, Paes de CA. The Electrophysiological Organization of the Embryonic Chick Heart. *J Gen Physiol*. 1965;49:351-363.
91. Lieberman M, Paes de CA. The Spread of Excitation in the Embryonic Chick Heart. *J Gen Physiol*. 1965;49:365-379.
92. Paff GH, Boucek RJ, Harrell TC. Observations on the development of the electrocardiogram. *Anat Rec*. 1968;160:575-582.
93. Arguello C, Alanis J, Pantoja O, Valenzuela B. Electrophysiological and ultrastructural study of the atrioventricular canal during the development of the chick embryo. *J Mol Cell Cardiol*. 1986;18: 499-510.
94. Arguello C, Alanis J, Valenzuela B. The early development of the atrioventricular node and bundle of His in the embryonic chick heart. An electrophysiological and morphological study. *Development*. 1988;102:623-637.
95. Chuck ET, Meyers K, France D, Creazzo TL, Morley GE. Transitions in ventricular activation revealed by two-dimensional optical mapping. *Anat Rec A Discov Mol Cell Evol Biol*. 2004;280:990-1000.
96. Lu Y, James TN, Yamamoto S, Terasaki F. Cardiac conduction system in the chicken: Gross anatomy plus light and electron microscopy. *Anat Rec*. 1993;236:493-510.
97. Anderson RH, Becker AE, Brechenmacher C, Davies MJ, Rossi L. The human atrioventricular junctional area. A morphological study of the AV mode and bundle. *Eur J Cardiol*. 1975;3:11-25.
98. Benninghoff A. Uber die Beziehungen des Reizleitungssystems und der Papillarmuskeln zu den Konturfasern des Herzschlandes. *Anat Anz*. 1923;57:186-208.
99. Marino TA, Truex RC, Marino DR. The development of the atrioventricular node and bundle in the ferret heart. *Am J Anat*. 1979;154:135-150.
100. Patten BM. The development of the sinoventricular conduction system. 1956;22:1-21.
101. James TN. Structure and function of the sinus node, AV node and His bundle of the human heart: part I - structure. *Progress in Cardiovascular Diseases*. 2002;45:235-267.
102. Scheinman MM, Yang Y. The history of AV nodal reentry. *Pacing Clin Electrophysiol*. 2005;28: 1232-1237.
103. Sedmera D, Wessels A, Trusk TC, Thompson RP, Hewett KW, Gourdie RG. Changes in activation sequence of embryonic chick atria correlate with developing myocardial architecture. *Am J Physiol Heart Circ Physiol*. 2006;291:H1646-H1652.
104. Christoffels VM, Smits GJ, Kispert A, Moorman AF. Development of the pacemaker tissues of the heart. *Circ Res*. 2010;106:240-254.

105. Jongbloed MRM, Schalij MJ, Poelmann RE, Blom NA, Fekkes ML, Wang Z, Fishman GI, Gittenberger-de Groot AC. Embryonic conduction tissue: a spatial correlation with adult arrhythmogenic areas? Transgenic CCS/lacZ expression in the cardiac conduction system of murine embryos. *J Cardiovasc Electrophysiol*. 2004;15:349-355.
106. Chuck ET, Freeman DM, Watanabe M, Rosenbaum DS. Changing activation sequence in the embryonic chick heart. Implications for the development of the His-Purkinje system. *Circ Res*. 1997;81:470-476.
107. Rothenberg F, Watanabe M, Eloff B, Rosenbaum D. Emerging patterns of cardiac conduction in the chick embryo: waveform analysis with photodiode array-based optical imaging. *Dev Dyn*. 2005;233:456-465.
108. Kolditz DP, Wijffels MCEF, Blom NA, Van der Laarse A, Markwald RR, Schalij MJ, Gittenberger-de Groot AC. Persistence of functional atrioventricular accessory pathways in post-septated embryonic avian hearts: implications for morphogenesis and functional maturation of the cardiac conduction system. *Circulation*. 2007;115:17-26.
109. Becker AE, Anderson RH, Durrer D, Wellens HJ. The anatomical substrates of wolff-parkinson-white syndrome. A clinicopathologic correlation in seven patients. *Circulation*. 1978;57:870-879.
110. Ko JK, Deal BJ, Strasburger JF, Benson DW, Jr. Supraventricular tachycardia mechanisms and their age distribution in pediatric patients. *Am J Cardiol*. 1992;69:1028-1032.
111. Gomes JA, Mehta D, Langan MN. Sinus node reentrant tachycardia. *Pacing Clin Electrophysiol*. 1995;18:1045-1057.
112. Lee PC, Chen SA, Hwang B. Atrioventricular node anatomy and physiology: implications for ablation of atrioventricular nodal reentrant tachycardia. *Curr Opin Cardiol*. 2009;24:105-112.
113. Haissaguerre M, Jais P, Shah DC, Takahashi A, Hocini M, Quiniou G, Garrigue S, Le MA, Le MP, Clementy J. Spontaneous initiation of atrial fibrillation by ectopic beats originating in the pulmonary veins. *N Engl J Med*. 1998;339:659-666.
114. Kurotobi T, Ito H, Inoue K, Iwakura K, Kawano S, Okamura A, Date M, Fujii K. Marshall vein as arrhythmogenic source in patients with atrial fibrillation: correlation between its anatomy and electrophysiological findings. *J Cardiovasc Electrophysiol*. 2006;17:1062-1067.
115. Stillitano F, Lonardo G, Zicha S, Varro A, Cerbai E, Mugelli A, Nattel S. Molecular basis of funny current (If) in normal and failing human heart. *J Mol Cell Cardiol*. 2008;45:289-299.
116. Lubitz SA, Benjamin EJ, Ellinor PT. Atrial fibrillation in congestive heart failure. *Heart Fail Clin*. 2010;6:187-200.
117. Shinohara T, Park HW, Han S, Shen MJ, Maruyama M, Kim D, Chen PS, Lin SF. Ca2+ clock malfunction in a canine model of pacing-induced heart failure. *Am J Physiol Heart Circ Physiol*. 2010;299:H1805-H1811.
118. Aanhaanen WT, Brons JF, Dominguez JN, Rana MS, Norden J, Airik R, Wakker V, de Gier-de Vries C, Brown NA, Kispert A, Moorman AF, Christoffels VM. The Tbx2+ primary myocardium of the atrioventricular canal forms the atrioventricular node and the base of the left ventricle. *Circ Res*. 2009;104:1267-1274.

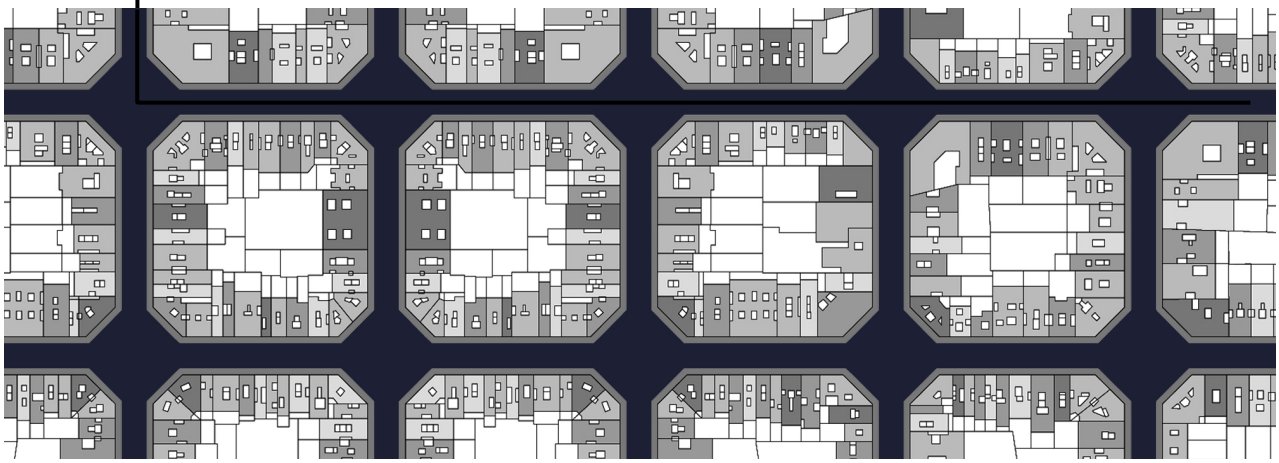

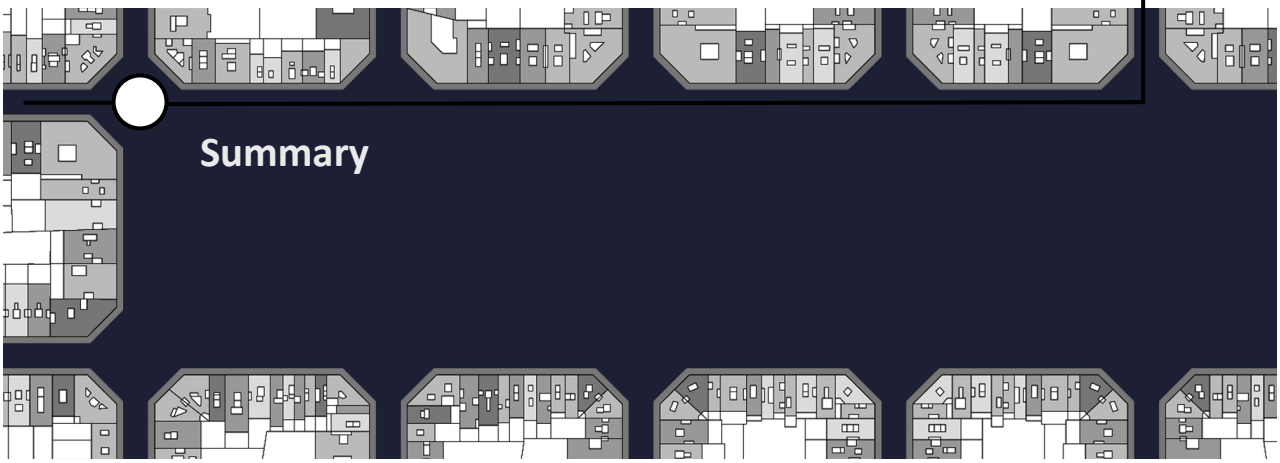
Summary

Summary

In this thesis we have described the cellular contribution of second heart field-derived cells to the developing heart, focusing on the morphological and functional development of the sinus venosus myocardium and components of the central cardiac conduction system (CCS), specifically the sinoatrial (SAN) and the atrioventricular (AVN) node. For this, we have studied the incorporation of cells from the posterior heart field (a subpopulation within the second heart field) to the venous pole of the heart in mouse, chicken and quail models using several immunohistochemical and molecular markers like *podoplanin*, *RhoA*, *PDGF*-family, *Id2* and *Hcn4*. We have also studied the changes in the embryonic electrogram in relation to potential arrhythmogenic substrates that could be explained by events during development.

In **chapter 1** we provided an overview on heart development and the development of the CCS. These two processes are closely related and abnormal development of the heart can result in abnormal CCS development. Within cardiac development, the recruitment of progenitor cells from the first and second heart field are essential. We have focused on the progenitor cells that will contribute to the venous pole of the heart (posterior heart field) both to a myocardial and a mesenchymal component, from which a partial contribution to the CCS is proposed. The composition and development of two major structures within the CCS, the SAN and AVN was reviewed.

In **chapter 2** we described the role of the transmembrane glycoprotein podoplanin in posterior heart field development. We investigated the role of *podoplanin* in development of the sinus venosus myocardium. *Podoplanin* mutants showed a generalized hypoplasia (underdevelopment) of the myocardial structures at the venous pole of the heart. The sinus venosus myocardium including the SAN, the myocardium lining the wall of the cardinal and pulmonary veins, the primary atrial septum and dorsal atrial wall were all hypoplastic in the *podoplanin* mutant embryos. Impaired myocardial formation was correlated with abnormal epithelial-to-mesenchymal transformation of the coelomic epithelium due to upregulated E-cadherin and downregulated RhoA, which are controlled by *podoplanin*. Our results demonstrate an important role for *podoplanin* in the development of the sinus venosus myocardium.

Chapter 3 further focused on the development of sinus venosus myocardium including the SAN in the chick by studying expression patterns of RhoA in relation to other markers, and by studying electrical activation patterns of the developing sinus venosus myocardium. During development, initial myocardium-wide expression of RhoA became restricted to the right-sided sinus venosus myocardium, comprising the SAN. Electrophysiological measurements revealed initial capacity of both atria to show the first electrical activity that in time shifted to a right-sided dominance, coinciding

with persistence of RhoA, Tbx18 and *Hcn4* and absence of Nkx2.5 expression in the definitive SAN. The remaining sinus venosus myocardium further differentiates towards a 'working myocardium phenotype'. We hypothesize an initial sinus venosus wide capacity to generate pacemaker signals, becoming confined to the definitive SAN. Lack of differentiation towards a chamber phenotype could explain ectopic pacemaker foci.

In **chapter 4** we described the expression patterns of PDGF-A, -C and PDFGR-α during chick heart development. The expression patterns observed were spatiotemporally associated with the development of the second heart field at the arterial and venous pole of the heart and the development of the proepicardial organ and its derivatives, the epicardium and the epicardium-derived cells (EPDCs). Inhibition of epicardial outgrowth resulted in abnormal expression of both ligands (PDGF-A, -C) and the receptor (PDFGR-α), whereas pharmacological inhibition of PDGFR-α signalling resulted in abnormal epicardial development. These findings suggest that PDGF-A, -C and PDGFR-α are involved in cardiac remodelling during development, specifically related to the ventricular compact and trabecular myocardium through epicardial-myocardial interactions.

In **chapter 5** we described the expression of the inhibitor of differentiation *Id2* during heart development in relation to the second heart field. A possible function for *Id2* in distal CCS patterning has been suggested. Id2 had a broad expression pattern in the heart and vascular system and was expressed in myocardial progenitor cells at both the inflow and outflow tract of the heart, as well as in cells of the endocardial, epicardial and neural crest cell lineage. It was not expressed in fully differentiated myocardial cells. *Id2* knockout embryos demonstrated severe cardiac defects that include abnormal orientation of the systemic and pulmonary drainage, abnormal myocardialization of systemic and pulmonary veins, hypoplasia of the SAN, atrial and ventricular septal defects and myocardial hypoplasia, and double outlet right ventricle. These abnormalities suggest a role for *Id2* in second heart field deployment.

In **chapter 6** we have studied expression patterns of the cation channel HCN4 during chick CCS development. In situ hybridisation for *Hcn4* in the chick had not been performed yet due to the lack of the sequence in the databases. After obtaining the full-length sequence for *Hcn4, w*e designed our own RNA probe to detect *Hcn4* during chick heart development. Expression was observed early in development in the primary heart tube. After looping of the heart had started, expression became restricted to transitional zones flanked by working myocardium, i.e. myocardium that will not contribute to the CCS. These transitional zones include the sinus venosus myocardium where the SAN develops, the atrioventricular canal myocardium, the primary fold (a myocardial zone between the developing ventricles), and the developing outflow tract. Further in development, *Hcn4* expression was restricted to

the SAN, the AVN, the common bundle, the bundle branches and the internodal and atrioventricular ring myocardium. Based on these results we have identified *Hcn4* as a marker of the developing CCS in the chick. Furthermore, we propose that expression patterns during development can explain the occurrence of arrhythmogenic anatomical predilection sites in adults.

Chapter 7 provided an overview of the morphological changes in SAN and AVN differentiation during avian heart development. We also provided baseline measurements of developmental changes in the electrogram as well as the results of our lineage tracing experiments. Initially, the entire sinus venosus myocardium shows a specific panel of markers and has the potential to generate the first electrical activity. At later stages both expression patterns and electrical activation patterns become restricted to the definitive right-sided SAN. Similarly, the restriction of expression pattern for specific cardiac markers is also observed in the atrioventricular canal myocardium, where the future AVN will develop and initially cannot be distinguished from the surrounding myocardium. Lineage tracing experiments present a potential sinoatrial contribution to the AVN area. On an electrophysiological level, we observed a significant increase in heart rate and atrioventricular delay during development. These results show that significant changes occur in both morphology and electrical properties of chick sinus venosus and atrioventricular ring myocardium during development, where the putative SAN and AVN will form, respectively. The broad electrical potential of these structures during development may form an explanation for the occurrence of predilection sites for arrhythmias in the adult.

Finally, **chapter 8** provides a general discussion on the data presented on this thesis. The development of the heart in relation to the formation of the CCS is discussed with focus on understanding the developmental processes that could account for potential arrhythmogenic substrates. We have provided evidence (**chapters 1, 3, 6** and**7**) that the embryonic area of the developing CCS is broader than what is found in the adult. Potentially, embryonic structures could retain or re-gain this potential which could lead to rhythm disturbances. The next necessary step involves thorough lineage tracing experiments to study the cellular composition of the pertinent CCS structures like the SAN or the AVN.

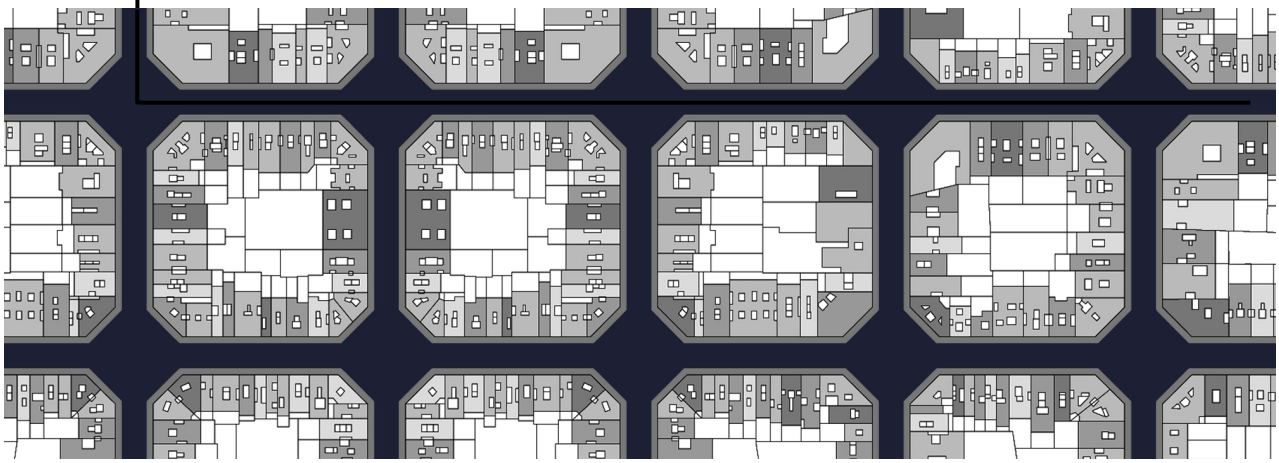

Samenvatting

Samenvatting

Dit proefschrift beschrijft de cellulaire bijdrage van het *second heart field* in de aanleg en ontwikkeling van het hart. De focus ligt daarbij op de morfologische en functionele ontwikkeling van het myocard (hartspierweefsel) van de sinus venosus en onderdelen van het centrale cardiale impuls-en geleidingssysteem, zoals de sinoatriale en de atrioventriculaire knoop. Om de rol van het *second heart field* in de aanleg en differentiatie van deze structuren te bestuderen, is er met name naar de rol van het *posterior heart field* (de bijdrage van het *second heart field* aan de veneuze pool) gekeken tijdens de hartontwikkeling van de muis, kip en kwartel. Hierbij is gebruik gemaakt van verschillende immunohistochemische en moleculaire markers, zoals podoplanine, RhoA, PDGF, Id2 en HCN4. Tevens zijn de elektrofysiologische veranderingen die tijdens de ontwikkeling in het embryonale hart plaatsvinden bestudeerd. Deze veranderingen hebben mogelijk een relatie met het ontstaan van specifieke hartritmestoornissen.

Hoofdstuk 1 geeft een overzicht over de aanleg en ontwikkeling van het hart inclusief het cardiale impuls-en geleidingssysteem. De aanleg van het hart en het impuls- en geleidingssysteem zijn nauw aan elkaar gerelateerd. Een verstoring in de hartontwikkeling kan dan ook resulteren in een abnormaal functionerend impuls- en geleidingssysteem. De bijdrage van de cellen van het *first heart field* en het *second heart field* is van essentieel belang in de aanleg van het hart. Dit hoofdstuk richt zich op de cellen die bijdragen aan de myocardiale en mesenchymale onderdelen van de veneuze pool (*posterior heart field*). Een deel van deze cellen draagt mogelijk bij aan de aanleg van het cardiale impuls- en geleidingssysteem. Tot slot wordt in dit hoofdstuk de huidige kennis geëvalueerd over de aanleg en samenstelling van de sinoatriale en de atrioventriculaire knopen. Beide structuren zijn belangrijke onderdelen van het cardiale impuls-en geleidingssysteem.

In Hoofdstuk 2 wordt de rol beschreven van het transmembraan eiwit *podoplanine* in de ontwikkeling van het *posterior heart field* en het sinus venosus myocard. Muizenembryo's met mutaties in het *podoplanine* gen hebben een gegeneraliseerde onderontwikkeling (hypoplasie) van de myocardiale structuren aan de veneuze pool van het hart. Het sinus venosus myocard, inclusief het myocard van de sinoatriale knoop, de wanden van de cardinaal- en pulmonaal venen, het primitieve atrium septum en de dorsale wand van het atrium zijn alle hypoplastisch in *podoplanine* knockout embryo's. Deze verstoorde aanleg van het myocard wordt gerelateerd aan een afwijkend 'epitheliaal naar mesenchymaal transformatie proces' (EMT) in het coeloomholte epitheel van *podoplanine* gemuteerde muizenembryo's. De verstoring van het EMT-proces wordt mogelijk veroorzaakt door een verhoogde expressie van E-cadherine en een verlaagde expressie van RhoA, welke normaliter door *podoplanine*

worden gereguleerd. Op basis van deze resultaten postuleren wij dat *podoplanine* een belangrijke rol heeft in de aanleg van het sinus venosus myocard.

In aansluiting op het voorgaande hoofdstuk, wordt in **hoofdstuk 3** de aanleg van het sinus venosus myocard inclusief de sinoatriale knoop tijdens de hartontwikkeling van de kip beschreven. De expressie van RhoA in relatie tot de expressie van andere (myocardiale) markers is bestudeerd, evenals de veranderingen in elektrofysiologische activatiepatronen in de sinus venosus van embryonale kippenharten. De expressie van RhoA wordt tijdens de vroege hartontwikkelingsstadia in het gehele hart waargenomen. Later in de ontwikkeling beperkt RhoA expressie zich (geleidelijk) tot de sinoatriale knoop. De elektrofysiologische metingen demonstreren dat de eerste activatie van de atria tijdens de vroege hartontwikkelingsstadia zowel in het toekomstige linker- als rechter atrium kan plaatsvinden. Tijdens de daarop volgende ontwikkelingsstadia wordt de primaire atriale activatie voornamelijk tot het rechter atrium beperkt. Deze elektrofysiologische dominantie van het rechter atrium gaat gepaard met een beperking van het immunohistochemische expressiepatroon tot de sinoatriale knoop. Het expressiepatroon van de sinoatriale knoop wordt gekenmerkt door aanwezigheid van RhoA, Tbx18 en *Hcn4* en afwezigheid van Nkx2.5. Het overige sinus venosus myocard differentieert richting een 'kamer fenotype'. We hypothetiseren dat het gehele sinus venosus myocard initieel het vermogen heeft om als pacemaker te kunnen fungeren. Gedurende de verdere ontwikkeling neemt de pacemaker capaciteit van het grootste deel van dit sinus venosus myocard af en uiteindelijk wordt de sinoatriale knoop de primaire pacemaker van het hart. Een verstoorde differentiatie van het embryonale sinus venosus myocard vormt een plausibele verklaring voor ectopische pacemaker foci in de atria.

In **hoofdstuk 4** worden de expressiepatronen van de groeifactoren PDGF-A, -C en de receptor PDGFR-α tijdens de hartontwikkeling van de kip beschreven. De expressiepatronen zijn spatiotemporeel geassocieerd met de aanleg en ontwikkeling van het *second heart field* aan zowel de arteriële- als de veneuze pool van het hart. Daarnaast zijn de expressiepatronen gerelateerd aan de ontwikkeling van het proepicard orgaan en de daarvan afkomstige structuren, het epicard en de epicard afgeleide cellen (EPDCs). Remming (inhibitie) van epicard-uitgroei resulteert in een abnormale expressie van zowel ligand (PDGF-A, -C) als receptor (PDGFR-α), terwijl farmacologische inhibitie van PDGFR-α leidt tot een gestoorde epicardiale ontwikkeling. Deze bevindingen suggereren dat *PDGF-A*, *-C* en *PDGFR*-α tijdens de hartontwikkeling betrokken zijn bij de remodellering van het hart. Deze remodellerende invloeden, welke gereguleerd worden door zogenaamde 'epicardiale-myocardiale interacties', vinden voornamelijk plaats in het compacte myocard van de ventrikels en in het trabekelsysteem.

Hoofdstuk 5 beschrijft de expressie van de differentiatieremmer (inhibitor of differentiation) *Id2* tijdens de hartontwikkeling in relatie tot het *second heart field.* Expressie van *Id2* wordt waargenomen in de cellen van het endotheel, epitheel en de neurale lijst. De expressie van *Id2* vertoont ook een uitgebreid patroon in het cardiovasculaire systeem en in de myocardiale voorlopercellen, die gelegen zijn bij zowel de arteriële- als de veneuze pool van het embryonale hart. Id2 is echter afwezig in volledig gedifferentieerde cardiomyocyten. Muizenembryo's met een mutatie in het *Id2*-gen laten een reeks van hartafwijkingen zien, waaronder een abnormale positie van zowel de systeem- als pulmonaalvenen (aders), een gestoorde aanleg van het myocard rondom deze venen, een onderontwikkeling (hypoplasie) van de sinoatriale knoop, defecten van het atrium-en ventrikel septum, algehele hypoplasie van het myocard en een zogenaamde double outlet right ventricle, waarbij de beide grote slagaders (aorta en truncus pulmonalis) boven de rechter ventrikel staan. De combinatie van deze afwijkingen suggereert dat *Id2* een belangrijke rol speelt in de regulatie van het *second heart field* in de aanleg en ontwikkeling van het hart.

Hoofdstuk 6 beschrijft het expressiepatroon van het 'cation-kanaal' HCN4 in de ontwikkeling van het cardiale impuls- en geleidingssysteem in de kip. In situ hybridisatie voor *Hcn4* in de kip was tot nog toe niet verricht wegens het ontbreken van de sequentie in databanken. Na het vaststellen van de volledige *Hcn4* sequentie, hebben we een *Hcn4* RNA probe ontwikkeld. Tijdens vroege embryonale ontwikkelingsstadia wordt *Hcn4* in het gehele primaire hartbuisje waargenomen. Na kromming van het hartbuisje beperkt de expressie van *Hcn4* zich tot zogenaamde transitionele zones of overgangszones die geflankeerd worden door het "werkmyocard", d.w.z. het myocard dat geen deel uitmaakt van het cardiale impuls- en geleidingssysteem. Deze transitionele zones omvatten het sinus venosus myocard waar de ontwikkeling van de sinoatriale knoop plaatsvindt, het myocard van het atrioventriculaire kanaal, de primaire plooi (een myocardiaal gebied dat gelegen is tussen de zich ontwikkelende ventrikels) en het myocard van de uitstroom van het hart. Uiteindelijk, in het foetale vierkamer-hart, beperkt de expressie van *Hcn4* zich tot de sinoatriale knoop, de atrioventriculaire knoop, de bundel van His, de bundel takken en het myocard van de internodale banen en de atrioventriculaire ringen. Op basis van deze data concluderen we dat *Hcn4* een marker is van het zich ontwikkelende cardiale impuls-en geleidingssysteem in de kip. Tevens kan het uitgebreide *Hcn4* expressiepatroon tijdens de embryonale ontwikkeling een goede verklaring vormen voor de aanwezigheid van anatomische voorkeurslocaties van hartritmestoornissen bij volwassen patienten.

Hoofdstuk 7 geeft een overzicht van de morfologische en histologische veranderingen van de sinoatriale en atrioventriculaire knoop tijdens de embryonale ontwikkeling van de kip en de kwartel. Ook worden de veranderingen van het elektrogram tijdens deze stadia weergegeven, evenals de resultaten van lineage tracing-experimenten. Vroeg in

de ontwikkeling heeft het gehele sinus venosus myocard een specifiek expressiepatroon van (immunohistochemische) markers en heeft dit gehele gebied de potentie om als cardiale pacemaker te fungeren. Op latere stadia van de ontwikkeling vindt restrictie plaats van zowel de pacemakercapaciteit als van dit specifieke (immuno-histochemische) expressiepatroon, die zich uiteindelijk zullen beperken tot het myocard van de (rechtszijdige) sinoatriale knoop. Hetzelfde proces rond (immunohistochemische) expressiepatronen voltrekt zich in het myocard van het atrioventriculaire kanaal, waar aanvankelijk het gebied van de toekomstige atrioventriculaire knoop niet van de omgeving te onderscheiden is. Lineage tracing experimenten laten een potentiële bijdrage van het sinoatriale myocard aan het atrioventriculaire knoopgebied zien. Op elektrofysiologisch gebied wordt tijdens de embryonale ontwikkeling een significante toename waargenomen van zowel de hartfrequentie als van de vertraging in atrioventriculaire geleiding van de cardiale impuls in de atrioventriculaire knoop. Deze data demonstreren dat tijdens de hartontwikkeling in de kip en kwartel significante morfologische en elektro-fysiologische veranderingen plaatsvinden in het myocard van zowel de sinus venosus als van de atrioventriculaire ring, waar de toekomstige sinoatriale knoop en de atrioventriculaire knoop worden aangelegd. We hypothetiseren dat het aanvankelijk brede myocardiale gebied dat initieel de prikkel kan initieren tijdens de embryonale ontwikkeling, een verklaring kan geven voor de voorkeurslocaties van hartritme-stoornissen.

Hoofdstuk 8 omvat de algemene discussie van dit proefschrift. Het hartontwikkelingsproces wordt besproken in relatie tot de aanleg en ontwikkeling van het cardiale impuls- en geleidingssysteem. Daarbij wordt een verband gelegd met het optreden van hartritmestoornissen op voorkeurslocaties in het (volwassen) hart. Zoals we hebben aangetoond in de **hoofdstukken 1**, **3**, **6** en **7** is het cardiale prikkel- en geleidingssysteem in het embryonale hart omvangrijker dan in een volwassen hart. Hierdoor zouden myocardiale gebieden, die een ‘embryonaal geleidingssysteem fenotype’ behouden of opnieuw verwerven, later in het leven hartritmestoornissen kunnen initieren.
Om het inzicht uit te breiden in de exacte cellijnen die bijdragen aan de aanleg van de verschillende onderdelen van het cardiale impuls- en geleidingssysteem, zoals de sinoatriale en de atrioventriculaire knoop, zijn lineage tracing experimenten in de toekomst van essentieel belang.

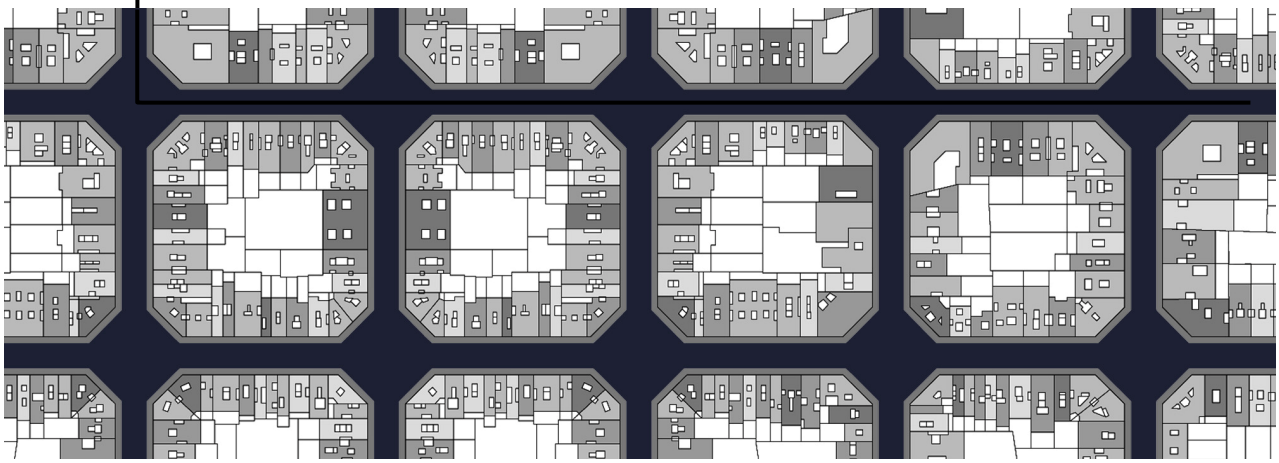

List of publications

List of publications

Grauss RW, Winter EM, van Tuyn J, Pijnappels DA, **Vicente Steijn R**, Hogers B, van der Geest RJ, de Vries AAF, Steendijk P, van der Laarse A, Gittenberger-de Groot AC, Schalij MJ, Atsma DE. Mesenchymal stem cells from ischemic heart disease patients improve left ventricular function after acute myocardial infarction. Am J Physiol Heart Circ Physiol. 2007 Oct; 293(4):H2438-47.

Winter EM, Grauss RW, Hogers B, van Tuyn J, van der Geest R, Lie-Venema H, **Vicente Steijn R**, Maas S, DeRuiter MC, deVries AA, Steendijk P, Doevendans PA, van der Laarse A, Poelmann RE, Schalij MJ, Atsma DE, Gittenberger-de Groot AC. Preservation of left ventricular function and attenuation of remodeling after transplantation of human epicardium-derived cells into the infarcted mouse heart. Circulation. 2007 Aug 21;116(8):917-27.

Mahtab EA, **Vicente-Steijn R**, Hahurij ND, Jongbloed MR, Wisse LJ, DeRuiter MC, Uhrin P, Zaujec J, Binder BR, Schalij MJ, Poelmann RE, Gittenberger-de Groot AC. Podoplanin deficient mice show a RhoA-related hypoplasia of the sinus venosus myocardium including the sinoatrial node. Dev Dyn. 2009 Jan;238(1):183-93.

Bax NA, Lie-Venema H, **Vicente-Steijn R**, Bleyl SB, Van Den Akker NM, Maas S, Poelmann RE, Gittenberger-de Groot AC. Platelet-derived growth factor is involved in the differentiation of second heart field-derived cardiac structures in chicken embryos. Dev Dyn. 2009 Oct;238(10):2658-69.

Vicente-Steijn R, Kolditz DP, Mahtab EA, Askar SF, Bax NA, VAN DER Graaf LM, Wisse LJ, Passier R, Pijnappels DA, Schalij MJ, Poelmann RE, Gittenberger-DE Groot AC, Jongbloed MR. Electrical activation of sinus venosus myocardium and expression patterns of RhoA and Isl-1 in the chick embryo. J Cardiovasc Electrophysiol. 2010 Nov;21(11):1284-92.

Vicente-Steijn R, Passier R, Wisse LJ, Schalij MJ, Poelmann RE, Gittenberger-de Groot AC, Jongbloed MRM. The funny current channel HCN4 delineates the developing cardiac conduction system in the chicken heart. Heart Rhythm. 2011. *in press*

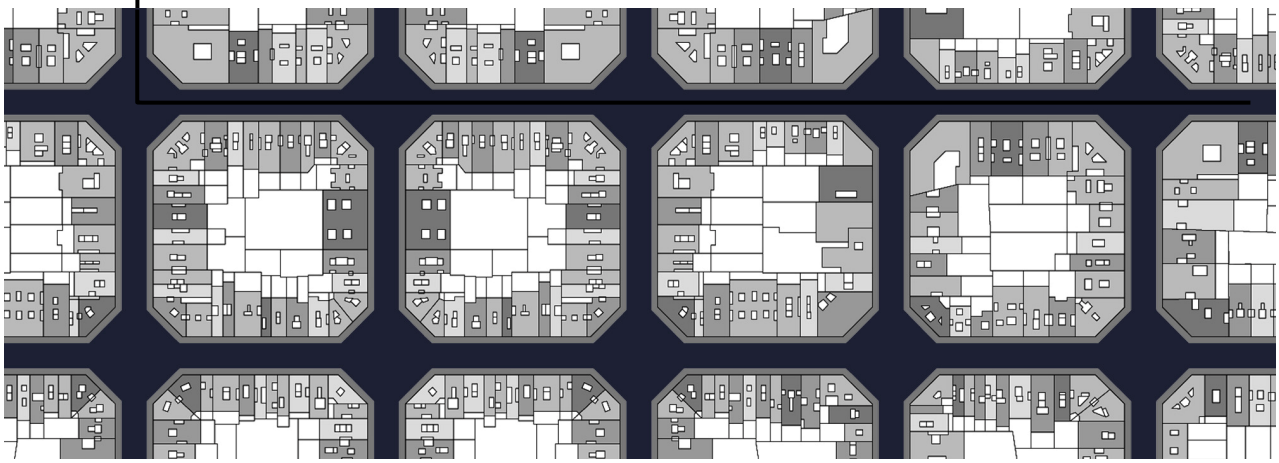

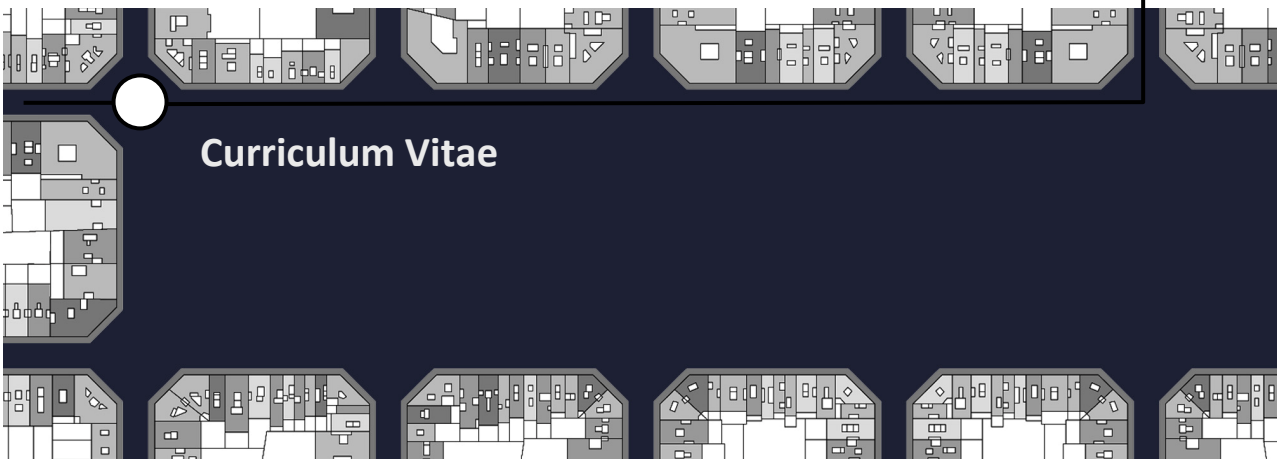
Curriculum Vitae

Curriculum Vitae

Rebecca Vicente Steijn was born on the 18th of February 1983 in Barcelona, Spain. She graduated from the Oak House British School (Barcelona) in 2000 where she conducted her final project on the hereditability of prostate cancer in patients of the Vall d'Hebron hospital. In September of 2000 she started her study of Human Biology at the Universitat Pompeu i Fabra in Barcelona. During her study she performed several international research internships. The first one was carried out at the Ruder Boscovic Institute in Zagreb, Croatia, where she studied the processes that control cellular aging in relation to cancer. Her first contact with muscle-related research came from her two internships at the Vrije Universiteit Medical Centre (VU) in Amsterdam at the department of Physiology. Under the supervision of dr. R.T. Jaspers she studied the cellular and functional composition of the iliofibularis muscle of the Xenopus to understand muscular remodelling for possible therapeutic applications. Her final research project was conducted at the Leiden University Medical Centre (LUMC) in Leiden at the department of Cardiology under the supervision of Prof. dr. A. van der Laarse. She studied the therapeutic effects of mesenchymal stem cells in myocardial infarction. She graduated in June of 2006.

In august of 2006 she started her PhD project at the department of Anatomy and Embryology under the supervision of Prof. dr. A.C. Gittenberger-de Groot, Prof. dr. R.E. Poelmann and dr. M.R.M. Jongbloed. The results of this research are described in this thesis. In March of 2011 she started her post-doc position at the same department in the group of Prof. dr. R.E. Poelmann.

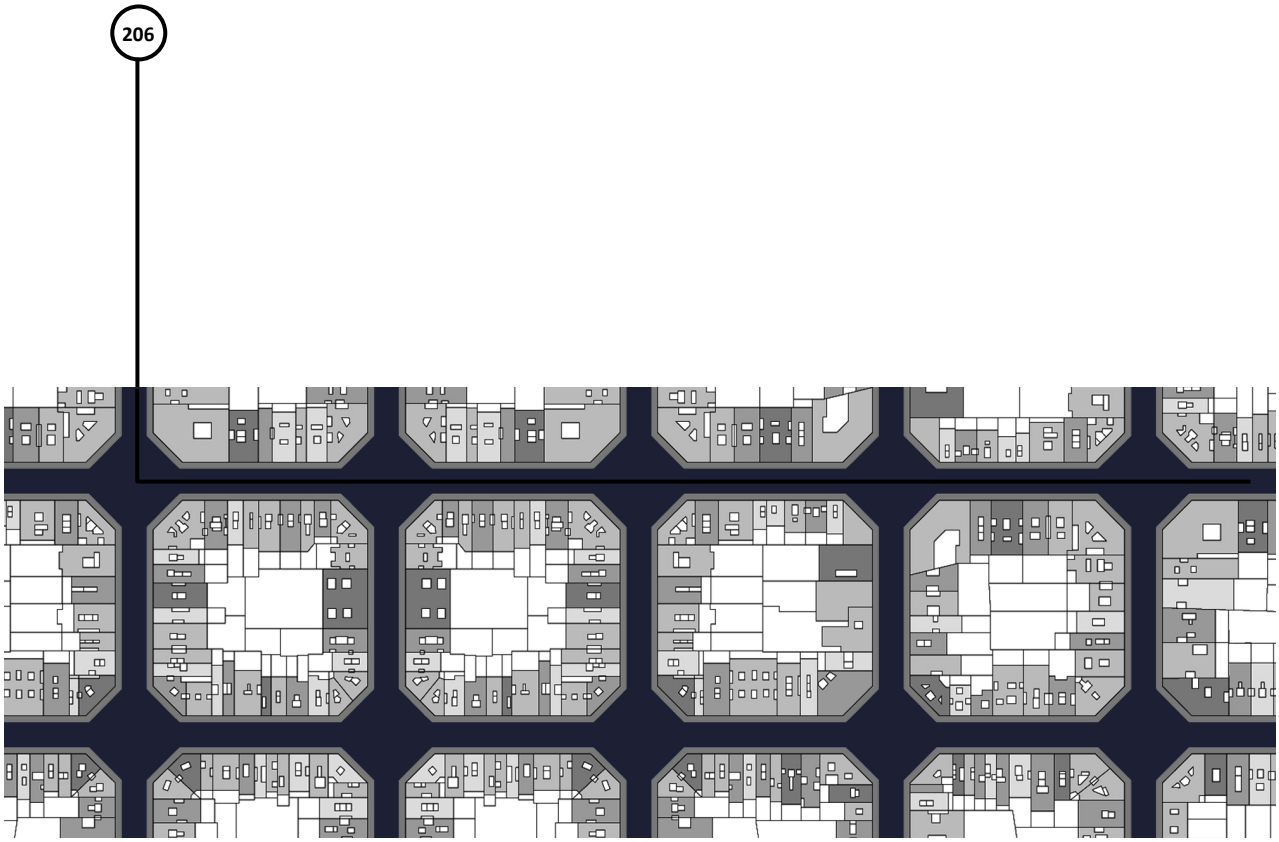
206

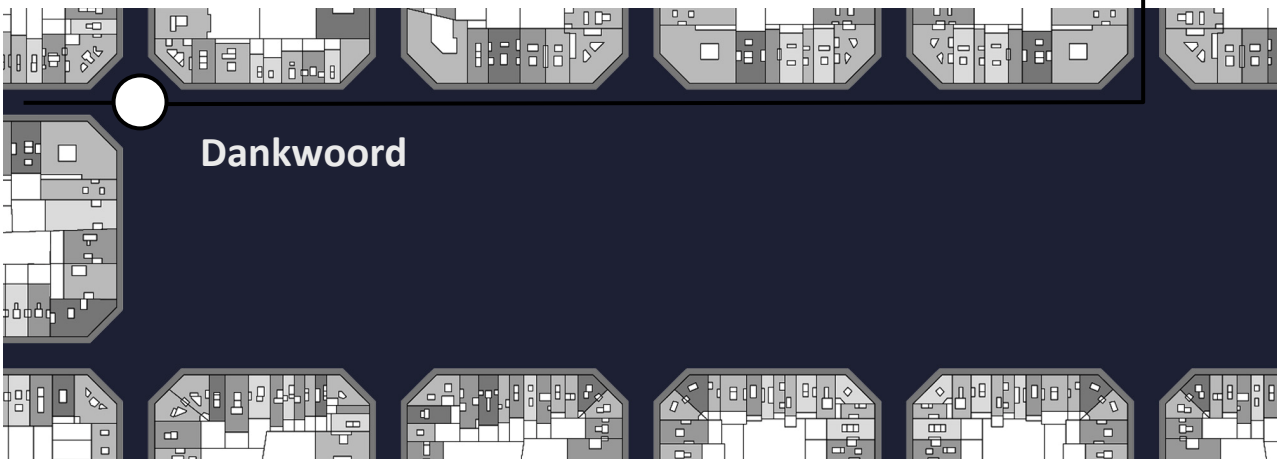
Dankwoord

Dankwoord

Veel collega's en vrienden hebben - direct of indirect - een belangrijke bijdrage geleverd aan dit proefschrift. Zij hebben mij zowel inhoudelijk als moreel enorm gesteund.

Bij de start van mijn promotieonderzoek had ik nauwelijks kennis van de hartontwikkeling en nog minder van die van kippen. Om de verschillende processen te kunnen doorgronden heeft mijn promotor Prof. dr. Rob Poelmann mij destijds intensief begeleid met urenlange microscoopsessies. Ik kijk met veel plezier terug naar het wekelijks overleg met hem, mijn andere promotor Prof. dr. Adri Gittenberger-de Groot en mijn co-promotor dr. Monique Jongbloed. In dit gezelschap hebben wij veel leuke 'brainstormsessies' gehad met spannende nieuwe ideeën tot gevolg. De discussies met Prof. dr. M.J. Schalij van de afdeling Cardiologie hebben herhaaldelijk geleid tot verrassende wendingen aan mijn onderzoek.
Dankzij de ondersteuning van mijn collega's van de afdeling Anatomie en Embryologie heb ik vier zeer leuke promotiejaren gehad. Ik wil de analisten Conny, Dorien, Jan, Jantine, Linda, Monica en Simone graag bedanken voor hun steun op het lab.
Saskia heeft mij met veel geduld geleerd hoe met kippenembryo's om te gaan. Ook kijk ik met veel genoegen terug naar de gezellige maar vooral nuttige sessies met Bert achter de 'Amira'. Zonder zijn expertise in 3D-reconstructies zou ik nog steeds niet goed weten hoe een hart ruimtelijk in elkaar zit. Bas Blankenvoort, Jan Lens en Ron Slagter hebben een onmisbare bijdrage geleverd aan de mooie figuren en tekeningen. Zonder deze creaties zou dit boekwerk een stuk minder fraai zijn geworden.
Ook Joke, Anne-Marie en Wies waren een fantastische steun tijdens mijn AIO-schap.
En ik heb dankbaar gebruik gemaakt van de computerkennis van Daniël en Paul.
De mede-AIO´s tijdens mijn promotieonderzoek (Anastasia, Appie, Brigit, Cathelijne, Cheryl, Denise, Fanneke, Harsha, Kim, Lida, Patty, Piet, Regina, Roderick, Stefan, Willemijn en Yvonne) hebben een belangrijke bijdrage geleverd aan de gezellige tijd binnen en buiten het lab.
Ik heb de adviezen van- en discussies met mijn huidige kamergenoot Margot altijd enorm gewaardeerd. Deze hebben veel toegevoegd aan mijn kennis en ervaring. Mijn 'tijdelijke' kamergenoten Heleen, Liesbeth, Nynke en Noortje wil ik bedanken voor de warmte waarmee zij mij aan het begin van mijn promotieonderzoek hebben ontvangen. De samenwerking met Nathan tijdens 'onze laatste loodjes' heeft ons beiden veel goeds gebracht.
Toine de Vries en Kim Janssen van de afdeling Moleculaire Cel Biologie wil ik bedanken voor de prettige samenwerking en ondersteuning.

De eerste kennismaking met hartgerelateerd onderzoek was tijdens mijn afstudeerstage. Ik kijk met veel plezier terug naar die tijd en wil mijn toenmalige begeleiders, Prof. dr. Arnoud van der Laarse en dr. Robert Grauss, hiervoor bedanken.

Ook dank aan mijn collega's van het lab van de afdeling Cardiologie. Na mijn stage bleef ik altijd welkom, wat in een goede samenwerking heeft geresulteerd. Arti, Cindy, Daniël, Lizet, Margreet, Melina, Minka, Niek, Saïd en Ton wil ik bedanken voor alle plezier op het lab.

Ook een speciaal woord van dank aan mijn vrienden in Nederland en Spanje. Zij hebben veel van mijn kanten gezien en waren er altijd om het (weer) gezellig te maken. In het bijzonder Tessa, die mij met onze afspraakjes en telefoongesprekken telkens weer voldoende energie gaf om een nieuwe onderzoeksuitdaging aan te gaan. Montse, mi mejor amiga desde que tengo tres años, siempre me ha apoyado - a veces a larga distancia - durante este período. Es más, sin pensárselo un minuto me dijo "sí" cuando le pregunté si me quería ayudar con el diseño de la portada de mi tésis. No tengo palabras para expresar mi gratitud, pero creo que tampoco hacen falta. [Montse, mijn allerbeste vriendin sinds mijn derde levensjaar, is altijd betrokken geweest en heeft mij - vaak op verre afstand - gesteund. Zij is zelfs zo gek geweest om "ja" te zeggen toen ik hulp vroeg voor mijn kaftontwerp. Woorden van dank schieten hiervoor tekort, maar zijn eigenlijk niet eens nodig.]

Ik wil mijn moeder, tevens mijn goede vriendin, in het bijzonder uitlichten. Zonder haar was ik nooit zo ver gekomen. Haar advies is altijd goud waard!

Een persoonlijk dankwoord richting mijn paranimfen Edris en Jacobien.
Edris, toen ik bij Anatomie begon hoorde ik al geruchten over 'die gekke Afghaan die je niet altijd serieus moest nemen'. Vervolgens kwam ik bij jou op de kamer. Ik kijk met een grote glimlach terug op onze wetenschappelijke discussies en gezellige momenten. Ik ben heel blij dat jij mijn paranimf wil zijn. Je bent een echte vriend!
Lieve Jaco, toen ik jou leerde kennen was jij de 'andere schoonzus' die ook promotieonderzoek deed. Maar het was iets met infecties, voor mij een onbekend terrein. Vervolgens hebben wij elkaar intensief leren kennen, onder andere op de door ons gedeelde Pyreneeën. Behalve dat je een fantastische schoonzus bent, zou ik je ook als paranimf niet willen missen.

En tot slot, mijn lieve Wouter. Jij hebt een belangrijke rol gespeeld bij mijn keuze voor Leiden als plaats om te promoveren. Jouw steun tijdens mijn promotieonderzoek kan ik niet in woorden uitdrukken. Maar wel je hulp bij het eruit halen van mijn 'niet-in-Nederland-geboren-en-getogen' trekjes in het Nederlandse taalgebruik. Zelfs tot aan het dankwoord toe (behalve dit stukje). Ik hoop dat wij heel lang samen van het leven zullen genieten!